Aus dem Institut für Transfusionsmedizin und Immunologie
der Medizinischen Fakultät Mannheim
Direktor: Prof. Dr. med. Harald Klüter

# Mechanism of action of adipose mesenchymal stromal cells reducing cisplatin-induced proximal tubular epithelial cell injury

Inauguraldissertation
zur Erlangung des
Doctor scientiarum humanarum (Dr. sc. Hum.)

der

Medizinischen Fakultät Mannheim
der Ruprecht-Karls-Universität
zu
Heidelberg

vorgelegt von
Eleonora Scaccia

Aus
Terracina, Italy
2025

Dekan: Herr Prof. Dr. med. Sergij Goerdt
Referentin: Frau Prof. (apl.) Dr. rer. nat. Karen Bieback

“*A mia figlia Noemi,*
*insegui sempre i tuoi sogni e non lasciare*
*che nessuno ti ostacoli lungo il cammino”*

**Sections/data reported within this dissertation are part of submitted/published manuscripts:**

Introduction chapter comprises material from the published review article "*Erika Rendra*, **Eleonora Scaccia***, Karen Bieback*. *Recent advances in understanding mesenchymal stromal cells. F1000Res. 2020 Feb 27:9:F1000 Faculty Rev-156. "*

The first part of the thesis contains material from the published article: "*Sandra Calcat-i-Cervera*, Erika Rendra*, **Eleonora Scaccia***, Francesco Amadeo*, Vivien Hanson, Bettina Wilm, Patricia Murray, Timothy O'Brien, Arthur Taylor and Karen Bieback*. *Harmonised culture procedures minimise but do not eliminate mesenchymal stromal cell donor and tissue variability in a decentralised multicentre manufacturing approach. Stem Cell Research & Therapy 14, 120 (2023)*. "

The second part of the thesis contains material from the published article: "*Renata Skovronova*, **Eleonora Scaccia***, Sandra Calcat-i-Cervera*, Benedetta Bussolati , Timothy O'Brien and Karen Bieback. Adipose stromal cells bioproducts as cell-free therapies: manufacturing and therapeutic dose determine in vitro functionality*. *J Transl Med. 2023 Oct 16;21(1):723.* "

The third part of the thesis contains material from the soon to be submitted article "***Eleonora Scaccia**, Erika Rendra, Isabell Moskal, Stefanie Uhlig, Francesca Pagano, Karen Bieback*. *Conditioned medium from Adipose Stromal Cells reduces cisplatin-induced proximal tubular epithelial cells apoptosis by downregulation of miR-181a-5p*"

*shared authorship

# TABLE OF CONTENTS

Page

# ABBREVIATIONS

| | |
|---|---|
| **A** | |
| AGO | Argonaut |
| AIF | Apoptosis-inducing factor |
| AKI | Acute renal injury |
| A-MSC | Adipose mesenchymal stromal cells |
| Apaf-1 | Protease-activating factor-1 |
| ATG | Autophagy-related gene |
| ATP | Adenosine triphosphate |
| **B** | |
| Bcl-2 | B-cell lymphoma 2 |
| BM-MSC | Bone marrow mesenchymal stromal cells |
| **C** | |
| CKD | Chronic kidney disease |
| ciPTEC | Conditionally immortalized proximal tubular epithelial cells |
| **D** | |
| DAVID | Database for Annotation, Visualization and Integrated Discovery |
| DM | Diabetes mellitus |
| DGCR8 | DiGeorge syndrome critical region 8 |
| dsRNA | Double-stranded RNA |
| DMEM | Dulbecco`modifield Eagle Medium |
| **E** | |
| ECM | Extracellular matrix |
| EGF | Epidermal Growth Factor |
| ESRD | Even terminal stage |
| ESRs | Early-stage researchers |
| EV | Extracellular Vesicle |
| **F** | |
| FBS | Fetal Bovine Serum |
| **G** | |
| GFP | green fluorescence protein |
| GFR | Rate of glomerular filtration |
| GTPase | Small nuclear guanine triphosphatase |
| GTPase | Small nuclear guanine triphosphatase |
| **H** | |
| HBSS | Hank`balanced salt solution |
| HFBR | Hollow fiber bioreactor |
| HGF | Hepatocyte growth factor |
| HK2 | Human kidney 2 |
| HLA | Human leukocyte antigen |
| HUVEC | Human umbilical vascular endothelial cells |
| **I** | |
| I/R | Ischaemia-Reperfusion |
| I3 | Triiodothyronine |
| IAPs | Inhibitor of apoptosis proteins |
| IDO | Indoleamine-pyrrole 2,3-dioxygenase |

| | |
|---|---|
| IFN- γ | Interferon gamma |
| IGF-1 | Insulin-like growth factor 1 |
| IL-1 | Interleukin-1 |
| IL-10 | Interleukin-10 |
| IL-12p40 | Interleukin-12p40 |
| IL-16 | Interleukin-6 |
| ISCT | International Society for Cellular Therapy |
| ISEV | Society of Extracellular Vesicles |
| ITS | Insulin-Transferrin-Sodium Selenite Supplement |
| ITS-G | Insulin-transferrin-selenium |
| **J** | |
| **K** | |
| KD | Kidney disease |
| KLF6 | Krüppel-like factor 6 |
| **L** | |
| lncRNA | Long non-coding RNA |
| **M** | |
| MAPK1 | Mitogen-activated protein kinase |
| MCSP | Melanoma |
| α-MEM | Minimum essential medium alpha |
| MHC | Major histocompatibility complex |
| miRNA | MicroRNA |
| MISEV | The Minimal information for studies of extracellular vesicles |
| Mit-A | Mithramycin-A |
| MMPs | Matrix metalloproteinases |
| MoA | Mechanism of action |
| mRNA | MessengerRNA |
| MSC | Mesenchymal Stromal Cell |
| MSC-CM | MSC-conditioned culture medium |
| MVBs | Multivesicular bodies |
| MVs | Microvesicles |
| **N** | |
| **O** | |
| **P** | |
| PBMC | Human peripheral blood mononuclear cells |
| PBS | Phophate buffer saline |
| PCR | Polymerase chain reaction |
| PFA | Perfluoroalkoxy alkanes |
| PGE2 | Prostaglandin E2 |
| PHA | Phytoemagglutinin-L |
| piRNA | Piwi-interacting RNA |
| **Q** | |
| **R** | |
| Ran | RAs-related Nuclear protein |
| RISC | RNA-induced suppression complex |
| RMTs | Cell-based regenerative medicine therapies |
| RNAi | RNA interference |
| ROS | Reactive oxygen species |
| RPMI | Roswell park Memorial Institute Medium |

| | |
|---|---|
| rRNA | ribosomal RNA |
| RTB | RenalToolBox |
| RT-qPCR | Reverse transcription-quantitative polymerase chain reaction |
| **S** | |
| siRNA | Small interfering RNA |
| SKI-II | Sphingosine kinase inhibitor |
| **T** | |
| TBS | Tris buffer saline |
| TBS-T | Tris buffer saline 1x + Tween |
| TF | Tissue factor |
| TFF | Tangential flow filtration |
| TGF - β | Transforming growth factor β |
| TGS | Tris/Glycine/SDS |
| TNF-α | Tumor necrosis factor- α |
| TRAIL | TNF-Related Apoptosis-Inducing Ligand |
| tRNA | transfer RNA |
| **U** | |
| UC-MSC | Umbilical cord mesenchymal stromal cells |
| **V** | |
| VEGF | Vascular endothelial growth factor |
| VEGFR-2 | Vascular endothelial growth factor receptor 2 |
| **W** | |
| WB | Western blot |
| WT | Wild-type |
| **X** | |
| **Y** | |
| **Z** | |
| ZNF | Zinc finger |

# 1 INTRODUCTION

## 1.1 Kidney disease

Kidney disease (KD) is a global public health problem that affects more than 750 million of the worldwide population and causes 5 to 10 million deaths each year [1, 2]. KD is considered the third fastest-growing cause of death worldwide and has a continuous rise in age-related mortality and socioeconomic conditions [3]. Various pathologies including obesity, diabetes and hepatitis B virus infections can cause kidney problems. At the same time, the progression of KD in turn becomes a risk factor for cardiovascular diseases [4], stroke and peripheral vascular disease and cancer [5].

Guidelines for the improvement of overall renal disease outcomes divide KD into two sub-classes: acute kidney injury (AKI) and chronic kidney disease (CKD) [6], that differ from each other in the duration of the disease, respectively <3 or >3 months. By definition, AKD precedes CKD, but AKD may also be overlapping on pre-existing CKD, due to another disease or due to an aggravation of the same disease [7].

**Chronic Kidney Disease**

Criteria for defining a kidney problem as a CKD are progressive and irreversible loss of kidney function evidenced by an estimated glomerular filtration rate (eGFR) of <60 ml/min per 1,73 $m^2$, the persistent presence of manifestations indicators of renal damage (proteinuria, active urinary sediments, histological damage, structural abnormalities or a history of kidney transplantation), or both, lasting more than 3 months [8].

The incidence of CKD is correlated with age; over 60% of people aged 80 have CKD, which increases their risk of developing cardiovascular disease and death [9]. The development of CKD is influenced by risk factors such as diabetes mellitus (DM), hypertension and obesity, patients with CKD are at increased risk of acute kidney injury (AKI), but at the same time, repeated episodes of AKI contribute to CKD progression [10].

**Acute Kidney Injury**

AKI is a clinical syndrome that includes all pathological conditions characterized by a reduction within 48h of kidney function, defined by an absolute increase in creatinine levels 0.3 mg/dl and/or a percentage increase in creatinine 1,5 times the basal value and/or a reduction in diuresis to values < 0,5 ml/KG /h for at least 6h or presence of anuria for at least 12h [11].

AKI affects 30-60% of seriously ill patients and is associated with acute morbidity and mortality [12] partly due to the absence of early diagnostic markers that lead to a delay in diagnosis and the application of preventive measures that can reduce the consequences of kidney damage.

Also, AKI is a very heterogeneous syndrome with varying etiology, pathophysiology and clinical presentation makes it difficult to search for a specific treatment [13].

### 1.1.1 Nephrocitotoxity

Kidneys receive about 25% of cardiac output, underlining their important role in physiology. As excretion organs, kidneys are naturally exposed to a large portion of circulating drugs and chemicals that may harm the kidney [14]. Nephrotoxicity results from a rapid decline in excretory mechanisms within the kidney, which promotes the accumulation of waste products generated during protein metabolism including urea, nitrogen and creatinine [15].

Due to the complexity of the kidneys, defining the pathophysiology of AKI is very difficult. A decrease in glomerular filtration rate can be caused by local alterations causing reversible tubular stress/tubular necrosis injury [16], or from already persistent diseases such as diabetes mellitus, hypertension and heart failure [17]. Ischemia/reperfusion (I/R) is the main cause of AKI, due to arterial occlusion during surgery, congestive heart failure or kidney transplantation [18]. I/R is characterised by a reduction in blood supply to the kidney followed by a restoration of perfusion. This reduction in oxygenation results in reduced ATP levels, metabolic impairment, apoptosis, and reactive oxygen species (ROS) production, and aggravate during the reperfusion period, causing sterile inflammation, vasoconstriction, and oxidative damage [19].

The most vulnerable site to injury due to hypoxia, toxic compounds, proteinuria, metabolic disorders and senescence, is the tubular epithelium. Tubular cell lesions can be lethal (causing cell death) or sub-lethal (cell injury can release pro-

inflammatory or pro-fibrotic mediators). Typically, after the insult follows a recovery phase characterised by the activation of protective and regenerative mechanisms in surviving cells that restore the properties and functions of epithelial cells [9]. If these mechanisms do not occur, the extent of damage can promote renal fibrosis and the progression of CKD. In CKD, loss of podocytes replaced by extracellular matrix protein (ECM), tubular cell lesions and subsequent tubular interstitial fibrosis, contribute to nephron loss [20].

The final stage of CKD is when irreversible loss of kidney function requires dialysis or kidney transplantation. The latter comes with high costs and significant limitations in organ availability [21, 22]. Therefore, to prevent renal injury from progressing to even end-stage (ESRD), it is crucial to identify more effective therapeutic strategies to attenuate renal injury [23].

### 1.1.2 Cisplatin

The kidneys are the major targets for the toxic effects of various chemical agents and thus drug-induced AKI is a frequent entity in clinical medicine. The incidence of nephrotoxic AKI is difficult to estimate due to the variabilities of patient populations and criteria of AKI, however it is reported to contribute to about 20% of patients treated with cisplatin [24].

Cisplatin (cis-diamminedichloroplatinum II) is a platinum-containing antineoplastic drug, first approved for clinical use in 1978. It is used alone or in combination with other therapy extensively to treat different malignancies [25]. However, the major limiting factors in the use of cisplatin are the side effects in normal tissues, which include neurotoxicity, ototoxicity, nausea and vomiting, and nephrotoxicity [26, 27].

Nephrotoxicity was reported in initial clinical trials of cisplatin chemotherapy [28]. Cisplatin nephrotoxicity occurs in about one-third of the patients undergoing cisplatin treatment [29, 30]. Clinically, cisplatin nephrotoxicity is often observed after 10 days of cisplatin administration and is manifested as reduced glomerular filtration rate, increased serum creatinine, and reduction of serum levels of magnesium and potassium.

The nephrotoxic effect produced by cisplatin is caused by its accumulation in the kidney, it is concentrated and reabsorbed by renal tubular cells (five times more than in the blood) [31], mainly in the S3 segment of the proximal tubules. Here the high density of negatively charged mitochondria in proximal tubular cells attracts the

positively charged cisplatin hydrolysed complexes [32]. Consequent mitochondrial dysfunction contributes to the lethal lesion of renal tubules and the subsequent loss of renal function. Still, the exact mechanism of the cisplatin action is not completely understood. However, it is known that cisplatin interacts primarily with genomic DNA, specifically the N7 position of guanine bases, causing inter- and intra-strand DNA crosslinks which perturb DNA synthesis and result in apoptosis, autophagy, nuclear and mitochondrial DNA damage and production of reactive oxygen species [33, 34].
The pathophysiology of cisplatin-induced AKI involves 4 major mechanisms (**Fig**. **1**):

**- Apoptosis**

The dosage of cisplatin determines whether cells die from necrosis or apoptosis [35]. In cell culture studies, it is shown that the use of high concentrations of cisplatin causes necrotic cells, on the contrary, apoptosis is caused by low concentrations. However, in vivo, cisplatin appears to induce both necrosis and apoptosis [36]. There are many pathways involved in apoptosis, but the intrinsic mitochondrial pathway is identified as the primary one responsible for cisplatin-induced nephrotoxicity. Cellular stress in the intrinsic pathway results in the activation of the pro-apoptotic B-cell lymphoma 2 (Bcl-2) family proteins, Bax and Bak, which form porous defects in the outer membrane of mitochondria, resulting in the release of apoptotic factors from the organelles [34, 37].

**- Oxidative stress**

Typical mechanisms of cisplatin-induced AKI are the generation of ROS, accumulation of lipid peroxidation products and suppressed antioxidant systems in the kidneys [38]. Inside the cell, cisplatin is converted into a reactively elevated form that reacts quickly with antioxidant molecules increasing oxidative stress. Or, cisplatin can compromise the respiratory chain with increased ROS production and cause mitochondrial dysfunction [39].

**- Inflammation**

Cisplatin, due to its pro-inflammatory nature, induces phosphorylation and subsequent translocation of nuclear transcription factor-kappa B (NF-$\kappa$B) in the nucleus through the degradation of its protein inhibitor I$\kappa$Bα. Within the nucleus, NF-$\kappa$B activates the transcription of inflammatory mediators including tumour necrosis

factor alpha (TNF-alpha) which in turn, induces the expression of other inflammatory cytokines and the recruitment of inflammatory cells in the kidney [24].

**- Vascular injury in the kidney**.

An additional component that characterizes the pathophysiology of cisplatin induced by AKI is renal vasoconstriction caused by endothelial dysfunction [40]. Cisplatin induces acute ischemic damage with a reduction in the medullary blood flow resulting in tubular cell injury. These renal hemodynamic changes may be associated with increased cytosolic calcium in glomerular arterioles [41].

Although many experimental therapies have been developed for the prevention and treatment of cisplatin-induced AKI, current clinical practice only includes supportive measures such as hydration, replacement of electrolyte losses and avoidance of other potentially nephrotoxic drugs, while waiting for renal function to recover [24].

Cisplatin has been used for decades in animal experiments to induce AKI, and it represents a commonly used model to study the therapeutic effects of mesenchymal stromal cell (MSC) [42].

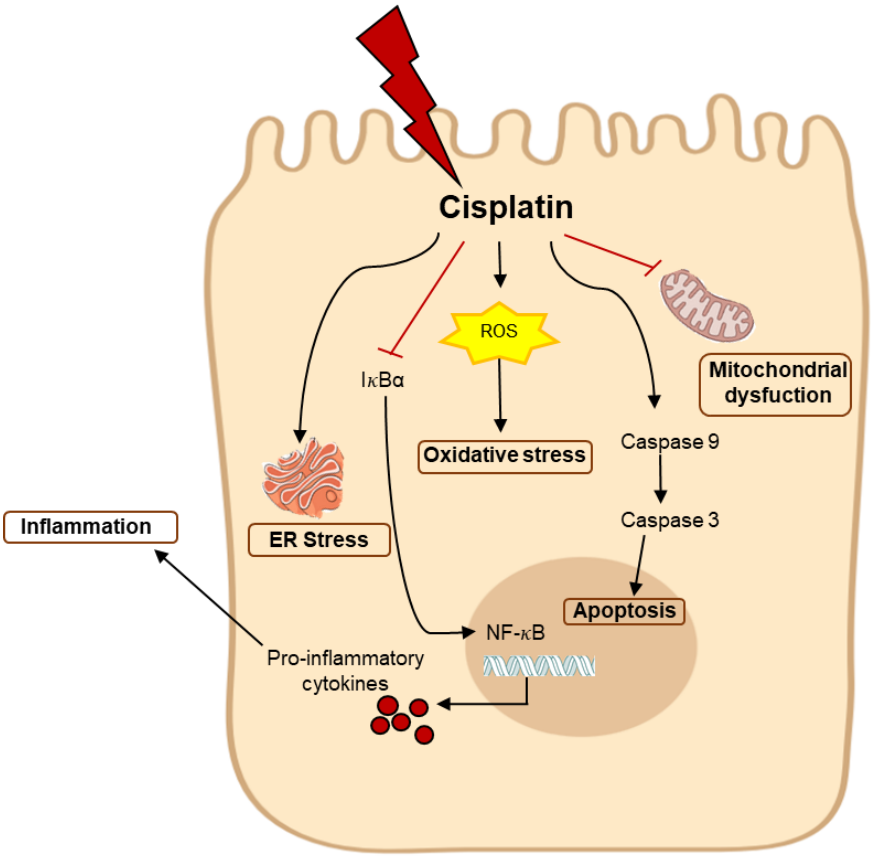


**Figure 1.** Pathway activated by the presence of cisplatin in renal epithelial cells.

### 1.1.3 Current therapy

End-stage kidney disease (ESRD) treatments currently only include dialysis and kidney transplantation [43]. The latter option is made even more difficult by the shortage of kidneys available for donation and an increase in the prevalence of people in need of a transplant [44]. The average waiting period for a kidney transplant varies between 3 and 7 years [45], while the age of people on dialysis is increasing [46]. Nevertheless, kidney transplantation seems to be the treatment with a better quality of life and increasing life expectancy compared with the dialysis treatment [47]. But at the same time, complications may occur after kidney transplantation such as the development of interstitial fibrosis and tubular atrophy, which may evolve into progressive kidney dysfunction also associated with vascular occlusion and glomerulosclerosis [48].

The limited effects of current therapy for KD underline the need for the development of novel therapeutic agents. At the moment, the protective effects of possible therapies such as the use of anti-inflammatory drugs, small interfering RNAs, remote ischemic preconditioning and MSC are being evaluated. MSC-based therapy appears to be an innovative approach to intervention with enormous potential for KD management, but the complexity of the mechanisms involved does not yet allow MSC to be used for large-scale clinical treatment [4, 49].

## 1.2 The Renaltoolbox Consortium

Chronic kidney disease is a serious disease that affects 850 million people worldwide. Only dialysis or kidney transplantation is available to replace kidney function, but alternative therapies such as cell-based regenerative medicine therapies (RMTs) are being considered. However, progress is currently limited because, for many RMTs, a lot of work is still needed to assess safety and efficacy and make safe therapy available to patients.

MSC are one of the mainly studied cell types for cellular-based therapies, thanks to their heterogeneous modes of action they are commonly studied in various diseases.

Currently, the therapeutic use of stem cells poses some challenges because the underlying mechanism of action of transplanted cells is largely unknown. In addition, the results of MSC therapy can be influenced by several variables, such as the experimental setting (MSC dose, treatment time, animal model) and the intrinsic

factors of transplanted cells plus the unpredictable crosstalk with various factors and cell types within the body upon transplantation, that may prime and alter the MSC functions.

For these reasons, a better understanding of the properties and behaviour of these stromal cells and their mechanism of action can contribute to the development of targeted therapies.

In line with this, cell-based therapeutics present intrinsically distinctive difficulties for development and application of potency assays.

Potency is defined in the International Conference on Harmonisation of Technical Requirements for Registration of Pharmaceuticals for Human Use Q6B guidelines as "the measure of the biological activity using a suitably quantitative biological assay (also called potency assay or bioassay), based on the attribute of the product which is linked to the relevant biological properties". (Guidance for Industry Potency Tests for Cellular and Gene Therapy Products. U.S. Department of Health and Human Services Food and Drug Administration Center for Biologics Evaluation and Research; 2011).

We expect rapid progress in the development of combinatorial potency tests based on increased knowledge of MSC biology and their mecahnisms of action, hopefully allowing for the formulation of tests that facilitate and speed up the transition from preclinical studies to clinical trials safer.

To address these challenges, a network of 15 academic, industry and charitable organisations was established, called RenalToolBox (RTB). The RenalToolBox network encomprised 15 early-stage researchers (ESRs) that worked in three interdisciplinary teams to address the following scientific objectives (**Fig. 2 and 3**):

1. **Develop novel tools for diagnosing kidney disease and assessing renal function** (Work Package 1).

   The main goal was to develop novel electronic devices, mathematical tools, molecular biomarkers and near-infrared tracers to diagnose and stage kidney disease, and to monitor disease progression and regression.

2. **Develop and apply cutting-edge imaging technologies to evaluate the safety and efficacy of MSC-based RMTs in a rodent model of kidney disease** (Work Package 2).

   By leveraging complementary imaging technologies for whole animals and image probes, the aim was to monitor the biological distribution of MSC and

study its safety with final tissue analysis. For the evaluation of efficacy, new in vivo imaging strategies and analysis tools were applied to monitor renal function and morphology longitudinally in the animals themselves. In particular, the 'clearing' technology, that makes the organs transparent, allowed for validation of the results in vivo of bio-distribution and accurately quantifiedthe extent of morphological damage.

3. **Establish the optimal source of MSC, develop a matrix of potency assays and explore therapeutic mechanisms** (Work Package 3).

   The aim was to compare the properties and therapeutic potential of adipose mesenchymal stromal cell (A-MSC), bone marrow mesenchymal stromal cells (BM-MSC) and umbilical cord mesenchymal stromal cell (UC-MSC) to develop a matrix of potency assays and to understand repair mechanisms. Moreover, it was decided to investigate secreted factors, microRNAs, immunomodulatory mechanisms and the role of mitochondrial transfer to underlie the mechanisms of action.

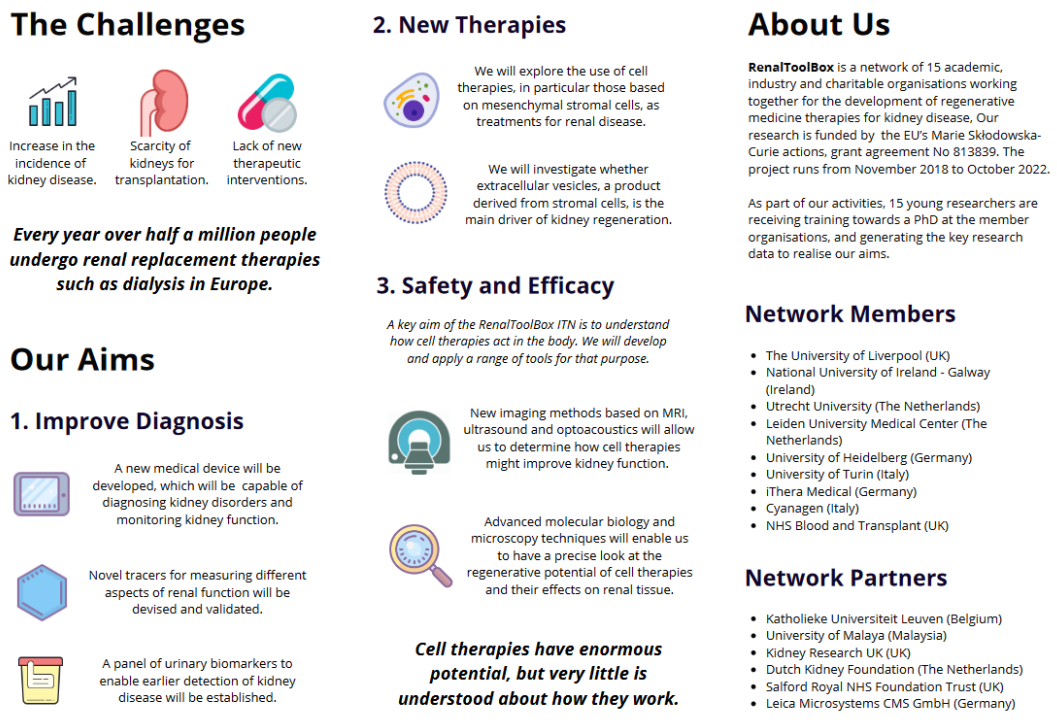


**Figure 2**. The RenalToolBox brochure that sums up the key points of the RTB network and specific research aims (taken from [50]).

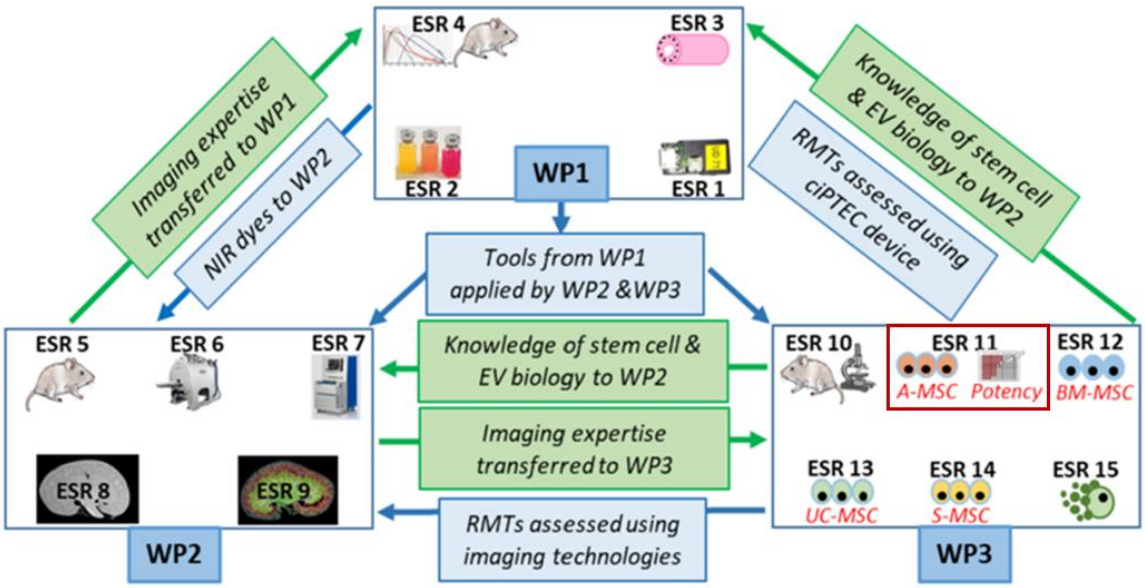


**Figure 3.** Overview of the research programme. The red box indicates my position in the programme. (The image was taken from the proposal application n°813839).

## 1.3 Mesenchymal Stromal Cell

Mesenchymal Stromal Cell (MSC) are non-hematopoietic, multipotent stromal/stem cells, that are present in almost all tissues and organs, including the bone marrow, periosteum, adipose tissue, pulp, synovium, umbilical cord, placenta and amniotic fluid [51, 52]. They were first identified in bone marrow by Friedenstein in the late 1960s and described as fibroblast-like cells, adherent to plastic, forming clones, with the ability to self-renew in vitro and differentiate into osteoblasts, chondrocytes and adipocytes [53]. Heterogeneity and discordances in terminology and criteria for stromal/stem cell, however, spread with increased research in the field. Therefore, the International Society for Cellular Therapy (ISCT) suggested the term “multipotent mesenchymal stromal cells” as consensus nomenclature [54].

### 1.3.1 Biological characteristics of MSC

The ISCT suggested minimal criteria to define MSC: (**1**) MSC must adhere to plastic under standard culture conditions; (**2**) more than 95% of the cells must express specific cell surface markers, notably CD73, CD90 and CD105, while lacking the expression of hematopoietic stem cell markers and autologous transplant rejection antigens such as CD45, CD34, CD14, CD11b, CD79α, CD19 and human leukocyte antigen (HLA)-DR; (**3**) in vitro, these cells must have the capacity to be induced to differentiate into adipocytes, osteoblasts and chondrocytes [55].

MSC demonstrate to have multi-lineage differentiation potential; in vitro, they can differentiate into the mesoderm lineage (bone, cartilage, fat, and connective tissues). Initially there have been some reports that these cells may even trans-differentiate into ectodermal (nerve and epithelial tissues) and endodermal cells (muscle and liver cells) [56, 57].

As a result of their ability to self-renew and differentiate into different cell lines, MSC perform regenerative functions by replacing dying cells in various tissues and for this reason, have become the favourite seed cells for tissue engineering, eventually even for kidney tissue engineering. Some studies demonstrate a successful differentiation of MSC into kidney cells. In mice, bone marrow-MSC (BM-MSC) isolated from transgenic mice for green fluorescence protein (GFP) and injected into a C57BL/6j syngeneic model have demonstrated the potential to differentiate into glomerular cells [58].

An important feature of MSC is their low immunogenicity. They show low expression of major histocompatibility complex (MHC) class I molecules but do not express MHC class II and costimulatory molecules, including B7-1 (CD80), B7-2 (CD86) and CD40 [59], unless stimulated. This is considered as an advantage allowing for allogeneic transplantation overcoming the HLA allogeneic barrier. However, many in vitro studies have shown that MSC can induce an immune response from allogeneic lymphocytes [60] . At the same time, in vivo experiments confirm that MSC do not induce an immune response after allogeneic transplantation [61].

### 1.3.2 MSC mechanism of action

#### 1.3.2.1 Immunomodulation

A very important function of MSC is the capacity to modulate immune responses. MSC have the ability to regulate mechanisms of both innate, as well as adaptive immune responses, through the modulation of cellular responses and the secretion of inflammatory mediators. The immunomodulation process takes place in many stages and includes recognition of the inflammatory response and migration of MSC to the site of injury, “licensing” or activation of MSC, if necessary, removal of pathogens and modulation of inflammation [62].

MSC-mediated immunosuppression is induced by pro-inflammatory cytokines present in the inflammatory microenvironment. Exposure of MSC to interferon (IFN)-γ increases the immune suppressive activity by stimulating the production of inhibitors

of inflammation, for example, indoleamine-pyrrole 2,3-dioxygenase (IDO), factor H, prostaglandin E2 (PGE2), transforming growth factor β (TGFβ) and hepatocyte growth factor (HGF). This licensing has been demonstrated in vitro, where the pre-treatment with IFN-γ stimulates MSC to secrete IDO in a dose-dependent manner, which inhibits the proliferation of CD8+ T cells [63]. This activation step has also been shown in vivo in a Graft vs Host Disease (GvHD) model, since recipients of IFN -γ −/− T cells did not respond to MSC treatment and succumbed to GVHD [64].

Interacting with macrophages, MSC promote their polarization from the M1 pro-inflammatory phenotype to M2 anti-inflammatory cells, reduce the production of pro-inflammatory cytokines such as tumor necrosis factor- α (TNF-α), interleukin-1 (IL-1), interleukin-6 (IL-6), interleukin-12p40 (IL-12p40), IFN- γ, and increase the secretion of anti-inflammatory cytokines, including interleukin-10 (IL-10) [65, 66]. Some in vitro observations have been confirmed in in vivo studies, showing the important role of MSC in educating macrophages and promoting tissue repair during injury resolution. For instance, applying MSC to treat renal damage after ischemia mitigated the infiltration of macrophages and increased the proportion of M2 macrophages, combined with an increase in IL-1/6 production and secretion of IL-10 at ischemic sites [67].

In the setting of kidney transplantation, there are several underlying mechanisms critically involved in MSC-induced graft protection. MSC injection reduced IFNγ and IL-6 levels in serum while increasing IL-10 as anti-inflammatory cytokine, suggesting that MSC reset the balance between T helper 1 and 2 cells. Furthermore, MSC infusion induces regulatory T cells (Treg), which significantly prolongs graft survival by Treg-dependent mechanisms and suppresses the receptor tyrosine kinase in monocyte/macrophage cells, preventing monocyte infiltration and acute rejection [68]. In general, these data suggest that MSC prevent kidney graft rejection due to a shift of T cells toward an immune suppressive phenotype.

#### 1.3.2.2 Homing and Hemocompatibility

One of the key benefits of MSC-based therapies is their ability to preferentially migrate to damaged tissues exhibiting inflammation [69]. Here, the transplanted MSC are considered to act as a ‘‘drug store’’ to support recovery or tissue regeneration [70] rather than by engrafting, integrating and differentiating per se within the tissue.

If transplanted locally at the target tissue, MSC can be directed to the site of injury via a chemokine gradient. Upon intravenous infusion, MSC can escape the bloodstream

via a multi-step process, exit the circulation and migrate to the injury site. The initial *tethering* phase is mediated by selectins expressed by endothelial cells and CD44 expressed by MSC. The interaction between these two factors makes it easier for MSC to start rolling along the vascular wall. The second phase, *activation*, is facilitated by protein-coupled chemokine G receptors, generally in response to inflammatory signals. Next, the integrins responsible for the *arrest* phase intervene and then the phase of *transmigration or diapedesis* begins, where MSC cross the endothelial cell layer and the basal membrane. To do this, MSC secrete matrix metalloproteinases (MMPs) to break down the endothelial basal membrane. Finally, MSC, attracted by chemotactic signals released during damage, migrate through the interstitium to the site of injury [71].

One of the biggest challenges facing in A-MSC therapies is improving their homing efficiency. In diverse kidney disease models such as AKI, I/R [72] and cisplatin-induced AKI [73], no significant evidence of cell migration to the kidney was found despite the therapeutic effect observed. The percentage of intravenously administered MSC that reach the target tissue was low, most of them tended to accumulate in the lung, spleen or liver (filter organs) [74], risking getting trapped as microemboli [75]. However, it has also been suggested that the MSC that home to certain organs such as the spleen may reduce inflammatory infiltrating cells. In contrast, a local transplantation to injured sites delivers a larger amount of MSC to the kidney that enhances endogenous renal stem cell proliferation but may promote capillary obstruction [18, 76].

In recent years there has been concern regarding thrombotic events in response to intravascular MSC therapy. Thromboembolic events can occur for several reasons, the relative large MSC that can be entrapped and occlude small vessels [77]. Or the expression of procoagulant molecules such as tissue factor (TF) can trigger the clotting cascade [78]. Thus, several studies recommend selecting for TF-negative MSC and to incorporate suitable anticoagulation strategies into clinical protocols, to mitigate any risk of thrombotic events [78].

In addition, in a previous study carried out by my research group, it is shown that MSC do not induce platelet activation and thereby thrombus formation, but through the activity of CD73 to generate antithrombotic adenosine to inhibit the overactivation of platelets [79].

#### 1.3.2.3 MSC therapy in the treatment of kidney disease

Pre-clinically, MSC therapy has been shown to positively affect kidney function and survival of the graft [80, 81]. Since the first successful clinical application of MSC in 2004 [82], research on therapeutic applications of MSC has expanded to currently record more than 500 clinical trials [83]. Among them, nine clinical trials use MSC as cell therapy in kidney transplantation.

The benefits of allogeneic MSC in cisplatin-induced AKI treatment are documented in several studies, where different cell sources, administration routes and approaches are tested to better understand the mechanisms of action involved [84-86]. In animal models of cisplatin-induced AKI, MSC therapy has shown encouraging therapeutic effects, mainly involving reno-protective trophic effects (**Fig. 4**). Is largely demonstrated that the anti-apoptotic mechanism is one of the main effects mediated by MSC, even though further analyses are necessary to clarify how this is accomplished.

In xenogenic studies, good results in terms of survival rate, kidney function and morphology were achieved through the application of different types of MSC. For example, the therapeutic effect of A-MSC was demonstrated for the first time in a cisplatin-induced AKI model in 2012 by *Kim et al*. where cells and their paracrine factors were tested, resulting in a reduction of renal tissue damage and an increase in survival rate [73]. Infusion of A-MSC has resulted in a vast therapeutic effect, including reductions in apoptotic cell death and the release of paracrine factors that exert an anti-inflammatory action by suppressing the release of TNF-α and IL-1 from renal tubular cells.

Other studies have proposed that A-MSC cells, when transplanted together with hematopoietic stem cells, show greater efficiency than when transplanted alone [87]. Or, pre-transplant A-MSC combined with hematopoietic stem cells, minimized the overall application of immune suppressants in kidney transplantation [88, 89].

Phase I of a pilot study started in 2011 [90] aiming to test the safety and efficacy of ex-vivo MSC to repair the kidney and improve renal function in patients with solid organ cancer who develop AKI after treatment with cisplatin. In this study, the patients were treated with a single systemic infusion of allogeneic BM-MSC with a 1-month follow-up.

Although many clinical trials have demonstrated promising outcomes of MSC-based therapy, the best source of MSC, the optimal timing, dosage, route and frequency of

administration, as well as long-term post-transplantation safety remain unclear. Nevertheless, it is expected that MSC will contribute substantially to the success of human kidney transplantation, while large-scale, multi-centre clinical trials are needed to further validate their clinical effects [91].

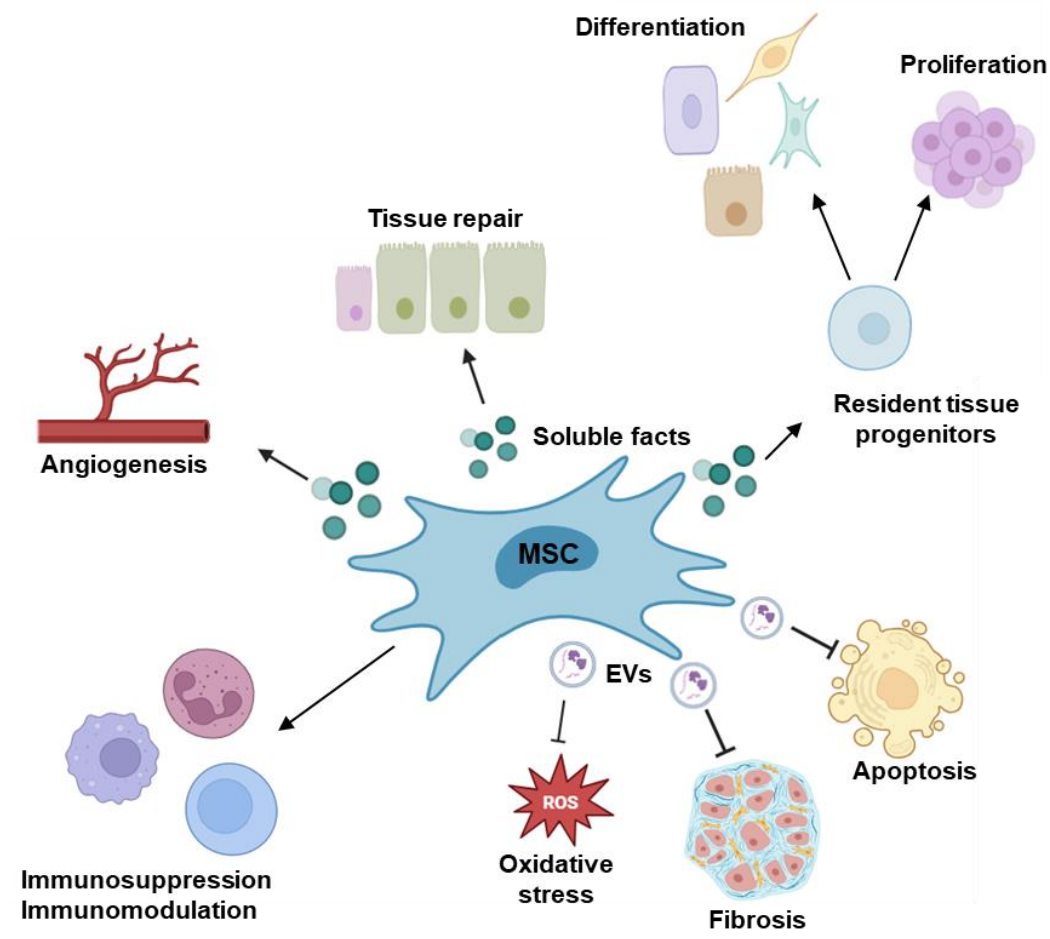


**Figure 4.** Schematic representation of MSC mechanism of action in kidney disease. This image was created using BioRender.

### 1.3.2.4 Paracrine effects

Until the early 20th century the use of MSC in regenerative medicine seemed the right choice given their ability to home at injury sites and to differentiate into different cell types, contributing to tissue repair. This theory was revised however when *Gnecchi and colleagues* revealed that MSC mediated their therapeutic effects by release/secretion of trophic molecules, now known as secretome. In 2005, it was described for the first time that the MSC-conditioned culture medium (MSC-CM) was capable of reproducing cardio-protective effects of MSC transplantation in myocardial

infarction [92], indicating that therapeutic efficacy can be mediated by the secreted factors alone, being able to activate the repair and regeneration of the damaged tissue.

Consequently, several clinical studies have infused MSC secretome in its entirety or individual paracrine factors to elicit a positive benefit in a wide range of therapeutic and immunomodulatory applications, including the treatment of skin wounds, distraction osteogenesis, and kidney injury [93, 94]. Confirmation comes from in vivo studies where both MSC and their conditioned medium (CM) were able to enhance kidney function [95]. In addition, the therapeutic power of CM has been associated with drug-induced cytotoxicity, MSC-CM inhibited epithelial-mesenchymal transition and improved renal fibrosis in kidney epithelial cells under cisplatin treatment [96].

MSC's secretome is described as a complex mixture of soluble products composed of protein-soluble fractions such as enzymes, cytokines and growth factors and a vesicular fraction including extracellular vesicles (EVs), microvesicles (MVs) or exosomes which are involved in the transfer of proteins and genetic material (e.g., microRNAs) to other cells, with promising therapeutic effects [97].

Several studies have shown that MSC support renal recovery through the release of growth factors such as vascular endothelial growth factor (VEGF), insulin-like growth factor 1 (IGF-1) and Hepatocyte Growth Factor (HGF). VEGF is also involved in angiogenesis, immunomodulation and cell survival. instead TGF-β is known to potentiate immunomodulation, cell growth, proliferation and differentiation, and wound healing. And HGF has been reported to be involved in immunomodulation, cell migration, development, and apoptosis [98, 99].

Data presented by *Villegas and co-workers* demonstrated that VEGF can act directly on renal epithelial cells via the vascular endothelial growth factor receptor 2 (VEGFR-2) receptor stimulating proliferation and promoting survival [100].

Cell-free therapy is now more and more discussed as alternative to cell-based therapies due to its advantages:

(**1**) Paracrine factors can be bioengineered and scaled to specific dosages.

(**2**) The nature of the secretome allows it to be stored and transported efficiently [101].

(**3**) The use of MSC secretome is more economical and practical for clinical applications, as it avoids invasive cell collection procedures.

(**4**) The administration of bioactive factors as a therapeutic product represents a safer alternative, without the risks of tumour development or emboli formation, entrapment in lung microvasculature, and less immunogenicity [102].

(**5**) The secretome or its components are beginning to be considered a potential active pharmaceutical component, where its vesicular component has revealed promising features e.g. for use as a drug delivery system.

The EVs can be designed to increase the levels of active molecules (proteins or RNA) already present in the EVs, or through transfection of the stem cells change their cargo. Furthermore, biodistribution/stability can be altered by changing the composition of surface molecules [103].

However, the main concern raised by various authors remains the absence of a standard protocol for MSC isolation/expansion, secretome production, collection, and bioprocessing [104].

## 1.4 Extracellular Vesicle

The term extracellular vesicle (EV) is commonly used in the scientific community to identify a heterogeneous population of vesicles delimited by a lipid bilayer. Typically, they are classified according to their origin and size [105].

EVs, especially exosomes, carry a wide range of bioactive factors such as proteins and lipids, as well as transcription factors, messenger RNA (mRNA), microRNA (miRNA), long non-coding RNA (lncRNA), DNA, and signal transduction molecules [106, 107]. The region of origin of EVs determines their phenotype, but mainly their function. Although MSC from different tissues, such as adipose tissue, human umbilical cord and bone marrow, share common therapeutic effects, the efficiency and regulatory pathways triggered by EVs can vary among the MSC subtypes. Indeed, MSC from tissues of different origins are not used identically for some diseases and target organs. Preclinical studies of MSC-EV typically select a source tissue that is closely associated with the organ where the disease is occurring or affected. The identification of miRNAs and protein markers based on unique expressions in the respective source tissue, has allowed to identify pathways where EVs are most involved. For example, BM-MSC-EVs have been shown to play an important anti-apoptosis and astrocyte differentiation role. A-MSC-EVs showed strong effects on phagocytosis, cell motility and osteoblast differentiation. Finally, UC-

MSC-EVs are reported to be involved in angiogenesis, improvement of spinal cord injury and regulation of various signalling pathways, such as IL-17 and TGF-beta signalling [108].

Exosomes and macrovesicles are part of the EV category and are often mixed up in literature, therefore the International Society of Extracellular Vesicles (ISEV) unified the nomenclatures and the methodologies for the isolation and characterization of EVs [105]. The "minimal information for studies of extracellular vesicles (MISEV)" provide a list of requirements for extracellular vesicles to be classified as vesicles. The main ones are (**1**) to quantify the number of cells secreting EV, (**2**) to determine the number of EV particles, (**3**) to define the presence of constituents associated with EV and (**4**) to define the existence of co-isolated components (**Fig. 5**). The correct characterization of EV is crucial to associate functions uniquely to EV rather than their co-isolated particles [109].

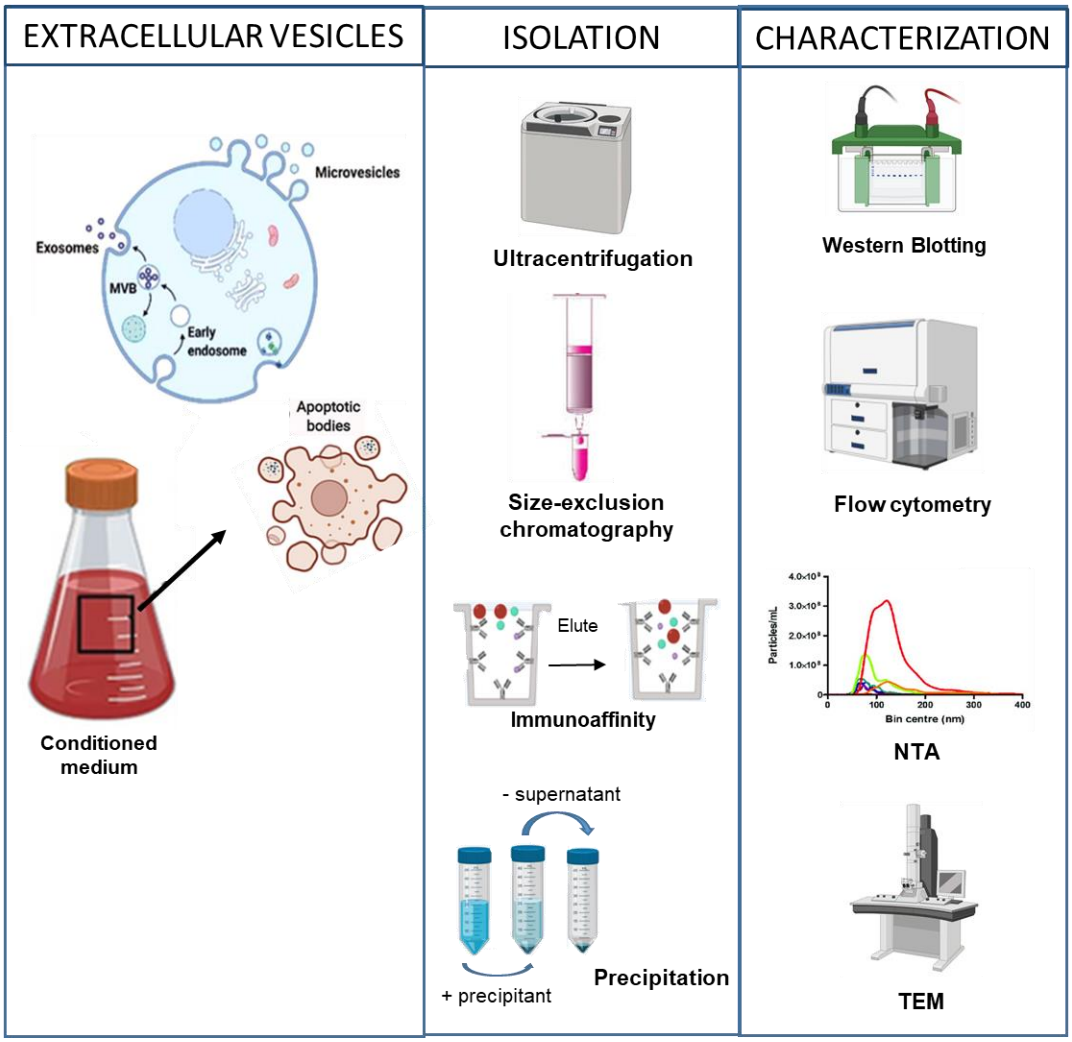


**Figure 5. Overview of commonly used EV isolation and characterization methods.** Some EV isolation methods are shown in the graph, ultracentrifugation and size exclusion chromatography are

the techniques used to isolate EV. The characterisation methods described are those we use in our work. NTA= indicates Nanoparticle Tracking Analysis; TEM= transmission electron microscopy. This image was created using BioRender.

Exosomes are the most characterized and widely studied EVs [110]. They are distinguished from macrovesicles by their size range (50-150 nm) and biogenesis. They are generated from the inward budding of late endocytic compartments, called multivesicular bodies (MVBs) and subsequently secreted to the extracellular environment as membranous vesicles upon fusion with the membrane plasma. Also, exosomes are characterized by the presence of evolutionarily conserved proteins, like tetraspanins (CD9, CD63 and CD81), heat shock proteins (HSP60, 70 and 90), MHC I and II classes, Alix and Tsg101.

Macrovesicles are in the range of 100-1000 nm and are formed through the direct budding of the plasma membrane. Their release is independent of MVB and does not require exocytosis. Finally, apoptotic bodies are large-size vesicles from 1 mm up to 5 mm and are shed by blebbing off the plasma membrane of apoptotic cells (**Fig. 6**) [103].

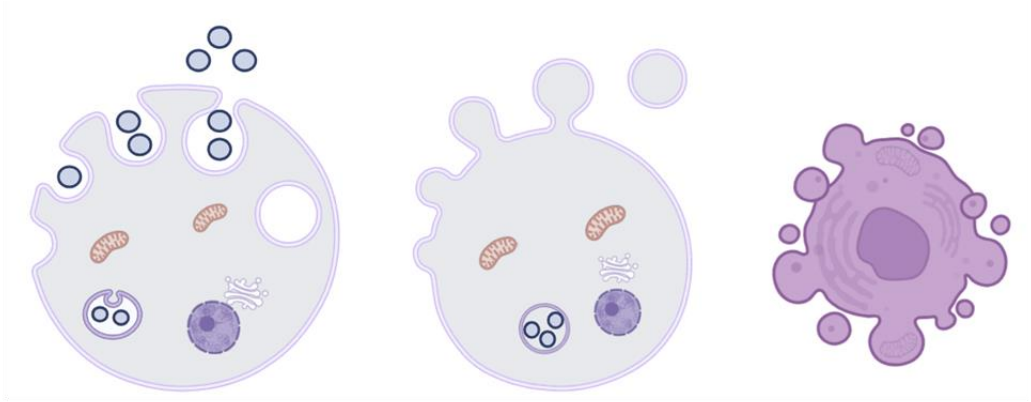

| | Exosome | Microvesicle | Apoptotic Bodies |
|---|---|---|---|
| **Size** | 50-150 nm | 100-1000 nm | 1-5 mm |
| **Protein marker** | CD81, CD63, CD9, Alix, Tsg101 | Selectins, integrin, CD40, | Caspase3, histones |
| **Composition** | Protein, lipids, coding RNA, non coding RNA, DNA | Protein, lipids, coding RNA, non coding RNA, DNA | |
| **Origin** | Multivesicular body | Plasma membrane | Plasma membrane |

**Figure 6.** Classification of Exosomes, microvesicles and apoptotic bodies according to ISEV criteria . This image was created using BioRender.

EVs have been shown to have key roles in cell-cell communication in health and disease.

EVs transmit information to the receptor cells through different mechanisms. One of these mechanisms is endocytosis, where the EV fuses with the membrane of the organelles and discharges their content in the cytoplasm. They may also merge with the membrane of the recipient cell to release their charge intracellularly, directly or through specific receptors. Finally, the membrane surfaces of EVs can trigger signalling cascades through receptor/ligand interactions without internalization [111].
EVs can provide various factors, which can regulate a range of biological functions, including cell proliferation, anti-apoptosis, anti-fibrosis, anti-inflammation, and angiogenesis [112]. For example, EVs isolated from MSC have demonstrated a therapeutic effect on kidney disease through immunomodulation and regeneration [113].

### 1.4.1 MSC-EVs in kidney disease

Like for other organs, several pre-clinical studies demonstrate that stromal/stem cell-derived EVs promote tissue repair and reduce inflammation in kidney disease [114]. In 2009*, Bruno et al*. proved that EVs isolated from human bone marrow MSC support epithelial cell survival in acute renal failure, stimulating their proliferation and preventing apoptosis [115]. In an animal model of renal I/R injury, EVs show to decrease epithelial tubular cell damage, increase cell proliferation and kidney function [116, 117]. Some data suggested that EVs have the ability to induce neovascularization in the kidney. It has been noted that the infusion of EV improves capillary renal density and reduces renal fibrosis in a rat model of an AKI [118]. Moreover, MSC-EV also have a beneficial effect in the treatment of toxic nephropathy induced by cisplatin and gentamycin by inhibiting mitochondrial apoptosis in epithelial tubular cells and cell proliferation induction [119] or ameliorated renal function and reducing the histological lesion of the disease [115].
It is well known that EV activity mainly involves the horizontal transfer of biologically active molecules and genetic information such as mitochondria, proteins, lipids, microRNAs (miRs), messenger RNAs (mRNAs) and transfer RNAs (tRNAs), influencing the function of the target cells [103, 120].
Among the various molecules present in the EV cargo, miRNAs have been considered critical elements in renal cell reprogramming. Their role has been highlighted with Drosha knockdown in stem cells that abolished the protective effect of EVs [121].

EVs also contain a protein component, *Kim et al*. reported the proteomic analysis of human bone marrow MSC-EVs by the Database for Annotation, Visualization and Integrated Discovery (DAVID) software and indicated that MSC-EVs contain 730 proteins, and these proteins are mainly involved in cell cycle, proliferation, migration, adhesion (for instance fibronectin, ezrin, Ras GTPase-activating-like protein IQGAP1, and integrin), signalling molecules (for instance mitogen-activated protein kinase (MAPK)1 and CDC42) and morphogenesis [122].

Translation of EV-based therapy into clinical practice requires clarification of several critical issues. Identifying optimal protocols for EV is the primary consideration for production, isolation and storage [123]. Nevertheless, prof-of-principle studies have been performed already in patients with chronic kidney disease (CKD) [103]. One trial was designed by *Nassar et al*. to assess the safety and therapeutic efficacy of umbilical cord MSC-EVs in ameliorating the progress of chronic kidney disease. In 20 patients with CKD an improvement of renal function was observed with amelioration of glomerular filtration and reduced blood urea and serum creatinine, one year after EV administration (2 doses). Moreover, patients showed a reduction in TNF-α levels and an increase TGF-β1 and IL-10 in plasma [124].

Through the use of more advanced techniques in production and isolation, large-scale production of EV has been established. EVs can be easily stored for long periods and transported as cryovials or even lyophilized. The possibility of EV bioengineering allows the design of treatments customized according to the pathophysiological aspects of the patient's kidney. Moreover, unlike drug delivery systems, such as liposomes and polymer micelles, the use of EVs has advantages in structural stability, non-toxicity, and low immunogenicity which are related issues with synthetic nanoparticles [125].

Although these cell-free therapies might promise to treat kidney lesions, clinical use still has challenges. The heterogeneity of MSC secretions obtained from different tissues could strongly influence the therapeutic potential. In addition, some preconditioning stimuli can affect the quality and quantity of trophic factors in the MSC-EV. Other important challenges are their safety, the analysis of MSC cell sources, the standardization of EV production and the development of methods to control the quality and safety of therapeutic EVs [103, 112, 126]. To identify the 'active substance/component' responsible for the biological activity of novel EV therapeutics, it is necessary to have a better understanding of their specific mechanisms.

## 1.5 microRNAs

One part of the various mechanisms by which MSC and EVs are considered to mediate their therapeutic effects is via the transfer of microRNAs. RNA transcripts include messenger RNA and non-coding RNA. The latter is divided into two main categories: small non-coding RNA (<200 nucleotides) and long non-coding RNA (lncRNA, >200 nucleotides). Some small non-coding RNAs, housekeeping RNAs, such as ribosomal RNA (rRNA) and transfer RNA (tRNA), are essential for cell physiology [127]. Another group of small RNAs, present in all eukaryotic organisms, negatively controls the expression of unwanted genetic material. Based on their length (20-30 nucleotides) and association with proteins of the Argonaut family (AGO), small RNAs have been classified into three classes: miRNA, small interfering RNA (siRNA), and piwi-interacting RNA (piRNA) [128]. MiRNA and siRNA are similar in both biochemical and functional terms: both are 19-20 nucleotides (nt) long; they have a 5'-phosphate and a 3'-hydroxyl end and are part of the RNA-induced suppression complex (RISC) that inhibits the expression of a specific gene. These molecules are distinguished by their original region: the miRNAs derive from a 60-70 nt long double-stranded region and siRNAs from long double-stranded RNA. They are also distinguished by their mechanism of action on target messengers: siRNA has a perfect base-pair that induces target cutting and degradation, while miRNA has imperfect base-pairing, with one or more mismatches in sequence complementarity; thus it blocks the translation of their respective target [129].

The latest release of the miRbase database (v22) contains 2654 human mature miRNAs sequences, which confirms their importance in gene expression regulation.

In the majority of organisms, miRNA is less abundant than mRNA and protein, because a single miRNA can regulate hundreds of messengers and, vice versa, a single mRNA can be regulated by several different miRNAs [130]. About 60% of human genes are cooperatively regulated by multiple miRNAs [131]. miRNAs were originally considered the "waste DNA" product, however, we know now that they are involved in the regulation of about 30% of all mammalian protein-coding genes and that they have different roles in the cell cycle, apoptosis, tissue development, division of stem cells and development of degenerative diseases [132, 133].

### 1.5.1 miRNA`s biogenesis

The biogenesis of miRNA is mediated by multiple steps: transcription of primary miRNA transcripts, nuclear processing by Drosha, nucleocytoplasmic export, cytoplasmic processing by Dicer, and formation of RNA-induced silencing complex (RISC) with Argonaute (Ago) proteins [134].

MiRNAs are generally synthesized as long primary transcripts, called pri-miRNA, from RNA polymerase II or III (**Fig. 7**). miRNAs are encoded as individual miRNA genes (monocistronic), as miRNA clusters (polycistronic), or in introns of protein-coding genes (intronic) [135]. Pri-miRNA (primary miRNA) are polyadenylated at the 3' and bind a 7-methylguatin at the 5'. Also, they maintain an internal hairpin-loop structure that will be recognized and processed within the nucleus by a tandem of interacting proteins: the RNA-binding protein DiGeorge syndrome critical region 8 (DGCR8) and nuclear enzyme RNase III Drosha. DGCR8 protein binds double-stranded RNA (dsRNA) recognizing the apical region of the hairpin and simultaneously stabilizes the Drosha binding that will process the dsRNA segment [136].

Once the pre-miRNA (precursor miRNA) is produced, it is exported from the nucleus via exportin-5, (XPO5)/RanGTP complex. Once in the cytoplasm, pre-miRNA is released from exportin-5 after GTP hydrolysis [137].

In the cytoplasm, pre-miRNA hairpin is processed by the Dicer ribonuclease, a type III endonuclease consisting of 2 double strand binding domains and two catalytic RNAse III domains, including Paz domain responsible for the first binding with pre-miRNA.

Paz recognizes the 3'OH at the free end of the pre-miRNA and this allows Dicer to bind with its double-strand binding domain. The two RNase III domains (the ones that will cut) are positioned at such a distance from the double strand and the Paz domain that produce 20-22 nt fragments with staggered ends of 2 nucleotides.

After cleavage, only one filament of the dsRNA is incorporated into the RISC complex. The selection of one or the other filament is based on the thermodynamic properties of the dsRNA: the less stable filament at 5' is the one that is usually loaded into AGO, and is deemed the guide strand. The unloaded strand is called the passenger strand, is cleaved by AGO2 and degraded by cellular machinery [138].

The post-transcriptional silencing of the target mRNA is due to the components of the RISC complex activated by the miRNA/mRNA pairing. The key protein components

of this complex are members of the Argonaut family consisting of a domain PAZ (Piwi Argonaute Zwille), involved in the link with miRNA, and a domain PIWI, involved in cutting. In humans, Ago2 is the only Argonaut protein capable of endonucleolytic cleavage [139]. Argonaute associated with miRNA binds to the 3′-untranslated region (3′-UTR) of mRNA and prevents the production of proteins in different ways. The recruitment of Argonaute proteins to targeted mRNA can induce deadenylation of the polyadenylated 3′-end and induce mRNA degradation. The Argonaute–miRNA complex can also affect the formation of functional ribosomes at the 5′-end of the mRNA by competing with translation initiation factors and/or abrogating ribosome assembly (translation initiation). In addition, the Argonaute–miRNA complex can alter protein production by recruiting cellular factors (peptidases, post-translational modifying enzymes) that will target the degradation of the growing polypeptides (translation elongation) [134, 140].

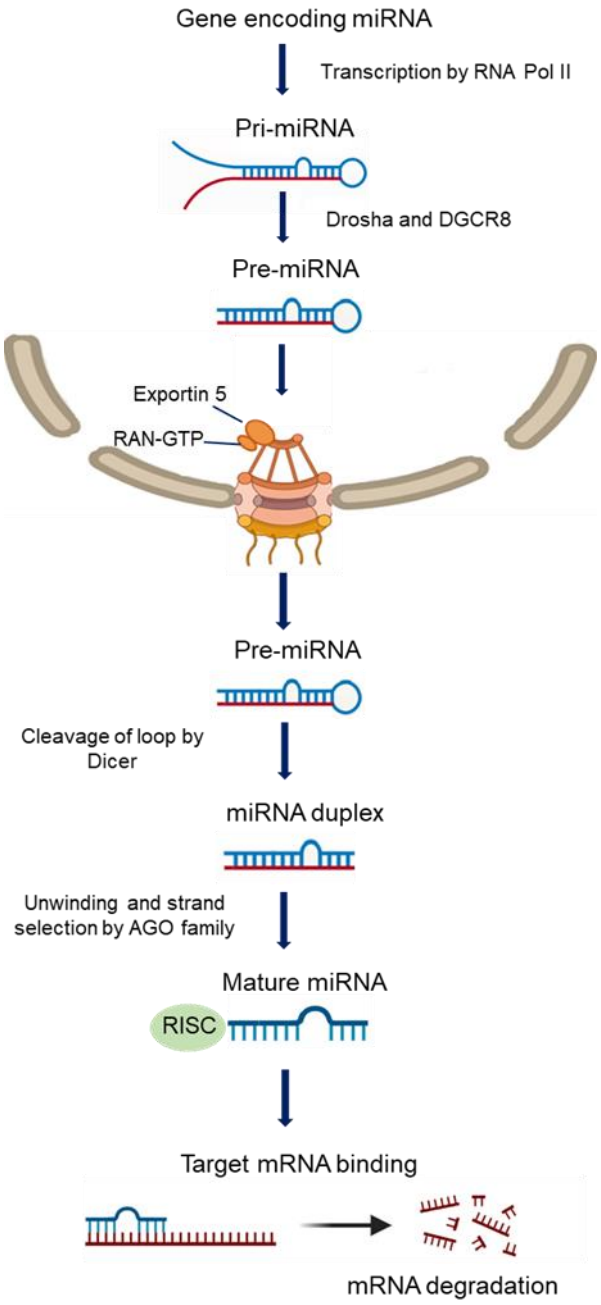


**Figure 7. MiRNA biogenesis.** Overview of microRNA (miRNA) biogenesis. This image was created using BioRender.

### 1.5.2 microRNAs in nephrotoxicity

In mammals, microRNAs are estimated to control the activity of ~50% of all protein-coding genes [141]. Here, microRNAs control different physiological processes such as metabolism, apoptosis, cell proliferation, stem cell division, muscle differentiation and brain morphogenesis. Accordingly, aberrations in their expression are related to a variety of pathologies, ranging from tumours to autoimmune diseases [142].

In recent years, the the involvement of miRNA in kidney disease has been gradually recognized. *Wei et al*. reported for the first time the essential involvement of miRNAs in ischemic AKI by using a proximal tubule-specific Dicer knockout mouse model. In the proximal tubule, microRNAs appear to promote cellular injury because a selective loss of Dicer in animals after three weeks of age confers resistance to ischemia-reperfusion injury [143].

Another study by *Zhu et al*. demonstrated changes in microRNA expression during renal IRI in laboratory rats. Using a gene microarray assay, it has been observed that cisplatin-induced kidney injury caused an upregulation in 36 miRNAs and downregulation in 8 miRNAs. One of these miRNA was mir-146b, which through its inhibition has been shown to play a role in the regulation of apoptosis [144].

In addition to mir-146b, another apoptosis-related miRNA is mir-34a. In addition, this miRNA was found to be a new downstream target of p53 making it important for therapeutic purposes. Its correlation with p53 has been demonstrated in vitro in mouse proximal tubular cells, the treatment with cisplatin upregulates the expression of mir-34a, and an inhibition of p53 abolishes its up-regulation. It has also been shown that if an antisense for mir-34 is used, apoptosis will increase and cell survival will be reduced [145].

Numerous studies have demonstrated that miRNAs can be released into extracellular fluids. Extracellular miRNAs can be used as biomarkers for a variety of diseases. The extracellular miRNAs can be delivered to target cells and they may act as autocrine, paracrine, and/or endocrine regulators to modulate cellular activities. MSC have been verified to be a safe and effective delivery vehicle for therapeutic miRNA treatment, through EVs [112].

An in vitro study reports the protective role of mir-1184 carried by EVs and released in target cells. A bioinformatics analysis was performed on the different expressions of miRNA in human kidney 2 (HK2) cells treated with 20 µM cisplatin for 48 h. Through this analysis, mir-1184 has been identified, which is also expressed in the MSC. With the transfection of the MSC, they produced an EV expressing mir-1184. Treatment of HK2 cells with these EVs showed a reduction of apoptosis through FOX1 and p27 kip1 which induces the G1 phase of the cell cycle [146].

MicroRNAs are highly conserved RNA non-coding between species, making them potential biomarkers in addition to their specific expression in different tissues or

pathological states, relatively simple laboratory methods for their analysis and stability in different body fluids (e.g., blood and urine, commonly used as samples because they can be collected using minimally invasive procedures) [147, 148].

For example, miR-21 in urinary and plasma was strongly associated with severe AKI [149] and miR-494 level in urinary was elevated earlier than serum creatinine level after I/R [150]. Mir-192 [151] or Mir-378a, 1839, 140, 26b, and let-7g [152] have been commonly modified into in vivo models of cisplatin-induced tubular lesions and considered biomarkers for nephrotoxicity [153, 154].

A potential clinical application would be to measure their expression and be able to predict the pathological condition of AKI or to distinguish a patient with AKI from one without.

The therapeutic approach includes two possibilities: the use of therapeutic miRNAs, through the use of a mimic one may be able to restore the expression of miRNA and therefore its biological function. Vice versa one may consider using miRNA inhibitors (anti-miRNA) to reduce the expression of upregulated miRNAs during pathogenesis.

There are already examples for clinical applications, in e.g. wound healing: A Phase 2 clinical trial was recently completed to test the effects of a miR-29 mimic drug (MRG-201; remlarsen) to prevent the formation of a fibrotic scar (hypertrophic scar or keloid) or cutaneous fibrosis [155]. In addition, Phase 1 and 1b clinical trials have been completed to test the effects of a miR-92a antagomir (MRG-110) in wound healing [155] and a miR-21 antagomir (CDR132L) to treat the effects of heart failure [156].

### 1.5.3 MiR-181a's family

A family of miRNA is a group of miRNAs that are derived from a common ancestor. Normally, members of a miRNA family are functionally similar but are not necessarily preserved in the primary sequence of the secondary structure. The miR-181 gene family is an ancient family that originated in the invertebrate urochord species. Phylogenetic analysis of the Mir-181 family in vertebrates has shown that the expansion of this gene family has occurred through gene duplication [157].

The miR -181 family has four members (Mir-181a, Mir-181b, Mir-181c and Mir-181d). Their binding region is complementary to a few hundred mRNAs identified so far, allowing members of the miR-181 family to regulate their target genes either by inhibitory binding to their mRNA or by activating the silencing complex and causing degradation of the target mRNA [158].

The mir-181 family recognizes the coding sequence for the C2H2 domain of zinc finger (ZNF) genes and down-regulates the expression of ZNFs, the regulators of transcription [159]. Thanks to this sequence recognition, the mir-181 family has access to the regulation of numerous cellular pathways. They are important in cellular development and differentiation, evidenced by their aberrant expression in cancers and autoimmunity [160].

A member of the miR-181 family, miR-181a, is described as a mitochondrial miRNA in human kidneys [161, 162]. Overexpression of miR-181a could enhance cell proliferation and as well reduce apoptosis of clear cell renal cell carcinoma via the down-regulation of Krüppel-like factor 6 (KLF6) expression [163]. Furthermore, HK-2 cells treated with cisplatin show a significant increase of miR-181a, which contributed to cell apoptosis and cell death by directly regulating target genes such as Bcl-2 and Bax. Inhibition of miR-181a promotes the expression of Bcl-2 and suppressed Bax, accompanied by the protection of proximal tubular cells from cisplatin injury [164]. Mir-181a also plays a protective role in chronic kidney disease, its over-expression reduces glomerular sclerosis and renal tubular epithelial injury in rats [165].

# 2 AIM OF THE STUDY

Cell-based regenerative medicine therapies based on MSC are opening new perspectives for treatment of numerous diseases. Still, despite the promising results, translation into the clinical scenario has not shown the expected results. Our limited understanding of the underlying mechanisms of cell-based RMTs is a barrier that makes it difficult to ascertain why some RMTs work well in animal models, but not so well in patients.

To understand the mechanisms of action of MSC and to be able to study its effects in the context of renal injury in vitro, we designed our work to answer 3 questions.

**AIM 1**. Is it possible to identify a specific source of MSC that is better suited for therapeutic applications?

**AIM 2**. Is the secretome as efficacious as MSC and if so, which part of the secretome reproduces the therapeutic effect?

**AIM 3**. Do microRNAs play a role in the protective effect of MSC?

**AIM 1. Is it possible to identify a specific source of MSC that is better suited for therapeutic applications?**

In an collaborative approach within the RTB consortium, we compared MSC from three different tissue sources to understand whether one or the other is better suited for therapeutic applications. Here, we pursued the following experiments:

- harmonize culture conditions
- ship the cells to the different centers to perform basic manufacturing and characterization steps, mimicking different decentralized production centres.

We hypothesised that using a common protocol could reduce site-to-site variation whilst maintaining the tissue and donor-specific differences. In the second part of the study, each centre performed individual assessments of the three MSC types. While the lab in Galway focused on the regenerative capacity of MSC, the lab in Liverpool assessed their homing capacity and in our lab we addressed immunomodulatory activities.

**AIM 2. Is the secretome as efficacious as MSC and if so, which part of the secretome reproduces the therapeutic effect?**

As introduced, various studies suggest that the secretome is as potent as the MSC themselves. Thus we asked whether it is the EV-enriched component or rather the secreted/protein-rich fraction which is active. To address this, we first established a AKI in vitro model based on cisplatin injury. Then we compared the EVs obtained using different isolation methodologies and the protein-rich fraction with the entire secretome to identify the component that had the maximum effectiveness in a multi-matrix assay of cisplatin-injury.

**AIM 3. Do microRNAs play a role in the protective effect of MSC?**

The final goal of the project was to validate and explain the molecular mechanisms behind the therapeutic effects of MSC derivatives in an in vitro injury model. We hypothesized that MSC-derived secretome exerts a protective effect, among others, modulating the expression of miRNA in post-transcriptional gene regulation in injured target cells. In particular, we focused on studying the change of microRNAs induced by the presence of the MSC-CM. For this purpose, first we tested the efficiency of MSC-CM in our cisplatin injury model, then we carried out a screening of microRNA identifying a possible microRNA sensitive to the action of MSC-CM. Finally, we tested its role in the protective effect of MSC-CM in an in vitro apoptosis assay.

# 3 MATERIALS AND METHODS

## 3.1 Material

### 3.1.1 Cells

| Cell type | Source / Manufacturer |
|---|---|
| Adipose derived human mesenchymal stromal cells (A-MSC) | Mannheim: Self isolated in laboratory. |
| | Mannheim Ethics Commission II (vote number 2006-192 N-MA); |
| Bone marrow derived human mesenchymal stromal cells (BM-MSC) | Galway |
| | Obtained from Lonza (Basel, Switzerland) |
| Umbilical cord blood-derived human mesenchymal stromal cells (UC-MSC) | Liverpool |
| | Isolated and obtained from NHS Blood and Translant in accordance to Declaration of Helsinki, before being transferred to University of Liverpool. |
| Human peripheral blood mononuclear cells (PBMC) | Previously isolated in laboratory leukapheresis samples. |
| | Provided kindly by the German Red Cross Blood Donor Service in Mannheim, Germany. Leukapheresis samples: Mannheim Ethics Commission II (vote number 2018-594N-MA). |
| Conditionally immortalized proximal tubular epithelial cells | Purchased from Cell4Pharma |
| Human umbilical vascular endothelial cells (HUVEC) | Previously isolated in laboratory<br>Ethical vote: MA-2023-567N-MA |

#### 3.1.1.1 Cell culture products

| Product | Company | Catalog No. |
|---|---|---|
| DMEM | PAN Biotech | P04-01500 |
| RPMI 1640 | Lonza | 12-918F |
| DMEM-F12 | ThermoFisher | 11039047 |

| | | |
|---|---|---|
| α-MEM | Gibco | 2561029 |
| EndoGRO-LS Complete Culture Media Kit | Sigma-Aldrich | SCME001 |
| Mesenchymal Stem Cell Adipogenic Differentiation Medium | Promocell | C-28016 |
| Mesenchymal Stem Cell Osteogenic Differentiation Medium | | C-28013 |
| Supplement mix Adipogenic Differentiation Medium | | C-39816 |
| Supplement mix Osteogenic Differentiation Medium | | C-39813 |
| Opti-MEM | Gibco, Thermo Fisher Scientific | 31985062 |
| Hoechst 33342 | Invitrogen | 917368 |
| Adipored assay reagent | Lonza | PT-7009 |
| OsteoImage™ Mineralization Assay | Lonza | PA-1503 |
| Collagenase NB 6 GMP Grade | Serva Electrophoresis | 17458 |
| Human allogeneic serum pooled from healthy AB donors (AB serum) | German Red Cross Blood Donor Service, Institute Mannheim | |
| Fetal Bovine Serum (FBS serum) | Gibco | 10270-106 (Lot 2Q7096K) |
| Penicillin/Streptomycin | PAN Biotech | P06-07100 |
| L-glutamine | | P04-80100 |
| Trypsin/EDTA | | P10-024100 |
| EDTA | Applichem | A3145,0500 |
| DPBS (1X) | Gibco | 14190-094 |
| HBSS | Sigma-Aldrich | H8264 |
| Dymethylsulphoxide (DMSO) | Wak-chemie Medical GmbH | WAK-DMSO-10 |
| IL-2 human recombinant | PromoCell | C-61240 |
| Phytoemagglutinin-L (PHA) | Merck Millipore | M5030 |

| | | |
|---|---|---|
| Interferron-y human recombinant (IFNγ) | R&D Systems | 285-IF |
| VEGF | Peprotech | 100-20-10UG |
| ZM32381 | ChemCruz | |
| Accutase | Sigma-Aldrich | |
| Insulin-Transferrin-Sodium Selenite Supplement (ITS) | | 11074547001 |
| Epidermal Growth Factor (EGF) human recombinant | | E9644 |
| Hydrocortisone | | H0135 |
| Triiodothyronine (I3) | | T5516 |
| PrestoBlue™ HS | Invitrogen | P50200 |
| Fibronectin | PromoCell | C-43060 |
| Apotracker | Biolegend | 427401 |
| Lipofectamine RNAiMAX | Thermo Fisher Scientific | 13778075 |
| Cisplatin | Teva® | |
| Antimicin A | Sigma-Aldrich | 1397-94-0 |

### 3.1.1.2 Cell culture media

| Media | Composition |
|---|---|
| Mesenchymal Stem Cell growth media (Part 1) | 500 ml α-MEM |
| | 10% FBS |
| | 100 U/ml penicillin and 10mg/ml streptomycin |
| | 4mM L-glutamine |
| Mesenchymal Stem Cell growth media (Part 2 and 3) | 500 ml DMEM |
| | 10%AB serum |
| | 100 U/ml penicillin and 10mg/ml streptomycin |
| | 4mM L-glutamine |
| DMEM FBS | 500 ml DMEM |
| | 10% FBS |

| | |
|---|---|
| | 1% Penicillin/Streptomycin |
| | 2% L-glutamine |
| CiPTEC Complete Culture Media | 500 ml DMEM-F12 |
| | 5 µg/ml Insulin, 5 µg/ml Transferin, 5ng/ml Sodium Selenite |
| | 10 ng/ml EGF |
| | 36 ng/ml Hydrocortisone |
| | 40 pg/ml I3 |
| | 10% FBS |
| CiPTEC Serum Free Media (SFM) | 500 ml DMEM-F12 |
| | 5 µg/ml Insulin, 5 µg/ml Transferin, 5ng/ml Sodium Selenite |
| | 10 ng/ml EGF |
| | 36 ng/ml Hydrocortisone |
| | 40 pg/ml I3 |
| PBMC Media | 500 ml RPMI |
| | 100 U/ml penicillin and 10mg/ml streptomycin |
| | 4mM L-glutamine |
| | 10% FBS |
| Huvec Media | 500 ml EndoGRO-LS medium |
| | 10% FBS |

### 3.1.2 Flow cytometry

#### 3.1.2.1 Flow cytometry solutions

| Name | Composition |
|---|---|
| FACS Buffer | 1L DPBS |
| | 0.4% BSA |
| | 0.02% $NaN_3$ |

| | |
|---|---|
| | Adjust to pH 7,4 |

### 3.1.2.2 Flow cytometry Antibodies

| Antibody | Fluorochrome | Clone | Manufacturer | Catalog No. |
|---|---|---|---|---|
| Anti-IDO | PE | eyedio | eBioscience | 12-9477-42 |
| **Human MSC characterization** | | | | |
| Anti-CD44 | PE | | BD Biosciences<br>BD Stemflow™ Human MSC Analysis Kit | 562245 |
| anti-CD73 | APC | | | |
| anti-CD90 | FITC | | | |
| anti-CD-105 | PerCP-Cy™ | | | |
| h-MSC Positive Isotype Cocktail control | | | | |
| h-MSC Negative Isotype Cocktail control | PE | | | |
| h-MSC Positive Cocktail control | | | | |
| h-MSC Negative Cocktail control | PE | | | |

### 3.1.2.3 Flow Cytometry buffers and reagents

| Product | Company | Catalog No. |
|---|---|---|
| Cell wash | BD Biosciences | 349524 |
| IC Fixation Buffer | eBioscience | 00-8222-49 |
| Permeabilization Buffer 10x | Invitrogen | 00-8333-56 |
| Cytotell Green | ATT Bioquest | 22253 |
| FcR blocking reagent (human) | Miltenyi | 130-059-901 |
| Fixable Viability dye eFluor450 (eF450) | Invitrogen | 65-0863-14 |

| | | |
|---|---|---|
| Precision Count beads | BioLegend | 424902 |

### 3.1.3 Western blot

#### 3.1.3.1 Western blot solutions

| Name | Composition |
|---|---|
| Tris buffer saline (TBS) 10x | 1L DPBS |
| | 6.05g Tris |
| | 8.76g NaCl |
| | Adjust to pH 7,6 |
| Tris buffer saline 1x + Tween (TBS-T) | TBS + 0.1% Tween 20 |
| Towbin buffer | 70% deionized water |
| | 20% methanol |
| | 10% 10X TGS |
| Blocking buffer | 5% BSA in TBS-T |

#### 3.1.3.2 Primary Antibodies

| Antibody | Dilution | Clone | Species | Manufacturer | Catalog No. |
|---|---|---|---|---|---|
| Anti human-Calnexin | 1:500 | E-10 | Mouse | Santa Cruz | sc-46669 |
| Anti-human p53 | 1:100 | DO-1 | Mouse | Santa Cruz | Sc-126 |
| Anti human-GAPDH | 1:1000 | | Rabbit | Abcam | Ab9485 |

#### 3.1.3.3 Secondary Antibodies

| Antibody | Dilution | Clone | Species | Manufacturer | Catalog No. |
|---|---|---|---|---|---|

| | | | | | |
|---|---|---|---|---|---|
| Anti-mouse HRP | 1:5000 | Polyclonal | Goat | GE Healthcare Bio-science AB | P0447 |
| Anti-rabbit HRP | 1:5000 | Polyclonal | Goat | GE Healthcare Bio-science AB | P0448 |

### 3.1.3.4 Western blot solutions and material

| Product | Company | Catalog No. |
|---|---|---|
| Run buffer, Tris/Glycine/SDS (TGS) | Bio-Rad | 1610772 |
| 4x Laemmli sample buffer | Bio-Rad | 161-0747 |
| β-mercaptoethanol | Sigma Aldrich | M7522-100ml |
| Page Ruler Plus | Thermo Fisher | 26619 |
| Precision plus protein, Dual colour standards | Bio-Rad | 1610374 |
| Pierce RIPA Buffer | Thermo Fisher | 89900 |
| Halt protease inhibitor single-use cocktail (100x) | Thermo Fisher | 78430 |
| Tween 20 | Serva | 37470.01 |
| 10X TGS | Bio-Rad | 161-0772 |
| Methanol | Carl Roth | 8388.5 |
| 10X TGS | Bio-Rad | 1610732 |
| Nitrocellulose blotting membrane | GE Healthcare Bio-science AB | 1060000 |
| Filter paper (Whatman) | Sigma Aldrich | WHA10537138 |
| Mini Trans-blot filter paper | Bio-Rad | 1703932 |
| Page blue | Thermo Fisher | #26616 |
| Albumin fraction V (bovine serum albumin) | Carl Roth | 8076.2 |
| Mini-PROTEAN TGX Precast gels, 4-15% | Bio-Rad | 456-1083DC |
| Criterion XT Precast gels; 4-12% | Bio-Rad | 345-0124 |

#### 3.1.3.5 Protein detection Reagents

| Product | Company | Catalog No. |
|---|---|---|
| L-Kynurenine | Santa Cruz | sc-202688 |
| Trichloroacetic acid | Fluka Riedel-de Haen | 33209 |
| 4-(Dimethylamino) benzaldehyde | Santa Cruz | sc-202888 |
| Sodium nitrite | AppliChem | A7014,0500 |
| Sulfanilamide | AppliChem | A3971,0100 |
| N-(1-Napthyl)-ethylendiamine dihydrochloride (Naphtylamine) | Carl Roth | 4342.1 |
| Double distilled water | Carl Roth | 3478.1 |

### 3.1.4 qPCR Kits and Reagent

| Product | Company | Catalog No. |
|---|---|---|
| miRneasy Micro kit | Qiagen | 217084 |
| SensiFAST ™ cDNA Synthesis Kit | Bioline | BIO-65054 |
| QIAzol Lysis Reagent | Qiagen | 79306 |
| miRNA 1st-Strand cDNA Synthesis Kit | Agilent | #600036 |
| miRNA QPCR Master Mix | Agilent | #600583 |
| RT2 Profiler PCR Array for nephrotoxicity | Qiagen | #330231 |
| LNA_181a-5p inhibitor | miRCURY LNA miRNA Qiagen | # 339131 |
| negative control inhibitor | | # 339136 |
| LNA_181a-5p mimic | | # 339173 |
| negative control mimic | | # 339173 |

#### 3.1.4.1 qPCR primer

| microRNA | Primer Sequence (5'-3') |
|---|---|
| hsa-miR-181a-5p | 5’-AACATTCAACGCTGTCGGTGAG-3’ |
| hsa-miR-125a-5p | 5’-CCTGAGACCCTTTACCTGTG-3’ |
| hsa-miR-146a-5p | 5’-TGAGAACTGAATTCCATGGGTT-3’ |
| hsa-U6 | 5’-CGCAAGGATGACACGCAAATTC-3’ |

### 3.1.5 Kits

| Product | Company | Catalog No. |
|---|---|---|
| BD Biosciences StemFlow Human MSC Analysis Kit | BD Biosciences | 562245 |
| CellTiter-Glo® Luminescent Cell Viability Assay | Promega | G7570 |
| Pierce BCA Protein Kit | Thermo Fisher | 23227 |

### 3.1.6 Other solutions

| Name | Composition |
|---|---|
| PBS/EDTA | 500 ml DPBS |
| | 2mM EDTA |
| Stopping Medium | 50 ml DPBS |
| | 10% FBS |
| Freezing Medium | FBS |
| | 10% DMSO |
| PFA 4% | 50 ml DPBS |
| | 4% PFA |

### 3.1.7 Consumable laboratory material

| Product | Company | Catalog No. |
|---|---|---|
| 25 $cm^2$ cell culture flasks | Thermo Fisher | 156367 |
| 75 $cm^2$ cell culture flasks | Thermo Fisher | 156499 |
| 175 $cm^2$ cell culture flasks | Thermo Fisher | 159910 |
| 6-well cell culture plate | Thermo Fisher | 140675 |

| | | |
|---|---|---|
| 12-well cell culture plate | Thermo Fisher | 150628 |
| 24-well cell culture plate | Thermo Fisher | 142475 |
| 96-well cell culture plate | Eppendorf | 0030 790.119 |
| 96-well black cell culture plate | Perkin Elmer | 6005550 |
| ImageLock 96 well plate | Essen BioScience | 4379 |
| Wound marker | Essen BioScience | 4563 |
| 15 ml Cell star tubes | Greiner Bio-one | 188271 |
| 50 ml Cell star tubes | Greiner Bio-one | 227261 |
| 10-20 µl sterile filter tips | Star Lab | S1120-3710 |
| 200 µl sterile filter tips | SurPhob | VT0243X |
| 1000 µl sterile filter tips | SurPhob | VT0263X |
| 1.25 ml Precision Dispenser (PD) sterile tips | Brand | 702386 |
| 2.5 ml PD sterile tips | Brand | 702388 |
| 5 ml PD sterile tips | Brand | 702390 |
| 10 ml PD sterile tips | Brand | 631060 |
| 5 ml serological sterile pipettes | Star Lab | 180806-069 |
| 10 ml serological sterile pipettes | Star Lab | 180720-070 |
| 25 ml serological sterile pipettes | Star Lab | 190105-071 |
| 50 ml centrifuge tube | Greiner bio-one | 227261 |
| 15 ml centrifuge tube | Greiner bio-one | 188271 |
| 100 kD MWCO concentration filter | Sartorius | VS2042 |
| Cell strainer, 70µm | Sarstedt | 83.3945.070 |
| Cell strainer, 100µm | Sarstedt | 83.3945.100 |
| 50 ml syringe | Dispomed | 21050 |
| 10 ml syringe | Dispomed | 20010 |
| 5 ml syringe | Braun | 4606051 |
| 1 ml syringe | BD Biosciences | 300013 |
| Rotilabo syringe filters 0.22 µm | Carl Roth | SE2M035I07 |

| | | |
|---|---|---|
| Syringe filters 0.45µm | NeoLab | 3-1904 |
| 0.2 ml thin-walled tubes with flat caps | Thermo Fisher | AB0622 |
| Cryopreservation tubes | Greiner Bio-one | 122278 |
| 1.5 ml tubes | Eppendorf | 0030 125.150 |
| 1.6 ml tubes (Low binding, DNA-DNase, RNase free) | Biozym Scientific | 710176 |
| 5 ml Polystyrene round bottom FACS tubes | Corning | 352052 |
| CASY cup | OMNI Life Science | 5651794 |
| Gloves | Hartmann | 3538071 |
| Pursept A Xpress | Schülke | SMH 230131 |
| Scalpels | Braun | 10567364 |
| PCR plate | Genaxxon bioscience | I2207.0050 |
| qEV10 35nm Column | IZON | #SP710799 |

#### 3.1.7.1 Laboratory equipment

| Device | Model | Manufacturer |
|---|---|---|
| Live imaging microscope | IncuCyte SX5 | Essen BioScience, Ltd. |
| Live imaging microscope | IncuCyte Zoom | Essen BioScience, Ltd. |
| Thermal Cycler | PTC0200 | Bio-Rad Laboratories GmbH |
| Light Cycler | Light Cycler® 960 | Roche |
| Centrifuge | ROTINA 420 | Hettich Zentrifugen |
| Centrifuge | ROTINA 420R | Hettich Zentrifugen |
| Centrifuge | 5415R | Eppendorf |
| Small Centrifuge | Minispin | Eppendorf |
| Cell counter | CASY | OMNI Life Science |
| Microscope | Axiovert 100 | ZEISS |

| | | |
|---|---|---|
| Microscope | Axiovert 40C | ZEISS |
| Microscope Camera | AxioCam M Rc | ZEISS |
| Sterile laminar flow hood | Hera safe | Thermo Fisher Electron Cooperation |
| Chemical flow hood | Airflow-Control EN14175 | Caspar and Co. Labora |
| Cell culture incubator | CB210 | Binder |
| Cell culture pump | Vacusafe Comfort | Integra Biosciences |
| Cell culture shaker | Lab Dancer | IKA |
| Water bath | WNE 7 | Memmert |
| Hollow Fiber Bioreactor | FiberCell systems | C2025D |
| pH-Meter | pH 211 | Hanna Instruments |
| Microplate reader | TECAN infinite M200PRO | TECAN |
| Flow cytometer | BD FACS Canto II | BD Biosciences |
| Chemiluminescent detector | FusionCapt Advanced Solo 4 | Vilbert Lourmat |
| Horizontal shaker | Thermo Mixer C | Eppendorf |
| Rotator | SB2 | Stuart |
| Chamber shaker | UniHood 650 | Edmund Bühler |
| Precision scale | EW 2200-2NM | Kern & Sohn |
| Precision scale | ABJ 22-4M | Kern & Sohn |
| Nitrogen tanks | Biosafe UN 1977 | Cryotherm |
| Autoclave | V-150 | Systec |
| Zetaview | PMX 220 ZetaView TWIN Laser | Particle Metrix |

### 3.1.8 Software for data analysis

| Software | Version | Company |
|---|---|---|
| FlowJo | 10 | FlowJo, LLC, Ashland, OR, USA |
| GraphPad Prism | 9 | GraphPad Software Inc. |

| | | |
|---|---|---|
| | | San Diego, USA |
| Word | Microsoft 10 | Redmond, WA, USA |
| Excel | | |
| PowerPoint | | |
| i-Control | 1.10 | TECAN |
| Image-J | | NIH |
| IncuCyte 2020B Software | | Essen BioScience, Ltd. |
| IncuCyte ZOOM 2018A | | Essen BioScience, Ltd. |
| GeneGlobe Data Analysis | | Qiagen |
| R-studio | 4.2.2 | RStudio Inc. Posit, PBC |
| Cytoscape | | Institute for System Biology |

## 3.2 Methods

### 3.2.1 AIM 1: Inter-laboratory study on the comparison of different MSC sources: study design

The first part of this thesis is a study running within the context of the RenalToolBox EU ITN Network, where my colleague and I contributed.

Within this study, we collaborated with researchers from the University of Liverpool (Liverpool, UK) and the University of Galway (Galway, Ireland) to assess the biological and therapeutic properties of MSC derived from bone marrow (BM-MSC, Galway), adipose tissue (A-MSC, Heidelberg), and umbilical cord (UC-MSC, Liverpool) in an inter-laboratory comparative study.

Within each centre, we isolated and expanded three different donors from one tissue source following the respective in-house standard procedures. Isolated and expanded MSC were then cryopreserved and internationally shipped to all the centres.

When all the centres received all the MSC types, the cells were thawed and expanded using harmonised culture conditions. These included, α-MEM basal

medium with 10% FBS (one batch for all centres, prechecked with the RenalToolBox consortium) and optimised seeding densities (300 cells/ $cm^2$ for A-MSC and 3,000 cells/$cm^2$ for BM- and UC-MSC) at 37 C with 5% (v/v) $CO_2$ and controlled humidity.

Part one of the inter-laboratory study was to compare the growth kinetics, the differentiation ability and the immunophenotype of all the MSC in each centres to assess the degree of variability of different handling, despite harmonized protocols. Part two of the study was that each centre analysed different functional attributes of the MSC to identify eventaual source-specific capacities. Specifically, we performed an assay to assess the inhibitory effect of MSC on proliferation of PBMCs, stimulated by the mitogen phytohemagglutin (PHA).

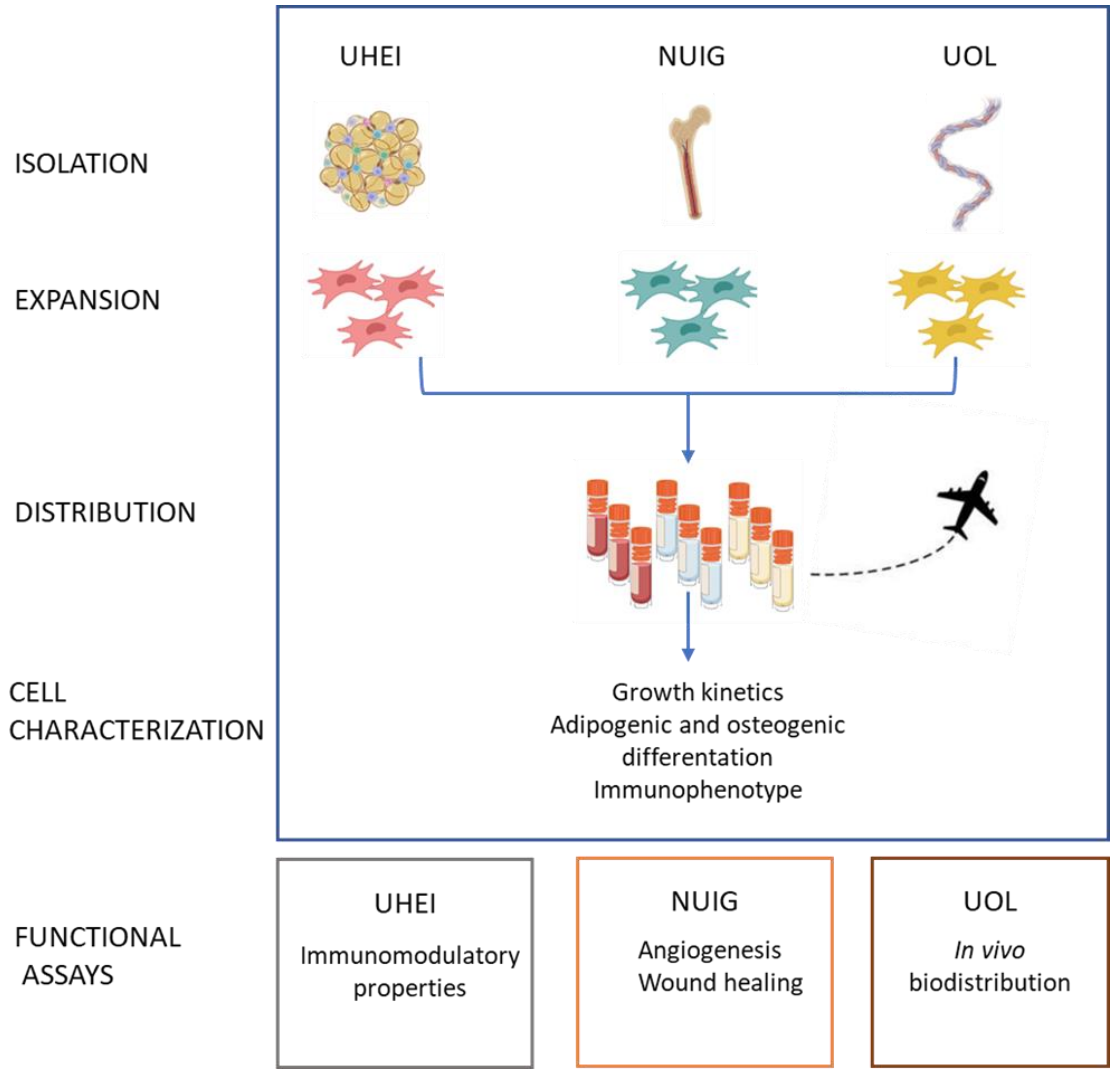


**Figure 8. Schematic representing study design and assay distribution across centres**. UHEI= University of Heidelberg, NUIG= University of Galway and UOL= University of Liverpool. This image was created using BioRender. The figure has been modified from [166].

#### 3.2.1.1 Adipose-derived mesenchymal stromal cell isolation

Adipose-derived mesenchymal stromal cells (A-MSC) were isolated from healthy donors after obtaining informed consent (Mannheim Ethics Commission II; vote numbers 2010-262 N-MA, 2009-210 N-MA, 49/05 and 48/05). Raw lipoaspirate samples were washed with sterile PBS to remove cellular debris and red blood cells by centrifugation at 420g for 10 minutes.

Samples were resuspended in DMEM (ratio 1:1) containing 0.15 PZU/ml NB6 collagenase for 45-60 min at 37°C with gentle agitation. At the end of incubation time, the collagenase was inactivated by adding an equal volume of DMEM/10% FBS, then centrifugated at 1200g for 10 minutes to obtain a high-density stromal vascular fraction (SVF) pellet. The supernatant was discarded and the pellet was incubated for 10 minutes at room temperature with erythrocyte lysis buffer to remove red blood cells. After a centrifugation step, the SVF pellet was resuspended in DMEM and filtered through a 100µm nylon mesh filter before centrifuging the filtrate at 1200g for 10 minutes to obtain the enriched SVF pellet. The pellet was resuspended in DMEM AB plated in a T25 or T75 culture flask (dependent on pellet size) and incubated overnight at 37°C, 5% $CO_2$. On the following day, we performed extensive washings with PBS of the plates to remove non-adherent and red blood cells, before media change. Cell morphology was constantly monitored by microscope observation and the media was changed two times for week. The resulting population of A-MSC cells were harvested and seeded in a new flask at a density of 300 cells/$cm^2$. Once 70-80% of confluence were reached, the cells were harvested with trypsin/EDTA, counted with the CASY cell counter and seeded again with a density of 300 cells/$cm^2$ for further experiments.

#### 3.2.1.2 A-MSC culture and cryopreservation

A-MSC were expanded until passage 3 at a density of 300 cells/$cm^2$ supplemented with 10% FBS serum 1% penicillin/streptomycin (100,000 U/ml penicillin and 10 mg/ml streptomycin; and 4 Mm L-glutamine in α-MEM. When the culture reached 70-80% of confluence, the cells were harvested with trypsin/EDTA and cryopreserved in FBS with 10% of DMSO. The cryovials were conserved in liquid nitrogen before being shipped to UOL and NUIG on dry ice.

### 3.2.1.3 BM and UC-MSC isolation and culture

BM- and UC-MSC, as for the A-MSC, were isolated in the respective institute and sent to the other centres. When all the institutes received the MSC, cells were thawed and cultured under harmonized culture conditions (**Table 1**) the basic MSC characterization was done and the results were compared between the centres and between the tissue sources.

**Table 1.** Harmonised culture conditions for RTB interlab study.

| HARMONISED CULTURE CONDITIONS | | |
|---|---|---|
| GROWTH CONDITIONS<br>• Minimal Essential Media α (α-MEM)<br>• 10% FBS | SEEDING DENSITY<br>• A-MSC 300 cells/cm$^2$<br>• BM-, UC-MSC 3000 cells/cm$^2$ | CRYOCONSERVATION<br>• 10% DMSO in FBS |

### 3.2.1.4 Growth kinetics

To assess the proliferation kinetics of the MSC, population doublings and doubling times of MSC from the three tissues sources were compared. A-, BM- and UC-MSC were thawed and cultured for at least one passage before their growth kinetics curves were calculated. After recovery from the cryopreservation, A-MSC were seeded at 300 cells/cm$^2$ density, while BM- and UC-MSC were seeded at 3000 cells/cm$^2$. Growth rate values were calculated following the equations of Population Doublings (PD) and Population Doubling Time (PDT), where Fcn stands for final cell number and Icn for Initial cell number.

$$\text{Population Duublings (PD)} = \frac{Log10\ (Fcn) - Log10\ (\text{Icn})}{Log10\ (2)}$$

$$\text{Population doubling Time (PDT)} = \frac{Culture\ duration}{PD}$$

#### 3.2.1.5 Adipogenic differentiation

MSC were tested for their adipogenic differentiation capacity. 5.700 cells/well were seeded in a 96-well plate and after 48h, cells were cultured in adipogenic differentiation media for 14 days. α-MEM 10% FBS condition was used as a negative control.

On the last differentiation day, MSC were fixed with 4% PFA for 30 minutes, washed and incubated with Hoechst-33342 (nuclear dye, 1:100 final concentration) for another 30 minutes. Hoechst fluorescence (excitation: 354 nm/emission: 442nm) was measured on a plate reader and taken as baseline to account for the cell numbers and to normalize the adipogenic signal against. To test for adipogenic differentiation, the AdipoRed assay was performed following the manufacturer's instructions. AdipoRed is a solution of Hydrophilic Stain Nile Red that when partitioned in a hydrophobic environment, it becomes fluorescent, which allows to quantify the intracellular lipid droplets typical of adipocytes.

After washing with PBS, AdipoRed (5 µl/well in a 96-well plate), was added to the plate containing 200 µl of PBS and incubated in the dark for 15 minutes.

Following incubation, AdipoRed fluorescence was measured on a plate reader at 485/572 nm. The AdipoRed signal was normalized against the Hoechst signal and presented as a fold change of the undifferentiated condition.

#### 3.2.1.6 Osteogenic differentiation

MSC were tested for their osteogenic differentiation capacity, 2.900 cells/well were seeded in a 96-well plate and after 48h, cultured in osteogenic differentiation media for 14 days. As for the adipogenic differentiation, αMEM 10% FBS condition was used as a negative control.

On the last differentiation day, MSC were fixed with 4% PFA for 30 minutes, washed and incubated with Hoechst-33342 (1:100 final concentration) for another 30 minutes. Hoechst fluorescence (excitation: 354 nm/emission: 442nm) was measured on a plate reader. To test for osteogenic differentiation, the Osteoimage mineralization assay was performed following the manufacturer's instructions.

The OsteoImage™ Mineralization Assay is a rapid, fluorescent in vitro assay for assessing bone cell mineralization, which is based on specific binding of the fluorescent OsteoImage™ Staining Reagent to the hydroxyapatite portion of bone-like nodules deposited by cells.

After washing with wash buffer, Osteoimage staining reagent (1:100 final dilution in Staining Reagent Dilution Buffer) was incubated with the cells for 30 minutes at RT. Following incubation, the staining solution was removed and three consecutive washing steps were performed with a wash buffer. Osteoimage fluorescence was measured on a plate reader at 492/520 nm. The Osteoimage signal was normalized on the Hoechst signal and presented as a fold change of the undifferentiated condition.

#### 3.2.1.7 Immunophenotyping analysis

To define their immunophenotype and assess similarities and eventual differences in marker expression, BM--, UC and A-MSC were characterized by flow cytometry. When the confluence reached the 70-80%, the cells were harvested and washed once with PBS and $1x10^5$ cells were collected in FACS tubes, resuspended in 100 µl of FACS buffer. 10 µl of FcR blocking reagent was added in each tube and let incubated at 4°C for 5 minutes. The MSC immunophenotype was measured using the BD Stemflow™ Human MSC Analysis Kit (containing FITC Anti-Human CD90, PE Anti-Human CD44, PerCP-Cy™ 5.5 Anti-HumanCD105, APC Anti-Human CD73, h-MSC Positive Isotype Cocktail control, PE h-MSC Negative Isotype Cocktail control, h-MSC Positive Cocktail control, PE h-MSC Negative Cocktail control) according to the manufacturer's instructions.
Staining was performed for 30 minutes in the dark at 4°C after which cells were washed twice with Cell wash and analysed. A total of 10,000 events were acquired with BD FACS Canto and fcs files were exported and the percentage of positive cells for the surface marker was obtained with FlowJo software.

#### 3.2.1.8 PBMC proliferation assay

To assess the immunomodulatory capacity of MSC, their ability to inhibit the proliferation of PBMCs in co-culture has been studied. PBMCs used in our experiments was isolated from leukapheresis samples from healthy donors, provided by the German Red Cross Blood Donor Service in Mannheim (Mannheim Ethics Commission; vote number 2018-594N-MA) and cryo-preserved in liquid nitrogen for further use.
MSC were seeded in a 96-well plate with a seeding density of 10,000 cells/well in α-MEM 10% FBS and allowed to attach overnight. The next day we started the co-culture with cryo-preserved PBMC. PBMCs were washed twice with PBS and stained

with the proliferation dye Cytotell Green (final concentration of 1:500 dilution from stock) to be able to follow the number of cell division by dye dilution. After 15 min incubation at 37°C, cells were washed 3 times with PBS, centrifuged and resuspended in a concentration of $10^5$ cells/200 µl in RPMI, supplemented with 10% FBS, L-glutamine, P/S, and 200 U/ml IL-2. $10^5$ PBMS were added directly on top of the MSC with a ratio of 1:10 MSC: PBMCs. To stimulate the PBMC's proliferation, PHA was added to the culture to a final concentration of 4,8 µg/ml. PBMCs cultured alone without MSC in the absence and presence of PHA served as negative and positive controls, respectively. After day 5, Cytotell green cells were harvested from co-culture and control conditions, technical replicates were pooled and collected in FACS tubes, washed and resuspended in FACS Buffer. PBMC proliferation was measured using a FACS Canto II and the fcs files were exported and analyzed with FlowJo.

#### 3.2.1.9 IFN-y stimulation and intracellular indoleamine 2,3-dioxygenase staining

Indoleamine 2,3-dioxygenase (IDO) -mediated tryptophan degradation suppresses T cell proliferation as already described in a previous study performed in our lab [167]. To assess whether MSC from the different sources differed with respect to their IDO production, we measured this after stimulation with interferon gamma.

MSC were seeded in a 6-well plate at a density of 5.000 cells/$cm^2$ in full α-MEM 10% FBS. Once seeded, cells were allowed to attach overnight and then were treated for 24 hours with IFN-γ (concentration 25 ng/ml), to assess specific IDO secretion. As negative control MSC were cultured in the absence of IFN-γ. After the treatment, MSC were harvested, washed with PBS and collected in FACS tubes and stained with Fixable Viability dye eF450 (1:4.000 final dilution) and incubated for 30 minutes at 4°C. The cell suspension was then incubated with IC fixation buffer for 30 minutes at room temperature. After washing/centrifuging samples twice with 1X permeabilisation buffer, cells were stained with PE-conjugated anti-IDO in 1X permeabilisation buffer for 30 minutes. Following this step, cells were washed twice and analyzed immediately at BD FACS Canto II and the FCS files were exported and analyzed with FlowJo. Data are represented as median fluorescence intensity (MFI) and percentage of positive cells.

### 3.2.2 AIM 2: Comparison of A-MSC bioproducts

Within AIM 2 of this thesis, the EVs, the protein fraction and the MSC-CM were compared to each other. The cells used in this study were the adipose-derived mesenchymal stromal cells (A-MSC) from lipoaspirates from three donors, processed at our lab at Medical Faculty Mannheim (University of Heidelberg) using α-MEM media and 10% fetal bovine serum at 37 ℃ with 5% CO2 and controlled humidity.

These three A-MSC batches were shipped as cryo-aliquots to the other two RTB centres which contributed to this study (the University of Galway and the University of Turin) to be cultured under identical harmonized culture conditions as described before. The bioproducts were derived from the conditioned medium of A-MSC in 3D culture (see below), purified by size exclusion chromatography (SEC) to produce (**1**) EV-SEC or the (**2**) protein-rich fraction or 2D culture cells, treated with ultracentrifugation to produce (**3**) EV-UC or after concentration to produce (**4**) the conditioned medium (CM) or (**5**) the respective washing (CM-WO) (**Fig. 9**)

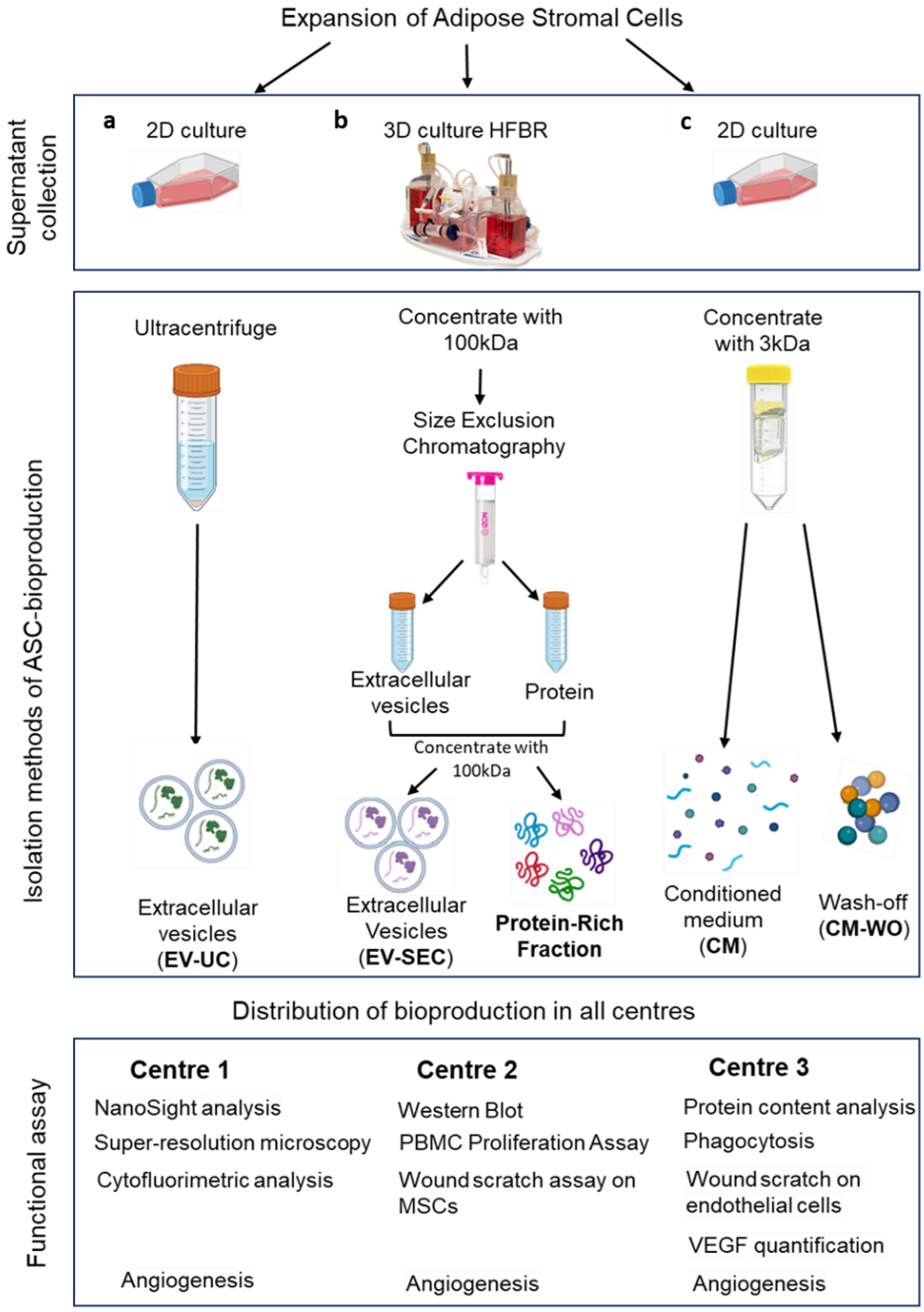


**Figure 9**. **Schematic representing the study design and the distribution of performed assays across the centres**. The A-MSC were cultured in 2D culture fasks in a serum-free medium for the production of bioproducts. (**a**) The supernatant was collected and then purified by ultracentrifugation EV-UC, (**b**) for EV-SEC, the A-MSC were cultured in a 3D hollow fiber bioreactor (HFBR), from which the supernatant was collected, concentrated and processed by SEC. EVs and protein fraction were concentrated with a 100 kDa filter. (**c**) Conditioned medium and wash-off: Finally, the A-MSC were cultured in 2D culture flasks, the supernatant was collected and concentrated with a 3 kDa filter and the conditioned medium and wash-of were collected during the process. The figure has been modified from [168].

#### 3.2.2.1 3D culture of A-MSC and collection of media

As in the first part, three different donors of A-MSC from lipo-aspirate were cultured at the density of 3,000 cells/cm$^2$ in α-MEM supplemented with 10% FBS serum 1% penicillin/streptomycin (100,000 U/ml penicillin and 10 mg/ml streptomycin; and 4Mm L-glutamine until passage 3. When the culture reached 70-80% of confluence, the cells were harvested with trypsin/EDTA and cryopreserved in FBS with 10% of DMSO. The cryo-aliquots were conserved in liquid nitrogen before being shipped to Turin and Galway on dry ice. A-MSC were cultured in all the centres under identical harmonized culture conditions and used from passages 4-6.

To gain a high amount of MSC-CM, we established a 3D culture of A-MSC within a hollow-fiber bioreactor. This allows for seeding a large amounts of cells on the basis of its hollow fiber technology, increases the area of seeding density and allows to harvest a CM rich in EV derived from millions of cells every day. A further advantage of this system is the reproduction of a more in vivo like environment compared to 2D cultures in flasks [169].

When the cells in passage 3 reached 80% confluence, A-MSC were harvested with trypsin/EDTA, counted and 14 × 10$^6$ cells were seeded in a hollow-fiber bioreactor cartridge (20 kDa MWCO, 450 cm$^2$, C2025D). Before injecting the cells, 'pre-culture steps' were carried out to initiate and activate the bioreactor, first PBS for 24 h, followed by fibronectin coating (concentration 30 µg/ml) overnight and 24h with only media without serum. After the pre-culture process, A-MSC were seeded in α-MEM without FBS in the extra-capillary space, instead, the serum was used in the circulating medium, at 37 °C with 5% $CO_2$ and controlled humidity for seven days without harvesting the supernatant, with regular monitoring of glucose levels. A-MSC were cultured for 4 weeks in the bioreactor and during this period, the supernatant was collected daily. Every day the supernatant was collected from the extra-capillary space, centrifuged for 5 min at 420 × g to remove cell debris, and stored at -80 °C. After 4 weeks, cells were harvested and counted to calculate the bio-product per producer cell concentration.

#### 3.2.2.2 EV isolation by size exclusion chromatography

Each A-MSC-CM collected previously and stored at -80°C was thawed at 4°C. Before starting the isolation procedure, the CM was centrifuged for 10 min at 300 x g and 20 min at 4,000 x g. After, the supernatant was filtered through a 0.2 µm syringe filter and concentrated with a 100 kD MWCO concentration filter to a final volume of 10 ml. The qEV10-IZON column 35 mm was washed with sterile PBS before adding 10 ml of the sample. Following the manufacturer's instruction, the EV fraction (EV-SEC) and the protein fraction (protein-rich fraction) were collected in falcon tubes and then concentrated to the final volume of 1,5 ml (Vivaspin 20, 100.000 MWCO PE). Each EV sample and the resultant supernatant containing the protein-rich-fraction were stored at -80°C until use in further experiments.

#### 3.2.2.3 EV/CM treatment

A-MSC-derived bioproducts were used at a ratio of 2:1 and 20:1, meaning ‘two’ or ‘twenty’ MSC cell equivalent bioproducts per each recipient cell. To calculate the cell equivalents, we counted the number of cells after harvesting and we used it to relate the number of particles/volumes generated of EVs and CM respectively for each bioproduct. For example, one bioreactor run generated 1.5 ml of EV-SEC from 14,000.000 A-MSC, converted into cells producing the bioproduct corresponds to 9,400 cell per ml (producer cell concentration).

#### 3.2.2.4 ZetaView analysis

Particle number and size distribution were measured with light scattering technology, NTA. One microliter of concentrated EV was diluted in 0.22 µm sterile-filtered PBS in a 1:1,000 dilution, EVs were visualized using the ZetaView device, kindly provided by the Deaprtment of Urology, Medical Faculty Mannheim. The device-specific configuration was as follows: 80% sensitivity, shutter 100, 11 positions were measured and 2 measurement cycles were performed. Amongst all measurements, 1 to 3 positions from a total of 11 were removed for analysis due to some values being out of range.

#### 3.2.2.5 Western blot analysis of EV markers

Proteins extracted from Hela cells were used as cellular control, and the pellet was resuspended in RIPA buffer (50 mM Tris-HCl, pH7.4, 150 mM NaCl, 1% Triton X-

100, 1% Na-deoxycholate, 0.1% SDS, 0.1 mM CaCl2, and 0.01 mM MgCl2 supplemented with protease inhibitor cocktail, incubated 30 min in ice vortexing every 10 min and centrifuged 20 min at 20.000 × g.

An equal volume of bioproducts and cell lysate (38 µl) was loaded and separated on 4–15% Mini-PROTEAN TGX Precast Gels. Bioproducts and cell lysates were resuspended in protein loading dye (Laemmli sample buffer with freshly added β-mercaptoethanol 10%; v/v) and boiled for 5 min at 95 °C before be separate by sodium dodecyl sulphate–polyacrylamide gel electrophoresis (SDS-PAGE) in Run buffer (composed by Tris/Glycine/SDS (TGS)). Proteins were subsequently blotted to a nitrocellulose blotting membrane (0.2 µm) in Towbin buffer (composed by 70% deionized water, 20% methanol and 10% 10X TGS). Membranes were blocked in 5% BSA in 0.1% Tween in TBS (TBS-T). After blocking, blots were probed against Calnexin (anti-calnexin antibody 1:500 dilution, E-10), diluted in 5% BSA/TBS-T. After overnight incubation at 4 °C, membranes were washed 3 times with TBS-T and subsequently incubated with the secondary antibody anti-mouse IgG HRP (1:5000 dilution) for 1 h at room temperature followed by washing. Blots were then developed using Western Bright ECL and protein bands were detected using the FusionCapt Advanced Solo 4.

#### 3.2.2.6 Effect of MSC bioproducts on PBMC proliferation

The capacity of MSC or their bioproducts to inhibit the induced proliferation of PBMCs was analysed as described in chapter 3.2.1.7. PBMC labelled with proliferation dye Cytotell Green ( were seeded at a 1:10 MSC/bioproduct: PBMC ratio in RPMI, supplemented with 10% FBS, 2% L-glutamine, 1% penicillin/streptomycin, and 200 U/ml IL-2. PBMC proliferation was stimulated with PHA (4.8 µg/ml). PBMCs cultured alone without MSC/bioproduction in the absence and presence of PHA served as negative and positive controls, respectively. After 5 days, PBMC proliferation was measured based on the dilution of Cytotell Green dye using a FACS Canto II (BD Biosciences) and the data were analysed with FlowJo Software.

#### 3.2.2.7 Effects of MSC bioproducts on A-MSC cell migration

To assess the migratory capacity of MSC, we made use of the so called wound scratch assay analysed by live cell microscopy. In this assy, cells are seeded as monolayer. Upon confluence, a scratch was made using a specific wound scratch

maker tool (96-well Wound Maker, Sartorius) to create precise and reproducible wounds in all the wells. The migration of the cells closing the wound was captured by live-cell imaging and then analysed using a specific analysis tool (IncuCyte, Essen Bioscience, Sartorius).

Specifically, 20.000 A-MSC were seeded in a 96-well Essen ImageLock™ plate and cultured overnight. Then, the cells were scraped with the 96-well Wound Maker. After creating the wounds, the monolayer were washed 2 times with PBS and A-MSC bio-products were added in different concentrations. Plates were then cultured and monitored using the IncuCyte ZOOM™ device; every 3 hours images were taken. These images were analysed 24 hours later using the Relative Wound Density algorithm to report data.

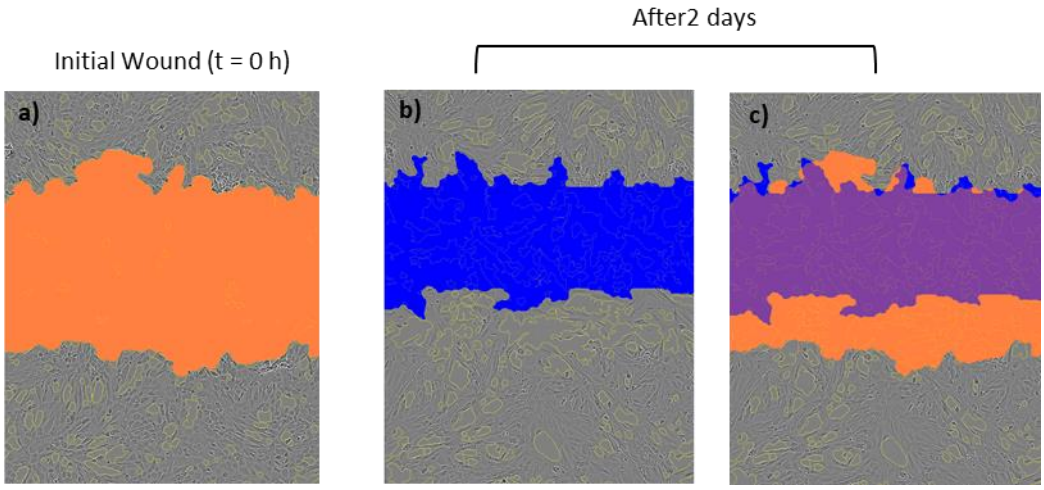


**Figure 10. Analysis of cell migration using a live cell imaging wound scratch assay (Incucyte)** **(a)** ciPTEC stage image taken at t = 0h post injury, yellow indicates the confluent mask and the orange area correspondsto the initial scratch wound mask**. (b)** ciPTEC phase image taken at 2 days, the blue area indicates the wound scratch area. **(c)** The purple color corresponds to the scratch wound mask indicating the overlap of wound scratch position after 2 days (blue) with the initial mask of the scratched wound (orange).

### 3.2.2.8 Effects of MSC bioproducts on capillary tube formation

We have previously shown that MSC-CM can promote capillary tube formation of HUVEVS on an extracellular matrix [170, 171]. Accordingly, we aimed to evaluate whether the MSC bioproducts differ in their potential to recapitulate this.

Human umbilical vascular endothelial cells (HUVEC) were thawed and cultured until passage 6 in EndoGRO-LS Complete Culture Media Kit. In vitro, the formation of capillary-like structures was performed on growth factor–reduced Matrigel (Galway

and Turin) or geltrex (Geltrex$^{TM}$ LDEV-free reduced growth factor matrix; Heidelberg) HUVEC cells were treated with EVs or CM as described before, seeded at a density of 10x10$^3$ cells/well on a 96 well plate. Positive control was full EndoGro-LS medium, negative control medium without VEGF and FBS (as used for all the conditions).
Galway and Heidelberg also tested the ability of the protein-rich fraction and CM to induce angiogenesis in the presence of VEGF inhibitor adding 1µM of ZM32381 to the culture.
Cells were periodically observed with a Nikon TE2000E inverted microscope and experimental results were recorded after 16 h; 3 images were taken per well (Galway and Turin). In Heidelberg, we used live cell imaging (IncuCyte Zoom) to monitor the network formation. Image analysis was performed with the ImageJ software v.1.53c, using the Angiogenesis Analyzer [172]. The data from three independent experiments were expressed as the mean ± SD of tube length in arbitrary units per field.

### 3.2.3 Part 3: Role of microRNAs in the protective effect of A-CM in n kidney injury model

#### 3.2.3.1 Proximal tubular epithelial cell culture and cisplatin-induced cell injury

To finally assess the effects of MSC, MSC bioproducts and specifically miRNAs on kidney injury, we first established a cell culture model of kidney injury. We focussed on human proximal tubule epithelial cells and used an immortalaized cell line, previously established by one of the collaboration partners within RTB [173]. We used conditionally immortalized PTEC (ciPTEC) obtained from Cell4Pharma (Oss, The Netherlands). This is a human renal cell line that mimics the proximal tubule cells of the kidney. Conditionally immortalised means that by changing the culture temeperature, cells can be transferred from proliferation (33 °C) to differentiation (37°C, reduced proliferation).
The ciPTECs were growing in phenol red-free Dulbecco's Modified Eagle's Medium F12 supplemented with 5 µg/mL insulin, 5 µg/mL transferrin, 5 µg/mL selenium, 35 ng/mL hydrocortisone 10 ng/mL epidermal growth factor, 40 pg/mL triiodothyronine and 10% (v/v) fetal bovine serum. ciPTECs were grown and expanded at 33° C, for the experiment, and were cultured overnight at 33° C the cells attached at the surface and the day after were moved at 37° C for 7 days of maturation.

To mimic the in vivo damage and establish an in vitro injury model, ciPTECs were exposed to different concentrations of cisplatin (15-250 µM), Antimycin A (2,5 nM-25 µM) or hydrogen peroxide (0,1 µM-0,6 µM) for 24 hours. Cell viability, metabolic activity and cell migration were then analyzed.
To study the protective role of A-CM, ciPTEC were treated with 15 µM cisplatin for 1h, after that time the medium was replaced with A-CM containing 15 µM cisplatin and treated for 23h. Cell viability, p53 expression, migration and apoptosis were analysed (see below). ciPTEC treated with control medium (ciPTEC SFM) served as the untreated (CTRL) and cisplatin-treated control (Cisplatin), respectively.

#### 3.2.3.2 A-MSC isolation, culture and preparation of A-MSC-conditioned medium

A-MSC were processed from the lipoaspirate of healthy donors after informed consent and in concordance with The Mannheim Ethics Commission II (vote 2011-215 N-MA), as previously described [79]. A-MSC were cultured using Dulbecco's Modified Eagle's Medium normal glucose (supplemented with 10% of pooled human allogeneic serum from five AB donors (German Red Cross Blood Donor Service Baden-Wurttemberg — Hessen, Institute Mannheim, Germany), 1% penicillin/streptomycin and 4 mM of L-glutamine. A-MSC were expanded, seeding 300 cells/cm2 at 37 °C with 5% $CO_2$ and controlled humidity. For preparing the CM, the A-MSC were seeded in a T175 flask with a seeding density of 3000 cells/$cm^2$ and once 60% confluent, the cells were washed 2 times with PBS. Then DMEM F12 without serum (SFM) was added for 24h. After 24h, the supernatant/CM was collected and centrifuged for 10 minutes at 300 × g and 20 minutes at 2,000 × g at 4°C. Thereafter, the CM was filtered through a 0.2 µm syringe filter and stored at -80 °C until further use. As a control medium, ciPTEC SFM was incubated in cell-free empty culture flasks at 37°C, 5% CO2, for 24 h and subjected to the same harvesting process described above.

#### 3.2.3.3 Assessment of ciPTEC viability

The viability of ciPTEC was measured using PrestoBlue™ HS probe after 24h of treatment with different concentrations of different compounds.

Presto Blue is a cell permeable resazurin-based solution that functions as a cell viability indicator. When added to live cells, the cell-reducing environment reduces resorufin to resazurin, a red compound and highly fluorescent.
ciPTECs were seeded at the density of 15.488/ well in a 96-well plate and treated for 24h with either cisplatin, antimycin A or hydrogen peroxide, after that the cells were washed once with HBSS and incubated for 30 minutes at 37 with 10 µl of PrestoBlue® cell viability reagent (diluted 1:10 in serum-free culture medium), in the dark. Fluorescence was measured using a microplate reader with ex/em: 560/590 nm. The results are presented as the fold change to the untreated ciPTECs.

#### 3.2.3.4 Assessment of ciPTEC metaboloc activity

To assess the metabolic activity of ciPTECs and the toxicity of different compounds, the intracellular ATP concentration was measured. The CellTiter-Glo® substrate was first reconstituted with CellTiter-Glo® buffer to obtain the complete reagent. 30 minutes before the assay, the kit and the culture plate were equilibrated at room temperature. After 24 h of treatment, the reagent was added with the same volume as the media in each well. To induce cell lysis, the cell culture plate was placed on an orbital shaker for 2 min and subsequently incubated at room temperature to stabilise the luminescent signal for 10 minutes. The signal was then read using a microplate reader (TECAN, M200). The results are presented as the fold change to the untreated ciPTECs**.**

#### 3.2.3.5 Assessment of ciPTEC migratory capacity

To assess ciPTEC migratory capacity, the cells were seeded as described before (chapter 3.2.2.7) in a 96-well Essen ImageLock™ plate, cultured and treated as described. To analyze the impact of cisplatin on cell migration, the 96-well WoundMaker tool was used to scratch precise and reproducible wounds in all the wells. After wound scratching, the medium was removed, the cells were washed 2 times with HBSS and fresh SFM or A-CM without cisplatin was added to the respective wells. The plate was then monitored using live cell imaging (IncuCyte Zoom, Essen BioScience, Sartorius), and every 3 hours pictures were taken with the software. The results were analyzed after 72 h. The relative wound density (%) algorithm was used to report data.

### 3.2.3.6 Assessment of ciPTEC apoptosis

To assess the cytotoxic effect on ciPTEC, an live cell imaging apoptosis assay was used. As we have shown previously that cisplatin induces mainly apoptosis and not necrosis/necroptosis [174], we focused on apoptosis in this study.

ciPTEC were seeded as described above (chapter 3.2.2.7). Then cells were pre-treated with/without cisplatin for 1h, and then with/without A-CM /SFM as control (plus cisplatin, respectively) for other 23 hours. To analyse the amount of apoptotic cells, the cisplatin-containing medium was removed after a total of 24 h, and new SFM or CM with 40 nM of Apotracker dye was added to the cells. The plate was then cultured and analysed using live cell imaging (IncuCyte SX5, Sartorius), and every 3 h a picture was taken over a period of 72 h. Using a defined processing definition, the total integrated intensity of green fluorescence (GCUxμ$^2$/image) was measured and normalized against the cell confluence (%). The data were displayed as relative value to cisplatin-treated ciPTEC in SFM (labelled as Cisplatin in the graphs).

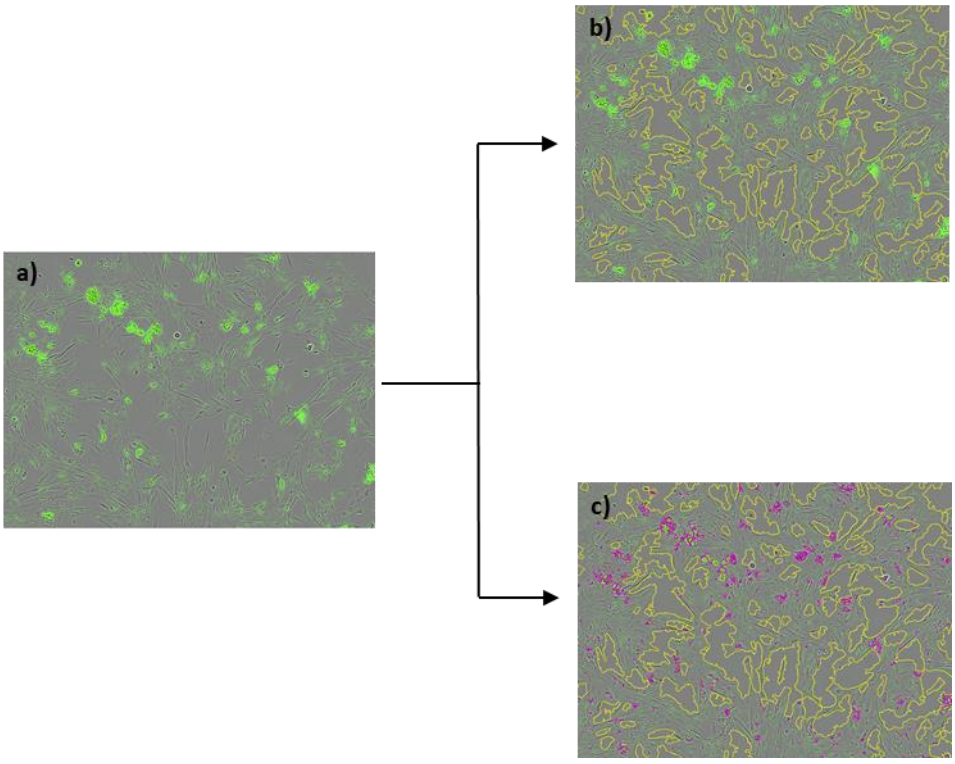


**Figure 11**. **The live cell imaging apoptosis assay**. **a**) ciPTEC phase image with green fluorescence indicating the apoptotic cells positive for the Apotracker dye. **b**) The yellow contours correspond to the mask that recognizes the ciPTEC and is used to calculate the cellular confluence. **c**) Along with the mask of the cells, purple indicates the mask that recognizes apotracker –positive cells, to measure the total integrated intensity of green fluorescence.

#### 3.2.3.7 p53 detection by Western blot

As second parameter for cell apoptosis, the level of p53 was measured by western blot. The pellet from ciPTEC (and Hela cells used as control) was resuspended in RIPA buffer (50 mM Tris-HCl, pH7.4, 150 mM NaCl, 1% Triton X-100, 1% Na-deoxycholate, 0.1% SDS, 0.1 mM $CaCl_2$, and 0.01 mM $MgCl_2$ supplemented with protease inhibitor cocktail, incubated 30 min on ice vortexing every 10 min and centrifuged 20 min at 20,000 × g. The protein concentration was determined using the Pierce BCA Protein Assay Kit, following the manufacturer's instructions. 10 µg of each sample were loaded and separated on 4–15% Mini-PROTEAN TGX Precast Gels. Cell lysates were treated with protein loading dye with freshly added β-mercaptoethanol 10%; v/v; and boiled for 5 min at 95 °C before SDS-PAGE. Proteins were subsequently blotted to a nitrocellulose blotting membrane (0.2 µm). Membranes were blocked in 5% BSA in 0.1% Tween in TBS (TBS-T). After blocking, blots were probed with the following primary antibodies diluted in 5% BSA/TBS-T: p53 (mouse, 1:100 dilution, DO-1,) and GAPDH (rabbit, dilution 1:1000, ab9485). After overnight incubation at 4 °C, membranes were washed 3 times with TBS-T and subsequently incubated with the secondary antibody dilution: polyclonal goat anti-mouse HRP (1:5000 dilution) and polyclonal goat anti-rabbit HRP (1:5000 dilution) for 1 h at room temperature followed by washing. Blots were then developed using Western Bright ECL and protein bands were detected using the FusionCapt Advanced Solo 4 . The protein bands were quantified with ImageJ software v.1.53c. The protein bands were quantified with ImageJ software v.1.53c. and normalise against the correspondent GAPDH values.

#### 3.2.3.8 Analysis of ciPTEC mRNA and miRNA expression

We further analysed gene expression of ciPTEC in response to cisplatin/A-CM treatments. First, a nephrotoxicity PCR array was performed to assess gene expression changes, second a sequencing of small RNAs to detect differentially expressed miRNAs. 3 independent technical replicates were used for the analysis.

##### 3.2.3.8.1 RNA isolation for the RT-qPCR array

To isolate total RNA, including small RNAs, the miRNeasy Micro kit was used. After 24h of treatment with cisplatin and MSC-CM, ciPTEC were harvested from a 12-well plate using 700 µl QIAzol Lysis Reagent homogenized by resuspension and

incubated for 5 minutes at room temperature. 140 µl of chloroform were added to each sample and shaken vigorously for 15 seconds, then incubated for 3 minutes at room temperature. Once the solution had homogenized, the samples were centrifuged at 4° at 12,000 xg for 15 minutes. The upper aqueous phase was transferred to a new collection tube, trying to avoid transferring any interphase. Next, 1.5 volumes of 100% ethanol were added to the aqueous phase and mixed thoroughly by pipetting. At that point, the samples were pipetted into an RNeasy MinElute spin and centrifuge at 8000 x g for 15 seconds at room temperature and after the flow-through was discarded. Now that the RNA is bound to the column, a series of washes was done, the first with 700 µl Buffer RWT followed by centrifugation at 8000 x g for 15 seconds. After discarding the flow-through, 500 µl Buffer RPE was added to the column, centrifuged at 8000 x g for 15 seconds and the flow-through discarded. Another wash step was performed with 500 µl of 80% ethanol and centrifuged for 2 min at ≥8000 x g. The RNeasy MinElute spin column was moved in a new 2 ml collection tube and centrifuged at full speed for 5 min with an open lid to dry the membrane. Finally, 14 µl RNase-free water was added directly to the centre of the spin column membrane and centrifuged for 1 min at full speed to elute the RNA.

The concentration of RNA was measured using a NanoQuant Plate™ and a microplate reader at 280 nm. The ratio of absorbance at 260 nm and 280 nm was also calculated and always exceeded the value of 2,0 indicating good purity. The samples were then stored in -80 ˚C freezer until further use.

#### 3.2.3.9 Polyadenylation Reaction and cDNA synthesis for qPCR

The synthesis of cDNA was performed using a miRNA 1st-Strand cDNA synthesis kit. The first step was the polyadenylation reaction, by adding the following components to separate RNase-free 0.5-ml microcentrifuge tubes as shown in **Table 2**.

**Table 2. Components of polyadenylation reaction**

| **Component** | **Volume per reaction** |
|---|---|
| RNase-free water | to a final volume to 20 µl |
| 5× poly A polymerase buffer | 4 µl |
| rATP (10 mM) | 1 µl |

| | |
|---|---|
| 200 ng of total RNA | X µl |
| E. coli poly A polymerase | 1 µl |

Briefly, the reaction was centrifuged to collect the contents at the bottom of the tubes and then incubated at 37°C for 30 minutes and after at 95°C for 5 minutes to terminate the adenylation. At the end of the reaction, all samples were immediately transferred to ice.

The second step was the 1st-Strand cDNA synthesis reaction. For each RNA sample, we prepared a cDNA synthesis reaction by adding the following components to RNase-free microcentrifuge tube, as shown in **Table 3**.

**Table 3. Component of cDNA synthesis reaction**

| **Component** | **Volume per reaction** |
|---|---|
| RNase-free water | to bring the final volume to 20 µl |
| 10× AffinityScript RT buffer | 2 µl |
| Polyadenylation reaction | 4 µl |
| dNTP mix (100 mM) | 0.8 µl |
| RT adaptor primer (10 µM) | 1.0 µl |
| AffinityScript RT/RNase Block enzyme mixture | 1.0 µl |

The reactions were mixed and briefly centrifuged before the incubation at 55°C for 5 minutes, at 25°C for 15 minutes, at 42°C for 30 minutes to allow reverse transcription of 1st-strand cDNA and at 95°C for 5 minutes to terminate reverse transcription. Then, 280 µl of RNase-free water was added to each reaction and stored in -20 ˚C freezer for future use.

### 3.2.3.10 Quantitaive PCR

qPCR was performed to determine the expression of miRNA. U6 small nuclear RNA was used as an endogenous control for miRNA analysis. The primers used are listed in Table qPCR primer (3.1.4.1). The miRNA QPCR master mix was used and the reagents were added as shown in **Table 4.**

**Table 4. Components of QPCR amplification reaction**

| Component | Volume per reaction |
|---|---|
| RNase-free water | to bring the final volume to 25 µl |
| 2× miRNA QPCR master mix | 12.5 µl |
| 3.125 µM universal reverse primer | 1.0 µl |
| 3.125 µM miRNA-specific forward primer | 1.0 µl |
| cDNA sample | 1.0 µl |

The qPCR was run using a Roche Light Cycler® 96 with the following cycles: 1 cycle for 10 minutes at 95°C and 40 cycles for 10 seconds at 95°C, 15 seconds at 60°C and 20 seconds at 72°C. The comparative $2^{-\Delta Ct}$ method was used for relative quantification and statistical analysis.

#### 3.2.3.11 Sequencing and bioinformatics analysis

CiPTEC mRNA was harvested 24h after cisplatin treatment with or without CM from n= 3 replicates and isolated using the miRNeasy Kit, after the isolation the samples were sent in service for sequencing. The small RNA sequencing was outsourced and performed at Novogene Corporation (Cambridge, UK). Before sequencing, the company monitored RNA degradation and contamination on 1% agarose gels. RNA purity was checked using the NanoPhotometer® spectrophotometer (IMPLEN, CA, USA). RNA integrity and quantitation were assessed using the RNA Nano 6000 Assay Kit of the Agilent Bioanalyzer 2100 system (Agilent Technologies, CA, USA).
All samples fulfilled the quality criteria.
Briefly, 3 µg of total RNA were used for library preparation and sample indexing with NEB Next Multiplex Small RNA Library Prep Set for Illumina (NEB USA). Library quality was assessed on the Agilent Bioanalyzer 2100 system using DNA High Sensitivity Chips.
The clustering of the index-coded samples was performed on a cBot Cluster Generation System using TruSeq SR Cluster Kit v3-cBot-HS (Illumina) for subsequent single-end 50 bp sequencing on the Illumina NovaSeq 6000 platform. Each library yielded an average of 13.44 +/- 2.12 million (mean +/- S.D.) reads per sample. Raw data were processed for adapter trimming and the obtained clean fragments were aligned using Bowtie software on the reference genome provided in miRbase 20.0. and checked for quality using FAST QC online tool. The percentage of

aligned reads was 71,10 +/- 1,26 % (mean +/- S.D.). MiRNA expression levels were estimated by TPM (transcript per million) through the following criteria [175]: Normalization formula: Normalized expression = mapped readcount/Total reads*1000000. Once we received raw data from Novogene, we continued with the analysis of differentially expressed miRNAs.

Differentially expressed miRNAs were evaluated using the DE-Seq R package. The P-values was adjusted using the Benjamini & Hochberg method. A corrected P-value of 0.05 was set as the threshold for significantly differential expression by default.

The graphical representation of data was performed on the average log10 transformed TPM of the Differentially expressed microRNAs (DEmiRNA) using the Pheatmap package in R [176]. The clustering analysis was performed on the Euclidean distance value which was normalised by row in the graphical representation. Each column is the result of three independent replicates.

The network building was performed using the Cytoscape online tool with the embedded KEGG pathway analysis, starting from the list of differentially expressed miRNAs.

#### 3.2.3.12 MiRNA transfection

To study the role of miR-181a-5p in the ciPTEC apoptosis, we inhibited or overexpresses the miRNA using a mix (called **siRNA mix**) composed of 20 pmol LNA_181a-5p inhibitor (**inhibitor**) or negative control (**NC-inhibitor**) (miRCURY LNA miRNA) or 10pmol LNA_181a-5p mimic (**mimic**) or negative control (**NC-mimic**) (miRCURY LNA miRNA), diluted in Opti-MEM. The siRNA mix was diluted with a second mix consisting of Opti-MeM medium containing lipofectamine (0,3 µl/100 µl Optimem) (**Lipofectamine® RNAiMAX mix**), at a 1:1 ratio and incubated at room temperature for 5 minutes, according to the manufacturer's instruction.

ciPTECs were treated for 1h with/without cisplatin, and then the medium was replaced for 23 h with/without A-CM containing 15 µM of Cisplatin and the respective 181a-5p inhibitor or 181a-5p mimic (or control). After 24h, the medium was discarded, the cells were washed twice with HBSS and fresh SFM or CM (without cisplatin) containing 40 nM of Apotracker was added to each well. As described before (chapter 3.2.3.6), ciPTEC apoptosis was monitored using live cell imaging for 3 days with 3h intervals and the total integrated intensity of green fluorescence (GCUxµm$^2$/image) and ciPTEC confluence (%) was measured.

#### 3.2.3.13 Statistics

Statistical analysis was performed using GraphPad Prism v9.4.2. Data were presented as mean ± standard deviation unless specified. *N* refers to the biological replicates for each donor per cell type, and *n* indicates the independent technical replicates. The statistical analyses run for each data set and the number of replicates are indicated in the figure legends. Statistical significance is indicated as the following: * $p < 0.05$, ** $p < 0.01$, *** $p < 0.001$, and **** $p < 0.0001$.. Additional information are reported in the corresponding figure legends.

# 4 RESULTS

## 4.1 AIM 1: Inter-laboratory study on the comparison of different MSC sources

A better understanding of cell-source differences/similarities would ease the road to overcoming some of the current challenges that the field is facing.

Until now, there is limited knowledge on which factors and to which extent induce variability in different MSC batches, tissue sources, culture conditions (media, serum source, seeding densities), culture plastics and so on and to which extent operator-based handling affects this. To address this, we performed an interlaboratory study within the RTB consortium to **a**) compare adipose (A-MSC), bone marrow (BM-MSC), umbilical cord (UC-MSC) MSC in an interlaboratory approach and **b**) to check additional quality attributes of the MSC which eventually could favour one tissue source against the others.

This work has been done together with my fellow PhD student Erika.

### 4.1.1 Cell culture harmonisation

The methods used by the three working groups in Heidelberg, Galway and Liverpool were harmonised to ensure reproducibility across centres. A common manufacturing protocol was defined, which included selecting a batch of fetal bovine serum, culture media, a defined cell seeding density and defined cryopreservation conditions.

The first step to harmonize cell culture protocols for MSC was to select a common plating density, as it can be critical for cell growth and change proliferation kinetics as MSC is a primary culture and has limited mitotic expansion potential [177]. To account for donor-to-donor variability, three individual batches (isolates from different donors) of each MSC source have been expanded and distributed within the network.

MSC from A-, BM- and UC-MSC were seeded at either 300 cells/cm$^2$ or 3,000 cells/cm$^2$ and cultured for at least 2 passages. Population doubling times were measured over time. Our results showed that A- and BM-MSC had lower cumulative population doublings when grown at high density (**Fig. 12 b,c**) and therefore a prolongation in their expansion time (**Fig. 12 a**). On the contrary, UC-MSC showed higher cumulative population doublings at 3,000 cells/cm$^2$ (**Fig. 12 d**), which translated to an decrease in doubling times.

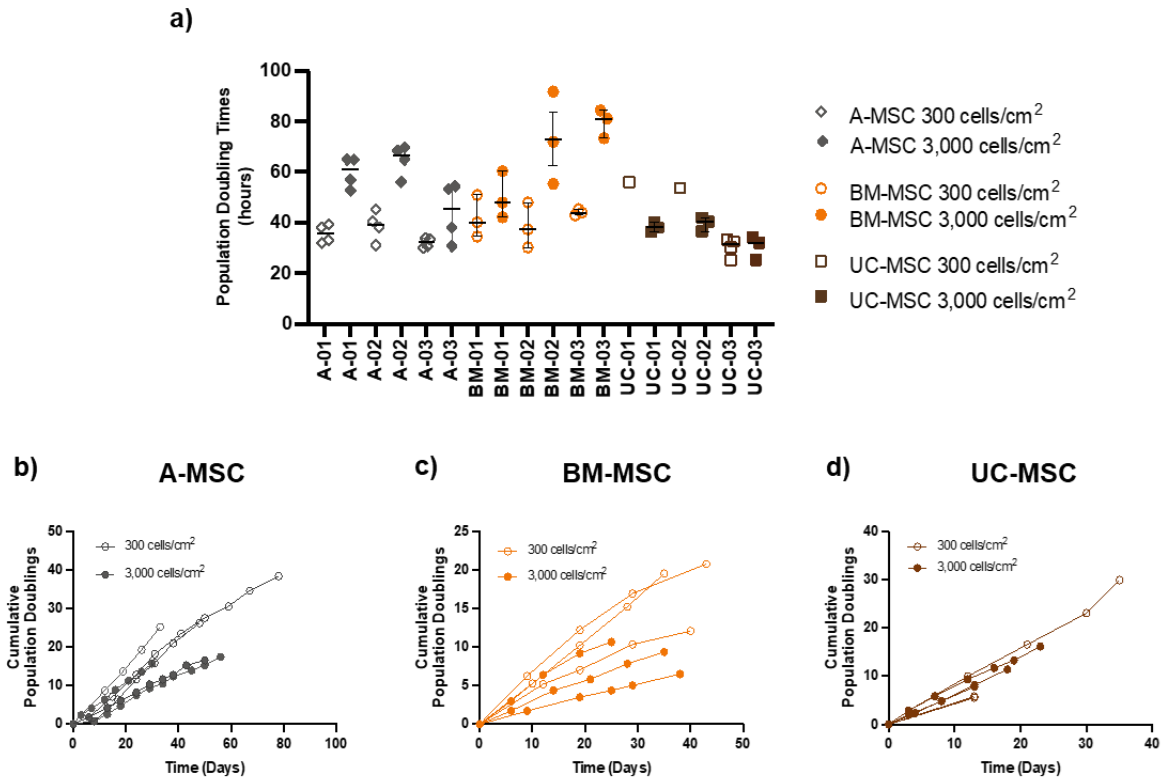


**Figure 12. Seeding density affects proliferation potential of MSC from different tissue sources**

Population doubling times of all MSC and both seeding density (**a**). Cumulative population doublings of (**b**) A-MSC (**c**) BM-MSC (**d**) UC-MSC seeding at 300 (empty symbols) and 3,000 cells/cm$^2$ (filled symbols) in all three different centres. All graphs N=3. The figure has been modified from [166].

### 4.1.2 Characterization of t MSC from different tissue sources

#### Growth kinetics

To assess whether proliferation capacity differs with respect to the tissue source, population kinetics were monitored for MSC grown between passages four and seven. A-, BM- and UC-MSC, each from three different donors, initiated in one laboratory, were shipped as cryopreserved aliquots to the three centres.

At these centres, each aliquot was thawed and cells were cultured according to the harmonised culture protocol (**Table 5**), for three passages in all the centres to determine their growth kinetics (**Fig. 13 a**).

**Table 5.** Harmonised and not harmonised conditions used in our experiment set-up

| HARMONISED CONDITIONS | NOT HARMONISED CONDITIONS |
|---|---|
| • Medium<br>• FBS<br>• Seeding density<br>• Calculation of PD and PDT<br>• FACS protocol<br>• Differentiation protocol | • Cell culture plastic<br>• Density for passaging<br>• Cell counting method |

Despite MSC being isolated in different laboratories and shipped internationally, there was a trend of consistent growth kinetics across all centres.

In all three centres, BM-MSC displayed lowest proliferation rates (PDT 90.81 ±10.57 hours, 66.78 ± 16.32 hours, 95.72 ± 28.02 hours in Heidelberg, Galway and Liverpool respectively). A-MSC proliferated fastest (43.17 ± 3.84 hours, 37.25 ± 1.64 hours, 51.10 ± 1.25 hours in Heidelberg, Galway and Liverpool respectively) followed by UC-MSC (68.07 ± 9.11 hours, 38.06 ± 1.04 hours, 46.06 ± 9.47 hours in Heidelberg, Galway and Liverpool respectively).

Site-to-site variations were also observed, especially for A- and UC-MSC where the doubling times were statistically significantly different when compared between different centres (**Fig. 13 a**).

**Adipogenic and osteogenic differentiation potential**

MSC are commonly identified by their ability to differentiate towards mesodermal lineages. Cell cultures were induced to undergo adipogenic and osteogenic differentiation using in-house protocols. Analysing their differentiation capacity, we found high levels of variability, mainly related to the inter-lab handling, tissue origin, and donor intrinsic factors. Our results showed that A- and BM-MSC were the two cell types capable of differentiating into adipocytes and osteocytes, while UC-MSC showed no differentiation potential into both lineages (**Fig. 13 b**).

In general, BM-MSC have shown a greater ability to differentiate in both lineages, although they demonstrated a high degree of variability when comparing both inter-laboratory data and donor-donor results. A-MSC showed similar levels of differentiation in all centers, except for one isolate. Comparing centres, data from Heidelberg and Liverpool were quite similar regarding the degree of differentiation against the undifferentiated control, whereas in Galway the differentiation of all MSC

remained relatively modest. There also the differences in the fold-change was more modest as within Heidelberg and Liverpool (**Fig. 13 b and c**).

**Immune phenotype**

Typically, MSC are defined by a combination of phenotypic characteristics, positive and negative markers, that are evaluated by flow cytometry [55]. All MSC sources showed consistently high levels (> 95%) of positive MSC markers, including CD73, CD90 and CD105 across all three centres (**Fig. 13 d, e and f**). Only A-MSC showed high levels of CD34 (10.21 ± 12.96% in Heidelberg and 18.40 ± 11.69% in Liverpool) and CD45 (10.81 ± 7.77% in Liverpool). Noticeable levels of HLA-DR were also observed in BM-MSC in Liverpool and Heidelberg (3.70 ± 3.36% and 7.33± 6.51% in Heidelberg and Liverpool, respectively), but not in Galway.

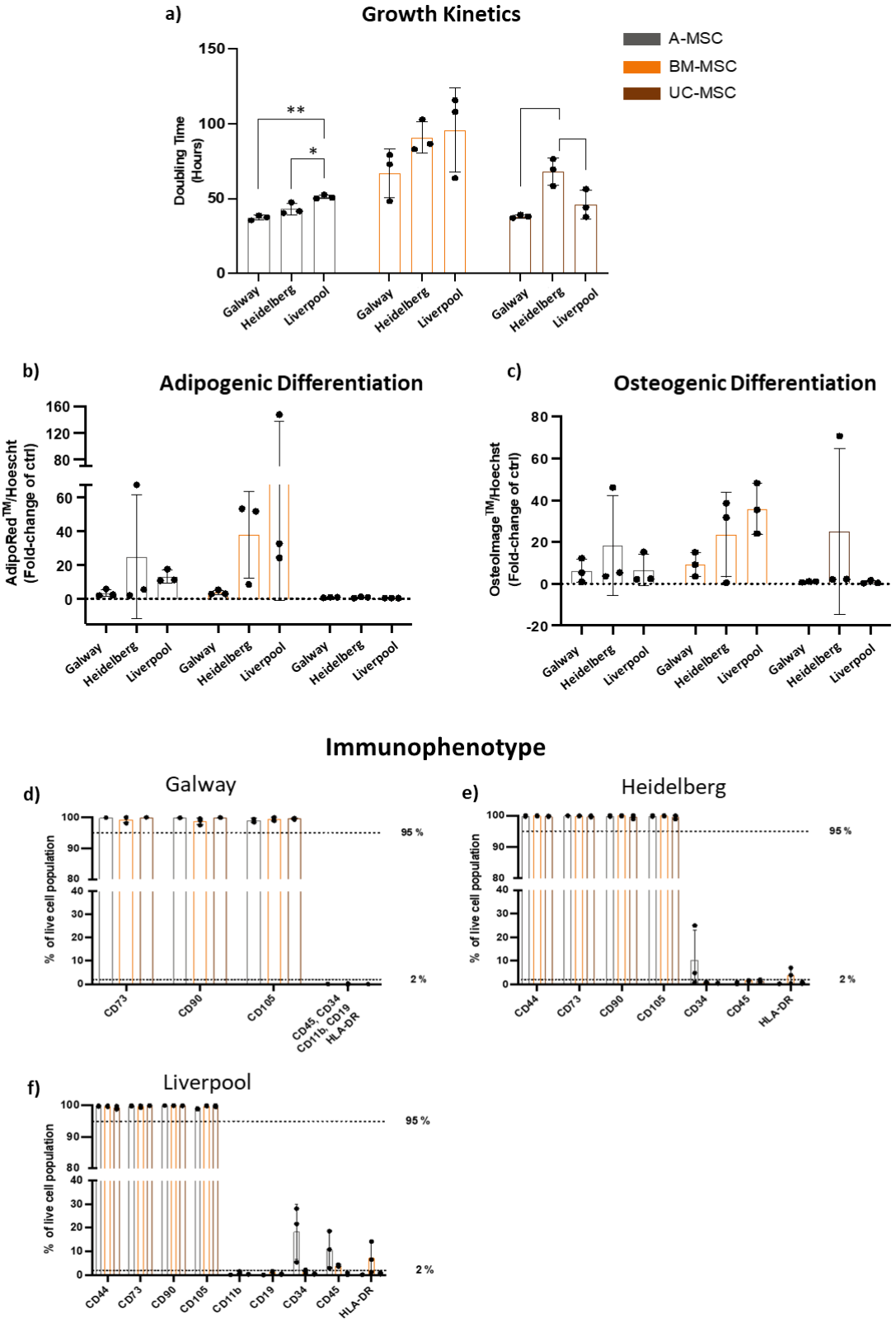


**Figure 13. Site and tissue-source dependent differences in proliferation kinetics, differentiation potential and marker expression MSC across independent laboratories.** (**a)** Doubling times of A- BM- and UC-MSC divide for site. (**b,c**) A-, BM- and UC-MSC differentiation capacity in adipogenic and osteogenic assay. (**g-i**) Analysis of the immunophenotype of A-, BM- and UC-MSC by flow cytometry. Data displayed as mean ± SD, N=3. One-way ANOVA with Tukey's multiple comparison corrections, * = $p < 0.05$, ** = $p < 0.001$, ** = $p < 0.001$, **** = $p < 0.001$. The figure has been modified from the [166].

### 4.1.3 Functional activity of different MSC sources

To investigate whether and to which extent MSC of different tissue sources differ, we assessed key functional characteristics. Immunomodulatory functions were tested in the site in Heidelberg, pro-angiogenic and pro-migratory function in the site in Galway. Further, the site in Liverpool performed an in vivo tracking of luminescently labelled MSC.

#### 4.1.3.1 Angiogenic and endothelial wound healing properties

In regenerative medicine, MSC have been suggested as a cell-therapy strategy because of their capacity to repair tissue and promote angiogenesis [178].

Our colleague in Galway addressed the pro-angiogenic and pro-migratory capacity of MSC-CM on human umbilical vein endothelial cells (HUVECs).

The angiogenic properties of conditioned media (CM) produced by A-, BM-, and UC-MSC respectively, were comparatively assessed in vitro by testing the ability of their secreted factors to stimulate tube-formation of endothelial cells when seeded on a Matrigel$^{TM}$ substrate. HUVEC treated with BM-CM formed a larger and more complex tubular network with a significant number of segments (F**ig. 14 a**), junctions (**Fig. 14 b**) and closed circuits (**Fig. 14 c**) compared to A- and UC-CM. Large donor-to-donor variability was observed across all cell sources, significant for BM-MSC. To quantify the amount of angiogenic factors in the MSC-CM, an antibody array was used . While all sources secreted comparable levels of angiogenic factors, there were differences in key factors like VEGF and IGFBP-1 and 2, which were higher in BM-MSC, or IL-8 and MCP-1, which were higher in UC-MSC (**Fig. 14 e**).

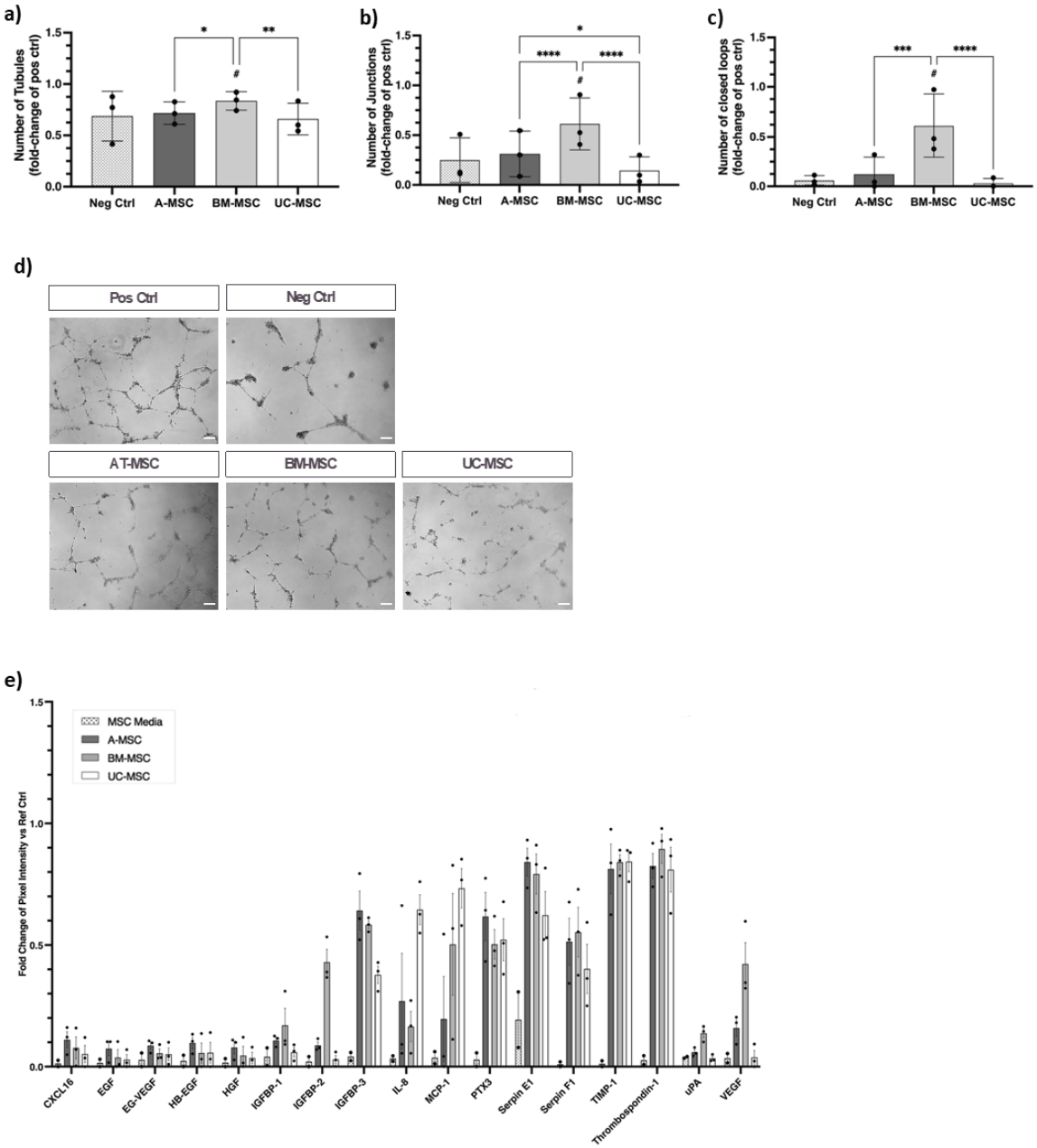


**Figure 14**. **MSC-CM exerts, source-dependently, pro-angiogenic activity**. (**a-c**) The graph reports the number of tubules, junctions and closed loops induced by treating HUVECs with CM from A-, BM- and UC-MSC, respectively. α-MEM served as negative control and EGM as positive control. (**d**) Representative phase contrast images of tubule-like networks in culture. (**e**) Differential angiogenic proteomic profile for each MSC-CM using an antibody array. Data is expressed as a fold change of the reference spots. Data is displayed as mean ± SD, N=3, n=3. Two-Way ANOVA with Tukey's multiple comparison corrections, * = $p < 0.05$, ** = $p < 0.001$, ** = $p < 0.0001$, **** = $p < 0.00001$. # Significance relative to negative control. The figure has been modified from [166] .

Subsequently, my colleague tested the ability of MSC-CM to induce endothelial cell migration in an in vitro wound healing scratch assay. As depicted in **Figure 15**, the addition of BM-CM resulted in a significant reduction in the scratch gap after 8 (35.03 ± 6.8 %) and 24 hours (58.3 ± 10.36 %) compared to the negative control (MEM-

Alpha) (13.73 ± 1.26 % at 8 hours and 3.5 ± 3.3 % at 24 hours). BM-CM was significantly superior to A-CM at 24 hours (22.4 ± 2.9 %) and UC-CM at 8 (18.01 ± 1.7 %) and 24 hours (18.1 ± 6.15) (**Fig. 15 e-f**). Noticeably, donors with enhanced endothelial wound healing properties were also prone to exhibit superior angiogenic properties.

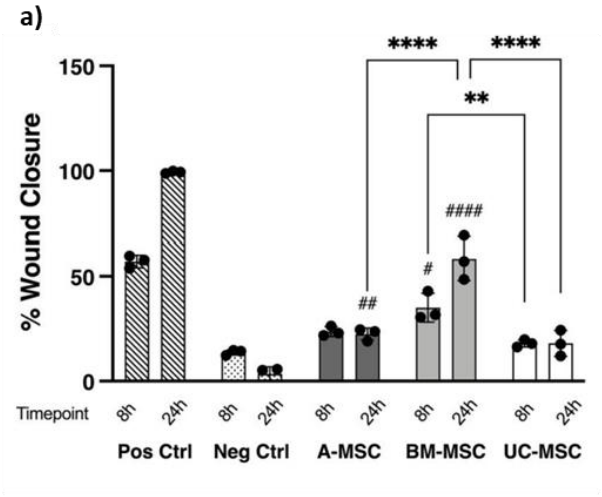


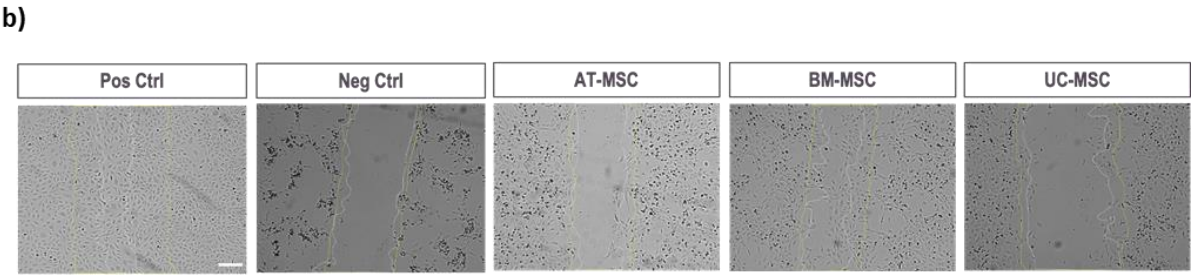


**Figure 15. BM-MSC-CM is superior to A- and UC-MSC-CM in inducing HUVEC migration in an in vitro wound scratch assay**

(**a**) A-, BM- and UC-CM induced endothelial cell migration in an in vitro wound healing model at and 24 hours after injury. (**b**) Representative phase contrast images at time 24 hours after scratch; yellow lines show the wound width at time 0 hours and white lines at time 8 hours after scratch. Data displayed as mean ± SD, N=3, n=3. Two-Way ANOVA with Tukey's multiple comparison corrections, * = $p < 0.05$, ** = $p < 0.001$, ** = $p < 0.0001$, **** = $p < 0.00001$. # Significance relative to negative control (serum-free α-MEM medium was used as negative control, α-MEM media with FBS was the positive control). The figure has been modified from [166] .

#### 4.1.3.2 Immunomodulatory properties

Immunomodulation is a key MSC therapeutic effect [178]. The ability to inhibit PHA-driven PBMC proliferation is often taken as a measure of immunomodulatory strength [179, 180]. To investigate the immunomodulatory capacity of MSC from different sources, their ability to inhibit PBMC proliferation upon PHA stimulation was tested in a co-culture setting. These experiments were performed in Heidelberg by my colleague Erika and me. **Figure 16 a** shows that all MSC were able to suppress PBMC proliferation, as reflected by a decrease in the number of proliferating PBMC when co-cultured with MSC compared to those cultured alone. A-MSC exhibited the highest degree of proliferation inhibition (0.17 ± 0.52 fold), followed by BM- (0.52 ± 0.07 fold) and UC-MSC (0.61 ± 0.21 fold). In addition, we compared the ability of MSC to inhibit PBMC proliferation with their ability to secrete IDO upon IFN-$\gamma$ stimulation [167]. The level of intracellular IDO, indicated by the mean fluorescence intensity (MFI) value, was highest in A-MSC, followed by BM- and UC-MSC. In addition, A-MSC showed greater donor-to-donor variability (**Fig. 16 b**). The percentage of cells positive for IDO staining showed the same order, A-MSC followed by BM- and UC-MSC; however, there was a decrease in variability in donor-to-donor variability observed in all MSC sources. (88.77 ± 12.04%, 76.17 ± 6.52% and 59.77 ± 14.15 % for A-, BM-, UC-MSC, respectively; **Fig. 16 c**).

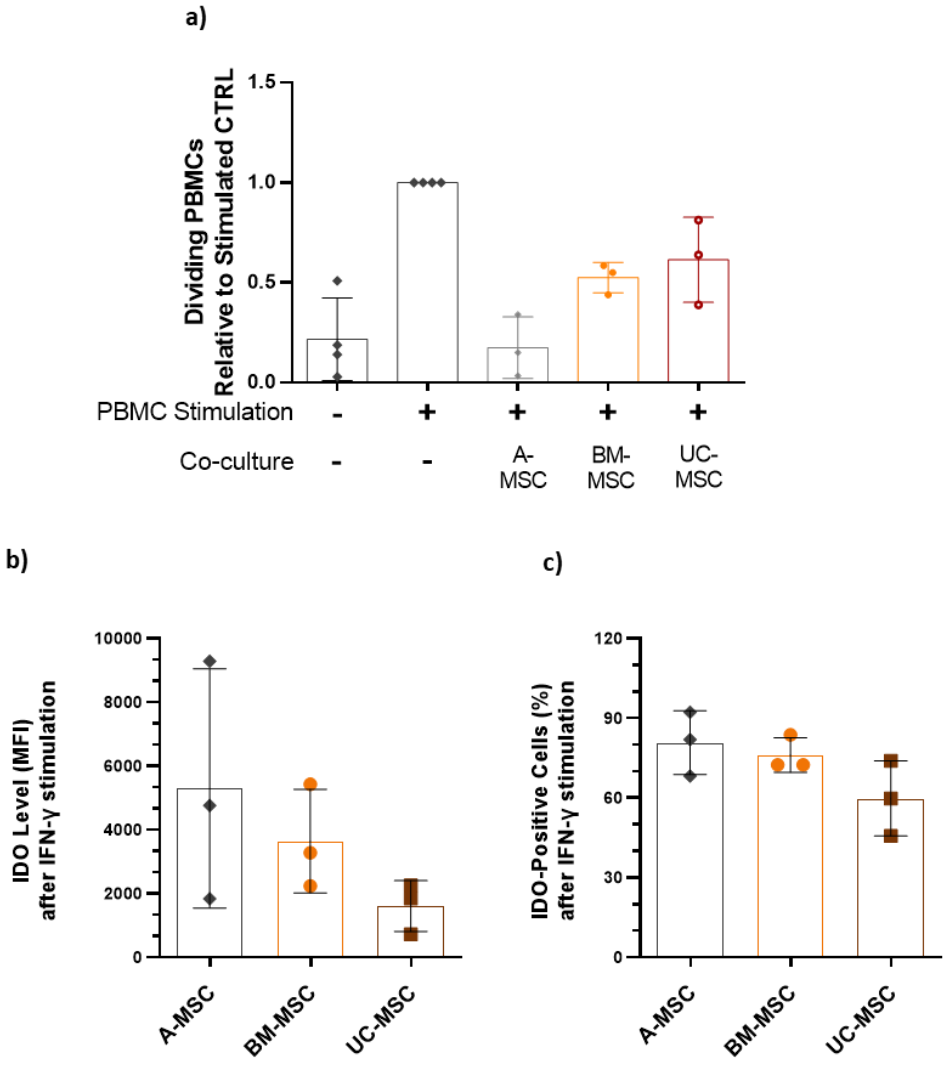


**Figure 16. A-MSC exert highest immunomodulatory capacity.**

(**a**) PBMC proliferation upon PHA stimulation after five days co-culture with MSC . All values were normalised to PHA-stimulated monocultured PBMCs. (**b**) Mean fluorescence intensity of intracellular IDO of MSC after being treated with IFN- γ for 24h. (**c**) The percentage of cells positive for IDO intracellular staining. Data are displayed as mean ± SD from N=3, n = 3. Two-Way ANOVA with Tukey's multiple comparison corrections, * = $p < 0.05$. The figure has been modified from [166] .

### 4.1.3.3 In vivo biodistribution in healthy mice

Finally, Liverpool compared the biodistribution of luc2 firefly luciferase positive MSC (FLuc+) following their intravenous administration to healthy C57BL/6J albino mice. The bioluminiscence images show that - immediately after administration - all the signals from the injected cells were directed towards the thoracic region of the body, which is the equivalent of the lungs, (**Fig. 17 a**). On day 0, all 3 cell sources showed a comparable signal for A, BM and UC cells respectively; **fig. 17 b**). 24h after infusion, the signal was strongly reduced and there was no sign of migration of the

cells from the lungs to other sites or organs. At this time point, the signal coming from the BM-MSC seemed lower than the signal coming from the two other cell types (**Fig. 17 a**). Three days after the administration, while most mice receiving BM cells did not show any signal, still a limited signal was detected in mice having received A- and UC-MSC, (**Fig. 17 a**). After seven days, no mice showed detectable bioluminescence (**Fig. 17 a**), and also the quantitative analysis of the bioluminescence signal showed no signal anymore (**Fig. 17 b**).

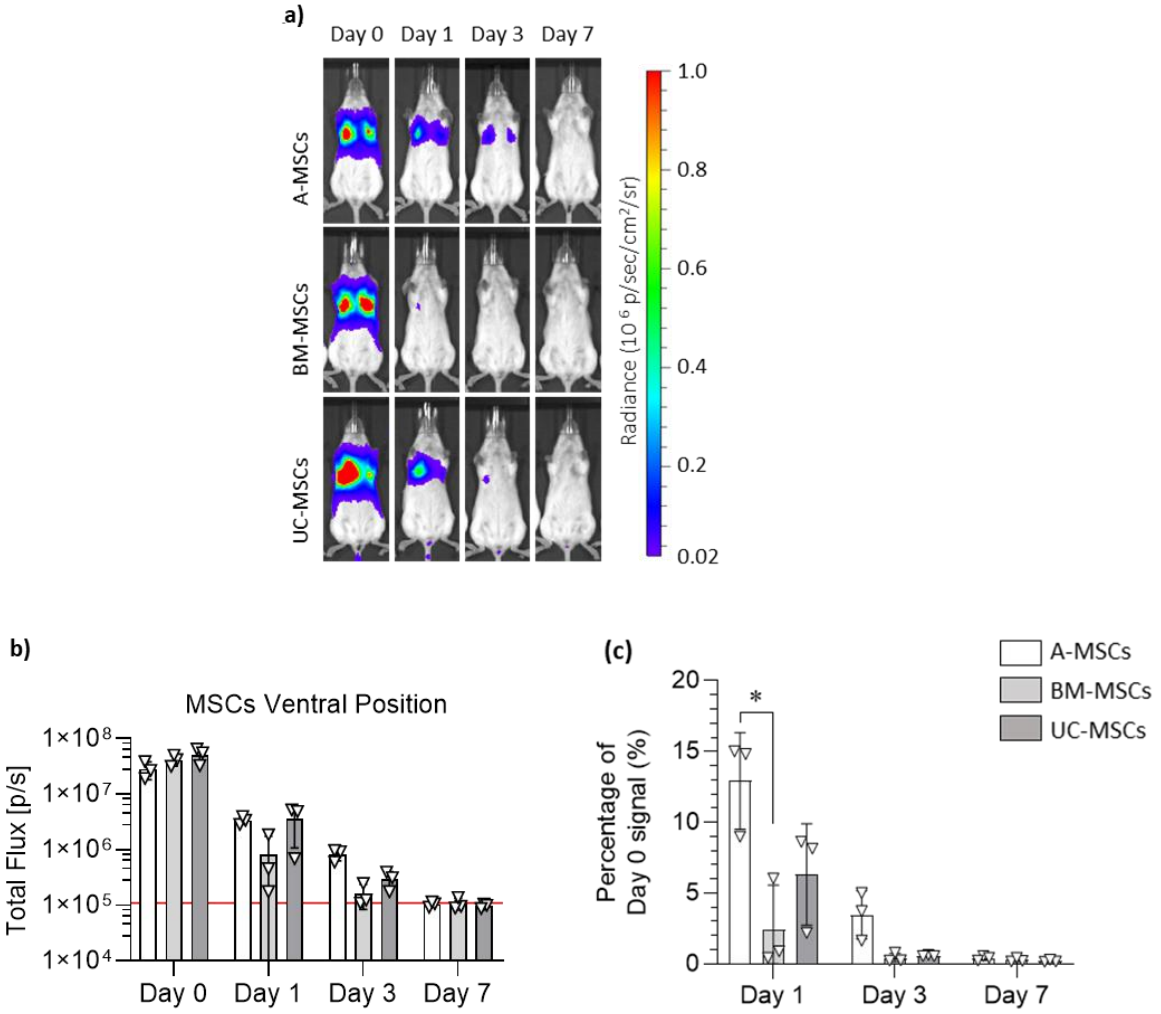


**Figure 17**. **In vivo biodistribution of MSC**. All MSC were entrapped in the lungs and were short-lived following IV administration. (**a**) Representative bioluminescence images of mice administered with FLuc expressing A-, BM- and UC-MSC on the day of administration of the cells (day 0), and after 1, 3 and 7 days (radiance scale from 0.2× $10^5$ to 1× $10^6$ p/s/cm2 /sr). (**b**) Light output (flux) as a function of time (days) from the three different types of MSC. (**c**) Signal at day 1, day 3, and day 7 normalised to day 0 signal. Data in charts are displayed as mean ± SD from three donors for each type of MSC (4

animals used per donor). Two-Way ANOVA with Tukey's multiple comparison corrections, *p<0.05. The figure shows the results obtained in Liverpool. The figure has been modified from [166].

## 4.2 AIM 2: Comparison of A-MSC bioproducts

As introduced, some researchers favour a paradigm shift, moving from cell-based therapies to the therapeutic application of the cells secretome, or bioproducts contained therein. From a clinical perspective, the CM appears advantageous, especially regarding safety and logistic issues such as ease of manufacturing, quality control and logistics. Recently, EVs emerged as candidate mediators of therapeutic activities within the secretome of MSC [103, 181].

In this part of the thesis, we have tried to deepen our knowledge on the differential effects of A-MSC bioproducts, analysing EVs isolated with different methods, the protein-rich fraction and the complete secretome in a multicenter comparative study as part of the RTB consortium activities. This work has been performed together with my colleagues in Galway and Turin (for details, see **Fig. 9**).

### 4.2.1 Impact of isolation method on EV phenotype

The first step was the characterisation of EVs obtained by UC or SEC from three different A-MSC donors. Both EV preparations, the CM and the protein-rich fraction were first measured by nanoparticle tracking analysis (NTA) in two centers using either the Nanosight or the Zetaview NTA, using established in house protocols.

Particle concentration per cell was comparable between donors and within one method (**Table 6 a**). The particle concentrations of EV-SEC, protein-rich fraction, and CM samples were similar in both centers and among each other. Even though the methods were different, the particles were all within the expected size range of EVs (70 nm - 300 nm), with EV preparations showing a smaller mean particle diameter of 128.98 and 167.2 nm compared to the protein-rich fraction with 134.17 and 246.93 nm respectively (**Table 6 b**).

**a) # of particles/$10^6$ cells**

| NanoSight | A-MSC | EV-UC | EV-SEC | Protein-rich fraction | CM | CM-WO |
|---|---|---|---|---|---|---|
| | Donor 1 | 6.38E+06 | 5.79E+08 | 1.06E+08 | 1.57E+07 | 1.06E+08 |
| | Donor 2 | 9.75E+06 | 3.28E+07 | 2.54E+07 | 1.28E+07 | 3.40E+07 |
| | Donor 3 | 4.67E+06 | 2.35E+08 | 1.65E+08 | 1.81E+07 | 2.88E+07 |

| ZetaView | A-MSC | EV-UC | EV-SEC | Protein-rich fraction | CM | CM-WO |
|---|---|---|---|---|---|---|
| | Donor 1 | 2.13E+08 | 7.72E+08 | 7.72E+07 | 2.10E+08 | 0 |
| | Donor 2 | 7.08E+08 | 7.83E+08 | 2.17E+07 | 3.00E+08 | 0 |
| | Donor 3 | 3.17E+08 | 1.52E+09 | 4.78E+08 | 3.00E+08 | 0 |

**b) Particle diameter (nm)**

| NanoSight | A-MSC | EV-UC | EV-SEC | Protein-rich fraction | CM | CM-WO |
|---|---|---|---|---|---|---|
| | Donor 1 | 123.6 | - | 135.9 | 98 | 165.5 |
| | Donor 2 | 128.8 | 99.2 | 141.8 | 98.1 | - |
| | Donor 3 | 113.7 | 179.6 | 124.8 | 160.3 | 122.9 |

| ZetaView | A-MSC | EV-UC | EV-SEC | Protein-rich fraction | CM | CM-WO |
|---|---|---|---|---|---|---|
| | Donor 1 | 139.7 | 119.4 | 209.0 | 136.4 | 0 |
| | Donor 2 | 190.2 | 308.5 | 273.2 | 118.8 | 0 |
| | Donor 3 | 126.2 | 119.6 | 258.6 | 114.4 | 0 |

**Table 6.** The nanoparticle tracking analysis of EV-UC, EV-SEC, the protein-rich fraction, CM and CM-WO (indicates the flow-through resulted from the concentration step of CM) samples each derived from 3 different A-MSC donors. The table has been modified from the article [168].

The composition of the EV populations were analysed and compared with the remainder of the samples via flow cytometry in Turin using a defined protocol (**Fig. 18 a**). No EV marker expression was found in the CM-WO, demonstrating the non-specificity of the particle count obtained by the nanodrop NTA analysis with these samples. Based on published recommendations [105], EVs shall express certain markers, such as the tetraspanins CD9, CD63 and CD81 [105]. EV-SEC and the CM showed higher expression of CD9 and CD63 compared to UC-EV. The protein-rich fraction showed higher expression of all tetraspanins than EV-UC. CD81 was weakly positive in CM, followed by the protein-rich fraction, while EVs were negative. Both EV preparations and CM were positive for the MSC markers CD44 and CD29, but their corresponding protein-rich fraction had no detectable MSC markers. Other

markers such as CD49e, CD146 and CD105 were almost exclusively present on the EV-UCs (**Fig. 18 a**). Analyzing the immunological markers, we observed similar levels of CD29, Melanoma (MCSP), and tyrosine-protein kinase transmembrane receptor ROR1 for all bioproducts, while CD142 (tissue factor, TF) was only present in EV-UC and CD133-1 on EV-SEC.

Characterisation of the surface markers and particle size was confirmed by super-resolution microscopy, staining for the tetraspanins CD9 (blue) and CD81 (red), and the MSC marker CD44 (green). All particles were positive for CD44 and tetraspanin expression, but the marker compositions of EV-SEC preparations were different from those of EV-UC and CM. Most particles were single tetraspanin positive, with EV-UC and CM were mainly CD81 positive and EV-SEC CD9 positive (**Fig. 18 b**).

As expected, the measurement of protein concentration in the bioproducts showed CM and protein-rich fraction with a higher amount of protein while a low amount was found in the EV-UC and non-detectable in EV-SEC and CM-WO (**Fig. 18 c**). As further proof of the purity of our EVs, with the western blot analysis, we confirmed the absence of subcellular components that may have contaminated the preparations, only the protein-rich fraction and positive control of Hela cell lysate were positive for the cytoplasmic marker Calnexin (**Fig. 18 d**)

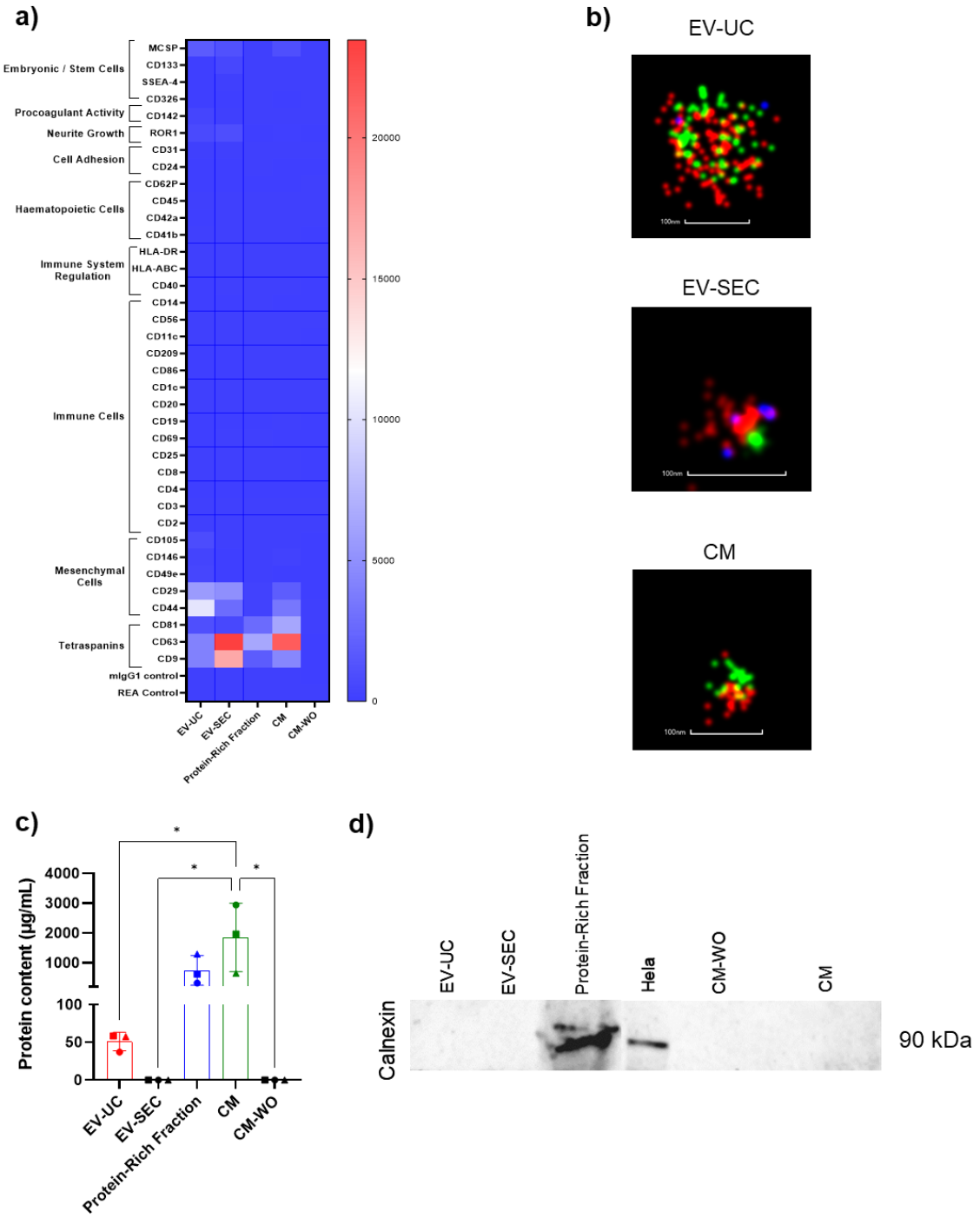


**Figure 18. Characterization of A-MSC bioproduction.** (**a**) FACS analysis using the MACSPlex exosomal kit. EV-UC, EV-SEC, Protein-rich fraction, CM and CM-WO were tested for 39 surface markers divided into groups based on their origin and function (embryonic cells, pro-coagulation activity, neurite growth, cell adhesion, hematopoietic cells, immune system regulation, immune cells, mesenchymal cells, tetraspanins and two controls). Data represented as a heatmap with the mean fluorescence intensity of N = 3 A-MSC donors per marker. (**b**) Representative super-resolution microscopy pictures of EV-UC, EV-SEC, CM. The samples are stained with CD81 red, CD44 green and CD9 blue. The scale bar is 100 nm. (**c**) Protein content analysis of EV-UC, EV-SEC, Protein-rich fraction, CM and CM-WO. (**d**) Western blot analysis of Calnexin of EV-UC, EV-SEC, Protein-rich fraction, CM-WO, CM. Cell lysates of Hela cells were used as a positive control.

Flow cytometry and super-resolution microscopy analysis was performed in Turin, protein concentration was measured in Galway and western blot analysis was performed in Heidelberg.
The figure has been modified from [168].

### 4.2.2 Differential immunomodulatory activities of A-MSC bioproducts

As described before, one key therapeutic feature of MSC is their immunododulatory capacity. Accordingly to compare the thereputic potency of the different A-MSC bioproducts, we first analyzed their immunosuppressive activity using two different assays. To best as possible adjust the concentration of the bioproducts, a cell equivalent dose for each factor was calculated and applied within the experiments.
Confirming previous observations [167, 182], the proliferation of mitogen-stimulated PBMC was inhibited exclusively by MSC being present in a direct co-culture. In contrast, no decrease in proliferation was seen when adding any of the EV preparations or the CM (**Fig. 19 a**). This showed that the lack of inhibitory activity was independent of the manufacturing mode of EVs, as both ultracentrifugation and SEC-isolated EVs lacked inhibitory strength. The flow-through resulting from the concentration step (CM-WO) was used as a control, likewise with no inhibitory activity.
However, when analysing the phagocytic activity of THP-1 monocyte-derived macrophage cells after LPS stimulation, different effects were seen. These experiments have been performed in Galway. The protein-rich fraction and the CM significantly enhanced the phagocytic activity of macrophages compared with the negative control (non-stimulated cells). It was superior to the EV-UC preparation, and also the EV-SEC stimulated a phagocytic capacity superior to the negative control and similar to that of the CM (**Fig. 19 b**).
Given the effectiveness of the EV-SEC, we tried to increase the concentration of both EVs and proteins by 10-fold and added 2 and 20 EVs (cell equivalents): THP1 cell. The higher EV concentration significantly enhanced the efficacy of both EV preparations, 10%/16.6% for 1:2/1:20 for EV-UC and 16.2%/24.2% for EV-SEC (**Fig. 19 c**), suggesting an immunomodulatory ability by EVs that depends on the dose and the isolation method used.

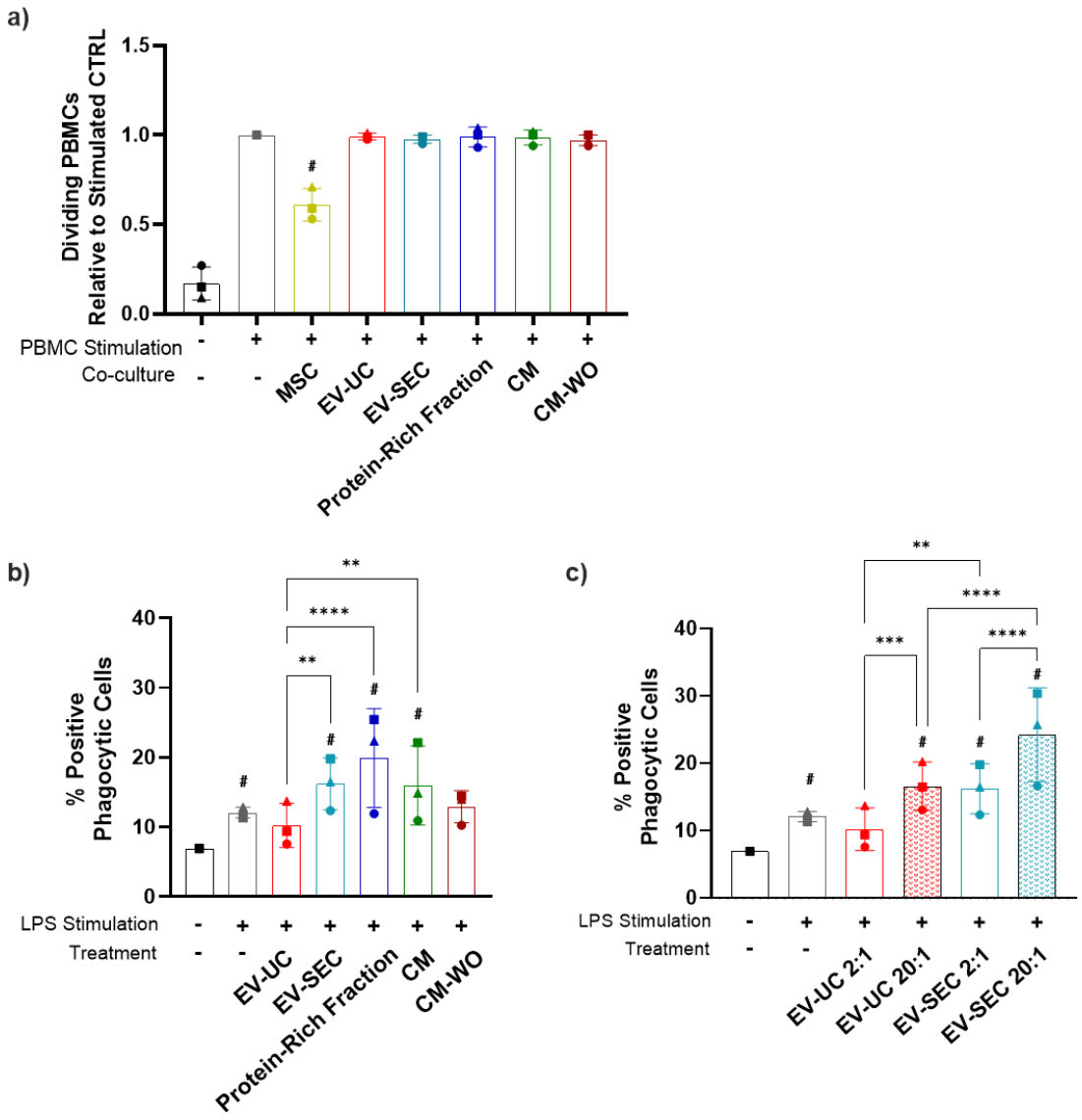


**Figure 19**. **Immunomodulatory properties of A-MSC bioproducts**. (**a**) PBMC proliferation after five days of co-culture with MSC under PHA stimulation. All values were normalized to PHA-stimulated monoculture PBMCs. (**b**) Phagocytic activity of LPS-stimulated THP-1 with EV: THP-1 cells ratio to 2:1, (**c**) phagocytic activity with increase of the EV: THP-1 cells ratio to 20:1. Data are represented as the mean ± SD of N = 3 A-MSC donors and n = 6 technical replicates. Statistical analysis was performed using Two-Way ANOVA with Tukey's multiple comparison test; * = $p < 0.05$, ** = $p < 0.001$, *** = $p < 0.0001$, **** = $p < 0.00001$. # Significance versus the negative control. The phagocytosis assay was performed in Galway. The figure has been modified from [168].

### 4.2.3 Effects of A-MSC bioproducts on cell migration

Next, we decided to investigate whether the methodology of isolation and preparation of the different bioproducts could also influence other key properties of MSC such as the induction of cell migration. The ability to induce cell migration was tested using

the in vitro wound scratch assay on endothelial cells (in Galway) and A-MSC (in Heidelberg).

The CM and the protein-rich fraction significantly enhanced endothelial cell migration after 8 hours of injury to levels of the positive control (to 8-fold and 7-fold compared to control, respectively) (**Fig. 20 a**). Although to a lesser extent, both EV preparations showed a similar impact on cell migration by increasing it by 4-fold compared to the control, while CM-WO stimulated migration only 3.1-fold.

The same effect was observed for all bioproducts promoting MSC migration. Although differences did not reach statistical significance, CM, the protein-rich fraction, and the EV-UC bioproducts showed a trend to enhance MSC migration (**Fig. 20 b**), while EV-SEC was less effective. As for the phagocytosis assay, by increasing the concentration it was possible to stimulate migration of MSC, this time the EV-UC showed a dose-dependent trend, instead EV-SEC at higher concentrations exerted only a marginal increase in MSC migration (**Fig. 20 c**).

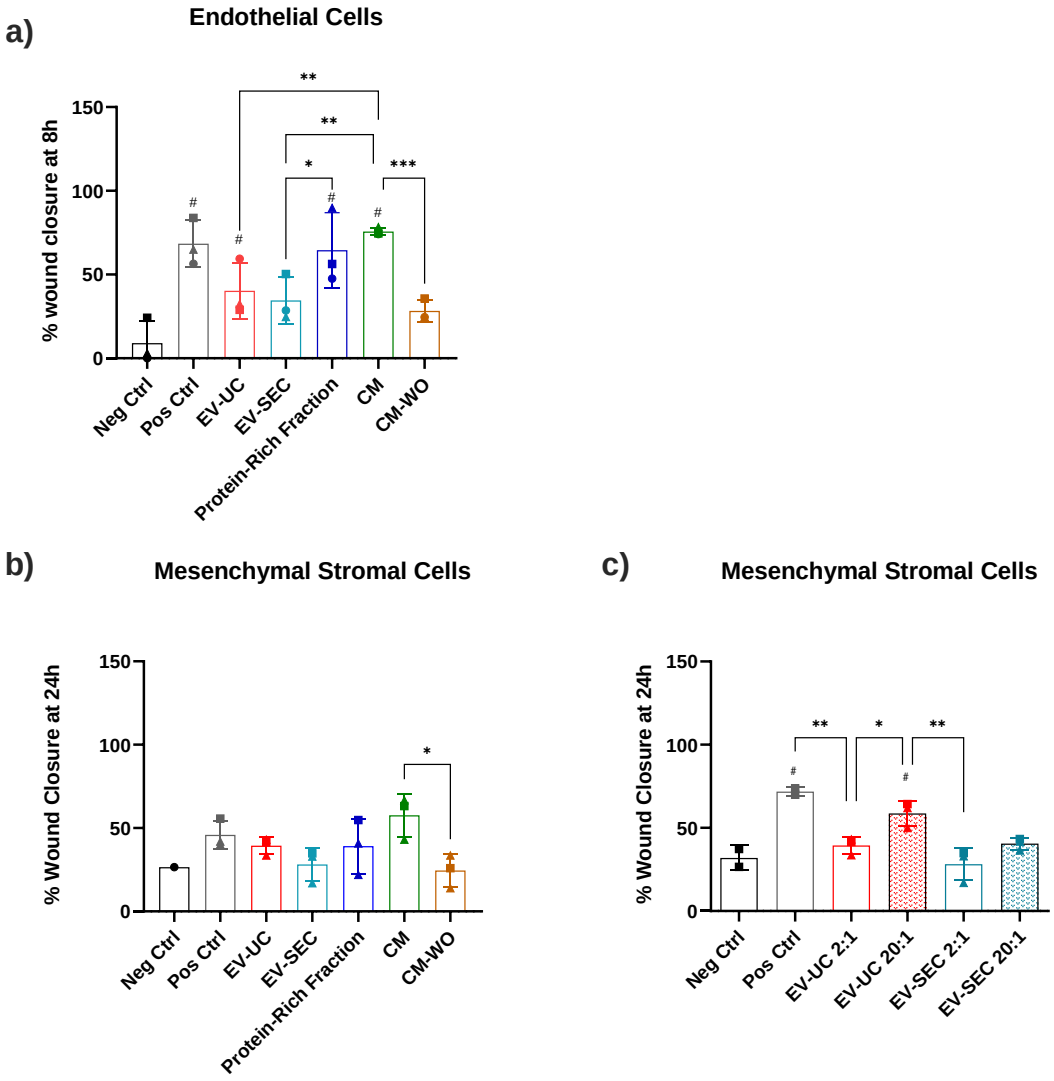


**Figure 20**. **Enhancement of cell migration by A-MSC bioproducts**. (**a**) Migratory capacity of endothelial cell migration in an in vitro wound healing model after 8h of the scratch. concerning the EndoGro-LS medium without FBS was used as negative control and EndoGro-LS medium with FBS and VEGF as positive control. (**b**) Migratory capacity of A-MSC in vitro wound healing model after 24 h after injury, α-MEM media without FBS was used as negative control and α-MEM media with FBS as positive control. (**c**) Migratory capacity of A-MSC with increasing in the ratio of EV:MSC. Data are represented as the mean ± SD of N = 3 A-MSC donors and n = 6 technical replicates. Statistical analysis was performed using Two-Way ANOVA with Tukey's multiple comparison test; * = $p < 0.05$, ** = $p < 0.001$, *** = $p < 0.0001$, **** = $p < 0.00001$. # Significance versus the negative control. Wound scratch assy on endothelial cell was performed in Galway, wound scratch assy on MSC was performed in Heidelberg. The figure has been modified from [168].

### 4.2.4 Effects of A-MSC bioproducts on angiogenesis

So far we have been able to observe marked differences in the efficacy of MSC bioproducts, in particular we have shown how different isolation methods can influence their function. Finally, we tested the bioproducts for their ability to induce angiogenesis/vascular tube formation. Arguing whether the international shipment of samples may have compromised their potential therapeutic effects, these assays were run again as a multicenter approach, in all three expert centres participating in this study using their established in-house methods. The angiogenic capacity of A-MSC bioproducts was taken as the ability to induce the formation of tubule-like structures in endothelial cells seeded on an extracellular matrix, either Matrigel™ or Geltrex. Results were normalized to the negative control (serum-free medium) and compared among centers, VEGF was added and used as positive control.

In general, the rates of angiogenesis induction were consistent across centers. CM and protein-rich-fraction induced tube-like formation to the highest degree, comparable to levels induced by VEGF, whereas EV-UC and EV-SEC induced only a moderate angiogenic effect (**Fig. 21 a and b**). The lack of angiogenic induction achieved by the EV preparations was confirmed when increasing the dose 10-fold. Despite a mild increase in tube formation generated by EV-SEC, all populations displayed comparable rates to that of the negative control (**Fig. 21 c**).

Based on these results, and to confirm the active role of VEGF in angiogenesis, we measured the levels of VEGF present in each of the bioproducts. As expected, VEGF was detected only in CM samples and protein-rich fraction, but not in EV and CM-WO populations (**Fig. 21 e**), similar to the total protein amount (**Fig. 21 c**). Moreover, upon adding ZM323881, a VEGFR2 inhibitor, the capacity of CM and the protein-rich fraction to stimulate tube formation (**Fig. 21 g-h**) was significantly reduced, thus confirming the critical role of VEGF in the tube formation assay.

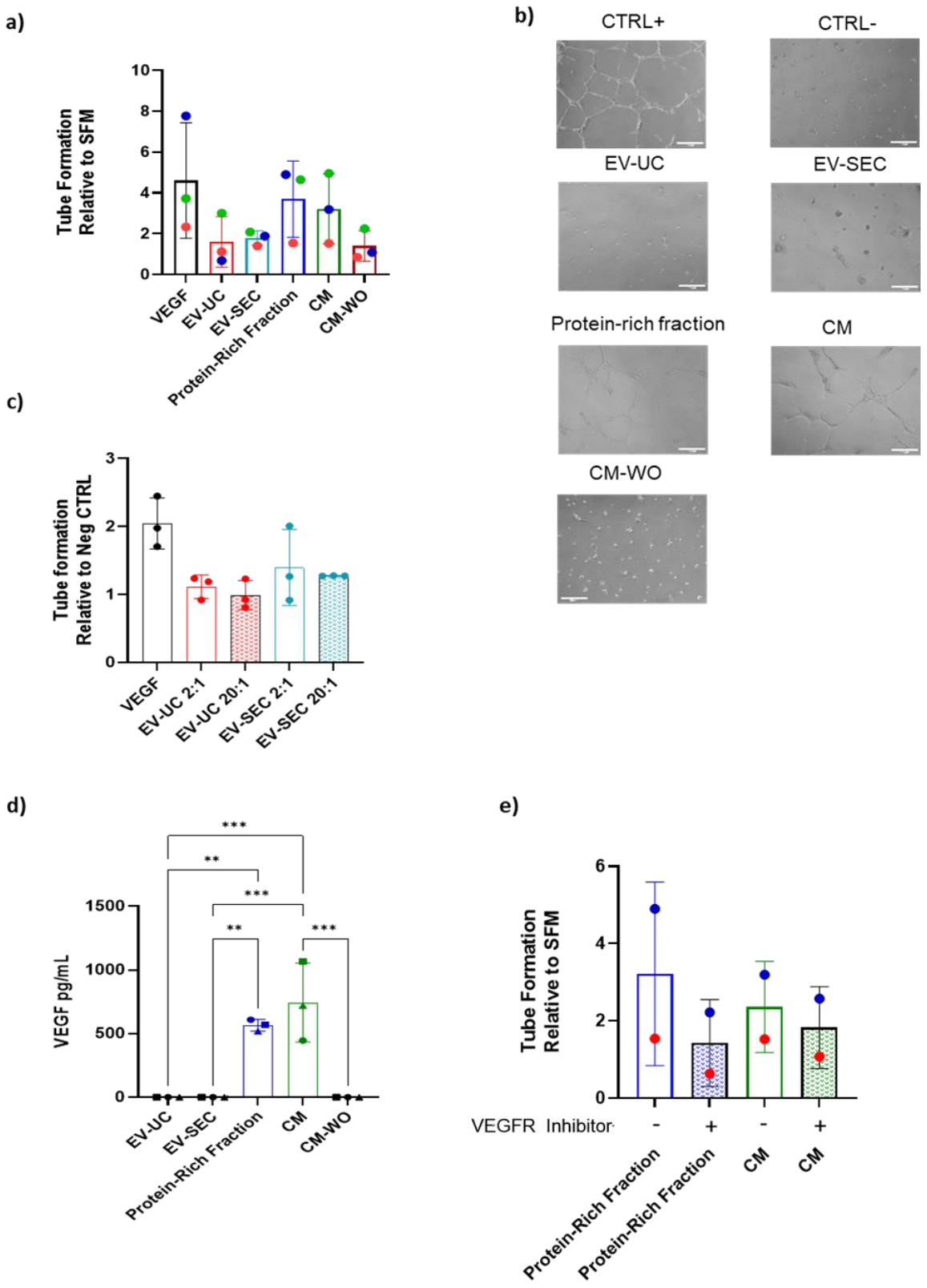


**Figure 21**. **Angiogenic properties of A-MSC-derived bioproducts**. Tube formation assay was chosen as inter-center comparison between centers. (**a**) Ability of A-MSC bioproducts to stimulate tube formation in vitro is represented as the relative tube formation of the negative control (EndoGRO-LS medium without VEGF). Dot colours represent the individual data from the 3 centers. (**b**) Representative phase contrast images of tubule-like networks in culture. (**c**) Tube formation assay with

increasing in the EV ratio to 20:1 (**d**) Measured of VEGF concentration in all bioproduction. (**e**) Tube formation assay with addition of 1 µM of ZM32381 in the CM and the protein-rich fraction preparations, this assay was performed in 2 centers. Data are represented as the mean ± SD of N = 3 A-MSC donors and n = 3 technical replicates per center. Statistical analysis was performed using One-Way ANOVA (D, E). * $p < 0.05$, ** $p < 0.01$, *** $p < 0.001$. The figure has been modified from [168].

## 4.3 AIM 3: Role of microRNAs in the protective effect of A-CM in an in vitro kidney injury model

### 4.3.1 Cisplatin cytotoxicity

In the third and final part of the thesis, we established an in vitro model capable of mimicking kidney cell damage. As a cellular model of acute kidney injury, the conditionally immortalised proximal tubule epithelial cell line (ciPTEC) was used for the experiments. We aimed to test the protective capacity of the A-MSC secretome in this injury model and then to identify the molecular mechanism activated by the presence of the secretome. We hypothesized that miRNAs are involved.

To establish the best nephrotoxicity model for our analysis, ciPTECs were treated with three compounds: cisplatin, antimycin A, and hydrogen peroxide. Each compound was tested at increasing concentrations in various read-outs; viability, apoptosis, intracellular levels of p53 and migration in the wound/scratch assay were chosen being reproducible and easy to quantify (**Fig. 22**).

Our goal was to find a concentration capable of moderate toxicity in order to test the capability of recovery induced by the A-CM. We observed the most robust and reproducible results using cisplatin as the toxic agent. After 24h of cisplatin treatment, all the biological functions were dose-dependently reduced (**Fig. 22 a,d,g**). Antimycin A, on the other hand, showed some impact only on cell viability (**Fig. 22 b**), though in a dose-independent manner. It did not compromise the metabolic and migratory activity, except for the higher concentration where we observed a reduction in cell migration (**Fig. 22 h**). A similar trend was found after treatment with hydrogen peroxide but only reducing cell viability, while metabolic activity and migration did not seem to have been affected by treatment (**Fig. 22 c,f, i**).

The treatment with a concentration of cisplatin of 15 µM was chosen for further experiments, it lowered viability significantly but not dramatically (25%), reduced metabolic activity (20%), and migration (36%).

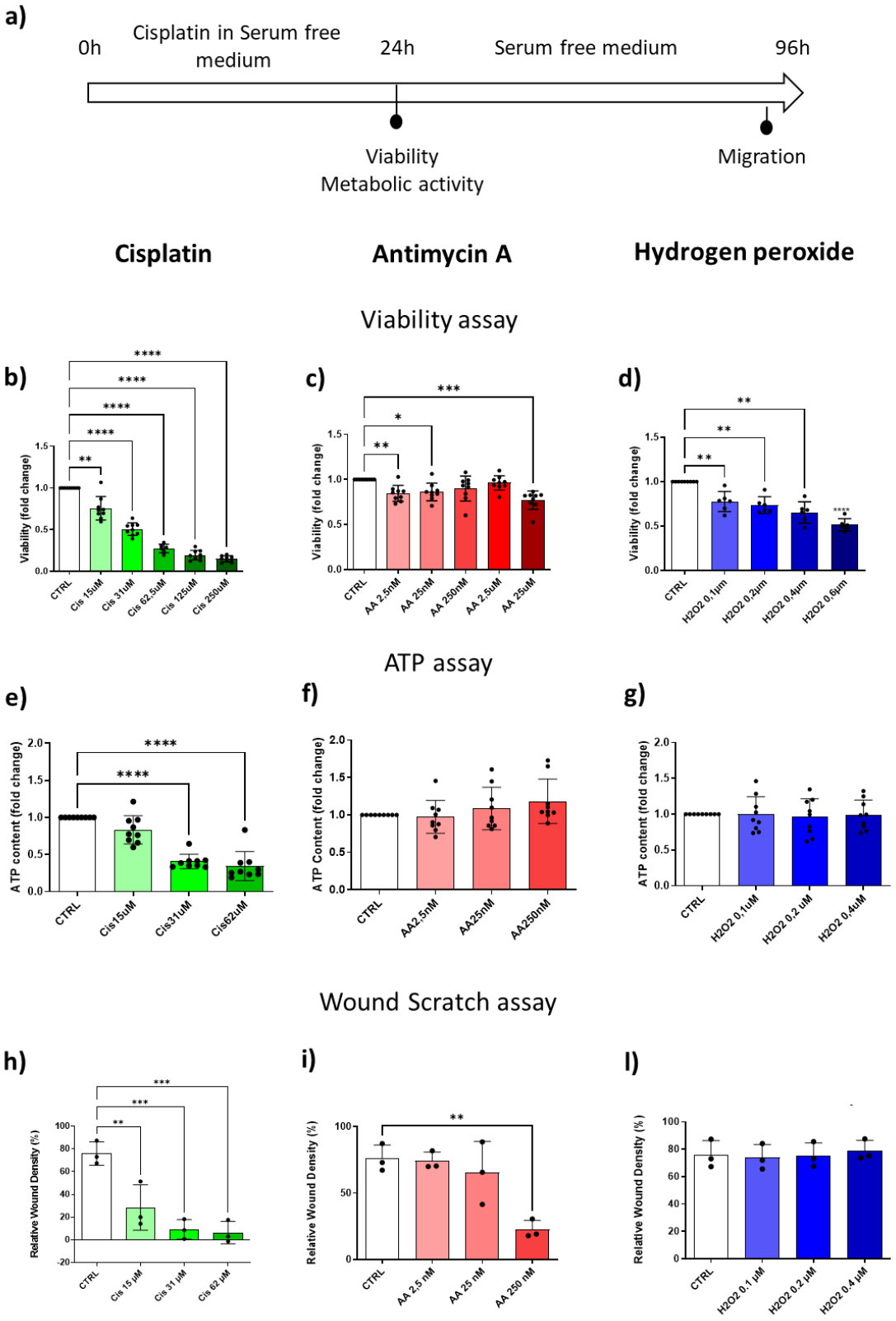


**Figure 22. Establishment of the in vitro injury model**

(**a**) Schematic overview of experimental set-up. CiPTECs were treated for 24h with different concentrations of cisplatin (Cis), antimycin A (AA) and hydrogen peroxide ($H_2O_2$). Viability (**b,c,d**), and metabolic activity (ATP production) (**e,f,g**) were evaluated after 24h of treatment. Data are displayed as normalised values against the untreated control (CTRL)**.** To assess their migratory capacity(**h,i,l**),

24 h post-treatments, the ciPTEC monolayer was scratched and the compounds-containing medium was discarded and replaced with fresh SFM. The closing of the wound was monitored using live cell imaging and quantified 3 days after the wound was made. Wound scratches were presented as relative wound density in %. n=3 independent experiments were performed. Data are displayed with mean ± SD. *p≤ 0.05, **p≤ 0.01, ***p ≤ 0.001 as calculated using One-Way ANOVA with Tukey's multiple comparisons test.

### 4.3.2 A-MSC-conditioned medium protects renal cells from cisplatin toxicity in vitro injury model.

Once we had chosen cisplatin and its concentration, we investigated the effect of A-MSC secretome on cisplatin-treated ciPTECs (**Fig. 23**).

For this purpose, ciPTEC were treated with cisplatin for 1h. Then A-CM was added to the cells for 23 hours. Overall by this a incubation with cisplatin for 24 hours was performed, allowing us to test the protective effect of A-CM. Cisplatin slightly, but significantly, reduced the viability of ciPTEC by 10% compared to untreated ciPTEC (**Fig. 23 b**). Cells treated with CM and cisplatin showed lowered viability as well. When analysing the expression of p53 a pronounced amelioration of cisplatin-mediated p53 induction by A-CM was observed (**Fig. 23 c**). Cisplatin significantly raised levels of p53 compared to untreated conditions (CTRL and A-CM), while the combination of cisplatin with A-CM (Cis-A-CM) tended to bring the expression levels of p53 back to normal (A-CM).

Although we have previously shown that EVs were not able to reproduce the effect of the secretome (chapter 4.2), we tested EVs in this experiment setup. Here, $5x10^8$ particles/ml of EV (same volume of protein) or the protein were added and incubated with/woithout cisplatin for 23 hours.

The EV fraction was not able to protect the ciPTEC from the cytotoxicity of cisplatin, unlike the protein fractions that were able to revert cell viability to levels comparable to the untreated ciPTECs (**Fig. 23 d)**.

The protective effect of A-CM was obvious when assessing apoptosis and migratory activity of ciPTEC. The treatment with only cisplatin significantly increased the number of apoptotic cells, but the addition of the CM reduced apoptosis by 64 % (**Fig. 23 f**). CM not only prevented cell death, but also promoted the migration of ciPTEC (**Fig. 23 g**). CM per se induced cell migration, slightly reduced upon cisplatin addition.

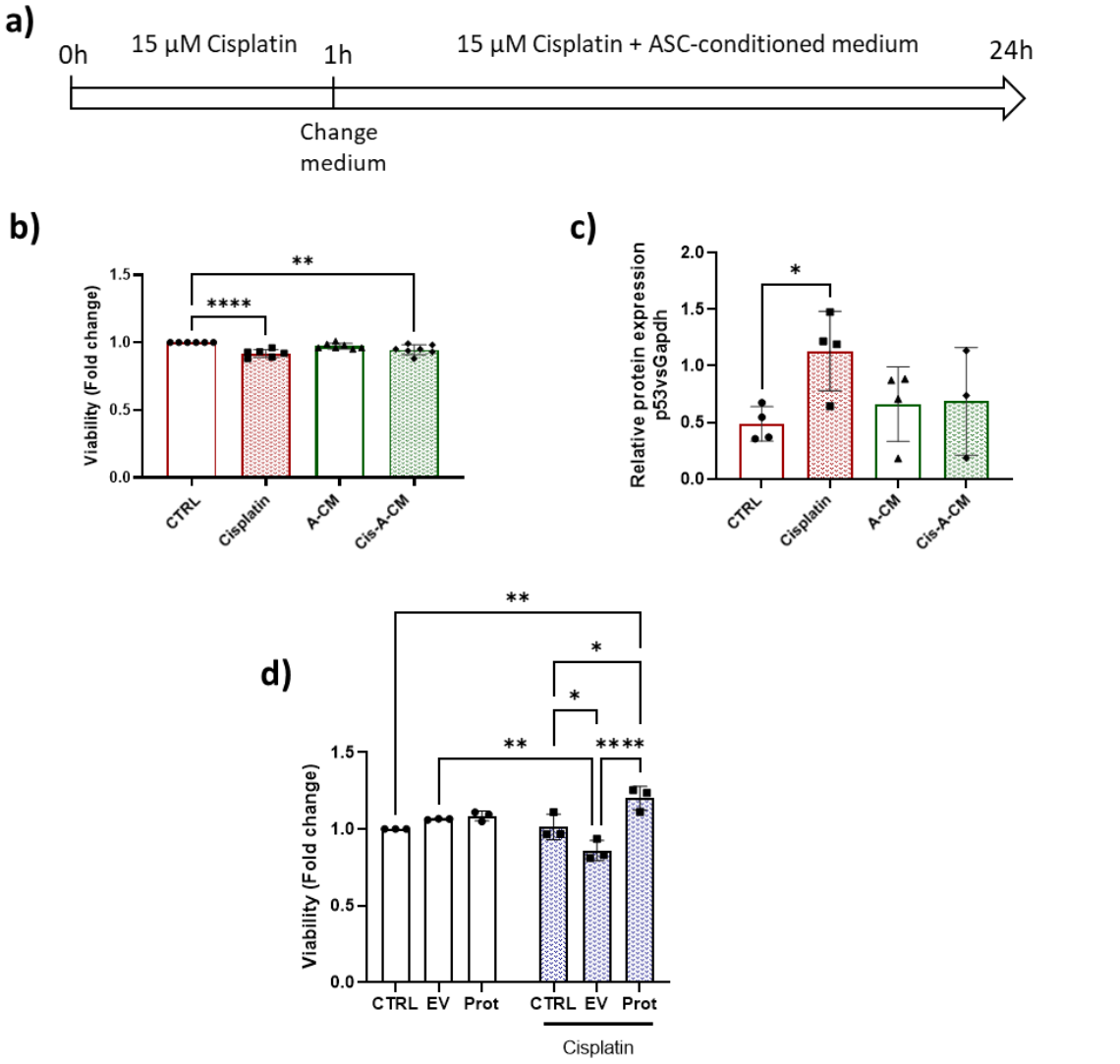
a)
0h
15 µM Cisplatin
1h
15 µM Cisplatin + ASC-conditioned medium
24h
Change medium
b)
Viability (Fold change)
CTRL
Cisplatin
A-CM
Cis-A-CM
c)
Relative protein expression p53vsGapdh
d)
Viability (Fold change)
CTRL EV Prot
CTRL EV Prot
Cisplatin
e)
15 µM Cisplatin
15 µM Cisplatin + ASC-conditioned medium
ASC-conditioned medium or SFM
0h
1h
24h
96h
Change medium
Wound Scratch
f)
Apoptotic Cells/Confluence on d3 (GCU x µm²/Image/%)
g)
Relative Wound Density (%)

**Figure 23**. **A-CM protected ciPTEC from cisplatin toxicity**. (**a, e**) Schematic overview of the experimental set-up. The effect of A-CM, derived from A-MSC was evaluated on the (**b**) viability and (**c**) levels of p53 protein in ciPTECs treated or untreated with only cisplatin for 1 hour and then in the presence or absence of A-CM for a total of 24 hours (n=4). In addition, (**d**) EVs and protein components derived from A-CM were tested on the viability of ciPTECs treated or untreated with cisplatin (n=3). Values were normalised against the untreated control cultured in a serum-free medium (CTRL). The following day, the cisplatin-containing medium was replaced with either CM or CTRL medium containing Apotracker to monitor the ciPTEC apoptosis for an additional 72 h. Apoptosis was quantified after 96h from the cisplatin treatment and normalised by the cell confluence (n=4) (**f**). To measure the migratory capacity, ciPTEC monolayer was scratched after 24h of cisplatin treatment and the wound closing was monitored for 72h. Data are displayed as individual values with mean ± SD. *p≤ 0.05, **p≤ 0.01, ***p ≤ 0.001, as calculated using ordinary one-way ANOVA Tukey's multiple comparisons test.

### 4.3.3 Cisplatin cytotoxicity changes miRNA profiles in renal proximal tubule cells

We postulated that A-CM exerted its protective effect by modulating miRNA expression in injured kidney cells. To prove this, small RNA from ciPTECs treated with/without cisplatin and with/without A-CM was isolated and small RNA-sequencing analysis was performed. Differentially expressed microRNAs (DEmiRNAs) were calculated using the DEseq2 algorithm. The highest number of significant DEmiRNAs was found when comparing A-CM and Cis-A-CM samples, suggesting that the effects observed might be due to miRNAs regulation. For further grouping the miRNAs with at least 1,000 reads and differentially expressed in at least one of the comparisons were selected (**Fig. 24 a**). From the obtained list of 37 miRNAs, we performed a bibliographic search looking for links between the various miRNAs within the list and the apoptosis pathway and on kidney related cellular systems. This approach led to three miRNA candidates: miR-181a-5p, miR-146a-5p and miR-125a-5p. Bioinformatic search for the gene targets by these miRNAs and involvement in the p53 pathway revealed a partial overlap, suggesting a potential role of the miRNAs in modulating apoptosis via p53.

The read counts data of the selected miRNAs showed downregulation in cisplatin-treated ciPTEC in both SFM and A-CM (**Fig. 24 c-e**). However, miR-181a-5p showed the highest reduction upon cisplatin treatment. This modulation was validated by RT-qPCR (**Fig. 24 f**). The differences observed in miR-146a-5p and miR-125a-5p did not

reach statistical significance (**Fig. 24 g-h**). Accordingly, we focused our attention on miR-181a-5p for subsequent functional analyses.

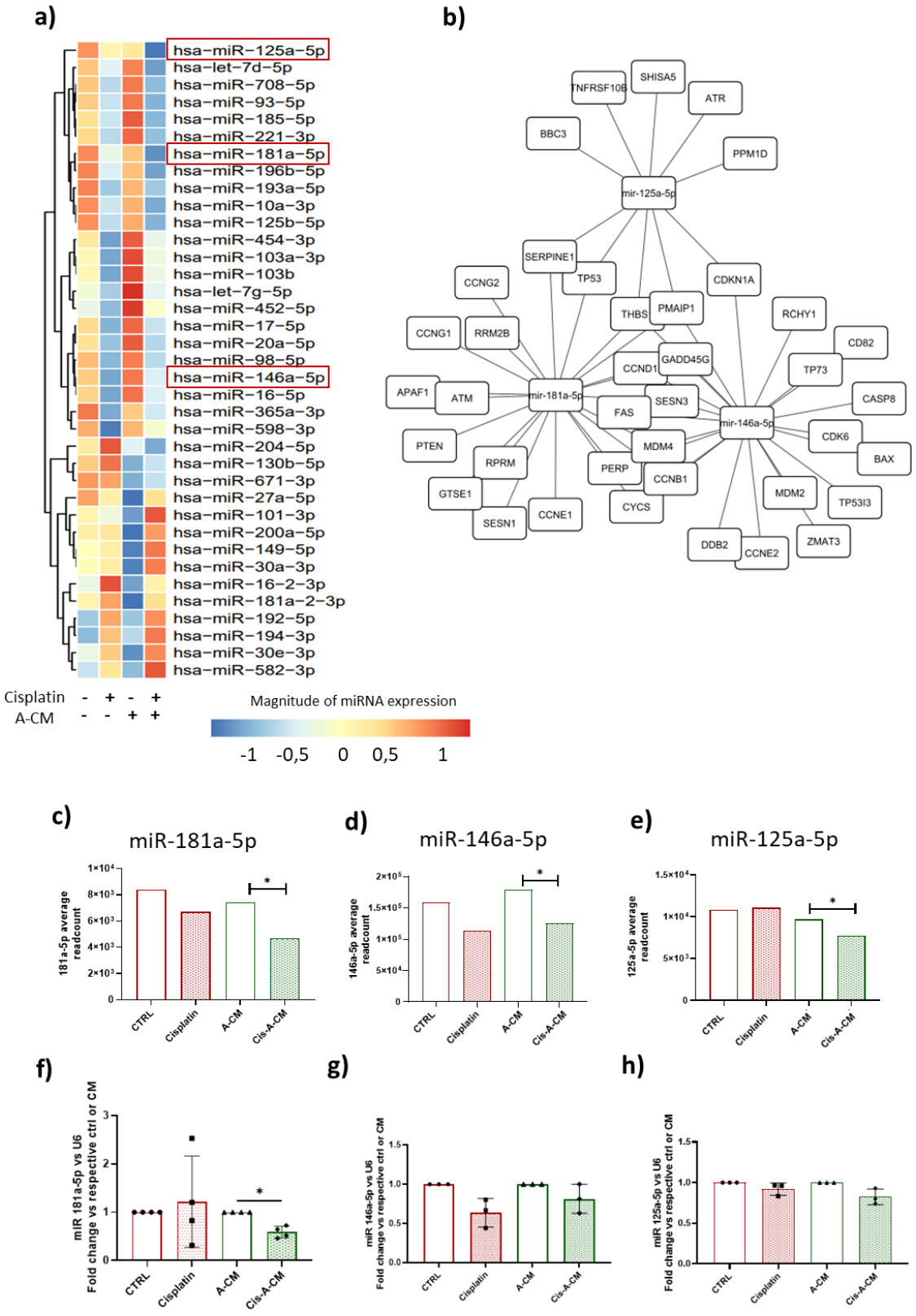

**Figure 24. Cisplatin cytotoxicity changes miRNA profiles in ciPTEC.** (**a**) The normalised log10 transformed miRNA read count data values are represented in the heatmap, the graph was generated using R-pheatmap package. Heat maps are showing the cluster of miRNA differentially expressed in ciPTEC treated with/without cisplatin and with/without A-CM. The colour scale indicates the expression level of the miRNA, with blue and red colours indicating low and high expression respect all the values. CTR and Cisplatin n=2; A-CM and Cis-A-CM n=4. (**b**) Based on the KEGG database, a network graph made with Cytoscape software shows that the selected miR-181a, miR-146-a and miR-125-a interact with each other within the p53 pathway. The read-count average obtained from the sequencing data showed the different expressions of (**c**) miR-181a-5p, (**d**) miR-146-a-5p and (**e**) miR-125-a5p in all the groups, the statistical analysis was performed to compare the treatment with the corresponding untreated control. Independent validation of sequencing results using RT-qPCR of (**f**) miR-181a (**g**) miR-146a and (**h**) miR-125a. Data are represented as the mean ± SD. N=3. Statistical analysis was performed using Student's t-test * $p < 0.05$.

### 4.3.4 MiR-181a regulates genes involved in nephrotoxicity

In a previous work conducted by my colleague Erika, a nephrotoxicity PCR array was performed to study the molecular pathways through which cisplatin and A-CM exert their effect. It has been shown that cisplatin affected ciPTECs gene expression profile, inducing nephrotoxicity, but this effect was largely recovered by CM. Genes affected by cisplatin and modulated by CM mainly included genes involved in apoptosis and oxidative stress [183]. I screened the data to identify that some of the genes in the nephrotoxicity PCR array were miR-181a targets. **Figure 25 a** illustrates that miR-181a-5p is involved in regulating genes involved in apoptosis (orange) and genes involved in nephrotoxicity (green).

Interestingly, the analysis of the specific mir-181a-5p target genes did not reveal any protective effect of A-CM as observed before (**Fig. 25 b-h**) [183], but the effect of cisplatin was still observed for CYR61, GAMT and VCAM-1 genes.

In addition, it was possible to associate gene expression levels with regulation by miR-181a. The upregulation of GAMT and CYR61 in Cis-A-CM group was compatible with the decrease of miR-181a-5p thus suggesting a de-repression of their expression at the post transcriptional level. Instead, VCAM, like miR-181a, showed a down regulation and this indicates that there is no microRNA regulation.

CYR61, SPP1, although statistically not significant, showed in trend to be downregulated by A-CM compared to cisplatin alone.

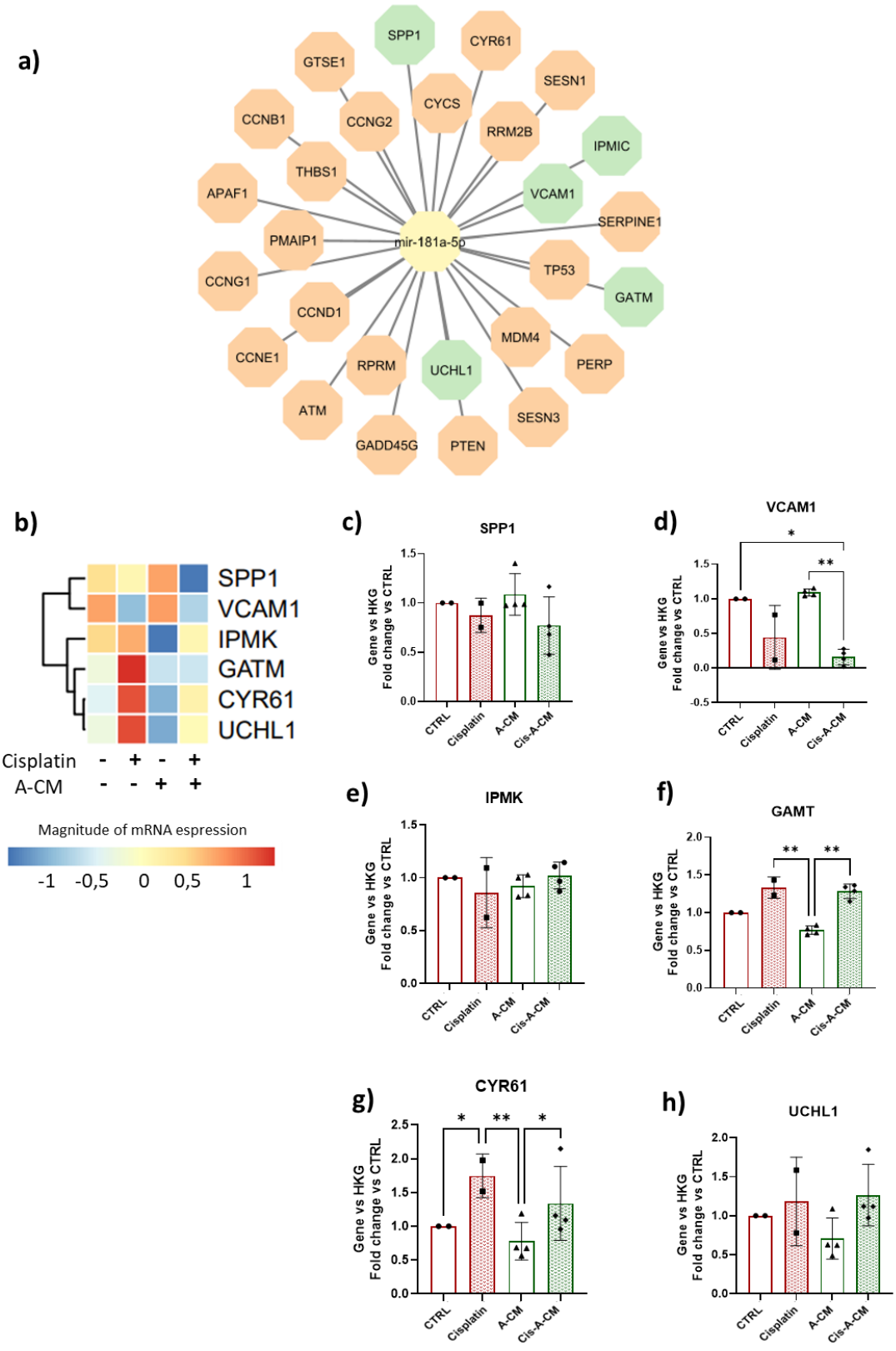


**Figure 25. MiR-181a's targets are involved in nephrotoxicity.** (**a**) Based on the KEGG database, a network graph made with Cytoscape shows miR-181a's target genes involved in the p53 pathway (orange) and nephrotoxicity (green). (**b**) Heat maps showing the results from a nephrotoxicity PCR array of mir-181a's target gene differentially expressed in ciPTEC treated with/without cisplatin and

with/without A-CM. The colour scale indicates the expression level of the genes, with blue and red colours indicating low and high expression respect all the values. Nephrotoxicity PCR array displayed as fold change versus the untreated control of (**c**) SPP1, (**d**) VCAM1, (**e**) IPMK, (**f**) GAMT, (**g**) CYR61, (**h**) UCHL1. N = CTRL=2, Cisplatin=2, A-CM=4 and Cis-A-CM=4. Data are represented as the mean ± SD. Statistical analysis was performed using Two-Way ANOVA with Tukey's multiple comparisons (**e, f**). * p <0.05, ** p <0.01. CTRL= untreated control, Cisplatin= cisplatin treatment, A-CM= adipose stromal cells conditioned medium, Cis-A-CM= cisplatin and conditioned medium treatment.

### 4.3.5 MiR-181a is involved in the protective role of A-CM reducing cisplatin apoptosis

To support our notion that miR-181a-5p is involved in the activity of A-CM rescuing ciPTEC from cisplatin-induced apoptosis, we performed functional experiments and inhibited or overexpressed miR-181a-5p by using an antisense inhibitor RNA or a miRNA mimic, respectively.

As schematized in the figure (**Fig. 26 a**), first we tested that our cells were transfected and that the expression of miR-181a was sensitive to the oligonucleotides added. Both the inhibitor (variation of 50% compared to the control) and the mimic (variation of 150 % compared to its control) modified the expression of miR-181a as expected (**Fig. 26 b and c**).

Assessing the effect on apoptosis upon cisplatin and A-CM treatment, we observe that lowering miR-181a expression by half led to an significant overall reduction of cisplatin-induced apoptosis, both in the cisplatin-only and in the cisplatin + A-CM group. In the cisplatin + A-CM group, an additive effect was seen (values: cisplatin + NC = 1.13+/- 0,22, cisplatin + inhibitor 0.50+/- 0,27, cisplatin + A-CM +NC: 0.71+/- 0,17, with inhibitor 0.10 +/-0,08) (**Fig. 26 e**).

This confirms data reported in literature where both in vitro and in vivo data showed a reduction in apoptosis related to the inhibition of mir-181a-5p [164, 184]. The CM further accentuated the miR-181a-5p anti-appototic effect due to the added inhibition of miR-181a-5p.

Based on published data, we expected to observe an increase in apoptosis upon miR-181-5p mimic addition/overexpression. However, our results failed to confirm this. The presence of miR-181-5p mimic in our system did not increase or decrease apoptosis, but interestingly the protective effect of the CM compared to the SFM was rather lost, and apoptosis rates were comparable to those in the respective cisplatin NC control (**Fig. 26 f**).

Overall, these data indicate that the MSC-CM can only influence the expression of miR-181a in combination with cisplatin. Only in this condition MSC-CM mediates a reduction in miR-181a expression, which probably activates signal cascades that reduce apoptosis.

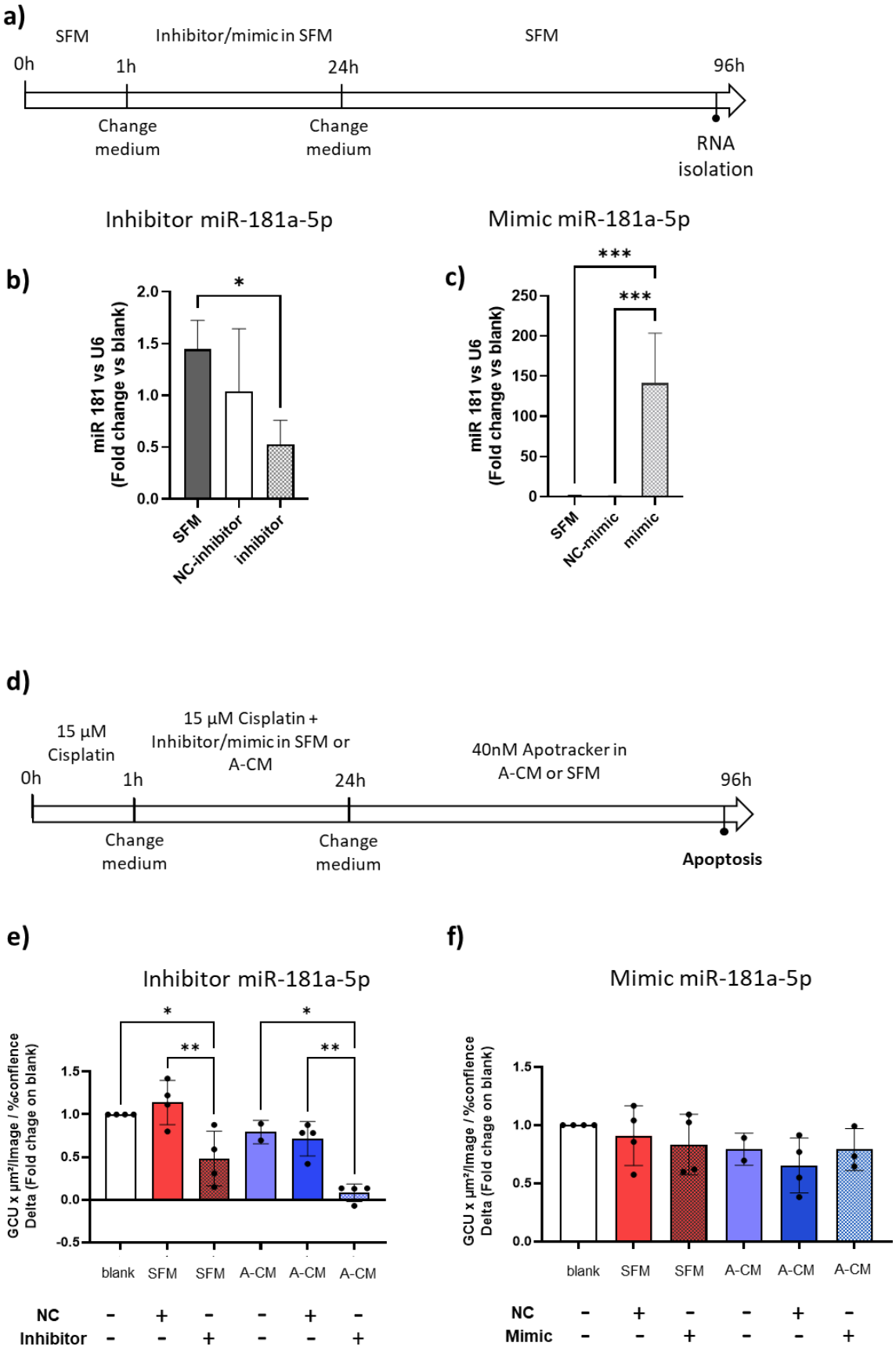


**Figure 26**. **Role of miR-181a in cisplatin toxicity.** (**a-d**) Schematic overview of the experimental set-up. (b) QPCR of inhibitor and (**c**) mimic effects on miR-181a-5p expression. Apoptosis assay

displayed as fold change of delta values (treated-untreated) with the presence of (**e**) miR-181a-5p inhibitor and (**f**) 181a-5p mimic. Data are represented as the mean ± SD. Statistical analysis was performed using One-Way ANOVA with Tukey's multiple comparison test * $p < 0.05$, ** $p < 0.01$, *** $p < 0.001$. (ciPTEC) n=4 and A-CM=3. SFM= basal medium, NC-mimic= negative control-mimic, NC-inhibitor= negative control-inhibitor, A-CM= adipose stromal cells conditioned medium, blank= basal medium with lipofectamine. GCU= green calibrated unit.

# 5 DISCUSSION

## 5.1 AIM 1: Inter-laboratory comparison of different MSC sources

MSC are used for different clinical applications, but the lack of standardisation and harmonisation of manufacturing protocols between laboratories hinders the clinical translation and comparability of therapeutic products [185].

MSC isolated from different tissue sources have unique and intrinsic properties depending on their origin and donor characteristics, making it difficult to standardise them [186]. Elucidating what makes each tissue source unique could help in predicting clinical potency and identifying the most effective MSC source in promoting regeneration and/or boosting the host endogenous repair mechanisms. Therefore, is necessary to understand their therapeutic potential to guarantee successful clinical translation.

For that purpose, work package 3 within the RenalToolBox ITN Network had one objective to biologically compare adipose (A-MSC), bone marrow (BM-MSC), umbilical cord (UC-MSC) mesenchymal stromal cells. Our specific aim in this work package was to investigate differences at phenotypic level and to compare mechanisms of action between MSC derived from different sources, with the future purpose of being able to identify the similarities and differences specific for the tissue source and application/assay. To achieve this goal we have designed an experimental plan (**Fig. 8**) where first we aimed to assess the impact of different decentralised production sites on MSC characteristics and second to understand differences in tissue source-specific properties.

Stroncek and colleagues have shown that and how variations in cell culture procedures affect the functional and molecular characteristics of cells to a much greater extent than the source material itself [187]. Considering these results, we tried to limit the variability given by different operators, media, culture protocol and donors, using predefined harmonised conditions by culturing all three MSC types in the same α-MEM medium supplemented with the same lot of FBS. Moreover, to properly compare the different sources, a seeding density optimal for the expansion of each cell type was identified and adopted across centres (**Table 1**). The original idea was to find a common growth density to grow all cell types, but this was not possible. The diversity due to the different tissues of origin was evident immediately, the A-MSC have shown to prefer a lower growth density than BM and UC-MSC.

Our study demonstrated that protocol harmonisation reduces but does not eliminate the centres variation while maintaining tissue and donor-specific differences.

In the biological comparison, the variability between centres and donor-donor continued to present in the kinetic results of growth, BM-MSC showed the longest doubling time and the highest inter-donor variability, and A-MSC consistently showed the least donor-to-donor variation regardless of where they were cultured (**Fig. 12**). However, a greater heterogenicity in cellular behaviour was obtained in the analysis of both adipogenic and osteogenic differentiation.

The analysis of adipogenic and osteogenic potential confirmed the known inter-donor variability that was consistent in all centres (**Fig. 13**). Despite the use of harmonized differentiation protocols and kits, the quantitative results varied considerably, demonstrating the great influence exerted by the operator. UC cells behaved similar in different centers showing no adipogenic or osteogenic potential. The reduced or whole lack of adipogenic differentiation potential has been repeatedly reported for perinatal MSC [188, 189]. However, the whole absence of in vitro osteogenic differentiation was rather unexpected, probably stressing the different needs of UC-MSC for osteo-induction [190].

In contrast, expression of surface markers (including CD73, CD90 and CD105) and lack of hematopoietic markers (including CD11b, CD19, CD34 and CD45) and major histocompatibility complex (MHC) class II (HLA-DR), showed uniformity in the results. Some variability was observed for the negative marker, in particular, A-MSC showed increased expression (>2%) of CD34 (Heidelberg and Liverpool) and CD45 (Liverpool) (**Fig. 13**). This variability may arise from affinity variables when using several monoclonal antibodies, as was previously reported in CD34 positivity of A-MSC early in culture [191-193]. Or similar initial expression of CD45 disappearing after prolonged culture observed in BM-MSC [194].

The site-to-site variation observed in the first part of our study may result from several factors independent of the use of standard protocols and which are difficult to predict: for example, diversity of operators, manual management of cell count and assessment of confluence for harvest. Another factor that could explain the variability is the shipment of cells in dry ice, the different times of shipping between centres may have affected cellular behaviour. To confirm our hypothesis studies are showing that cryopreservation not only affects cell proliferation [195], but also affects the differentiation potential [196] and immunosuppressive properties [197].

At the moment, there is limited knowledge about the specific properties of tissue that can predict clinical efficacy of MSC. Considering the significant effect that the origin tissue can have on functional properties, we provided a comparison of different sources of MSC, evaluating their basic characteristics. This comparison was performed in a single expert centre.

In Galway, the angiogenic profile of CM obtained from 3 different sources was evaluated. CM from BM-MSC showed superior abilities to form tubule-like structures and induce endothelial cell migration in vitro (**Fig. 14**). Moreover, the overall presence and concentration of angiogenic factors within the CM were found to be superior in BM preparations with increased relative levels of tubulogenesis-driving factors such as VEGF [98, 198]. The variability of the donor is a well-known phenomenon that we have observed also within our study, influencing the variability of reports in the literature. For example, studies show higher proangiogenic capacities [199] and higher secretion of VEGF in BM-MSC cultures [51] as in our case, while others reported increased tube formation and angiogenic bioactivity in the A-MSC secretome [200, 201]. This phenomenon underlines the need to dissect the donor characteristics and variability in autologous and allogeneic contexts to obtain favourable clinical results [202] The same trend was observed when analysing the migratory ability, BM-CM displayed a superior ability to induce endothelial cell migration followed by A-CM and finally UC-CM (**Fig. 15**).

Many studies have shown the ability of MSC to modulate the activation, proliferation and function of various immune cells of MSC and to produce cytokines in response to different stages of the inflammation process [203].

MSC-mediated effects on T cell proliferation depend on different mechanisms, which also involve IDO activity [69]. IDO has been implicated as the key factor responsible for inhibiting PBMC proliferation from tryptophan catabolism to kynurenine [204].

In a previous study conducted in our laboratory, we demonstrated that the suppression of T cell proliferation in vitro matched the increased secretion of IDO in A-MSC, resulting in a reduction in tryptophan and an increase in kynurenin levels in their conditioned media [167]. The immunomodulatory activity of MSC is influenced by stimuli present in the microenvironment, it has been shown that the stimulation of MSC with IFN-γ, has resulted in the up-regulation of IDO that has enhanced the suppressive potential of MSC on PBMC stimulated [205, 206].

In the literature, there are several studies in which MSC derived from different tissues are compared, but the results are very often conflicting. In a comparison between BM and A-MSC, for example, A-MSC exerted more potent immunomodulatory effects because they exhibited greater IDO activity and stronger expression of IFN-γ [207]. In another study comparing MSC from BM, A and Wharton's jelly, again, A-MSC resulted to be the most potent population in inhibiting allogeneic-induced T cell proliferation [208].

With our study, we reproduced this data. A-MSC had the highest ability to inhibit PBMC proliferation, and showed the highest level of intracellular IDO expression upon IFN-γ stimulation, followed by BM and UC-MSC (**Fig. 16**). These data supported previous data from our group, where A-MSC exerted the highest immunomodulatory strength, followed by BM and in that case umbilical cord blood-derived MSC [167]. However, there are also conflicting data proposing BM-MSC as the cellular source to have a superior immunosuppressive effect over A-MSC [209], or MSC from umbilical cord/Wharton's jelly possesses the strongest inhibitory effect on T cell proliferation compared to A-MSC, BM-MSC, and placenta-MSC [210]. Our data clearly demonstrate that data comparability is hard in MSC, as there is a huge impact of handling and processing. The manufacturing process may change cellular behavior even further. Thus it might be more important to optimize, harmonise and standardize manufacturing processes individually, **a**) for the cellulr source and eventually more importantly **b**) for the clinical indication.

It should also be noted that in vitro data cannot represent the complex in vivo situation [211]. The inflammatory context is defined by a variety of cell types and stimulating factors that affect the behaviour of MSC and modify their interaction with the immune system [203]. Therefore, future studies should be designed to understand whether the similarities/disparity of in vitro results are related to similar functions in vivo and whether it is possible to predict cellular behaviour in vivo by studying its biological properties.

One important part of our RTB study was to compare the biodistribution of MSC following their administration to healthy mice. For these experiments we decided to test intravenous administration of MSC. This is the technique commonly used in clinical trials [212], although it is known that most cells tend to accumulate in the lung, spleen or liver as filtering organs [74]. Further risks of this administration technique are

the possibility of forming (micro)emboli [75, 213], and the reduction of the actual number of cells capable of reaching the affected site [214]. For example, 83% of administered MSC were found in the lungs instead of the heart one hour after intravenous administration in a mouse myocardial infarction model [215].

We also noticed the trapping of cells in the lungs - immediately after infusion - independent of the tissue source. A significant drop in the bioluminescence signal from the lungs was observed in the first 24 hours after injection. Luminescence signals from both BM and UC-MSC disappeared early. Only A-MSC appeared to reside in the lungs for a slightly longer period, here a weak signal was still observable on day 3 post-infusion, but no signal was detected 7 days after injection. The bioluminescence signal was only detected in the lungs and no other organs, indicating trapping and subsequent degradation (**Fig. 17**). The decrease in signal observed after 24h probably suggests the death of the injected cells, as demonstrated earlier by *Haolu Wang et al*. They found that 30 minutes after intravenous injection the MSC were trapped in the microvessels of the lungs and liver, and only 28% of these survived after 24 hours [216]. It would be of interest to perform these experiments within an injury model, as previous reports showed that upon presence of an injury, MSC can egress the lung after initial entrapping and migrate towards the inflammatory cues [217]. This result is consistent with various reports [218, 219] and confirms that this effect is not influenced by the origin of MSC. Trapping in the lung has discussed initially to be of risk for the patient, due to pulmonary embolism for instance. However, the safety profile of infused MSC is very high, this is now well documented by the various clinical studies. Still unknown is whether lung entrapment may limit therapeutic success [75, 212, 220-222] or rather trigger MSC to release trophic factors [223]. In fact, the cell death 24h post-infusion is not necessarily a bad result, indeed it seems to be a necessary step for the activation of the immune system. This is now called the “hypothesis of dying stem cells". The apoptosis of transplanted MSC modulates innate and adaptive immune responses [219, 224]. A study on GVHD revealed that patients with immune cells that could induce MSC apoptosis responded to MSC therapy, suggesting that MSC apoptosis plays a role in the clinical response [225].

With our inter-laboratory study, we highlighted the importance of comparing different types of MSC, which may have benefits in specific therapeutic contexts. A-MSC have

shown improved immunoregulatory abilities, BM-MSC had superior angiogenic properties and wound healing, while UC-MSC appeared to be the least potent of all three sources within the analysis performed. However, the proposed assays cannot capture all the properties and attributes from each tissue source and need further validation in specific injury models in vitro and in vivo to confirm their ability to predict therapeutic potency. More importantly are our interlab comparison data that clearly indicate the impact of individual processing. To overcome this issue, a strict harmonisation and training is required to train operators within one center but also across centers, to increase reproducibility and reliability and to allow comparison of clinical data. This is most important to move the field forward and speed up translation and patients access to novel MSC-based therapies.

## 5.2 AIM 2: Comparison of A-MSC bioproduction

In the context of MSC products, potency assays are typically designed to evaluate a paracrine regenerative or reparative mechanism because it is widely accepted that these represent the predominant mechanisms by which MSC exert their effects, rather than through direct engraftment or differentiation of the cells towards a cellular lineage.

More and more studies in recent years attribute the main therapeutic effects of MSC to their paracrine factors, secretome and extracellular vesicles, which represent a new and safer method of treating medical conditions than direct cell-based therapies. Their non-living nature gives them a therapeutic advantage for their stability, lower immune response, and ease in terms of transport and storage [101]. The term secretome includes several components of a different nature that are involved in different pathways, for this reason being able to identify the component that can have a therapeutic impact in a specific application would make cell-free therapy even more effective.

Due to their role in cellular communication, EVs are the secretome component in the focal point of research across multiple scientific fields. The ability of EVs to carry and deliver molecular messages across distances within the body positions them as central players in both normal physiology and disease. Despite growing interest, much remains unknown about EV biogenesis and mode of action [226].

### 5.2.1 The importance of isolation and characterization protocols of bio-products

There are discrepant data in the literature regarding the effectiveness of cell-free MSC bioproducts. Whereas some researchers claim that the secretome or the EVs therein can recapitulate the entire therapeutic effects of MSC and used them as cell-free therapies [227, 228], our data do not support this theory, at least regarding EVs.

In this part of the thesis, we wanted to investigate the A-MSC secretome in more detail studying the different components and testing their efficiency in vitro, analysing several aspects involved in tissue regeneration. To our knowledge, our work represents one of the few studies characterizing and comparing EVs obtained with different isolation methodologies and the protein-rich fraction to the whole secretome to identify the component that had the greatest efficacy in a variety of assays and in an inter-laboratory approach (**Fig. 9**).

Protocols for the isolation and characterisation of EVs are subject to discussion.
The choice of EV isolation methods should be based on an assessment of several factors, as well as the specific research issue(s) and experimental design, as explained by *Poupardin R. et al*. The authors, combining the results published in the field of EV research over the last ten years, have identified the connections between the source of EV, the isolation method, cargo and function, highlighting the complexity of their interrelationship [229].
Researchers can select from a wide range of commercial and in-house isolation methods, each with their advantages and disadvantages [230, 231]. For example, for differential ultracentrifugation, there are reports on how variables such as run time, centrifugation speed, and rotor type impact both EV yield and contamination with non-EV material [232, 233]. In an inter-laboratory EV isolation comparison, in which our research group participated, a predefined differential centrifugation protocol was used to analyse separately the degree of reproducibility between the participants in each isolation cycle rather than between the different independent isolations. It has been shown that, regardless of the use of standardised protocols, the variability of results remained, due to the use of different equipment and operators. They also highlighted the consolidated impact of storage conditions and freeze-thaw cycles on isolated vesicles [234]. The study, however, did not account for the eventual loss of efficiency of EVs due to breaking/degradation of the EVs due to the massive ultracentrifugation force [235].
Accordingly, the initial hypothesis of our study was that the EVs isolated by ultracentrifugation might be ineffective due to shear-rate induced degradation, instead, the use of SEC could lead to more functional EVs.

In accordance with the international guidance [105], the bioproducts were analysed and evaluated for their concentration, diameter, specific membrane and intracellular markers (**Fig. 18**). However, the results derived from the quantification of particle number surprised: we observed a large difference in particle concentration when measuring the same sample with two different NTA systems (**Table. 6**). This shows that differences in the technology, the setting, the accuracy and precision of different NTA technologies plus eventually the shipping of frozen EVs can affect the final results [236]. This underlines the need for transparent reporting of experimental details,

as asked for by the Society for Extracellular Vesicles [237]. A few authors, including us, suggest calculating and reporting cell equivalents rather than particle concentrations, especially for dose-effective studies. Comparing EV concentrations of different preparations within one NTA system documented that the different culture systems (bioreactor vs 2D flask) yielded higher EV numbers, consistent with previous reports that showed improved production of EVs in the bioreactor [238].

Despite the NTA results, we expected to achieve a higher particle concentration with the use of the bioreactor. A 3-D hollow fiber bioreactor has the advantage over a 2D culture of presenting more *in vivo* as an environment for cultured cells, and the possibility of collecting CM in a small volume [169]. As per protocol and as reported in other studies, we collected CM from the bioreactor every day [239, 240], in our study for 3 weeks, expecting to obtain a higher concentration of EV than what was obtained. One possible explanation could be the concentration steps of CM before and after isolation with the SEC. It has been shown that EVs have different binding capacities to the various membrane filters and this during the concentration process could cause the "loss" of some of them. One possible explanation for these results may be that we used PES 100kDa as membrane, which may have negatively affected the concentration of EVs. One study compared the binding capacity of EVs with different types of membranes indicating that centrifugal filters with a regenerated cellulose membrane and a pore size of 10kDa are required to concentrate EVs without a significant loss [241].

Our results have confirmed our hypothesis regarding EV-UC.I In our in vitro tests we did not see a beneficial effect as often reported in the literature. Although commonly used, this isolation technique has disadvantages such as the damage to EVs caused by various ultracentrifuge steps. In addition, another problem is the formation of EV aggregates from ultracentrifugation and high-speed pellet compaction which can reduce the efficiency of EV insulation [242].

In contrast, EV-SEC is considered to maintain their integrity, biological activity and initial abundance during gel filtration, moving with the fluid flow under a small differential pressure; however, the vesicle fraction obtained is diluted and requires additional concentration steps [242].

Unlike hypothesized, we have not been able to demonstrate a higher efficiency of EV-SEC, they have only marginally outperformed EV-UC and only in some aspects in

our in vitro tests. Our idea of more efficient EV-SEC was further refuted in a recent work has classified EV isolation procedures into three arbitrary groups based on the combination of yield and purity of the final sample her, the SEC was classified together with UC as “the isolation methods with medium yield and purity“. This may explain why we have not found major differences between the two methods [243]. In this study, the ultimate goal was to compare two isolation methods, but a future approach could be the use of EV derived by combining the two methods. Considering the complexity of finding a single standardized approach for EV separation from any fluid, a new strategy is combining orthogonal isolation methods to achieve the ideal mixture of purity and recovery for the intended EV use [243].

### 5.2.2 EVs exert functional activity dose-dependently, but only in certain assays

The only test in which all bioproducts failed was the analysis of T-cell proliferation, they were unable to suppress T cell proliferation (**Fig.19**). While studies show that EV successfully suppresses mitogen-induced T-cell proliferation, others (ourselves included) failed to reproduce such observations [182]. In our previous work, we demonstrated that the vesicular component does not mediate the inhibition of PBMC but rather the secretome of MSC, yet only once the cells were previously stimulated with IFNγ, which stimulates the MSC to secrete IDO into the conditioned medium [63, 167]. Also, Papait and co-workers reported recently that A-MSC-derived EV, isolated by ultracentrifugation, did not inhibit anti-CD3-driven T cell proliferation or modulated Th1/Th2/Th17/Treg differentiation [244].

Some studies, in contrast to our results, have shown the capacity of EVs to modulate the immune cell response [245-251].

This discrepancy is probably due to a different experimental setting. As our previous studies suggest, at least in our setting suppression of T cell proliferation is largely based on an IDO-dependent mechanism and therefore our EVs, unlike cells, showed no effect. In addition, some reports prefer to pre-condition MSC to obtain more functional EVs. For example, IDO-overexpressed MSC-derived exosomes promoted renal self-recovery after IR-induced AKI by the regulation of macrophage polarization. The repair ability was significantly higher than the parental MSC-Exo [251]. In addition to the isolation method that can affect the efficiency of EVs, there is also the heterogeneity of donors from which they are isolated. To confirm, MSC-EV

preparations isolated from different donors differentially affected the CD4+ and CD8+ T cell subset responsiveness and in addition, they noted that only one preparation of EV suppressed the proliferation of T cells [245].

EVs, however, have been shown to enhance the phagocytic activity of macrophages. *Carceller et al*. found that EVs can increase the phagocytic activity of LPS-stimulated macrophages [252]. In our case, we have noticed that it was the protein component that had a greater effect on macrophages. With lower efficiency, even both EV preparations activated macrophages in higher dose. In particular, the SEC method seemed to approach the CM effect (**Fig.19**). These data are supported by findings by *Papait et al*, who also compared A-MSC conditioned medium in toto, the EV-free and the EV-UC preparation on macrophage differentiation. They suggest that the ability of the secretome to modulate the immune cell response is mediated mainly by factors not carried by EV. These authors demonstrated the ineffectiveness of EV preparation in macrophage polarization to M1 or M2 despite the use of four different doses (100 - 10µl with an EV concentration mean of 9.9 $x10^5$ EV/µl) unlike the EV- free fraction which instead showed an efficiency comparable to the secretome in whole [244].

There may be different explanations for why in some studies EV modulates the immune system and in others not. As discussed above, these discordant results may depend on different experimental setting. Another factor to consider is the heterogeneity of MSC, which may secrete heterogeneous types of EV with distinct proteomic profiles suggesting distinct biological functions [253]. Therefore, a specific function cannot be generalized to all EVs secreted by the same type of MSC.
Or, a strong impact on the functions of MSC-derived EVs is given by MSC culture conditions used to produce CM from which EVs are isolated. The extracellular microenvironment indeed affects the composition of EVs and the resulting biological activities [254].
In our case growth factors/cytokines are more likely to be responsible for the immunomodulatory effect. The immunomodulatory property of MSC has been attributed to several factors, among which the most studied are IL-10 [255], IDO [63] (previously discussed), HGF [256], TGF-b [223] and PGE2 [257].

Further we also evaluated the angiogenic properties of our A-MSC bioproducts in an in vitro tubulogenesis assay (**Fig. 21**) given that in all three participating labs respective assays were established [258]. To minimize variability, we however tried to harmonize the assay protocol and the endothelial cells culture. Nevertheless, we observed large variety in data, most likely because different extracellular matrix-like (ECM) substrates were used, different matrigel batches and geltrex, and different endothelial cell donors. Despite these variances, we observed a similar trend. EVs, regardless of the isolation method and different operators, did not show an angiogenic effect. Given that CM and the protein fraction were highly active, we speculated that VEGF is important, as shown before by our group [170]. We observed increased angiogenic ability in samples with high levels of VEGF (protein-rich fraction and in CM), compared to EV preparations where levels were low (**Fig.18**). Further confirmation was obtained by inhibiting VEGF-receptor 2 in both protein-rich fraction and CM, resulting in a diminution of angiogenic efficiency (**Fig. 21**) [259].

### 5.2.3 The non-purity of EV can lead to a misattribution of their therapeutic effect

The effectiveness of EVs has been questioned in recent years, studies show that the beneficial effect seen with the use of EVs is actually due to contamination with the protein fraction. *Whittaker E. et al.* show that the presence or absence of EVs in CM does not influence in vitro angiogenesis and wound healing efficiency. Importantly, this study discusses that efficacy can be explained when EV preparations were not purified to a high degree. It also discusses that very high concentrations are required to show effects, far higher than those at which they were found in the conditioned medium [260].

Vice versa, *Forteza-Genestra et al.* demonstrated in a model of chondrocyte differentiation that the contaminating factors had negative effects on EV efficacy, the impurities co-isolated with the EV caused deleterious effects on extracellular matrix component expression in chondrogenic cells [259].

In addition, EV and the protein fraction isolated with SEC were compared with EV-UC in an in vitro functional study, noting that treatment with EV-UC had similar effects on the expression of ECM components from the protein fraction treatment. It has been demonstrated that the deleterious effect is caused by contamination with co-

precipitated elements when isolated by ultracentrifugation; this contamination can be removed by using a purification method such as SEC [259].

When we talk about contamination of EVs, however, a distinction must be made between contamination with soluble factors or with the proteins that constitute the external layer named corona [261].

This protein coating significantly influences the EV's interactions with cells, tissues, and the immune system. It can also affect recipient cells' stability, the uptake of EVs and also seems to be relevant for the EV function [262].

Some studies have shown the involvement of corona proteins in angiogenesis and immunomodulation. It has been shown that EV isolates with tangential flow filtration (TFF) lose their angiogenic function after being further purified with UC [263] which is known to be a method that depletes the corona of synthetic nanoparticles [264]. Also, it has been demonstrated that EVs with a reconstituted protein-corona of known growth factors are more effective in stimulating angiogenesis than either EVs or growth factors alone [265]. Interesting results have been obtained for immunomodulation. Dose-dependent inhibition of T cell proliferation was observed only with cells and their corona-bearing TFF-EVs but not by TFF-separated soluble factors. In contrast, further separation with the SEC reduced the immunomodulatory capacity of EV-SEC, but showed a significant immunomodulatory activity of the late fractions in which they probably contain the corona protein [265].

From the literature, it would appear that SEC [265, 266], together with UC, are isolation methods that remove corona proteins from EVs. Based on this evidence, we can speculate that one reason why we have not found EV functionality was the removal of corona proteins. Probably, if we had used a 'gentle' approach to the insulation of electric vehicles, such as TFF, we would have obtained a higher power of EV than methods like the SEC that produce EV as well but less functional.

The presence of a protein corona can complicate the study of EVs as it can interfere with the interpretation of their behavior in different experimental setups.

Also, the application of different EV quantification methods such as protein concentration or absolute EV counts with NanoSight makes it difficult to identify the possible effective dose and replicate the results reported in literature.

Our data clearly indicate that conditioned medium is effective in a variety of in vitro assays.

I certain assays we could identify the most important soluble factors, IDO, for instance in mediating inhibition of T cell proliferation, or VEGF in mediating angiogenic tube-like formation.
In the setting of cisplatin injury, we also figured out that CM is highly active preventing from cisplatin-mediated apoptosis. EVs were not involved in this setting as depletion of EVs had no neutralizing effect [183]. My colleague Erika figured out that the free thiol content was important acting as ROS scavengers. Early data indicated a correlation between the free thiol content in the CM and the protection from cisplatin-induced apoptosis [183].
A more detailed investigation adding a variety of different inhibitors, however, indicated that MSC CM inhibits apoptosis by different mechanisms, most likely involving suppression of oxidative stress and subsequent regulated cell death [174].

In our study, we proposed an MSC-conditioned medium as a valid alternative to its cellular counterpart. However, several challenges must be overcome to make this technology clinically available and utilise the MSC secretome as a cell-free therapeutic. It is a very dynamic and complex component that varies according to the tissue from which the cells are isolated, to the donors and in response to different culture conditions [101, 267, 268]. Importantly, in the choice of secretome component to be used, it must also be considered that the secretome of MSC contains proteins and RNA, which can alter the genome of the cells of the recipient, some of which may be oncogenic [269].
To properly characterize and assess the therapeutic potential of the MSC secretome, our data strengthen the requirements for standardization of protocols for the expansion of MSC cultures, the collection, storage and transport of the secretome, and the isolation of defined components and subsequent characterization [267].

## 5.3 AIM 3: Role microRNA in the protective effect of A-CM in injury model

The previous chapters highlighted already that the mechanisms of action of MSC are multifaceted, complex, and responsive to the local milieu and involve both a cellular and humoral response.
So far our work has been based on predicting the behaviour of MSC or their bioproducts in a series of different assays that reflect the major mechanisms of action

of MSC. The data indicated that the MSC secretome is an important mediator and the exact mechanism will be hard to identify- if at all.

### 5.3.1 A-MSC-conditioned medium protects proximal tubular epithelial cells from cisplatin-cytotoxicity

Within a previous study, we investigated the therapeutic effect of MSC, in that specific case ABCB5+ skin-derived MSC, in an in vivo model of cisplatin nephrotoxicity. MSC grafted intravenously and intraperitoneally into a cisplatin-induced AKI murine model modulated mRNA expression toward an anti-inflammatory and pro-regenerative state. This happened despite an apparent lack of amelioration of renal damage at physiological, metabolic, and histological levels [174]. Accordingly, we postulated that the timepoint of infusion was too late to rescue from the high degree of injury.

For the in vitro model, we thus adapted the protocol to assess the preventive, rather than the therapeutic activity. Whereas my colleague Erika analyzed in detail the anti-apoptotic/anti-oxidative and immunomodulatory function of A-CM in this model [183], I hypothesized that A-CM, especially the EVs contained therein, can ameliorate cisplatin toxicity by modulating miRNAs.

### 5.3.2 Cisplatin nephrotoxicity affects the expression of microRNAs

First, we recapitulated the protective role of A-CM in preventing cisplatin-induced apoptosis in ciPTEC evaluating the expression status of protein p53, the so called "genome guardian", after 24h and apoptosis at day 3 (**Fig. 23**). P53 is one of the first proteins activated in a condition of cellular stress and promotes apoptosis by increasing the expression of genes leading to the permeabilization of the mitochondrial outer membrane and the release of apoptogenic factors [270]. Our data showed that cisplatin activated p53, as already demonstrated [24], and that the A-CM prevented cisplatin-induced p53 upregulation in line with apoptosis reduction. Unlike initially hypothesized, EVs were not involved in this protective action as EV depletion did not neutralize the protective effect of the CM on inhibiting apoptosis [183].

In contrast to other studies, we focused our analysis on the molecular response in the injured cells treated with MSC-CM. Previous studies working with EVs typically addressed the miRNA cargo of the EVs [229, 271]. We, however, postulated that factors

delived by the MSC-CM may modify the miRNA composition in the responder cells, by this mediating protection from the injury.

The comparative sequencing analysis of miRNA in ciPTEC treated/untreated with cisplatin or the combination of cisplatin and A-CM revealed that miRNAs were indeed modulated during the injury and affected by CM treatment. In particular, our screening allowed us to identify three candidates: mir-181a, mir-146a and mir-125a, whose expression has been documented to be cisplatin sensitive and involved in cancer and apoptosis pathways (**Fig. 24**).

mir-146 expression, for instance, was down-regulated in non-small cell lung cancer compared to parental cells making them resistant to cisplatin, but the over-expression reversed this situation [272]. In a mouse AKI model, the overexpression of miR-146 decreased the levels of serum creatinine and blood urea nitrogen and the apoptosis of renal cells, suggesting its protective role in renal function [273].

MiR-125a upregulation, observed in cisplatin-resistant non-small cell lung cancer cells, reduced the resistance to cisplatin, proliferation, migration, invasion and epithelial-mesenchymal transition and also promoted apoptosis [274].

The miR-181s family has recently been recognized to play a vital role in many cancers, including multiple myeloma [275], breast cancer [276], leukaemia [277], and hepatocellular carcinoma [278]. The dysregulation of miR-181a-5p has been implicated in various types of cancer and functions as an oncomiR or tumour inhibitor. The function of miR-181a-5p does not depend on a specific target, but rather on the collective impact of its targets, which may include both tumour suppressors and oncogenes [279].

Mir 181a-5p has been indicated as a possible novel potential biomarker in human diseases and tumours [280, 281] and its expression has also been associated with drug resistance including cisplatin-resistance [282, 283]. Expression of miR181a has been shown to be sensitive to cisplatin treatment in HK-2 cells, inhibition of microRNA-181a led to a reduction in the number of apoptotic cells upon cisplatin treatment [164] .

### 5.3.3 MiR-181a-5p is involved in the apoptotic pathway

Having observed that cisplatin and A-CM affected expression of some miRNAs, we focused on miR-181a-5p due to its well-described role in nephrotoxicity and apoptosis (**Fig. 25**). It was also the miRNA that was independently validated by RT-qPCR to have a significant expression change, downregulated in the presence of

cisplatin plus A-CM (**Fig. 24**). In our system, the inhibition of miR-181a reduced cell death, especially in the cisplatin group treated with A-CM. The inhibition of miR-181a caused a reduction of apoptosis both in the ciPTEC treated with basal medium and CM (**Fig. 26**), confirming the data reported in literature where both in vivo and in vitro showed a reduction of apoptosis-related inhibition of mir-181a-5p [184]. Also, *Han-Yu Zhu et al*. demonstrated the involvement of mir-181a in HK-2 cell apoptosis after cisplatin treatment. They noted that the treatment with cisplatin induced apoptosis and miR-181a levels, but the apoptosis was reduced upon addition of a microRNA-181a inhibitor with Bcl-2 up-regulated and Bax down-regulated [164] (**Fig.27**).

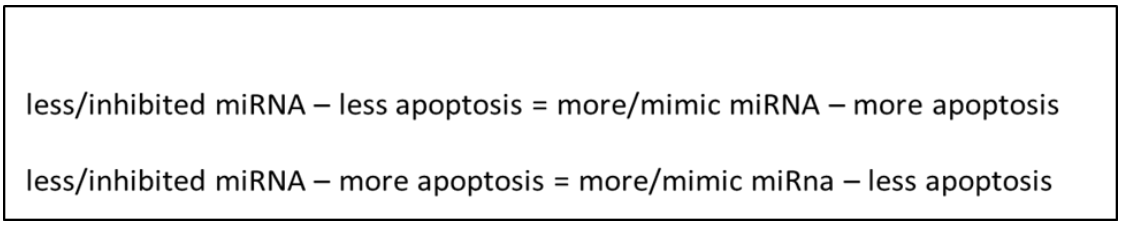


**Figure 27. Schematic version of the two possible roles of miRNA involved in apoptosis.**
Inhibition of a miRNA may be associated with a reduction in apoptosis levels, conversely, an increase in miRNA results in an increase in apoptosis. This phenomenon may be due to an indirect control of miRNA on pro-apoptotic protein. Inhibition of miRNA induces an increase in its target which in turn causes a decrease in pro-apoptotic proteins and consequently a decrease in apoptosis. The reverse phenomenon is achieved by an increase in miRNA expression. Instead in a situation of direct control of miRNA on pro-apoptotic proteins, inhibition/increase of miRNA causes an increase/decrease in levels of pro-apoptotic proteins with an increase/decrease in apoptosis.

Checking the PCR data of my colleague Erika for specific miR-181a-5p targets, however, did not reveal a clear change. Thus, we proceeded assessing the effect of down- and upregulation of miRNA-181a-5p. Our results showed that the conditioned medium accentuated the anti-apoptotic effect due to the inhibition of miR-181a-5p, in contrast, the mimic did not influence the cell death, moreover a protective effect of CM was not observed. From these data we can assume that the CM protects cells from cisplatin cytotoxicity by the downregulation of miR-181a. However, the increase in miR-181a-5p expression seems to interfere with the action of the CM.

Considering the in vitro data and our sequencing data, we hypothesized that there may be a correlation between miR-181a and p53. The reduction of apoptosis can be explained by the link between miR-181a and p53. Infusion of A-MSC reduced

apoptosis in the kidney by acting on the mitochondrial apoptosis pathway, attenuating the activation of p53 and consequently decreasing the expression of pro-apoptotic molecule Bax and cleaved caspase-9 and -3 [73]. *Liu et al.* revealed that miR-181a inhibition reduced the expression of p53 and Bax, while also increasing the expression of Bcl-2, which led to a reduction in apoptosis. A miR-181a mimic increased the expression of p53 and Bax and reduced the expression of Bcl-2 [284]. Other researchers proposed a binding of miR-181a to p53 which consequently regulates apoptosis [285].

To test this hypothesis, we crosschecked data from our previous study. Here, human xenogeneic ABCB5 + MSC grafted into a cisplatin-induced nephrotoxicity in a rat model, modulated cisplatin-induced changes in gene expression. The GSEA analysis showed 49 significant differentially expressed pathways. Cisplatin led to the upregulation of apoptosis and modulation of the p53 signalling pathways. Normalized enrichment scores of the p53 pathway were found 2.1 and 1.9-fold increased by microarray and RNA seq, respectively upon cisplatin treatment. Upon ABCB5 treatment, however, a number of genes were downregulated in the p53 signalling pathway [174] (**Fig. 28**).

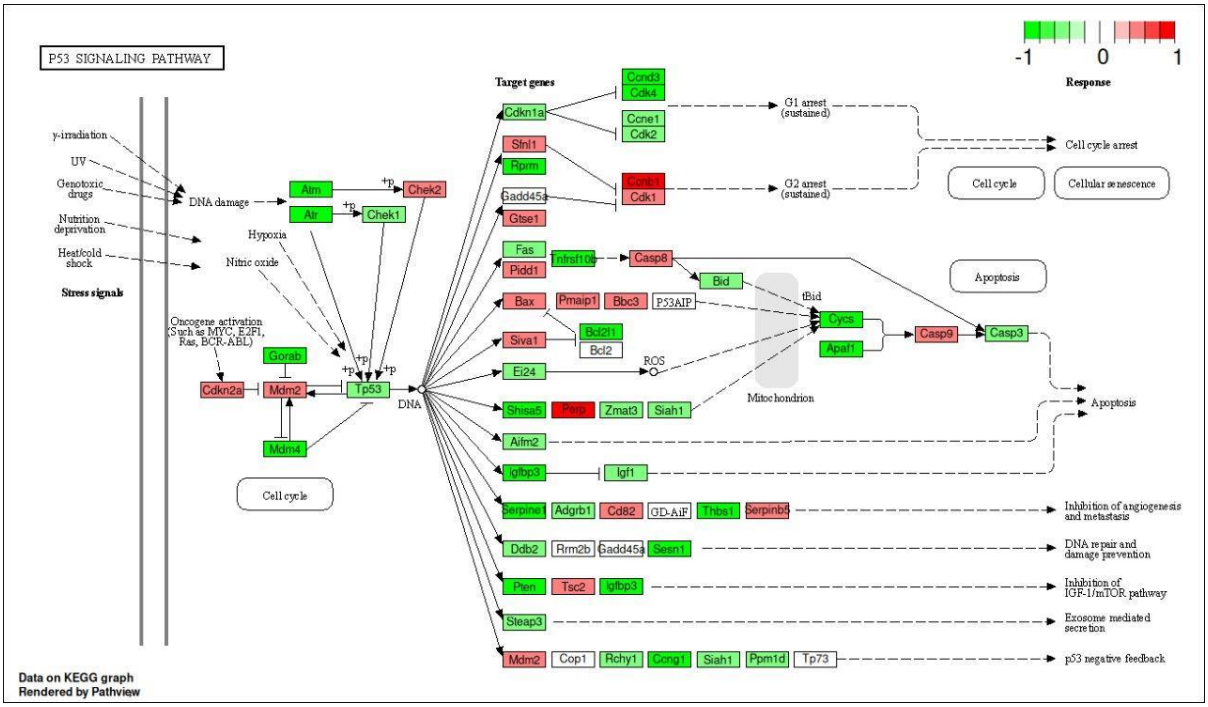

**Figure 28.** Changes in gene expression in the p53 pathway in response to treatment with ABCB5+ MSC. Downregulated protein are displayed in green, and upregulated proteins in red. Data generated by Christina Daniele.

An interesting report explains the correlation between miR-181a and p53. *Tsang et al.* propose that miR-181 is involved in a type II circuit with p53. Two self-regulation cycles of miRNA and their targets are described, called feedback and feedforward cycles, or type I and type II circuits, respectively [286] (**Fig. 29**). In a type I circuit, both the miRNA and its target are positively regulated; this loop type is probably responsible for homeostasis and steady levels of proteins. Contrary, a type II circuit describes a miRNA that negatively regulates its target (positive feedback loop) while its target directly or indirectly suppresses the transcription of the respective miRNA. Less target means less inhibitory action on the miRNA, a pathway that ultimately shuts down target expression, contrary to the type I circuit, where a balance is the result [287].

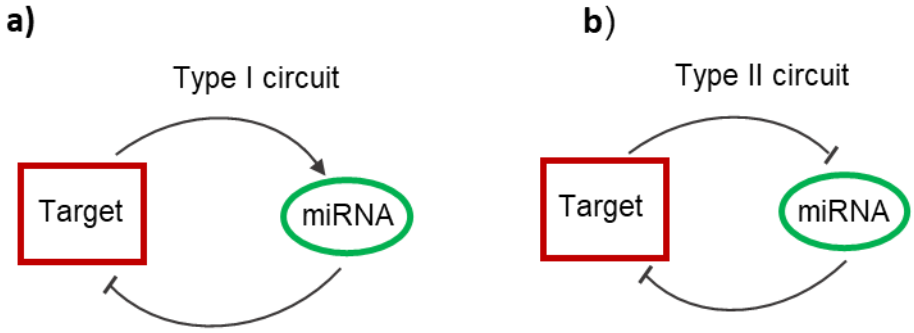


**Figure 29.** Different autoregulatory loops of miRNAs and their targets. (**a**) Type I circuit: miRNA inhibits the expression of its target, whereas the target acts as a transcription factor that activates the miRNA. (**b**) Type II circuit: the target has a negative effect on the miRNA expression, which leads to further inhibition of target expression.

Yet, most likely additional proteins act as a bridge between mir-181a and p53 (**Table 7**). *Liu et al.* revealed that miR-181a regulates p53 degradation, ubiquitination, and transcriptional activity by targeting BIRC6, a known regulator of p53. They showed that the inhibition of miR-181a ameliorates 5- Fluorouracil-induced renal cell cytotoxicity. Mir-181a inhibition leads to increased expression of its target BIRC6,

which can induce p53 degradation, therefore mitochondrial-dependent apoptosis is not activated [284].

Another possible linker between mir-181a and p53 is SIRT1 which contributes to the induction of P53 deacetylation, and inhibition of p53-dependent apoptosis [288]. In temporomandibular joint osteoarthritis, the increase of miR-181a-5p expression induced a reduction of its direct target SIRT1, inducing the activation of p53-dependent chondrocyte apoptosis [289].

Our data suggest a protective role of A-CM targeting the miR-181a - apoptosis axis activated by cisplatin (**Fig.30**). A variety of studies indicate that MSC/ A-MSC could directly transfer miR-181a-5b via extracellular vesicles and by this regulate the immune balance but also control differentiation [290, 291]. Here, however, we did not investigate the miRNAs transferred by MSC/MSC-CM or their extracellular vesicles, but rather the response profile of ciPTEC treated with A-CM. In addition, we observed a reduction of miR-181a-5p, however significantly changed only in the cisplatin plus A-CM treatment group. This suggests another player to be involved responsible for miR-181-5p downregulation. One candidate which eventually could be involved is lncRNA-P21, its role was analysed in a model of sepsis-induced acute lung injury. MSC-derived exosomal lncRNA-P21 was upregulated after LPS treatment and was able to inhibit lung cell apoptosis and repair lung lesions induced by LPS acting as a mir-181a sponge. Mir-181a down-regulation allowed the up-regulation of SIRT1 and consequently a reduction of apoptosis [292].

**Table 7.** In this table we have summarized the role of miR-181a in apoptosis, reporting possible targets that function as a bridge between miRNA and apoptotic proteins.

| MiRNA regulation expression | Target | Cell type | Outcome | Reference |
|---|---|---|---|---|
| Mimic of miR-181a | Decrease of KLF6 | Glomerular mesangial cell | Promote apoptosis of GMCs stimulated by high glucose | 293 |
| knockdown of miR-181a | Increase of BIRC6 | Mesangial cells | Ehanced 5-Fluorouracil - induced apoptosis through p53-dependent mitochondrial pathway | 284 |

| | | | | |
|---|---|---|---|---|
| Increase of miR-181a | Decrease of SIRT1 | Temporomandibular joint osteoarthritis mice model | Activation of p53-dependent chondrocyte apoptosis | 289 |
| Increase of miR-181a | Decrease of CBLB | Human esophageal cancer cell line OE19 | Increase in cisplatin-induced apoptosis | 294 |
| Mimic of miR-181a | Inhibition of PVT1 | Human non-small cell lung cancer | Enhanced responses of combination of Xiaoji Decoction and cisplatin on inhibition of cell lung cancer | 295 |
| Upregulation of miR-181a-5p | Inhibition of SP1 | Human non-small cell lung cancer | Increase the sensitivity to cisplatin and reduce the tumor size and weight | 295 |

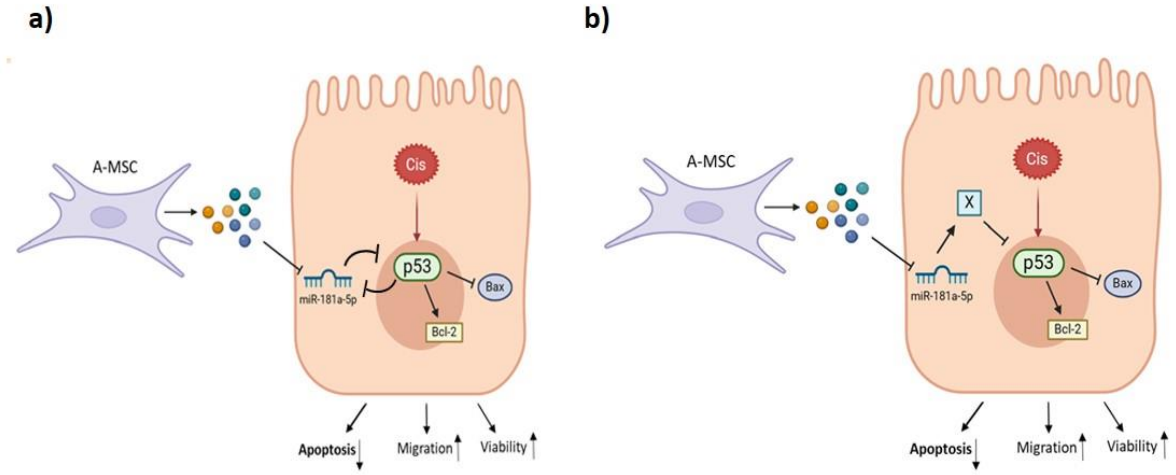


**Figure 30. Different models for the mechanism of A-CM mediated protection against cisplatin injury via the regulation of miR-181a-apoptosis axis**. (**a**) miR-181a is involved in direct relationship with p53. The down-regulation of miR-181a counteracts the activation of p53 by cisplatin, thus activating a type II circuit. (**b**) We propose that mir-181a is involved in an indirect relationship with p53 involving eventually a third protein that acts as a bridge between the two. A-CM reduces the levels of mir-181a, this allows its target (X) to inhibit p53. Inhibition of p53 induces the expression of anti-apoptotic proteins such as Bcl-2 and prevents the expression of apoptotic proteins such as Bax. As a consequence, A-CM mediates a protection from cisplatin-induced apoptosis, increasing the vitality and migratory capacity of ciPTECs. This graph was constructed using BioRender.

Identifying the cascade of signals that change according to microRNA expression is a challenge. A microRNA can have multiple targets and the target genes of a microRNA can change under different experimental conditions. It has been reported that miR 181a-5p is environment-dependent, especially in tumours. The binding of miR 181a-5p to multiple targets (which may be oncogenes or tumour suppressor genes) and their different expression patterns in various cancer types often leads to conflicting results [279]. Due to this uncertainty, more research are needed to provide a detailed understanding of miR 181a-5p, its role in apoptosis and why it is significantly changed only in the combined setting cisplatin plus A-CM.

### 5.3.4 A-CM protects from cisplatin injury but may interfere with cisplatins cytostatic therapeutic action

The data presented here and in our previous studies suggest that A-CM can ameliorate the cytotoxic effects of cisplatin, preventing apoptosis and as shown previously polarizing macrophages to the pro-regenerative and anti-inflammatory phenotype.
Therefore, a therapeutic scenario could be to administer A-CM to patients concomitantly with cisplatin to prevent any nephrotoxic side effects. However, this kind of therapy may eventually intervene with the desired anti-cancer benefit of cisplatin.

It is now known that cross-talk between MSC and cancer cells causes both pro-tumour and anti-tumour effects, raising safety concerns for clinical application in oncology [296]. MSC that help with tissue repair and regeneration may also support tumor functions. MSC release cytokines and growth factors that may act as oncogenic factors altering the recipient cells and promoting immunosuppressive effects [101]. Or, in response to soluble factors secreted by cancer cells, they can differentiate into cancer associated fibroblasts, a type of cell in the tumour microenvironment capable of promoting tumorigenesis [297]. At the same time, these cells have potent tumor-suppressive effects that have been exploited as cancer therapeutics. For example, the release of cytotoxic agents, such as TNF-Related Apoptosis-Inducing Ligand (TRAIL) or inflammatory mediators, such as the multifunctional cytokine TGFβ, can induce the apoptosis in different types of cancer [298]. Eventually, a specific tissue-targeting strategy could be a solution, one that

delivers protective MSC-secretome components to the tissue that needs protected and chemotherapy-enhancing factors to the tumor site.

To overcome the problems related to cell use, it is proposed to follow a safer approach that includes the use of secretome and its components. The advantage of using nonliving components is that they are more stable, can be sterilized, are less immunogenic and are easy to transport and store. However, protocols for isolation, characterisation, storage and delivery need to be standardized to ensure effective quality control, as we discussed above extensively [101].

Nanoparticle-based drug delivery systems have also gained attention. Microcapsules designed with alginate, cellulose and agarose have shown benefits in cell-based anti-cancer therapies [299, 300]. For example, by administering alginate-encapsulated cells that express soluble leucine-rich repeats and immunoglobulin-like domains 1, tumor growth in orthotopic patient-derived glioblastoma xenograft mice model was inhibited [300]. Biomaterials can be designed to have their own anti cancer activities. Gliadel, a biodegradable medical plant made of polyfeprosan, is inserted into the resection cavity and slowly releases the anti-cancer agent, bringing small benefits to patients who receive surgical removal of brain tumors [301].

Nanotherapies have a greater therapeutic effect because they can target multiple pathways, are less dependent on doses of drugs and thus mitigate adverse effects. They also have the ability to increase the bioavailability and solubility of different drugs by facilitating their dispersion and accumulation in cancer tissues while minimizing toxic effects in benign tissues [63].

In conclusion, we first highlighted the protective role of A-CM against the cytotoxic effect of cisplatin.

In addition, we identified one pathway through which CM can protect kidney cells, namely through the down-regulation of miR-181a-5p, which in turn attenuates apoptosis by regulating p53. This, in line with our previous data documents both the anti-apoptotic and immunoregulatory properties of the MSC secretome in reducing cisplatin cytotoxicity. However, before suggesting a clinical implementation, safety studies are required to understand whether the protective mechanisms may interfere with the actual intention of cisplatin use, the anticancer treatment.

With our study, we confirmed the preventive effect of A-CM towards apoptosis induced by cisplatin, and also identified mir-181a as its target. Our data confirm the involvement of miRNA in apoptosis and are limited to a theoretical description of possible targets involved in the process.

A future step would be to analyze how the p53 protein varies in the presence of miR-181a inhibitor and downstream signal cascade proteins such as Bcl-2 and Bax. Then, based on the results, it could be further investigated whether the link between miR-181a and p53 is direct or indirect.

We are aware that our results are limited to an in vitro experimental condition, it might be interesting to test in vivo the role of miR-181a in the apoptosis pathway.

# 6 SUMMARY

Kidney disease is a serious health problem worldwide, with an increasing prevalence. New research has made it possible to better understand the pathophysiology of kidney disease. However, there are still limited treatment options to stop or reverse the progression of the disease. Therefore, the development of new strategies for the treatment of kidney diseases is a critical area of research. In this context, cell-based therapy could be a promising strategy and is currently the focus of preclinical studies. Within an International Training Network entitled RenalToolBox, we investigated whether MSC could offer a novel cell-based therapy modality. Many questions remain open and in our study we addressed three:

1. Is it possible to identify a specific source of MSC that is better suited for therapeutic applications?
2. Is the secretome as efficacious as MSC and if so, which part of the secretome reproduces the therapeutic effect?
3. Do microRNAs play a role in the protective effect of MSC?

In **Aim 1**, we established harmonised tissue culture conditions for the expansion of adipose, bone marrow and umbilical cord MSC between three independent centres to study the reproducibility of these procedures and their impact on their biological characteristics and functionality both in vitro and in vivo. With this inter-laboratory study, we were able to accentuate the importance of adopting harmonised protocols that reduce, but do not eliminate, site-to-site variation, while specific differences in tissues and donors remain evident. Despite the use of a common protocol, the different types of MSC demonstrated individual properties, which can have benefits in specific therapeutic contexts.

In **Aim 2**, we focused on the study of secretome to understand which component was able to replicate the therapeutic effect. Our goal was to test the in vitro efficacy of different secretome components regarding different aspects of tissue regeneration and at the same time to understand how the different isolation methodologies can influence the final results. Extracellular vesicles (EVs), regardless of the method of isolation, failed to replicate the results obtained by the secretome, in contrast, the protein fraction showed an effect very close to that of the secretome. We have shown

that depending on the isolation method, contamination with protein residues can alter the results and misinform about the true efficiency of EVs. On the other hand, increased EV concentration in some applications increased effectiveness, indicating that purity and dose affect the final functionality.

In **Aim 3** we aimed to test the secretome in a situation of cellular damage in order to identify the beneficial effects and the molecular mechanisms involved to propose a therapeutic strategy. The administration of the conditioned medium protected the kidney cells by reducing cisplatin cytotoxicity. The conditioned medium acted on different cellular aspects, maintaining cell viability, maintaining p53 levels low, reducing apoptosis and, also, stimulating cell migration. We demonstrated that the conditioned medium reduced cell death by inhibiting the expression of mir-181a. We propose a so-called type II regulatory circuit by which A-MSC CM and cisplatin affect p53 expression/apoptosis and the counteracting miR-181a expression.

# 7 REFERENCES


1. Levin, A, Tonelli, M, Bonventre, J, Coresh, J, Donner, JA, Fogo, AB, Fox, CS, Gansevoort, RT, Heerspink, HJL, Jardine, M, Kasiske, B, Kottgen, A, Kretzler, M, Levey, AS, Luyckx, VA, Mehta, R, Moe, O, Obrador, G, Pannu, N, Parikh, CR, Perkovic, V, Pollock, C, Stenvinkel, P, Tuttle, KR, Wheeler, DC, Eckardt, KU, participants, ISNGKHS: Global kidney health 2017 and beyond: a roadmap for closing gaps in care, research, and policy. *Lancet,* 390**:** 1888-1917, 2017. https://doi.org/10.1016/S0140-6736(17)30788-2
2. Rota, C, Morigi, M, Imberti, B: Stem Cell Therapies in Kidney Diseases: Progress and Challenges. *Int J Mol Sci,* 20, 2019. https://doi.org/10.3390/ijms20112790
3. Mortality, GBD, Causes of Death, C: Global, regional, and national life expectancy, all-cause mortality, and cause-specific mortality for 249 causes of death, 1980-2015: a systematic analysis for the Global Burden of Disease Study 2015. *Lancet,* 388**:** 1459-1544, 2016. https://doi.org/10.1016/S0140-6736(16)31012-1
4. Chen, F, Chen, N, Xia, C, Wang, H, Shao, L, Zhou, C, Wang, J: Mesenchymal Stem Cell Therapy in Kidney Diseases: Potential and Challenges. *Cell Transplant,* 32**:** 9636897231164251, 2023. https://doi.org/10.1177/09636897231164251
5. Tsai, WC, Wu, HY, Peng, YS, Ko, MJ, Wu, MS, Hung, KY, Wu, KD, Chu, TS, Chien, KL: Risk Factors for Development and Progression of Chronic Kidney Disease: A Systematic Review and Exploratory Meta-Analysis. *Medicine (Baltimore),* 95**:** e3013, 2016. https://doi.org/10.1097/MD.0000000000003013
6. Stevens, PE, Levin, A, Kidney Disease: Improving Global Outcomes Chronic Kidney Disease Guideline Development Work Group, M: Evaluation and management of chronic kidney disease: synopsis of the kidney disease: improving global outcomes 2012 clinical practice guideline. *Ann Intern Med,* 158**:** 825-830, 2013. https://doi.org/10.7326/0003-4819-158-11-201306040-00007
7. Levey, AS: Defining AKD: The Spectrum of AKI, AKD, and CKD. *Nephron,* 146**:** 302-305, 2022. https://doi.org/10.1159/000516647
8. Kidney Disease: Improving Global Outcomes, CKDWG: KDIGO 2024 Clinical Practice Guideline for the Evaluation and Management of Chronic Kidney Disease. *Kidney Int,* 105**:** S117-S314, 2024. https://doi.org/10.1016/j.kint.2023.10.018
9. Ruiz-Ortega, M, Rayego-Mateos, S, Lamas, S, Ortiz, A, Rodrigues-Diez, RR: Targeting the progression of chronic kidney disease. *Nat Rev Nephrol,* 16**:** 269-288, 2020. https://doi.org/10.1038/s41581-019-0248-y
10. Duan, J, Wang, C, Liu, D, Qiao, Y, Pan, S, Jiang, D, Zhao, Z, Liang, L, Tian, F, Yu, P, Zhang, Y, Zhao, H, Liu, Z: Prevalence and risk factors of chronic kidney disease and diabetic kidney disease in Chinese rural residents: a cross-sectional survey. *Sci Rep,* 9**:** 10408, 2019. https://doi.org/10.1038/s41598-019-46857-7
11. Khwaja, A: KDIGO clinical practice guidelines for acute kidney injury. *Nephron Clin Pract,* 120**:** c179-184, 2012. https://doi.org/10.1159/000339789
12. Hoste, EAJ, Kellum, JA, Selby, NM, Zarbock, A, Palevsky, PM, Bagshaw, SM, Goldstein, SL, Cerda, J, Chawla, LS: Global epidemiology and outcomes of

acute kidney injury. *Nat Rev Nephrol,* 14**:** 607-625, 2018. https://doi.org/10.1038/s41581-018-0052-0
13. Kellum, JA, Prowle, JR: Paradigms of acute kidney injury in the intensive care setting. *Nat Rev Nephrol,* 14**:** 217-230, 2018. https://doi.org/10.1038/nrneph.2017.184
14. Wu, Y, Connors, D, Barber, L, Jayachandra, S, Hanumegowda, UM, Adams, SP: Multiplexed assay panel of cytotoxicity in HK-2 cells for detection of renal proximal tubule injury potential of compounds. *Toxicol In Vitro,* 23**:** 1170-1178, 2009. https://doi.org/10.1016/j.tiv.2009.06.003
15. Bellomo, R, Kellum, JA, Ronco, C: Acute kidney injury. *Lancet,* 380**:** 756-766, 2012. https://doi.org/10.1016/S0140-6736(11)61454-2
16. Garofalo, AM, Lorente-Ros, M, Goncalvez, G, Carriedo, D, Ballen-Barragan, A, Villar-Fernandez, A, Penuelas, O, Herrero, R, Granados-Carreno, R, Lorente, JA: Histopathological changes of organ dysfunction in sepsis. *Intensive Care Med Exp,* 7**:** 45, 2019. https://doi.org/10.1186/s40635-019-0236-3
17. Ishani, A, Xue, JL, Himmelfarb, J, Eggers, PW, Kimmel, PL, Molitoris, BA, Collins, AJ: Acute kidney injury increases risk of ESRD among elderly. *J Am Soc Nephrol,* 20**:** 223-228, 2009. https://doi.org/10.1681/ASN.2007080837
18. Torres Crigna, A, Daniele, C, Gamez, C, Medina Balbuena, S, Pastene, DO, Nardozi, D, Brenna, C, Yard, B, Gretz, N, Bieback, K: Stem/Stromal Cells for Treatment of Kidney Injuries With Focus on Preclinical Models. *Front Med (Lausanne),* 5**:** 179, 2018. https://doi.org/10.3389/fmed.2018.00179
19. Eltzschig, HK, Eckle, T: Ischemia and reperfusion--from mechanism to translation. *Nat Med,* 17**:** 1391-1401, 2011. https://doi.org/10.1038/nm.2507
20. Hodgkins, KS, Schnaper, HW: Tubulointerstitial injury and the progression of chronic kidney disease. *Pediatr Nephrol,* 27**:** 901-909, 2012. https://doi.org/10.1007/s00467-011-1992-9
21. Abecassis, M, Bartlett, ST, Collins, AJ, Davis, CL, Delmonico, FL, Friedewald, JJ, Hays, R, Howard, A, Jones, E, Leichtman, AB, Merion, RM, Metzger, RA, Pradel, F, Schweitzer, EJ, Velez, RL, Gaston, RS: Kidney transplantation as primary therapy for end-stage renal disease: a National Kidney Foundation/Kidney Disease Outcomes Quality Initiative (NKF/KDOQITM) conference. *Clin J Am Soc Nephrol,* 3**:** 471-480, 2008. https://doi.org/10.2215/CJN.05021107
22. Grange, C, Tritta, S, Tapparo, M, Cedrino, M, Tetta, C, Camussi, G, Brizzi, MF: Stem cell-derived extracellular vesicles inhibit and revert fibrosis progression in a mouse model of diabetic nephropathy. *Sci Rep,* 9**:** 4468, 2019. https://doi.org/10.1038/s41598-019-41100-9
23. Aghajani Nargesi, A, Lerman, LO, Eirin, A: Mesenchymal stem cell-derived extracellular vesicles for kidney repair: current status and looming challenges. *Stem Cell Res Ther,* 8**:** 273, 2017. https://doi.org/10.1186/s13287-017-0727-7
24. Ozkok, A, Edelstein, CL: Pathophysiology of cisplatin-induced acute kidney injury. *Biomed Res Int,* 2014**:** 967826, 2014. https://doi.org/10.1155/2014/967826
25. Gomez-Ruiz, S, Maksimovic-Ivanic, D, Mijatovic, S, Kaluderovic, GN: On the discovery, biological effects, and use of Cisplatin and metallocenes in anticancer chemotherapy. *Bioinorg Chem Appl,* 2012**:** 140284, 2012. https://doi.org/10.1155/2012/140284
26. Shiraishi, F, Curtis, LM, Truong, L, Poss, K, Visner, GA, Madsen, K, Nick, HS, Agarwal, A: Heme oxygenase-1 gene ablation or expression modulates cisplatin-induced renal tubular apoptosis. *Am J Physiol Renal Physiol,* 278**:** F726-736, 2000. https://doi.org/10.1152/ajprenal.2000.278.5.F726

27. Lebwohl, D, Canetta, R: Clinical development of platinum complexes in cancer therapy: an historical perspective and an update. *Eur J Cancer,* 34**:** 1522-1534, 1998. https://doi.org/10.1016/s0959-8049(98)00224-x
28. Hill, JM, Speer, RJ: Organo-platinum complexes as antitumor agents (review). *Anticancer Res,* 2**:** 173-186, 1982.
29. Arany, I, Safirstein, RL: Cisplatin nephrotoxicity. *Semin Nephrol,* 23**:** 460-464, 2003. https://doi.org/10.1016/s0270-9295(03)00089-5
30. Beyer, J, Rick, O, Weinknecht, S, Kingreen, D, Lenz, K, Siegert, W: Nephrotoxicity after high-dose carboplatin, etoposide and ifosfamide in germ-cell tumors: incidence and implications for hematologic recovery and clinical outcome. *Bone Marrow Transplant,* 20**:** 813-819, 1997. https://doi.org/10.1038/sj.bmt.1700980
31. Griffin, BR, Faubel, S, Edelstein, CL: Biomarkers of Drug-Induced Kidney Toxicity. *Ther Drug Monit,* 41**:** 213-226, 2019. https://doi.org/10.1097/FTD.0000000000000589
32. Qian, W, Nishikawa, M, Haque, AM, Hirose, M, Mashimo, M, Sato, E, Inoue, M: Mitochondrial density determines the cellular sensitivity to cisplatin-induced cell death. *Am J Physiol Cell Physiol,* 289**:** C1466-1475, 2005. https://doi.org/10.1152/ajpcell.00265.2005
33. Zhu, S, Pabla, N, Tang, C, He, L, Dong, Z: DNA damage response in cisplatin-induced nephrotoxicity. *Arch Toxicol,* 89**:** 2197-2205, 2015. https://doi.org/10.1007/s00204-015-1633-3
34. Pabla, N, Dong, Z: Cisplatin nephrotoxicity: mechanisms and renoprotective strategies. *Kidney Int,* 73**:** 994-1007, 2008. https://doi.org/10.1038/sj.ki.5002786
35. Lieberthal, W, Triaca, V, Levine, J: Mechanisms of death induced by cisplatin in proximal tubular epithelial cells: apoptosis vs. necrosis. *Am J Physiol,* 270**:** F700-708, 1996. https://doi.org/10.1152/ajprenal.1996.270.4.F700
36. Ramesh, G, Reeves, WB: TNFR2-mediated apoptosis and necrosis in cisplatin-induced acute renal failure. *Am J Physiol Renal Physiol,* 285**:** F610-618, 2003. https://doi.org/10.1152/ajprenal.00101.2003
37. McSweeney, KR, Gadanec, LK, Qaradakhi, T, Ali, BA, Zulli, A, Apostolopoulos, V: Mechanisms of Cisplatin-Induced Acute Kidney Injury: Pathological Mechanisms, Pharmacological Interventions, and Genetic Mitigations. *Cancers (Basel),* 13, 2021. https://doi.org/10.3390/cancers13071572
38. Aydinoz, S, Uzun, G, Cermik, H, Atasoyu, EM, Yildiz, S, Karagoz, B, Evrenkaya, R: Effects of different doses of hyperbaric oxygen on cisplatin-induced nephrotoxicity. *Ren Fail,* 29**:** 257-263, 2007. https://doi.org/10.1080/08860220601166487
39. Kruidering, M, Van de Water, B, de Heer, E, Mulder, GJ, Nagelkerke, JF: Cisplatin-induced nephrotoxicity in porcine proximal tubular cells: mitochondrial dysfunction by inhibition of complexes I to IV of the respiratory chain. *J Pharmacol Exp Ther,* 280**:** 638-649, 1997.
40. Winston, JA, Safirstein, R: Reduced renal blood flow in early cisplatin-induced acute renal failure in the rat. *Am J Physiol,* 249**:** F490-496, 1985. https://doi.org/10.1152/ajprenal.1985.249.4.F490
41. Kawai, Y, Nakao, T, Kunimura, N, Kohda, Y, Gemba, M: Relationship of intracellular calcium and oxygen radicals to Cisplatin-related renal cell injury. *J Pharmacol Sci,* 100**:** 65-72, 2006. https://doi.org/10.1254/jphs.fp0050661
42. Sharp, CN, Doll, MA, Dupre, TV, Shah, PP, Subathra, M, Siow, D, Arteel, GE, Megyesi, J, Beverly, LJ, Siskind, LJ: Repeated administration of low-dose

cisplatin in mice induces fibrosis. *Am J Physiol Renal Physiol,* 310**:** F560-568, 2016. https://doi.org/10.1152/ajprenal.00512.2015
43. Levey, AS, Atkins, R, Coresh, J, Cohen, EP, Collins, AJ, Eckardt, KU, Nahas, ME, Jaber, BL, Jadoul, M, Levin, A, Powe, NR, Rossert, J, Wheeler, DC, Lameire, N, Eknoyan, G: Chronic kidney disease as a global public health problem: approaches and initiatives - a position statement from Kidney Disease Improving Global Outcomes. *Kidney Int,* 72**:** 247-259, 2007. https://doi.org/10.1038/sj.ki.5002343
44. Wolfe, RA, Roys, EC, Merion, RM: Trends in organ donation and transplantation in the United States, 1999-2008. *Am J Transplant,* 10**:** 961-972, 2010. https://doi.org/10.1111/j.1600-6143.2010.03021.x
45. Mathur, AK, Ashby, VB, Sands, RL, Wolfe, RA: Geographic variation in end-stage renal disease incidence and access to deceased donor kidney transplantation. *Am J Transplant,* 10**:** 1069-1080, 2010. https://doi.org/10.1111/j.1600-6143.2010.03043.x
46. Himmelfarb, J, Ikizler, TA: Hemodialysis. *N Engl J Med,* 363**:** 1833-1845, 2010. https://doi.org/10.1056/NEJMra0902710
47. Garcia, GG, Harden, P, Chapman, J, World Kidney Day Steering, C: The global role of kidney transplantation. *Am J Nephrol,* 35**:** 259-264, 2012. https://doi.org/10.1159/000336371
48. Nankivell, BJ, Borrows, RJ, Fung, CL, O'Connell, PJ, Allen, RD, Chapman, JR: The natural history of chronic allograft nephropathy. *N Engl J Med,* 349**:** 2326-2333, 2003. https://doi.org/10.1056/NEJMoa020009
49. Yan, MT, Chao, CT, Lin, SH: Chronic Kidney Disease: Strategies to Retard Progression. *Int J Mol Sci,* 22, 2021. https://doi.org/10.3390/ijms221810084
50. RenalToolBox: RenalToolBox_brochure, 2020. https://renaltoolbox.org/wp-content/uploads/2020/10/RenalToolBox_brochure.pdf
51. Kern, S, Eichler, H, Stoeve, J, Kluter, H, Bieback, K: Comparative analysis of mesenchymal stem cells from bone marrow, umbilical cord blood, or adipose tissue. *Stem Cells,* 24**:** 1294-1301, 2006. https://doi.org/10.1634/stemcells.2005-0342
52. Peired, AJ, Sisti, A, Romagnani, P: Mesenchymal Stem Cell-Based Therapy for Kidney Disease: A Review of Clinical Evidence. *Stem Cells Int,* 2016**:** 4798639, 2016. https://doi.org/10.1155/2016/4798639
53. Friedenstein, AJ, Chailakhjan, RK, Lalykina, KS: The development of fibroblast colonies in monolayer cultures of guinea-pig bone marrow and spleen cells. *Cell Tissue Kinet,* 3**:** 393-403, 1970. https://doi.org/10.1111/j.1365-2184.1970.tb00347.x
54. Horwitz, EM, Le Blanc, K, Dominici, M, Mueller, I, Slaper-Cortenbach, I, Marini, FC, Deans, RJ, Krause, DS, Keating, A, International Society for Cellular, T: Clarification of the nomenclature for MSC: The International Society for Cellular Therapy position statement. *Cytotherapy,* 7**:** 393-395, 2005. https://doi.org/10.1080/14653240500319234
55. Dominici, M, Le Blanc, K, Mueller, I, Slaper-Cortenbach, I, Marini, F, Krause, D, Deans, R, Keating, A, Prockop, D, Horwitz, E: Minimal criteria for defining multipotent mesenchymal stromal cells. The International Society for Cellular Therapy position statement. *Cytotherapy,* 8**:** 315-317, 2006. https://doi.org/10.1080/14653240600855905
56. Pittenger, MF, Mackay, AM, Beck, SC, Jaiswal, RK, Douglas, R, Mosca, JD, Moorman, MA, Simonetti, DW, Craig, S, Marshak, DR: Multilineage potential

of adult human mesenchymal stem cells. *Science,* 284**:** 143-147, 1999. https://doi.org/10.1126/science.284.5411.143

57. Divya, MS, Roshin, GE, Divya, TS, Rasheed, VA, Santhoshkumar, TR, Elizabeth, KE, James, J, Pillai, RM: Umbilical cord blood-derived mesenchymal stem cells consist of a unique population of progenitors co-expressing mesenchymal stem cell and neuronal markers capable of instantaneous neuronal differentiation. *Stem Cell Res Ther,* 3**:** 57, 2012. https://doi.org/10.1186/scrt148
58. Imasawa, T, Utsunomiya, Y, Kawamura, T, Zhong, YU, Nagasawa, R, Okabe, M, Maruyama, N, Hosoya, T, Ohno, T: The potential of bone marrow-derived cells to differentiate to glomerular mesangial cells. *J Am Soc Nephrol,* 12**:** 1401-1409, 2001. https://doi.org/10.1681/ASN.V1271401
59. Spaas, JH, De Schauwer, C, Cornillie, P, Meyer, E, Van Soom, A, Van de Walle, GR: Culture and characterisation of equine peripheral blood mesenchymal stromal cells. *Vet J,* 195**:** 107-113, 2013. https://doi.org/10.1016/j.tvjl.2012.05.006
60. Nauta, AJ, Fibbe, WE: Immunomodulatory properties of mesenchymal stromal cells. *Blood,* 110**:** 3499-3506, 2007. https://doi.org/10.1182/blood-2007-02-069716
61. Koc, ON, Day, J, Nieder, M, Gerson, SL, Lazarus, HM, Krivit, W: Allogeneic mesenchymal stem cell infusion for treatment of metachromatic leukodystrophy (MLD) and Hurler syndrome (MPS-IH). *Bone Marrow Transplant,* 30**:** 215-222, 2002. https://doi.org/10.1038/sj.bmt.1703650
62. English, K: Mechanisms of mesenchymal stromal cell immunomodulation. *Immunol Cell Biol,* 91**:** 19-26, 2013. https://doi.org/10.1038/icb.2012.56
63. Hong, J, Hueckelhoven, A, Wang, L, Schmitt, A, Wuchter, P, Tabarkiewicz, J, Kleist, C, Bieback, K, Ho, AD, Schmitt, M: Indoleamine 2,3-dioxygenase mediates inhibition of virus-specific CD8(+) T cell proliferation by human mesenchymal stromal cells. *Cytotherapy,* 18**:** 621-629, 2016. https://doi.org/10.1016/j.jcyt.2016.01.009
64. Polchert, D, Sobinsky, J, Douglas, G, Kidd, M, Moadsiri, A, Reina, E, Genrich, K, Mehrotra, S, Setty, S, Smith, B, Bartholomew, A: IFN-gamma activation of mesenchymal stem cells for treatment and prevention of graft versus host disease. *Eur J Immunol,* 38**:** 1745-1755, 2008. https://doi.org/10.1002/eji.200738129
65. Francois, M, Romieu-Mourez, R, Li, M, Galipeau, J: Human MSC suppression correlates with cytokine induction of indoleamine 2,3-dioxygenase and bystander M2 macrophage differentiation. *Mol Ther,* 20**:** 187-195, 2012. https://doi.org/10.1038/mt.2011.189
66. Maggini, J, Mirkin, G, Bognanni, I, Holmberg, J, Piazzon, IM, Nepomnaschy, I, Costa, H, Canones, C, Raiden, S, Vermeulen, M, Geffner, JR: Mouse bone marrow-derived mesenchymal stromal cells turn activated macrophages into a regulatory-like profile. *PLoS One,* 5**:** e9252, 2010. https://doi.org/10.1371/journal.pone.0009252
67. Li, W, Zhang, Q, Wang, M, Wu, H, Mao, F, Zhang, B, Ji, R, Gao, S, Sun, Z, Zhu, W, Qian, H, Chen, Y, Xu, W: Macrophages are involved in the protective role of human umbilical cord-derived stromal cells in renal ischemia-reperfusion injury. *Stem Cell Res,* 10**:** 405-416, 2013. https://doi.org/10.1016/j.scr.2013.01.005
68. Gregorini, M, Bosio, F, Rocca, C, Corradetti, V, Valsania, T, Pattonieri, EF, Esposito, P, Bedino, G, Collesi, C, Libetta, C, Frassoni, F, Dal Canton, A,

Rampino, T: Mesenchymal stromal cells reset the scatter factor system and cytokine network in experimental kidney transplantation. *BMC Immunol,* 15**:** 44, 2014. https://doi.org/10.1186/s12865-014-0044-1

69. Shi, Y, Wang, Y, Li, Q, Liu, K, Hou, J, Shao, C, Wang, Y: Immunoregulatory mechanisms of mesenchymal stem and stromal cells in inflammatory diseases. *Nat Rev Nephrol,* 14**:** 493-507, 2018. https://doi.org/10.1038/s41581-018-0023-5
70. Caplan, AI: Why are MSCs therapeutic? New data: new insight. *J Pathol,* 217**:** 318-324, 2009. https://doi.org/10.1002/path.2469
71. Ullah, M, Liu, DD, Thakor, AS: Mesenchymal Stromal Cell Homing: Mechanisms and Strategies for Improvement. *iScience,* 15**:** 421-438, 2019. https://doi.org/10.1016/j.isci.2019.05.004
72. Katsuno, T, Ozaki, T, Saka, Y, Furuhashi, K, Kim, H, Yasuda, K, Yamamoto, T, Sato, W, Tsuboi, N, Mizuno, M, Ito, Y, Imai, E, Matsuo, S, Maruyama, S: Low serum cultured adipose tissue-derived stromal cells ameliorate acute kidney injury in rats. *Cell Transplant,* 22**:** 287-297, 2013. https://doi.org/10.3727/096368912X655019
73. Kim, JH, Park, DJ, Yun, JC, Jung, MH, Yeo, HD, Kim, HJ, Kim, DW, Yang, JI, Lee, GW, Jeong, SH, Roh, GS, Chang, SH: Human adipose tissue-derived mesenchymal stem cells protect kidneys from cisplatin nephrotoxicity in rats. *Am J Physiol Renal Physiol,* 302**:** F1141-1150, 2012. https://doi.org/10.1152/ajprenal.00060.2011
74. Kraitchman, DL, Tatsumi, M, Gilson, WD, Ishimori, T, Kedziorek, D, Walczak, P, Segars, WP, Chen, HH, Fritzges, D, Izbudak, I, Young, RG, Marcelino, M, Pittenger, MF, Solaiyappan, M, Boston, RC, Tsui, BM, Wahl, RL, Bulte, JW: Dynamic imaging of allogeneic mesenchymal stem cells trafficking to myocardial infarction. *Circulation,* 112**:** 1451-1461, 2005. https://doi.org/10.1161/CIRCULATIONAHA.105.537480
75. Furlani, D, Ugurlucan, M, Ong, L, Bieback, K, Pittermann, E, Westien, I, Wang, W, Yerebakan, C, Li, W, Gaebel, R, Li, RK, Vollmar, B, Steinhoff, G, Ma, N: Is the intravascular administration of mesenchymal stem cells safe? Mesenchymal stem cells and intravital microscopy. *Microvasc Res,* 77**:** 370-376, 2009. https://doi.org/10.1016/j.mvr.2009.02.001
76. Humphreys, BD, Bonventre, JV: Mesenchymal stem cells in acute kidney injury. *Annu Rev Med,* 59**:** 311-325, 2008. https://doi.org/10.1146/annurev.med.59.061506.154239
77. Shiratsuki, S, Terai, S, Murata, Y, Takami, T, Yamamoto, N, Fujisawa, K, Burganova, G, Quintanilha, LF, Sakaida, I: Enhanced survival of mice infused with bone marrow-derived as compared with adipose-derived mesenchymal stem cells. *Hepatol Res,* 45**:** 1353-1359, 2015. https://doi.org/10.1111/hepr.12507
78. Oeller, M, Laner-Plamberger, S, Hochmann, S, Ketterl, N, Feichtner, M, Brachtl, G, Hochreiter, A, Scharler, C, Bieler, L, Romanelli, P, Couillard-Despres, S, Russe, E, Schallmoser, K, Strunk, D: Selection of Tissue Factor-Deficient Cell Transplants as a Novel Strategy for Improving Hemocompatibility of Human Bone Marrow Stromal Cells. *Theranostics,* 8**:** 1421-1434, 2018. https://doi.org/10.7150/thno.21906
79. Netsch, P, Elvers-Hornung, S, Uhlig, S, Kluter, H, Huck, V, Kirschhofer, F, Brenner-Weiss, G, Janetzko, K, Solz, H, Wuchter, P, Bugert, P, Bieback, K: Human mesenchymal stromal cells inhibit platelet activation and aggregation

involving CD73-converted adenosine. *Stem Cell Res Ther,* 9**:** 184, 2018. https://doi.org/10.1186/s13287-018-0936-8

80. Baulier, E, Favreau, F, Le Corf, A, Jayle, C, Schneider, F, Goujon, JM, Feraud, O, Bennaceur-Griscelli, A, Hauet, T, Turhan, AG: Amniotic fluid-derived mesenchymal stem cells prevent fibrosis and preserve renal function in a preclinical porcine model of kidney transplantation. *Stem Cells Transl Med,* 3**:** 809-820, 2014. https://doi.org/10.5966/sctm.2013-0186
81. De Martino, M, Zonta, S, Rampino, T, Gregorini, M, Frassoni, F, Piotti, G, Bedino, G, Cobianchi, L, Dal Canton, A, Dionigi, P, Alessiani, M: Mesenchymal stem cells infusion prevents acute cellular rejection in rat kidney transplantation. *Transplant Proc,* 42**:** 1331-1335, 2010. https://doi.org/10.1016/j.transproceed.2010.03.079
82. Le Blanc, K, Rasmusson, I, Sundberg, B, Gotherstrom, C, Hassan, M, Uzunel, M, Ringden, O: Treatment of severe acute graft-versus-host disease with third party haploidentical mesenchymal stem cells. *Lancet,* 363**:** 1439-1441, 2004. https://doi.org/10.1016/S0140-6736(04)16104-7
83. ClinicalTrials. http:///clinicaltrials.gov
84. Bi, B, Schmitt, R, Israilova, M, Nishio, H, Cantley, LG: Stromal cells protect against acute tubular injury via an endocrine effect. *J Am Soc Nephrol,* 18**:** 2486-2496, 2007. https://doi.org/10.1681/ASN.2007020140
85. Cheng, K, Rai, P, Plagov, A, Lan, X, Kumar, D, Salhan, D, Rehman, S, Malhotra, A, Bhargava, K, Palestro, CJ, Gupta, S, Singhal, PC: Transplantation of bone marrow-derived MSCs improves cisplatinum-induced renal injury through paracrine mechanisms. *Exp Mol Pathol,* 94**:** 466-473, 2013. https://doi.org/10.1016/j.yexmp.2013.03.002
86. Moustafa, FE, Sobh, MA, Abouelkheir, M, Khater, Y, Mahmoud, K, Saad, MA, Sobh, MA: Study of the Effect of Route of Administration of Mesenchymal Stem Cells on Cisplatin-Induced Acute Kidney Injury in Sprague Dawley Rats. *Int J Stem Cells,* 9**:** 79-89, 2016. https://doi.org/10.15283/ijsc.2016.9.1.79
87. Vanikar, AV, Trivedi, HL, Feroze, A, Kanodia, KV, Dave, SD, Shah, PR: Effect of co-transplantation of mesenchymal stem cells and hematopoietic stem cells as compared to hematopoietic stem cell transplantation alone in renal transplantation to achieve donor hypo-responsiveness. *Int Urol Nephrol,* 43**:** 225-232, 2011. https://doi.org/10.1007/s11255-009-9659-1
88. Vanikar, AV, Trivedi, HL, Kumar, A, Gopal, SC, Patel, HV, Gumber, MR, Kute, VB, Shah, PR, Dave, SD: Co-infusion of donor adipose tissue-derived mesenchymal and hematopoietic stem cells helps safe minimization of immunosuppression in renal transplantation - single center experience. *Ren Fail,* 36**:** 1376-1384, 2014. https://doi.org/10.3109/0886022X.2014.950931
89. Trivedi, HL, Vanikar, AV, Kute, VB, Patel, HV, Gumber, MR, Shah, PR, Dave, SD, Trivedi, VB: The effect of stem cell transplantation on immunosuppression in living donor renal transplantation: a clinical trial. *Int J Organ Transplant Med,* 4**:** 155-162, 2013.
90. Negri, M: Mesenchymal Stem Cells In Cisplatin-Induced Acute Renal Failure In Patients With Solid Organ Cancers, 2011. ClinicalTrials.gov
91. Chen, C, Hou, J: Mesenchymal stem cell-based therapy in kidney transplantation. *Stem Cell Res Ther,* 7**:** 16, 2016. https://doi.org/10.1186/s13287-016-0283-6
92. Gnecchi, M, He, H, Liang, OD, Melo, LG, Morello, F, Mu, H, Noiseux, N, Zhang, L, Pratt, RE, Ingwall, JS, Dzau, VJ: Paracrine action accounts for marked protection of ischemic heart by Akt-modified mesenchymal stem cells. *Nat Med,* 11**:** 367-368, 2005. https://doi.org/10.1038/nm0405-367

93. Ankrum, JA, Ong, JF, Karp, JM: Mesenchymal stem cells: immune evasive, not immune privileged. *Nat Biotechnol,* 32**:** 252-260, 2014. https://doi.org/10.1038/nbt.2816
94. Leiker, M, Suzuki, G, Iyer, VS, Canty, JM, Jr., Lee, T: Assessment of a nuclear affinity labeling method for tracking implanted mesenchymal stem cells. *Cell Transplant,* 17**:** 911-922, 2008. https://doi.org/10.3727/096368908786576444
95. Zhuang, Q, Ma, R, Yin, Y, Lan, T, Yu, M, Ming, Y: Mesenchymal Stem Cells in Renal Fibrosis: The Flame of Cytotherapy. *Stem Cells Int,* 2019**:** 8387350, 2019. https://doi.org/10.1155/2019/8387350
96. Liu, B, Ding, F, Hu, D, Zhou, Y, Long, C, Shen, L, Zhang, Y, Zhang, D, Wei, G: Human umbilical cord mesenchymal stem cell conditioned medium attenuates renal fibrosis by reducing inflammation and epithelial-to-mesenchymal transition via the TLR4/NF-kappaB signaling pathway in vivo and in vitro. *Stem Cell Res Ther,* 9**:** 7, 2018. https://doi.org/10.1186/s13287-017-0760-6
97. Teixeira, FG, Carvalho, MM, Sousa, N, Salgado, AJ: Mesenchymal stem cells secretome: a new paradigm for central nervous system regeneration? *Cell Mol Life Sci,* 70**:** 3871-3882, 2013. https://doi.org/10.1007/s00018-013-1290-8
98. Maacha, S, Sidahmed, H, Jacob, S, Gentilcore, G, Calzone, R, Grivel, JC, Cugno, C: Paracrine Mechanisms of Mesenchymal Stromal Cells in Angiogenesis. *Stem Cells Int,* 2020**:** 4356359, 2020. https://doi.org/10.1155/2020/4356359
99. Boomsma, RA, Geenen, DL: Mesenchymal stem cells secrete multiple cytokines that promote angiogenesis and have contrasting effects on chemotaxis and apoptosis. *PLoS One,* 7**:** e35685, 2012. https://doi.org/10.1371/journal.pone.0035685
100. Villegas, G, Lange-Sperandio, B, Tufro, A: Autocrine and paracrine functions of vascular endothelial growth factor (VEGF) in renal tubular epithelial cells. *Kidney Int,* 67**:** 449-457, 2005. https://doi.org/10.1111/j.1523-1755.2005.67101.x
101. Phelps, J, Sanati-Nezhad, A, Ungrin, M, Duncan, NA, Sen, A: Bioprocessing of Mesenchymal Stem Cells and Their Derivatives: Toward Cell-Free Therapeutics. *Stem Cells Int,* 2018**:** 9415367, 2018. https://doi.org/10.1155/2018/9415367
102. Gowen, A, Shahjin, F, Chand, S, Odegaard, KE, Yelamanchili, SV: Mesenchymal Stem Cell-Derived Extracellular Vesicles: Challenges in Clinical Applications. *Front Cell Dev Biol,* 8**:** 149, 2020. https://doi.org/10.3389/fcell.2020.00149
103. Grange, C, Skovronova, R, Marabese, F, Bussolati, B: Stem Cell-Derived Extracellular Vesicles and Kidney Regeneration. *Cells,* 8, 2019. https://doi.org/10.3390/cells8101240
104. Kusuma, GD, Carthew, J, Lim, R, Frith, JE: Effect of the Microenvironment on Mesenchymal Stem Cell Paracrine Signaling: Opportunities to Engineer the Therapeutic Effect. *Stem Cells Dev,* 26**:** 617-631, 2017. https://doi.org/10.1089/scd.2016.0349
105. Thery, C, Witwer, KW, Aikawa, E, Alcaraz, MJ, Anderson, JD, Andriantsitohaina, R, Antoniou, A, Arab, T, Archer, F, Atkin-Smith, GK, Ayre, DC, Bach, JM, Bachurski, D, Baharvand, H, Balaj, L, Baldacchino, S, Bauer, NN, Baxter, AA, Bebawy, M, Beckham, C, Bedina Zavec, A, Benmoussa, A, Berardi, AC, Bergese, P, Bielska, E, Blenkiron, C, Bobis-Wozowicz, S, Boilard, E, Boireau, W, Bongiovanni, A, Borras, FE, Bosch, S, Boulanger, CM, Breakefield, X, Breglio, AM, Brennan, MA, Brigstock, DR, Brisson, A, Broekman, ML,

Bromberg, JF, Bryl-Gorecka, P, Buch, S, Buck, AH, Burger, D, Busatto, S, Buschmann, D, Bussolati, B, Buzas, EI, Byrd, JB, Camussi, G, Carter, DR, Caruso, S, Chamley, LW, Chang, YT, Chen, C, Chen, S, Cheng, L, Chin, AR, Clayton, A, Clerici, SP, Cocks, A, Cocucci, E, Coffey, RJ, Cordeiro-da-Silva, A, Couch, Y, Coumans, FA, Coyle, B, Crescitelli, R, Criado, MF, D'Souza-Schorey, C, Das, S, Datta Chaudhuri, A, de Candia, P, De Santana, EF, De Wever, O, Del Portillo, HA, Demaret, T, Deville, S, Devitt, A, Dhondt, B, Di Vizio, D, Dieterich, LC, Dolo, V, Dominguez Rubio, AP, Dominici, M, Dourado, MR, Driedonks, TA, Duarte, FV, Duncan, HM, Eichenberger, RM, Ekstrom, K, El Andaloussi, S, Elie-Caille, C, Erdbrugger, U, Falcon-Perez, JM, Fatima, F, Fish, JE, Flores-Bellver, M, Forsonits, A, Frelet-Barrand, A, Fricke, F, Fuhrmann, G, Gabrielsson, S, Gamez-Valero, A, Gardiner, C, Gartner, K, Gaudin, R, Gho, YS, Giebel, B, Gilbert, C, Gimona, M, Giusti, I, Goberdhan, DC, Gorgens, A, Gorski, SM, Greening, DW, Gross, JC, Gualerzi, A, Gupta, GN, Gustafson, D, Handberg, A, Haraszti, RA, Harrison, P, Hegyesi, H, Hendrix, A, Hill, AF, Hochberg, FH, Hoffmann, KF, Holder, B, Holthofer, H, Hosseinkhani, B, Hu, G, Huang, Y, Huber, V, Hunt, S, Ibrahim, AG, Ikezu, T, Inal, JM, Isin, M, Ivanova, A, Jackson, HK, Jacobsen, S, Jay, SM, Jayachandran, M, Jenster, G, Jiang, L, Johnson, SM, Jones, JC, Jong, A, Jovanovic-Talisman, T, Jung, S, Kalluri, R, Kano, SI, Kaur, S, Kawamura, Y, Keller, ET, Khamari, D, Khomyakova, E, Khvorova, A, Kierulf, P, Kim, KP, Kislinger, T, Klingeborn, M, Klinke, DJ, 2nd, Kornek, M, Kosanovic, MM, Kovacs, AF, Kramer-Albers, EM, Krasemann, S, Krause, M, Kurochkin, IV, Kusuma, GD, Kuypers, S, Laitinen, S, Langevin, SM, Languino, LR, Lannigan, J, Lasser, C, Laurent, LC, Lavieu, G, Lazaro-Ibanez, E, Le Lay, S, Lee, MS, Lee, YXF, Lemos, DS, Lenassi, M, Leszczynska, A, Li, IT, Liao, K, Libregts, SF, Ligeti, E, Lim, R, Lim, SK, Line, A, Linnemannstons, K, Llorente, A, Lombard, CA, Lorenowicz, MJ, Lorincz, AM, Lotvall, J, Lovett, J, Lowry, MC, Loyer, X, Lu, Q, Lukomska, B, Lunavat, TR, Maas, SL, Malhi, H, Marcilla, A, Mariani, J, Mariscal, J, Martens-Uzunova, ES, Martin-Jaular, L, Martinez, MC, Martins, VR, Mathieu, M, Mathivanan, S, Maugeri, M, McGinnis, LK, McVey, MJ, Meckes, DG, Jr., Meehan, KL, Mertens, I, Minciacchi, VR, Moller, A, Moller Jorgensen, M, Morales-Kastresana, A, Morhayim, J, Mullier, F, Muraca, M, Musante, L, Mussack, V, Muth, DC, Myburgh, KH, Najrana, T, Nawaz, M, Nazarenko, I, Nejsum, P, Neri, C, Neri, T, Nieuwland, R, Nimrichter, L, Nolan, JP, Nolte-'t Hoen, EN, Noren Hooten, N, O'Driscoll, L, O'Grady, T, O'Loghlen, A, Ochiya, T, Olivier, M, Ortiz, A, Ortiz, LA, Osteikoetxea, X, Ostergaard, O, Ostrowski, M, Park, J, Pegtel, DM, Peinado, H, Perut, F, Pfaffl, MW, Phinney, DG, Pieters, BC, Pink, RC, Pisetsky, DS, Pogge von Strandmann, E, Polakovicova, I, Poon, IK, Powell, BH, Prada, I, Pulliam, L, Quesenberry, P, Radeghieri, A, Raffai, RL, Raimondo, S, Rak, J, Ramirez, MI, Raposo, G, Rayyan, MS, Regev-Rudzki, N, Ricklefs, FL, Robbins, PD, Roberts, DD, Rodrigues, SC, Rohde, E, Rome, S, Rouschop, KM, Rughetti, A, Russell, AE, Saa, P, Sahoo, S, Salas-Huenuleo, E, Sanchez, C, Saugstad, JA, Saul, MJ, Schiffelers, RM, Schneider, R, Schoyen, TH, Scott, A, Shahaj, E, Sharma, S, Shatnyeva, O, Shekari, F, Shelke, GV, Shetty, AK, Shiba, K, Siljander, PR, Silva, AM, Skowronek, A, Snyder, OL, 2nd, Soares, RP, Sodar, BW, Soekmadji, C, Sotillo, J, Stahl, PD, Stoorvogel, W, Stott, SL, Strasser, EF, Swift, S, Tahara, H, Tewari, M, Timms, K, Tiwari, S, Tixeira, R, Tkach, M, Toh, WS, Tomasini, R, Torrecilhas, AC, Tosar, JP, Toxavidis, V, Urbanelli, L, Vader, P, van Balkom, BW, van der Grein, SG, Van Deun, J, van Herwijnen,

MJ, Van Keuren-Jensen, K, van Niel, G, van Royen, ME, van Wijnen, AJ, Vasconcelos, MH, Vechetti, IJ, Jr., Veit, TD, Vella, LJ, Velot, E, Verweij, FJ, Vestad, B, Vinas, JL, Visnovitz, T, Vukman, KV, Wahlgren, J, Watson, DC, Wauben, MH, Weaver, A, Webber, JP, Weber, V, Wehman, AM, Weiss, DJ, Welsh, JA, Wendt, S, Wheelock, AM, Wiener, Z, Witte, L, Wolfram, J, Xagorari, A, Xander, P, Xu, J, Yan, X, Yanez-Mo, M, Yin, H, Yuana, Y, Zappulli, V, Zarubova, J, Zekas, V, Zhang, JY, Zhao, Z, Zheng, L, Zheutlin, AR, Zickler, AM, Zimmermann, P, Zivkovic, AM, Zocco, D, Zuba-Surma, EK: Minimal information for studies of extracellular vesicles 2018 (MISEV2018): a position statement of the International Society for Extracellular Vesicles and update of the MISEV2014 guidelines. *J Extracell Vesicles,* 7**:** 1535750, 2018. https://doi.org/10.1080/20013078.2018.1535750

106. Phinney, DG, Pittenger, MF: Concise Review: MSC-Derived Exosomes for Cell-Free Therapy. *Stem Cells,* 35**:** 851-858, 2017. https://doi.org/10.1002/stem.2575
107. Pegtel, DM, Gould, SJ: Exosomes. *Annu Rev Biochem,* 88**:** 487-514, 2019. https://doi.org/10.1146/annurev-biochem-013118-111902
108. Ding, Z, Greenberg, ZF, Serafim, MF, Ali, S, Jamieson, JC, Traktuev, DO, March, K, He, M: Understanding molecular characteristics of extracellular vesicles derived from different types of mesenchymal stem cells for therapeutic translation. *Extracell Vesicle,* 3, 2024. https://doi.org/10.1016/j.vesic.2024.100034
109. Consortium, E-T, Van Deun, J, Mestdagh, P, Agostinis, P, Akay, O, Anand, S, Anckaert, J, Martinez, ZA, Baetens, T, Beghein, E, Bertier, L, Berx, G, Boere, J, Boukouris, S, Bremer, M, Buschmann, D, Byrd, JB, Casert, C, Cheng, L, Cmoch, A, Daveloose, D, De Smedt, E, Demirsoy, S, Depoorter, V, Dhondt, B, Driedonks, TA, Dudek, A, Elsharawy, A, Floris, I, Foers, AD, Gartner, K, Garg, AD, Geeurickx, E, Gettemans, J, Ghazavi, F, Giebel, B, Kormelink, TG, Hancock, G, Helsmoortel, H, Hill, AF, Hyenne, V, Kalra, H, Kim, D, Kowal, J, Kraemer, S, Leidinger, P, Leonelli, C, Liang, Y, Lippens, L, Liu, S, Lo Cicero, A, Martin, S, Mathivanan, S, Mathiyalagan, P, Matusek, T, Milani, G, Monguio-Tortajada, M, Mus, LM, Muth, DC, Nemeth, A, Nolte-'t Hoen, EN, O'Driscoll, L, Palmulli, R, Pfaffl, MW, Primdal-Bengtson, B, Romano, E, Rousseau, Q, Sahoo, S, Sampaio, N, Samuel, M, Scicluna, B, Soen, B, Steels, A, Swinnen, JV, Takatalo, M, Thaminy, S, Thery, C, Tulkens, J, Van Audenhove, I, van der Grein, S, Van Goethem, A, van Herwijnen, MJ, Van Niel, G, Van Roy, N, Van Vliet, AR, Vandamme, N, Vanhauwaert, S, Vergauwen, G, Verweij, F, Wallaert, A, Wauben, M, Witwer, KW, Zonneveld, MI, De Wever, O, Vandesompele, J, Hendrix, A: EV-TRACK: transparent reporting and centralizing knowledge in extracellular vesicle research. *Nat Methods,* 14**:** 228-232, 2017. https://doi.org/10.1038/nmeth.4185
110. Willms, E, Cabanas, C, Mager, I, Wood, MJA, Vader, P: Extracellular Vesicle Heterogeneity: Subpopulations, Isolation Techniques, and Diverse Functions in Cancer Progression. *Front Immunol,* 9**:** 738, 2018. https://doi.org/10.3389/fimmu.2018.00738
111. Todorova, D, Simoncini, S, Lacroix, R, Sabatier, F, Dignat-George, F: Extracellular Vesicles in Angiogenesis. *Circ Res,* 120**:** 1658-1673, 2017. https://doi.org/10.1161/CIRCRESAHA.117.309681
112. Tsuji, K, Kitamura, S, Wada, J: Immunomodulatory and Regenerative Effects of Mesenchymal Stem Cell-Derived Extracellular Vesicles in Renal Diseases. *Int J Mol Sci,* 21, 2020. https://doi.org/10.3390/ijms21030756

113. Colombo, M, Raposo, G, Thery, C: Biogenesis, secretion, and intercellular interactions of exosomes and other extracellular vesicles. *Annu Rev Cell Dev Biol,* 30**:** 255-289, 2014. https://doi.org/10.1146/annurev-cellbio-101512-122326
114. Cantaluppi, V, Biancone, L, Quercia, A, Deregibus, MC, Segoloni, G, Camussi, G: Rationale of mesenchymal stem cell therapy in kidney injury. *Am J Kidney Dis,* 61**:** 300-309, 2013. https://doi.org/10.1053/j.ajkd.2012.05.027
115. Bruno, S, Grange, C, Deregibus, MC, Calogero, RA, Saviozzi, S, Collino, F, Morando, L, Busca, A, Falda, M, Bussolati, B, Tetta, C, Camussi, G: Mesenchymal stem cell-derived microvesicles protect against acute tubular injury. *J Am Soc Nephrol,* 20**:** 1053-1067, 2009. https://doi.org/10.1681/ASN.2008070798
116. Gatti, S, Bruno, S, Deregibus, MC, Sordi, A, Cantaluppi, V, Tetta, C, Camussi, G: Microvesicles derived from human adult mesenchymal stem cells protect against ischaemia-reperfusion-induced acute and chronic kidney injury. *Nephrol Dial Transplant,* 26**:** 1474-1483, 2011. https://doi.org/10.1093/ndt/gfr015
117. Lindoso, RS, Collino, F, Bruno, S, Araujo, DS, Sant'Anna, JF, Tetta, C, Provero, P, Quesenberry, PJ, Vieyra, A, Einicker-Lamas, M, Camussi, G: Extracellular vesicles released from mesenchymal stromal cells modulate miRNA in renal tubular cells and inhibit ATP depletion injury. *Stem Cells Dev,* 23**:** 1809-1819, 2014. https://doi.org/10.1089/scd.2013.0618
118. Zou, X, Gu, D, Xing, X, Cheng, Z, Gong, D, Zhang, G, Zhu, Y: Human mesenchymal stromal cell-derived extracellular vesicles alleviate renal ischemic reperfusion injury and enhance angiogenesis in rats. *Am J Transl Res,* 8**:** 4289-4299, 2016.
119. Wang, B, Jia, H, Zhang, B, Wang, J, Ji, C, Zhu, X, Yan, Y, Yin, L, Yu, J, Qian, H, Xu, W: Pre-incubation with hucMSC-exosomes prevents cisplatin-induced nephrotoxicity by activating autophagy. *Stem Cell Res Ther,* 8**:** 75, 2017. https://doi.org/10.1186/s13287-016-0463-4
120. Quesenberry, PJ, Dooner, MS, Aliotta, JM: Stem cell plasticity revisited: the continuum marrow model and phenotypic changes mediated by microvesicles. *Exp Hematol,* 38**:** 581-592, 2010. https://doi.org/10.1016/j.exphem.2010.03.021
121. Collino, F, Bruno, S, Incarnato, D, Dettori, D, Neri, F, Provero, P, Pomatto, M, Oliviero, S, Tetta, C, Quesenberry, PJ, Camussi, G: AKI Recovery Induced by Mesenchymal Stromal Cell-Derived Extracellular Vesicles Carrying MicroRNAs. *J Am Soc Nephrol,* 26**:** 2349-2360, 2015. https://doi.org/10.1681/ASN.2014070710
122. Kim, HS, Choi, DY, Yun, SJ, Choi, SM, Kang, JW, Jung, JW, Hwang, D, Kim, KP, Kim, DW: Proteomic analysis of microvesicles derived from human mesenchymal stem cells. *J Proteome Res,* 11**:** 839-849, 2012. https://doi.org/10.1021/pr200682z
123. Eirin, A, Lerman, LO: Mesenchymal Stem/Stromal Cell-Derived Extracellular Vesicles for Chronic Kidney Disease: Are We There Yet? *Hypertension,* 78**:** 261-269, 2021. https://doi.org/10.1161/HYPERTENSIONAHA.121.14596
124. Nassar, W, El-Ansary, M, Sabry, D, Mostafa, MA, Fayad, T, Kotb, E, Temraz, M, Saad, AN, Essa, W, Adel, H: Umbilical cord mesenchymal stem cells derived extracellular vesicles can safely ameliorate the progression of chronic kidney diseases. *Biomater Res,* 20**:** 21, 2016. https://doi.org/10.1186/s40824-016-0068-0

125. Lv, LL, Feng, Y, Tang, TT, Liu, BC: New insight into the role of extracellular vesicles in kidney disease. *J Cell Mol Med,* 23**:** 731-739, 2019. https://doi.org/10.1111/jcmm.14101
126. Correa, RR, Juncosa, EM, Masereeuw, R, Lindoso, RS: Extracellular Vesicles as a Therapeutic Tool for Kidney Disease: Current Advances and Perspectives. *Int J Mol Sci,* 22, 2021. https://doi.org/10.3390/ijms22115787
127. Huang, YK, Yu, JC: Circulating microRNAs and long non-coding RNAs in gastric cancer diagnosis: An update and review. *World J Gastroenterol,* 21**:** 9863-9886, 2015. https://doi.org/10.3748/wjg.v21.i34.9863
128. Ha, M, Kim, VN: Regulation of microRNA biogenesis. *Nat Rev Mol Cell Biol,* 15**:** 509-524, 2014. https://doi.org/10.1038/nrm3838
129. Macfarlane, LA, Murphy, PR: MicroRNA: Biogenesis, Function and Role in Cancer. *Curr Genomics,* 11**:** 537-561, 2010. https://doi.org/10.2174/138920210793175895
130. Pritchard, CC, Cheng, HH, Tewari, M: MicroRNA profiling: approaches and considerations. *Nat Rev Genet,* 13**:** 358-369, 2012. https://doi.org/10.1038/nrg3198
131. Hogg, DR, Harries, LW: Human genetic variation and its effect on miRNA biogenesis, activity and function. *Biochem Soc Trans,* 42**:** 1184-1189, 2014. https://doi.org/10.1042/BST20140055
132. Lewis, BP, Burge, CB, Bartel, DP: Conserved seed pairing, often flanked by adenosines, indicates that thousands of human genes are microRNA targets. *Cell,* 120**:** 15-20, 2005. https://doi.org/10.1016/j.cell.2004.12.035
133. Hwang, HW, Mendell, JT: MicroRNAs in cell proliferation, cell death, and tumorigenesis. *Br J Cancer,* 94**:** 776-780, 2006. https://doi.org/10.1038/sj.bjc.6603023
134. Leitao, AL, Enguita, FJ: A Structural View of miRNA Biogenesis and Function. *Noncoding RNA,* 8, 2022. https://doi.org/10.3390/ncrna8010010
135. Lee, Y, Kim, M, Han, J, Yeom, KH, Lee, S, Baek, SH, Kim, VN: MicroRNA genes are transcribed by RNA polymerase II. *EMBO J,* 23**:** 4051-4060, 2004. https://doi.org/10.1038/sj.emboj.7600385
136. Blahna, MT, Hata, A: Smad-mediated regulation of microRNA biosynthesis. *FEBS Lett,* 586**:** 1906-1912, 2012. https://doi.org/10.1016/j.febslet.2012.01.041
137. Beezhold, KJ, Castranova, V, Chen, F: Microprocessor of microRNAs: regulation and potential for therapeutic intervention. *Mol Cancer,* 9**:** 134, 2010. https://doi.org/10.1186/1476-4598-9-134
138. Khvorova, A, Reynolds, A, Jayasena, SD: Functional siRNAs and miRNAs exhibit strand bias. *Cell,* 115**:** 209-216, 2003. https://doi.org/10.1016/s0092-8674(03)00801-8
139. Valencia-Sanchez, MA, Liu, J, Hannon, GJ, Parker, R: Control of translation and mRNA degradation by miRNAs and siRNAs. *Genes Dev,* 20**:** 515-524, 2006. https://doi.org/10.1101/gad.1399806
140. O'Brien, J, Hayder, H, Zayed, Y, Peng, C: Overview of MicroRNA Biogenesis, Mechanisms of Actions, and Circulation. *Front Endocrinol (Lausanne),* 9**:** 402, 2018. https://doi.org/10.3389/fendo.2018.00402
141. Rajewsky, N: microRNA target predictions in animals. *Nat Genet,* 38 Suppl**:** S8-13, 2006. https://doi.org/10.1038/ng1798
142. Faruq, O, Vecchione, A: microRNA: Diagnostic Perspective. *Front Med (Lausanne),* 2**:** 51, 2015. https://doi.org/10.3389/fmed.2015.00051

143. Wei, Q, Bhatt, K, He, HZ, Mi, QS, Haase, VH, Dong, Z: Targeted deletion of Dicer from proximal tubules protects against renal ischemia-reperfusion injury. *J Am Soc Nephrol,* 21**:** 756-761, 2010. https://doi.org/10.1681/ASN.2009070718
144. Zhu, Y, Yu, J, Yin, L, Zhou, Y, Sun, Z, Jia, H, Tao, Y, Liu, W, Zhang, B, Zhang, J, Wang, M, Zhang, X, Yan, Y, Xue, J, Gu, H, Mao, F, Xu, W, Qian, H: MicroRNA-146b, a Sensitive Indicator of Mesenchymal Stem Cell Repair of Acute Renal Injury. *Stem Cells Transl Med,* 5**:** 1406-1415, 2016. https://doi.org/10.5966/sctm.2015-0355
145. Bhatt, K, Zhou, L, Mi, QS, Huang, S, She, JX, Dong, Z: MicroRNA-34a is induced via p53 during cisplatin nephrotoxicity and contributes to cell survival. *Mol Med,* 16**:** 409-416, 2010. https://doi.org/10.2119/molmed.2010.00002
146. Zhang, J, He, W, Zheng, D, He, Q, Tan, M, Jin, J: Exosomal-miR-1184 derived from mesenchymal stem cells alleviates cisplatin-associated acute kidney injury. *Mol Med Rep,* 24, 2021. https://doi.org/10.3892/mmr.2021.12435
147. Wei, Q, Mi, QS, Dong, Z: The regulation and function of microRNAs in kidney diseases. *IUBMB Life,* 65**:** 602-614, 2013. https://doi.org/10.1002/iub.1174
148. Liu, Z, Wang, S, Mi, QS, Dong, Z: MicroRNAs in Pathogenesis of Acute Kidney Injury. *Nephron,* 134**:** 149-153, 2016. https://doi.org/10.1159/000446551
149. Du, J, Cao, X, Zou, L, Chen, Y, Guo, J, Chen, Z, Hu, S, Zheng, Z: MicroRNA-21 and risk of severe acute kidney injury and poor outcomes after adult cardiac surgery. *PLoS One,* 8**:** e63390, 2013. https://doi.org/10.1371/journal.pone.0063390
150. Lan, YF, Chen, HH, Lai, PF, Cheng, CF, Huang, YT, Lee, YC, Chen, TW, Lin, H: MicroRNA-494 reduces ATF3 expression and promotes AKI. *J Am Soc Nephrol,* 23**:** 2012-2023, 2012. https://doi.org/10.1681/ASN.2012050438
151. Pavkovic, M, Riefke, B, Ellinger-Ziegelbauer, H: Urinary microRNA profiling for identification of biomarkers after cisplatin-induced kidney injury. *Toxicology,* 324**:** 147-157, 2014. https://doi.org/10.1016/j.tox.2014.05.005
152. Wolenski, FS, Shah, P, Sano, T, Shinozawa, T, Bernard, H, Gallacher, MJ, Wyllie, SD, Varrone, G, Cicia, LA, Carsillo, ME, Fisher, CD, Ottinger, SE, Koenig, E, Kirby, PJ: Identification of microRNA biomarker candidates in urine and plasma from rats with kidney or liver damage. *J Appl Toxicol,* 37**:** 278-286, 2017. https://doi.org/10.1002/jat.3358
153. Kanki, M, Moriguchi, A, Sasaki, D, Mitori, H, Yamada, A, Unami, A, Miyamae, Y: Identification of urinary miRNA biomarkers for detecting cisplatin-induced proximal tubular injury in rats. *Toxicology,* 324**:** 158-168, 2014. https://doi.org/10.1016/j.tox.2014.05.004
154. Jeon, BS, Lee, SH, Hwang, SR, Yi, H, Bang, JH, Tham, NTT, Lee, HK, Woo, GH, Kang, HG, Ku, HO: Identification of urinary microRNA biomarkers for in vivo gentamicin-induced nephrotoxicity models. *J Vet Sci,* 21**:** e81, 2020. https://doi.org/10.4142/jvs.2020.21.e81
155. Gallant-Behm, CL, Piper, J, Lynch, JM, Seto, AG, Hong, SJ, Mustoe, TA, Maari, C, Pestano, LA, Dalby, CM, Jackson, AL, Rubin, P, Marshall, WS: A MicroRNA-29 Mimic (Remlarsen) Represses Extracellular Matrix Expression and Fibroplasia in the Skin. *J Invest Dermatol,* 139**:** 1073-1081, 2019. https://doi.org/10.1016/j.jid.2018.11.007
156. Taubel, J, Hauke, W, Rump, S, Viereck, J, Batkai, S, Poetzsch, J, Rode, L, Weigt, H, Genschel, C, Lorch, U, Theek, C, Levin, AA, Bauersachs, J, Solomon, SD, Thum, T: Novel antisense therapy targeting microRNA-132 in patients with heart failure: results of a first-in-human Phase 1b randomized,

double-blind, placebo-controlled study. *Eur Heart J,* 42**:** 178-188, 2021. https://doi.org/10.1093/eurheartj/ehaa898

157. Yang, Z, Wan, X, Gu, Z, Zhang, H, Yang, X, He, L, Miao, R, Zhong, Y, Zhao, H: Evolution of the mir-181 microRNA family. *Comput Biol Med,* 52**:** 82-87, 2014. https://doi.org/10.1016/j.compbiomed.2014.06.004
158. Lim, LP, Lau, NC, Garrett-Engele, P, Grimson, A, Schelter, JM, Castle, J, Bartel, DP, Linsley, PS, Johnson, JM: Microarray analysis shows that some microRNAs downregulate large numbers of target mRNAs. *Nature,* 433**:** 769-773, 2005. https://doi.org/10.1038/nature03315
159. Huang, S, Wu, S, Ding, J, Lin, J, Wei, L, Gu, J, He, X: MicroRNA-181a modulates gene expression of zinc finger family members by directly targeting their coding regions. *Nucleic Acids Res,* 38**:** 7211-7218, 2010. https://doi.org/10.1093/nar/gkq564
160. Calin, GA, Croce, CM: MicroRNA signatures in human cancers. *Nat Rev Cancer,* 6**:** 857-866, 2006. https://doi.org/10.1038/nrc1997
161. Marques, FZ, Romaine, SP, Denniff, M, Eales, J, Dormer, J, Garrelds, IM, Wojnar, L, Musialik, K, Duda-Raszewska, B, Kiszka, B, Duda, M, Morris, BJ, Samani, NJ, Danser, AJ, Bogdanski, P, Zukowska-Szczechowska, E, Charchar, FJ, Tomaszewski, M: Signatures of miR-181a on the Renal Transcriptome and Blood Pressure. *Mol Med,* 21**:** 739-748, 2015. https://doi.org/10.2119/molmed.2015.00096
162. Su, R, Lin, HS, Zhang, XH, Yin, XL, Ning, HM, Liu, B, Zhai, PF, Gong, JN, Shen, C, Song, L, Chen, J, Wang, F, Zhao, HL, Ma, YN, Yu, J, Zhang, JW: MiR-181 family: regulators of myeloid differentiation and acute myeloid leukemia as well as potential therapeutic targets. *Oncogene,* 34**:** 3226-3239, 2015. https://doi.org/10.1038/onc.2014.274
163. Lei, Z, Ma, X, Li, H, Zhang, Y, Gao, Y, Fan, Y, Li, X, Chen, L, Xie, Y, Chen, J, Wu, S, Tang, L, Zhang, X: Up-regulation of miR-181a in clear cell renal cell carcinoma is associated with lower KLF6 expression, enhanced cell proliferation, accelerated cell cycle transition, and diminished apoptosis. *Urol Oncol,* 36**:** 93 e23-93 e37, 2018. https://doi.org/10.1016/j.urolonc.2017.09.019
164. Zhu, HY, Liu, MY, Hong, Q, Zhang, D, Geng, WJ, Xie, YS, Chen, XM: Role of microRNA-181a in the apoptosis of tubular epithelial cell induced by cisplatin. *Chin Med J (Engl),* 125**:** 523-526, 2012.
165. Liu, L, Pang, XL, Shang, WJ, Xie, HC, Wang, JX, Feng, GW: Over-expressed microRNA-181a reduces glomerular sclerosis and renal tubular epithelial injury in rats with chronic kidney disease via down-regulation of the TLR/NF-kappaB pathway by binding to CRY1. *Mol Med,* 24**:** 49, 2018. https://doi.org/10.1186/s10020-018-0045-2
166. Calcat, ICS, Rendra, E, Scaccia, E, Amadeo, F, Hanson, V, Wilm, B, Murray, P, O'Brien, T, Taylor, A, Bieback, K: Harmonised culture procedures minimise but do not eliminate mesenchymal stromal cell donor and tissue variability in a decentralised multicentre manufacturing approach. *Stem Cell Res Ther,* 14**:** 120, 2023. https://doi.org/10.1186/s13287-023-03352-1
167. Torres Crigna, A, Uhlig, S, Elvers-Hornung, S, Kluter, H, Bieback, K: Human Adipose Tissue-Derived Stromal Cells Suppress Human, but Not Murine Lymphocyte Proliferation, via Indoleamine 2,3-Dioxygenase Activity. *Cells,* 9, 2020. https://doi.org/10.3390/cells9112419
168. Skovronova, R, Scaccia, E, Calcat, ICS, Bussolati, B, O'Brien, T, Bieback, K: Adipose stromal cells bioproducts as cell-free therapies: manufacturing and

therapeutic dose determine in vitro functionality. *J Transl Med,* 21**:** 723, 2023. https://doi.org/10.1186/s12967-023-04602-9

169. Systems, F: Hollow Fiber Bioreactor Protocol for Mesenchymal Stem Cells, 2021. FiberCell-Systems-Hollow-Fiber-Bioreactor-Protocol-for-Mesenchymal-Stem-Cells.pdf (fibercellsystems.com)
170. Fiori, A, Hammes, HP, Bieback, K: Adipose-derived mesenchymal stromal cells reverse high glucose-induced reduction of angiogenesis in human retinal microvascular endothelial cells. *Cytotherapy,* 22**:** 261-275, 2020. https://doi.org/10.1016/j.jcyt.2020.02.005
171. Kremer, H, Gebauer, J, Elvers-Hornung, S, Uhlig, S, Hammes, HP, Beltramo, E, Steeb, L, Harmsen, MC, Sticht, C, Klueter, H, Bieback, K, Fiori, A: Pro-angiogenic Activity Discriminates Human Adipose-Derived Stromal Cells From Retinal Pericytes: Considerations for Cell-Based Therapy of Diabetic Retinopathy. *Front Cell Dev Biol,* 8**:** 387, 2020. https://doi.org/10.3389/fcell.2020.00387
172. Carpentier, G, Berndt, S, Ferratge, S, Rasband, W, Cuendet, M, Uzan, G, Albanese, P: Angiogenesis Analyzer for ImageJ - A comparative morphometric analysis of "Endothelial Tube Formation Assay" and "Fibrin Bead Assay". *Sci Rep,* 10**:** 11568, 2020. https://doi.org/10.1038/s41598-020-67289-8
173. Wilmer, MJ, Saleem, MA, Masereeuw, R, Ni, L, van der Velden, TJ, Russel, FG, Mathieson, PW, Monnens, LA, van den Heuvel, LP, Levtchenko, EN: Novel conditionally immortalized human proximal tubule cell line expressing functional influx and efflux transporters. *Cell Tissue Res,* 339**:** 449-457, 2010. https://doi.org/10.1007/s00441-009-0882-y
174. Rendra, E, Crigna, AT, Daniele, C, Sticht, C, Cueppers, M, Kluth, MA, Ganss, C, Frank, MH, Gretz, N, Bieback, K: Clinical-grade human skin-derived ABCB5+ mesenchymal stromal cells exert anti-apoptotic and anti-inflammatory effects in vitro and modulate mRNA expression in a cisplatin-induced kidney injury murine model. *Front Immunol,* 14**:** 1228928, 2023. https://doi.org/10.3389/fimmu.2023.1228928
175. Zhou, L, Chen, J, Li, Z, Li, X, Hu, X, Huang, Y, Zhao, X, Liang, C, Wang, Y, Sun, L, Shi, M, Xu, X, Shen, F, Chen, M, Han, Z, Peng, Z, Zhai, Q, Chen, J, Zhang, Z, Yang, R, Ye, J, Guan, Z, Yang, H, Gui, Y, Wang, J, Cai, Z, Zhang, X: Integrated profiling of microRNAs and mRNAs: microRNAs located on Xq27.3 associate with clear cell renal cell carcinoma. *PLoS One,* 5**:** e15224, 2010. https://doi.org/10.1371/journal.pone.0015224
176. Team, RC: R: A Language and Environment for Statistical Computing. R Foundation for Statistical Computing, Vienna. 2021.
177. Bruder, SP, Jaiswal, N, Haynesworth, SE: Growth kinetics, self-renewal, and the osteogenic potential of purified human mesenchymal stem cells during extensive subcultivation and following cryopreservation. *J Cell Biochem,* 64**:** 278-294, 1997. https://doi.org/10.1002/(sici)1097-4644(199702)64:2<278::aid-jcb11>3.0.co;2-f
178. Bieback, K, Kuci, S, Schafer, R: Production and quality testing of multipotent mesenchymal stromal cell therapeutics for clinical use. *Transfusion,* 59**:** 2164-2173, 2019. https://doi.org/10.1111/trf.15252
179. Le Blanc, K, Tammik, L, Sundberg, B, Haynesworth, SE, Ringden, O: Mesenchymal stem cells inhibit and stimulate mixed lymphocyte cultures and mitogenic responses independently of the major histocompatibility complex. *Scand J Immunol,* 57**:** 11-20, 2003. https://doi.org/10.1046/j.1365-3083.2003.01176.x

180. Ketterl, N, Brachtl, G, Schuh, C, Bieback, K, Schallmoser, K, Reinisch, A, Strunk, D: A robust potency assay highlights significant donor variation of human mesenchymal stem/progenitor cell immune modulatory capacity and extended radio-resistance. *Stem Cell Res Ther,* 6**:** 236, 2015. https://doi.org/10.1186/s13287-015-0233-8
181. Johnson, J, Shojaee, M, Mitchell Crow, J, Khanabdali, R: From Mesenchymal Stromal Cells to Engineered Extracellular Vesicles: A New Therapeutic Paradigm. *Front Cell Dev Biol,* 9**:** 705676, 2021. https://doi.org/10.3389/fcell.2021.705676
182. Gouveia de Andrade, AV, Bertolino, G, Riewaldt, J, Bieback, K, Karbanova, J, Odendahl, M, Bornhauser, M, Schmitz, M, Corbeil, D, Tonn, T: Extracellular vesicles secreted by bone marrow- and adipose tissue-derived mesenchymal stromal cells fail to suppress lymphocyte proliferation. *Stem Cells Dev,* 24**:** 1374-1376, 2015. https://doi.org/10.1089/scd.2014.0563
183. Rendra, E, Uhlig, S, Moskal, I, Thielemann, C, Kluter, H, Bieback, K: Adipose Stromal Cell-Derived Secretome Attenuates Cisplatin-Induced Injury In Vitro Surpassing the Intricate Interplay between Proximal Tubular Epithelial Cells and Macrophages. *Cells,* 13, 2024. https://doi.org/10.3390/cells13020121
184. Li, W, Qiu, X, Jiang, H, Han, Y, Wei, D, Liu, J: Downregulation of miR-181a protects mice from LPS-induced acute lung injury by targeting Bcl-2. *Biomed Pharmacother,* 84**:** 1375-1382, 2016. https://doi.org/10.1016/j.biopha.2016.10.065
185. Liu, S, de Castro, LF, Jin, P, Civini, S, Ren, J, Reems, JA, Cancelas, J, Nayak, R, Shaw, G, O'Brien, T, McKenna, DH, Armant, M, Silberstein, L, Gee, AP, Hei, DJ, Hematti, P, Kuznetsov, SA, Robey, PG, Stroncek, DF: Manufacturing Differences Affect Human Bone Marrow Stromal Cell Characteristics and Function: Comparison of Production Methods and Products from Multiple Centers. *Sci Rep,* 7**:** 46731, 2017. https://doi.org/10.1038/srep46731
186. Wu, LW, Wang, YL, Christensen, JM, Khalifian, S, Schneeberger, S, Raimondi, G, Cooney, DS, Lee, WP, Brandacher, G: Donor age negatively affects the immunoregulatory properties of both adipose and bone marrow derived mesenchymal stem cells. *Transpl Immunol,* 30**:** 122-127, 2014. https://doi.org/10.1016/j.trim.2014.03.001
187. Stroncek, DF, Jin, P, McKenna, DH, Takanashi, M, Fontaine, MJ, Pati, S, Schafer, R, Peterson, E, Benedetti, E, Reems, JA: Human Mesenchymal Stromal Cell (MSC) Characteristics Vary Among Laboratories When Manufactured From the Same Source Material: A Report by the Cellular Therapy Team of the Biomedical Excellence for Safer Transfusion (BEST) Collaborative. *Front Cell Dev Biol,* 8**:** 458, 2020. https://doi.org/10.3389/fcell.2020.00458
188. Karagianni, M, Brinkmann, I, Kinzebach, S, Grassl, M, Weiss, C, Bugert, P, Bieback, K: A comparative analysis of the adipogenic potential in human mesenchymal stromal cells from cord blood and other sources. *Cytotherapy,* 15**:** 76-88, 2013. https://doi.org/10.1016/j.jcyt.2012.11.001
189. Al Ghrbawy, NM, Afify, RA, Dyaa, N, El Sayed, AA: Differentiation of Bone Marrow: Derived Mesenchymal Stem Cells into Hepatocyte-like Cells. *Indian J Hematol Blood Transfus,* 32**:** 276-283, 2016. https://doi.org/10.1007/s12288-015-0581-7
190. Majore, I, Moretti, P, Stahl, F, Hass, R, Kasper, C: Growth and differentiation properties of mesenchymal stromal cell populations derived from whole human

umbilical cord. *Stem Cell Rev Rep,* 7**:** 17-31, 2011. https://doi.org/10.1007/s12015-010-9165-y

191. Quirici, N, Scavullo, C, de Girolamo, L, Lopa, S, Arrigoni, E, Deliliers, GL, Brini, AT: Anti-L-NGFR and -CD34 monoclonal antibodies identify multipotent mesenchymal stem cells in human adipose tissue. *Stem Cells Dev,* 19**:** 915-925, 2010. https://doi.org/10.1089/scd.2009.0408
192. Bourin, P, Bunnell, BA, Casteilla, L, Dominici, M, Katz, AJ, March, KL, Redl, H, Rubin, JP, Yoshimura, K, Gimble, JM: Stromal cells from the adipose tissue-derived stromal vascular fraction and culture expanded adipose tissue-derived stromal/stem cells: a joint statement of the International Federation for Adipose Therapeutics and Science (IFATS) and the International Society for Cellular Therapy (ISCT). *Cytotherapy,* 15**:** 641-648, 2013. https://doi.org/10.1016/j.jcyt.2013.02.006
193. Lin, CS, Ning, H, Lin, G, Lue, TF: Is CD34 truly a negative marker for mesenchymal stromal cells? *Cytotherapy,* 14**:** 1159-1163, 2012. https://doi.org/10.3109/14653249.2012.729817
194. Yeh, SP, Chang, JG, Lin, CL, Lo, WJ, Lee, CC, Lin, CY, Chiu, CF: Mesenchymal stem cells can be easily isolated from bone marrow of patients with various haematological malignancies but the surface antigens expression may be changed after prolonged ex vivo culture. *Leukemia,* 19**:** 1505-1507, 2005. https://doi.org/10.1038/sj.leu.2403795
195. Al-Saqi, SH, Saliem, M, Quezada, HC, Ekblad, A, Jonasson, AF, Hovatta, O, Gotherstrom, C: Defined serum- and xeno-free cryopreservation of mesenchymal stem cells. *Cell Tissue Bank,* 16**:** 181-193, 2015. https://doi.org/10.1007/s10561-014-9463-8
196. Bahsoun, S, Coopman, K, Akam, EC: Quantitative assessment of the impact of cryopreservation on human bone marrow-derived mesenchymal stem cells: up to 24 h post-thaw and beyond. *Stem Cell Res Ther,* 11**:** 540, 2020. https://doi.org/10.1186/s13287-020-02054-2
197. Francois, M, Copland, IB, Yuan, S, Romieu-Mourez, R, Waller, EK, Galipeau, J: Cryopreserved mesenchymal stromal cells display impaired immunosuppressive properties as a result of heat-shock response and impaired interferon-gamma licensing. *Cytotherapy,* 14**:** 147-152, 2012. https://doi.org/10.3109/14653249.2011.623691
198. Lehman, N, Cutrone, R, Raber, A, Perry, R, Van't Hof, W, Deans, R, Ting, AE, Woda, J: Development of a surrogate angiogenic potency assay for clinical-grade stem cell production. *Cytotherapy,* 14**:** 994-1004, 2012. https://doi.org/10.3109/14653249.2012.688945
199. Du, WJ, Chi, Y, Yang, ZX, Li, ZJ, Cui, JJ, Song, BQ, Li, X, Yang, SG, Han, ZB, Han, ZC: Heterogeneity of proangiogenic features in mesenchymal stem cells derived from bone marrow, adipose tissue, umbilical cord, and placenta. *Stem Cell Res Ther,* 7**:** 163, 2016. https://doi.org/10.1186/s13287-016-0418-9
200. Hsiao, ST, Asgari, A, Lokmic, Z, Sinclair, R, Dusting, GJ, Lim, SY, Dilley, RJ: Comparative analysis of paracrine factor expression in human adult mesenchymal stem cells derived from bone marrow, adipose, and dermal tissue. *Stem Cells Dev,* 21**:** 2189-2203, 2012. https://doi.org/10.1089/scd.2011.0674
201. Kim, Y, Kim, H, Cho, H, Bae, Y, Suh, K, Jung, J: Direct comparison of human mesenchymal stem cells derived from adipose tissues and bone marrow in mediating neovascularization in response to vascular ischemia. *Cell Physiol Biochem,* 20**:** 867-876, 2007. https://doi.org/10.1159/000110447

202. Mastrolia, I, Foppiani, EM, Murgia, A, Candini, O, Samarelli, AV, Grisendi, G, Veronesi, E, Horwitz, EM, Dominici, M: Challenges in Clinical Development of Mesenchymal Stromal/Stem Cells: Concise Review. *Stem Cells Transl Med,* 8**:** 1135-1148, 2019. https://doi.org/10.1002/sctm.19-0044
203. Kronsteiner, B, Wolbank, S, Peterbauer, A, Hackl, C, Redl, H, van Griensven, M, Gabriel, C: Human mesenchymal stem cells from adipose tissue and amnion influence T-cells depending on stimulation method and presence of other immune cells. *Stem Cells Dev,* 20**:** 2115-2126, 2011. https://doi.org/10.1089/scd.2011.0031
204. Fiori, A, Uhlig, S, Kluter, H, Bieback, K: Human Adipose Tissue-Derived Mesenchymal Stromal Cells Inhibit CD4+ T Cell Proliferation and Induce Regulatory T Cells as Well as CD127 Expression on CD4+CD25+ T Cells. *Cells,* 10, 2021. https://doi.org/10.3390/cells10010058
205. Liang, C, Jiang, E, Yao, J, Wang, M, Chen, S, Zhou, Z, Zhai, W, Ma, Q, Feng, S, Han, M: Interferon-gamma mediates the immunosuppression of bone marrow mesenchymal stem cells on T-lymphocytes in vitro. *Hematology,* 23**:** 44-49, 2018. https://doi.org/10.1080/10245332.2017.1333245
206. Ryan, JM, Barry, F, Murphy, JM, Mahon, BP: Interferon-gamma does not break, but promotes the immunosuppressive capacity of adult human mesenchymal stem cells. *Clin Exp Immunol,* 149**:** 353-363, 2007. https://doi.org/10.1111/j.1365-2249.2007.03422.x
207. Li, CY, Wu, XY, Tong, JB, Yang, XX, Zhao, JL, Zheng, QF, Zhao, GB, Ma, ZJ: Comparative analysis of human mesenchymal stem cells from bone marrow and adipose tissue under xeno-free conditions for cell therapy. *Stem Cell Res Ther,* 6**:** 55, 2015. https://doi.org/10.1186/s13287-015-0066-5
208. Najar, M, Raicevic, G, Boufker, HI, Fayyad Kazan, H, De Bruyn, C, Meuleman, N, Bron, D, Toungouz, M, Lagneaux, L: Mesenchymal stromal cells use PGE2 to modulate activation and proliferation of lymphocyte subsets: Combined comparison of adipose tissue, Wharton's Jelly and bone marrow sources. *Cell Immunol,* 264**:** 171-179, 2010. https://doi.org/10.1016/j.cellimm.2010.06.006
209. Xishan, Z, Baoxin, H, Xinna, Z, Jun, R: Comparison of the effects of human adipose and bone marrow mesenchymal stem cells on T lymphocytes. *Cell Biol Int,* 37**:** 11-18, 2013. https://doi.org/10.1002/cbin.10002
210. Li, X, Bai, J, Ji, X, Li, R, Xuan, Y, Wang, Y: Comprehensive characterization of four different populations of human mesenchymal stem cells as regards their immune properties, proliferation and differentiation. *Int J Mol Med,* 34**:** 695-704, 2014. https://doi.org/10.3892/ijmm.2014.1821
211. Mattar, P, Bieback, K: Comparing the Immunomodulatory Properties of Bone Marrow, Adipose Tissue, and Birth-Associated Tissue Mesenchymal Stromal Cells. *Front Immunol,* 6**:** 560, 2015. https://doi.org/10.3389/fimmu.2015.00560
212. Moll, G, Ankrum, JA, Kamhieh-Milz, J, Bieback, K, Ringden, O, Volk, HD, Geissler, S, Reinke, P: Intravascular Mesenchymal Stromal/Stem Cell Therapy Product Diversification: Time for New Clinical Guidelines. *Trends Mol Med,* 25**:** 149-163, 2019. https://doi.org/10.1016/j.molmed.2018.12.006
213. Schrepfer, S, Deuse, T, Reichenspurner, H, Fischbein, MP, Robbins, RC, Pelletier, MP: Stem cell transplantation: the lung barrier. *Transplant Proc,* 39**:** 573-576, 2007. https://doi.org/10.1016/j.transproceed.2006.12.019
214. Prockop, DJ: Repair of tissues by adult stem/progenitor cells (MSCs): controversies, myths, and changing paradigms. *Mol Ther,* 17**:** 939-946, 2009. https://doi.org/10.1038/mt.2009.62

215. Lee, RH, Pulin, AA, Seo, MJ, Kota, DJ, Ylostalo, J, Larson, BL, Semprun-Prieto, L, Delafontaine, P, Prockop, DJ: Intravenous hMSCs improve myocardial infarction in mice because cells embolized in lung are activated to secrete the anti-inflammatory protein TSG-6. *Cell Stem Cell,* 5**:** 54-63, 2009. https://doi.org/10.1016/j.stem.2009.05.003
216. Wang, H, Liang, X, Xu, ZP, Crawford, DH, Liu, X, Roberts, MS: A physiologically based kinetic model for elucidating the in vivo distribution of administered mesenchymal stem cells. *Sci Rep,* 6**:** 22293, 2016. https://doi.org/10.1038/srep22293
217. Rustad, KC, Gurtner, GC: Mesenchymal Stem Cells Home to Sites of Injury and Inflammation. *Adv Wound Care (New Rochelle),* 1**:** 147-152, 2012. https://doi.org/10.1089/wound.2011.0314
218. Eggenhofer, E, Benseler, V, Kroemer, A, Popp, FC, Geissler, EK, Schlitt, HJ, Baan, CC, Dahlke, MH, Hoogduijn, MJ: Mesenchymal stem cells are short-lived and do not migrate beyond the lungs after intravenous infusion. *Front Immunol,* 3**:** 297, 2012. https://doi.org/10.3389/fimmu.2012.00297
219. de Witte, SFH, Luk, F, Sierra Parraga, JM, Gargesha, M, Merino, A, Korevaar, SS, Shankar, AS, O'Flynn, L, Elliman, SJ, Roy, D, Betjes, MGH, Newsome, PN, Baan, CC, Hoogduijn, MJ: Immunomodulation By Therapeutic Mesenchymal Stromal Cells (MSC) Is Triggered Through Phagocytosis of MSC By Monocytic Cells. *Stem Cells,* 36**:** 602-615, 2018. https://doi.org/10.1002/stem.2779
220. Wang, S, Guo, L, Ge, J, Yu, L, Cai, T, Tian, R, Jiang, Y, Zhao, R, Wu, Y: Excess Integrins Cause Lung Entrapment of Mesenchymal Stem Cells. *Stem Cells,* 33**:** 3315-3326, 2015. https://doi.org/10.1002/stem.2087
221. Nystedt, J, Anderson, H, Tikkanen, J, Pietila, M, Hirvonen, T, Takalo, R, Heiskanen, A, Satomaa, T, Natunen, S, Lehtonen, S, Hakkarainen, T, Korhonen, M, Laitinen, S, Valmu, L, Lehenkari, P: Cell surface structures influence lung clearance rate of systemically infused mesenchymal stromal cells. *Stem Cells,* 31**:** 317-326, 2013. https://doi.org/10.1002/stem.1271
222. Lipowsky, HH, Bowers, DT, Banik, BL, Brown, JL: Mesenchymal Stem Cell Deformability and Implications for Microvascular Sequestration. *Ann Biomed Eng,* 46**:** 640-654, 2018. https://doi.org/10.1007/s10439-018-1985-y
223. Ko, JH, Lee, HJ, Jeong, HJ, Kim, MK, Wee, WR, Yoon, SO, Choi, H, Prockop, DJ, Oh, JY: Mesenchymal stem/stromal cells precondition lung monocytes/macrophages to produce tolerance against allo- and autoimmunity in the eye. *Proc Natl Acad Sci U S A,* 113**:** 158-163, 2016. https://doi.org/10.1073/pnas.1522905113
224. Preda, MB, Neculachi, CA, Fenyo, IM, Vacaru, AM, Publik, MA, Simionescu, M, Burlacu, A: Short lifespan of syngeneic transplanted MSC is a consequence of in vivo apoptosis and immune cell recruitment in mice. *Cell Death Dis,* 12**:** 566, 2021. https://doi.org/10.1038/s41419-021-03839-w
225. Galleu, A, Riffo-Vasquez, Y, Trento, C, Lomas, C, Dolcetti, L, Cheung, TS, von Bonin, M, Barbieri, L, Halai, K, Ward, S, Weng, L, Chakraverty, R, Lombardi, G, Watt, FM, Orchard, K, Marks, DI, Apperley, J, Bornhauser, M, Walczak, H, Bennett, C, Dazzi, F: Apoptosis in mesenchymal stromal cells induces in vivo recipient-mediated immunomodulation. *Sci Transl Med,* 9, 2017. https://doi.org/10.1126/scitranslmed.aam7828
226. Margolis, L, Sadovsky, Y: The biology of extracellular vesicles: The known unknowns. *PLoS Biol,* 17**:** e3000363, 2019. https://doi.org/10.1371/journal.pbio.3000363

227. Giebel, B, Kordelas, L, Borger, V: Clinical potential of mesenchymal stem/stromal cell-derived extracellular vesicles. *Stem Cell Investig,* 4**:** 84, 2017. https://doi.org/10.21037/sci.2017.09.06
228. Tertel, T, Dittrich, R, Arsene, P, Jensen, A, Giebel, B: EV products obtained from iPSC-derived MSCs show batch-to-batch variations in their ability to modulate allogeneic immune responses in vitro. *Front Cell Dev Biol,* 11**:** 1282860, 2023. https://doi.org/10.3389/fcell.2023.1282860
229. Poupardin, R, Wolf, M, Maeding, N, Paniushkina, L, Geissler, S, Bergese, P, Witwer, KW, Schallmoser, K, Fuhrmann, G, Strunk, D: Advances in Extracellular Vesicle Research Over the Past Decade: Source and Isolation Method are Connected with Cargo and Function. *Adv Healthc Mater,* 13**:** e2303941, 2024. https://doi.org/10.1002/adhm.202303941
230. Patel, GK, Khan, MA, Zubair, H, Srivastava, SK, Khushman, M, Singh, S, Singh, AP: Comparative analysis of exosome isolation methods using culture supernatant for optimum yield, purity and downstream applications. *Sci Rep,* 9**:** 5335, 2019. https://doi.org/10.1038/s41598-019-41800-2
231. Mussack, V, Wittmann, G, Pfaffl, MW: Comparing small urinary extracellular vesicle purification methods with a view to RNA sequencing-Enabling robust and non-invasive biomarker research. *Biomol Detect Quantif,* 17**:** 100089, 2019. https://doi.org/10.1016/j.bdq.2019.100089
232. Cvjetkovic, A, Lotvall, J, Lasser, C: The influence of rotor type and centrifugation time on the yield and purity of extracellular vesicles. *J Extracell Vesicles,* 3, 2014. https://doi.org/10.3402/jev.v3.23111
233. Livshits, MA, Khomyakova, E, Evtushenko, EG, Lazarev, VN, Kulemin, NA, Semina, SE, Generozov, EV, Govorun, VM: Isolation of exosomes by differential centrifugation: Theoretical analysis of a commonly used protocol. *Sci Rep,* 5**:** 17319, 2015. https://doi.org/10.1038/srep17319
234. Torres Crigna, A, Fricke, F, Nitschke, K, Worst, T, Erb, U, Karremann, M, Buschmann, D, Elvers-Hornung, S, Tucher, C, Schiller, M, Hausser, I, Gebert, J, Bieback, K: Inter-Laboratory Comparison of Extracellular Vesicle Isolation Based on Ultracentrifugation. *Transfus Med Hemother,* 48**:** 48-59, 2021. https://doi.org/10.1159/000508712
235. Tengler, L, Tiedtke, M, Schutz, J, Bieback, K, Uhlig, S, Theodoraki, MN, Nitschke, K, Worst, TS, Seiz, E, Scherl, C, Rotter, N, Ludwig, S: Optimization of extracellular vesicles preparation from saliva of head and neck cancer patients. *Sci Rep,* 14**:** 946, 2024. https://doi.org/10.1038/s41598-023-50610-6
236. Bachurski, D, Schuldner, M, Nguyen, PH, Malz, A, Reiners, KS, Grenzi, PC, Babatz, F, Schauss, AC, Hansen, HP, Hallek, M, Pogge von Strandmann, E: Extracellular vesicle measurements with nanoparticle tracking analysis - An accuracy and repeatability comparison between NanoSight NS300 and ZetaView. *J Extracell Vesicles,* 8**:** 1596016, 2019. https://doi.org/10.1080/20013078.2019.1596016
237. Lotvall, J, Hill, AF, Hochberg, F, Buzas, EI, Di Vizio, D, Gardiner, C, Gho, YS, Kurochkin, IV, Mathivanan, S, Quesenberry, P, Sahoo, S, Tahara, H, Wauben, MH, Witwer, KW, Thery, C: Minimal experimental requirements for definition of extracellular vesicles and their functions: a position statement from the International Society for Extracellular Vesicles. *J Extracell Vesicles,* 3**:** 26913, 2014. https://doi.org/10.3402/jev.v3.26913
238. Jeske, R, Liu, C, Duke, L, Canonicco Castro, ML, Muok, L, Arthur, P, Singh, M, Jung, S, Sun, L, Li, Y: Upscaling human mesenchymal stromal cell production in a novel vertical-wheel bioreactor enhances extracellular vesicle secretion

and cargo profile. *Bioact Mater,* 25**:** 732-747, 2023. https://doi.org/10.1016/j.bioactmat.2022.07.004

239. Gobin, J, Muradia, G, Mehic, J, Westwood, C, Couvrette, L, Stalker, A, Bigelow, S, Luebbert, CC, Bissonnette, FS, Johnston, MJW, Sauve, S, Tam, RY, Wang, L, Rosu-Myles, M, Lavoie, JR: Hollow-fiber bioreactor production of extracellular vesicles from human bone marrow mesenchymal stromal cells yields nanovesicles that mirrors the immuno-modulatory antigenic signature of the producer cell. *Stem Cell Res Ther,* 12**:** 127, 2021. https://doi.org/10.1186/s13287-021-02190-3
240. Cao, J, Wang, B, Tang, T, Lv, L, Ding, Z, Li, Z, Hu, R, Wei, Q, Shen, A, Fu, Y, Liu, B: Three-dimensional culture of MSCs produces exosomes with improved yield and enhanced therapeutic efficacy for cisplatin-induced acute kidney injury. *Stem Cell Res Ther,* 11**:** 206, 2020. https://doi.org/10.1186/s13287-020-01719-2
241. Vergauwen, G, Dhondt, B, Van Deun, J, De Smedt, E, Berx, G, Timmerman, E, Gevaert, K, Miinalainen, I, Cocquyt, V, Braems, G, Van den Broecke, R, Denys, H, De Wever, O, Hendrix, A: Confounding factors of ultrafiltration and protein analysis in extracellular vesicle research. *Sci Rep,* 7**:** 2704, 2017. https://doi.org/10.1038/s41598-017-02599-y
242. Konoshenko, MY, Lekchnov, EA, Vlassov, AV, Laktionov, PP: Isolation of Extracellular Vesicles: General Methodologies and Latest Trends. *Biomed Res Int,* 2018**:** 8545347, 2018. https://doi.org/10.1155/2018/8545347
243. Clos-Sansalvador, M, Monguio-Tortajada, M, Roura, S, Franquesa, M, Borras, FE: Commonly used methods for extracellular vesicles' enrichment: Implications in downstream analyses and use. *Eur J Cell Biol,* 101**:** 151227, 2022. https://doi.org/10.1016/j.ejcb.2022.151227
244. Papait, A, Ragni, E, Cargnoni, A, Vertua, E, Romele, P, Masserdotti, A, Perucca Orfei, C, Signoroni, PB, Magatti, M, Silini, AR, De Girolamo, L, Parolini, O: Comparison of EV-free fraction, EVs, and total secretome of amniotic mesenchymal stromal cells for their immunomodulatory potential: a translational perspective. *Front Immunol,* 13**:** 960909, 2022. https://doi.org/10.3389/fimmu.2022.960909
245. Kordelas, L, Schwich, E, Dittrich, R, Horn, PA, Beelen, DW, Borger, V, Giebel, B, Rebmann, V: Individual Immune-Modulatory Capabilities of MSC-Derived Extracellular Vesicle (EV) Preparations and Recipient-Dependent Responsiveness. *Int J Mol Sci,* 20, 2019. https://doi.org/10.3390/ijms20071642
246. Bremer, M, Nardi Bauer, F, Tertel, T, Dittrich, R, Horn, PA, Borger, V, Giebel, B: Qualification of a multidonor mixed lymphocyte reaction assay for the functional characterization of immunomodulatory extracellular vesicles. *Cytotherapy,* 25**:** 847-857, 2023. https://doi.org/10.1016/j.jcyt.2023.03.009
247. Mouloud, Y, Staubach, S, Stambouli, O, Mokhtari, S, Kutzner, TJ, Zwanziger, D, Hemeda, H, Giebel, B: Calcium chloride declotted human platelet lysate promotes the expansion of mesenchymal stromal cells and allows manufacturing of immunomodulatory active extracellular vesicle products. *Cytotherapy,* 26**:** 988-998, 2024. https://doi.org/10.1016/j.jcyt.2024.04.069
248. Madel, RJ, Borger, V, Dittrich, R, Bremer, M, Tertel, T, Phuong, NNT, Baba, HA, Kordelas, L, Staubach, S, Stein, F, Haberkant, P, Hackl, M, Grillari, R, Grillari, J, Buer, J, Horn, PA, Westendorf, AM, Brandau, S, Kirschning, CJ, Giebel, B: Independent human mesenchymal stromal cell-derived extracellular vesicle preparations differentially attenuate symptoms in an advanced murine graft-

versus-host disease model. *Cytotherapy,* 25**:** 821-836, 2023. https://doi.org/10.1016/j.jcyt.2023.03.008

249. Bauer, FN, Tertel, T, Stambouli, O, Wang, C, Dittrich, R, Staubach, S, Borger, V, Hermann, DM, Brandau, S, Giebel, B: CD73 activity of mesenchymal stromal cell-derived extracellular vesicle preparations is detergent-resistant and does not correlate with immunomodulatory capabilities. *Cytotherapy,* 25**:** 138-147, 2023. https://doi.org/10.1016/j.jcyt.2022.09.006
250. Shigemoto-Kuroda, T, Oh, JY, Kim, DK, Jeong, HJ, Park, SY, Lee, HJ, Park, JW, Kim, TW, An, SY, Prockop, DJ, Lee, RH: MSC-derived Extracellular Vesicles Attenuate Immune Responses in Two Autoimmune Murine Models: Type 1 Diabetes and Uveoretinitis. *Stem Cell Reports,* 8**:** 1214-1225, 2017. https://doi.org/10.1016/j.stemcr.2017.04.008
251. Xie, X, Yang, X, Wu, J, Tang, S, Yang, L, Fei, X, Wang, M: Exosome from indoleamine 2,3-dioxygenase-overexpressing bone marrow mesenchymal stem cells accelerates repair process of ischemia/reperfusion-induced acute kidney injury by regulating macrophages polarization. *Stem Cell Res Ther,* 13**:** 367, 2022. https://doi.org/10.1186/s13287-022-03075-9
252. Carceller, MC, Guillen, MI, Gil, ML, Alcaraz, MJ: Extracellular Vesicles Do Not Mediate the Anti-Inflammatory Actions of Mouse-Derived Adipose Tissue Mesenchymal Stem Cells Secretome. *Int J Mol Sci,* 22, 2021. https://doi.org/10.3390/ijms22031375
253. Kowal, J, Arras, G, Colombo, M, Jouve, M, Morath, JP, Primdal-Bengtson, B, Dingli, F, Loew, D, Tkach, M, Thery, C: Proteomic comparison defines novel markers to characterize heterogeneous populations of extracellular vesicle subtypes. *Proc Natl Acad Sci U S A,* 113**:** E968-977, 2016. https://doi.org/10.1073/pnas.1521230113
254. Burrello, J, Monticone, S, Gai, C, Gomez, Y, Kholia, S, Camussi, G: Stem Cell-Derived Extracellular Vesicles and Immune-Modulation. *Front Cell Dev Biol,* 4**:** 83, 2016. https://doi.org/10.3389/fcell.2016.00083
255. Abumaree, MH, Al Jumah, MA, Kalionis, B, Jawdat, D, Al Khaldi, A, Abomaray, FM, Fatani, AS, Chamley, LW, Knawy, BA: Human placental mesenchymal stem cells (pMSCs) play a role as immune suppressive cells by shifting macrophage differentiation from inflammatory M1 to anti-inflammatory M2 macrophages. *Stem Cell Rev Rep,* 9**:** 620-641, 2013. https://doi.org/10.1007/s12015-013-9455-2
256. Deng, Y, Zhang, Y, Ye, L, Zhang, T, Cheng, J, Chen, G, Zhang, Q, Yang, Y: Umbilical Cord-derived Mesenchymal Stem Cells Instruct Monocytes Towards an IL10-producing Phenotype by Secreting IL6 and HGF. *Sci Rep,* 6**:** 37566, 2016. https://doi.org/10.1038/srep37566
257. Wang, J, Liu, Y, Ding, H, Shi, X, Ren, H: Mesenchymal stem cell-secreted prostaglandin E(2) ameliorates acute liver failure via attenuation of cell death and regulation of macrophage polarization. *Stem Cell Res Ther,* 12**:** 15, 2021. https://doi.org/10.1186/s13287-020-02070-2
258. Sanz-Nogues, C, O'Brien, T: In vitro models for assessing therapeutic angiogenesis. *Drug Discov Today,* 21**:** 1495-1503, 2016. https://doi.org/10.1016/j.drudis.2016.05.016
259. Forteza-Genestra, MA, Antich-Rossello, M, Calvo, J, Gaya, A, Monjo, M, Ramis, JM: Purity Determines the Effect of Extracellular Vesicles Derived from Mesenchymal Stromal Cells. *Cells,* 9, 2020. https://doi.org/10.3390/cells9020422

260. Whittaker, TE, Nagelkerke, A, Nele, V, Kauscher, U, Stevens, MM: Experimental artefacts can lead to misattribution of bioactivity from soluble mesenchymal stem cell paracrine factors to extracellular vesicles. *J Extracell Vesicles,* 9**:** 1807674, 2020. https://doi.org/10.1080/20013078.2020.1807674
261. Heidarzadeh, M, Zarebkohan, A, Rahbarghazi, R, Sokullu, E: Protein corona and exosomes: new challenges and prospects. *Cell Commun Signal,* 21**:** 64, 2023. https://doi.org/10.1186/s12964-023-01089-1
262. Ragni, E, Taiana, M: Mesenchymal stromal cells-extracellular vesicles: protein corona as a camouflage mechanism? *Extracell Vesicles Circ Nucl Acids,* 5**:** 722-727, 2024. https://doi.org/10.20517/evcna.2024.78
263. Andrade, AC, Wolf, M, Binder, HM, Gomes, FG, Manstein, F, Ebner-Peking, P, Poupardin, R, Zweigerdt, R, Schallmoser, K, Strunk, D: Hypoxic Conditions Promote the Angiogenic Potential of Human Induced Pluripotent Stem Cell-Derived Extracellular Vesicles. *Int J Mol Sci,* 22, 2021. https://doi.org/10.3390/ijms22083890
264. Blundell, E, Healey, MJ, Holton, E, Sivakumaran, M, Manstana, S, Platt, M: Characterisation of the protein corona using tunable resistive pulse sensing: determining the change and distribution of a particle's surface charge. *Anal Bioanal Chem,* 408**:** 5757-5768, 2016. https://doi.org/10.1007/s00216-016-9678-6
265. Wolf, M, Poupardin, RW, Ebner-Peking, P, Andrade, AC, Blochl, C, Obermayer, A, Gomes, FG, Vari, B, Maeding, N, Eminger, E, Binder, HM, Raninger, AM, Hochmann, S, Brachtl, G, Spittler, A, Heuser, T, Ofir, R, Huber, CG, Aberman, Z, Schallmoser, K, Volk, HD, Strunk, D: A functional corona around extracellular vesicles enhances angiogenesis, skin regeneration and immunomodulation. *J Extracell Vesicles,* 11**:** e12207, 2022. https://doi.org/10.1002/jev2.12207
266. Toth, EA, Turiak, L, Visnovitz, T, Cserep, C, Mazlo, A, Sodar, BW, Forsonits, AI, Petovari, G, Sebestyen, A, Komlosi, Z, Drahos, L, Kittel, A, Nagy, G, Bacsi, A, Denes, A, Gho, YS, Szabo-Taylor, KE, Buzas, EI: Formation of a protein corona on the surface of extracellular vesicles in blood plasma. *J Extracell Vesicles,* 10**:** e12140, 2021. https://doi.org/10.1002/jev2.12140
267. Teixeira, FG, Panchalingam, KM, Assuncao-Silva, R, Serra, SC, Mendes-Pinheiro, B, Patricio, P, Jung, S, Anjo, SI, Manadas, B, Pinto, L, Sousa, N, Behie, LA, Salgado, AJ: Modulation of the Mesenchymal Stem Cell Secretome Using Computer-Controlled Bioreactors: Impact on Neuronal Cell Proliferation, Survival and Differentiation. *Sci Rep,* 6**:** 27791, 2016. https://doi.org/10.1038/srep27791
268. Billing, AM, Ben Hamidane, H, Dib, SS, Cotton, RJ, Bhagwat, AM, Kumar, P, Hayat, S, Yousri, NA, Goswami, N, Suhre, K, Rafii, A, Graumann, J: Comprehensive transcriptomic and proteomic characterization of human mesenchymal stem cells reveals source specific cellular markers. *Sci Rep,* 6**:** 21507, 2016. https://doi.org/10.1038/srep21507
269. Taverna, S, Pucci, M, Alessandro, R: Extracellular vesicles: small bricks for tissue repair/regeneration. *Ann Transl Med,* 5**:** 83, 2017. https://doi.org/10.21037/atm.2017.01.53
270. Seth, R, Yang, C, Kaushal, V, Shah, SV, Kaushal, GP: p53-dependent caspase-2 activation in mitochondrial release of apoptosis-inducing factor and its role in renal tubular epithelial cell injury. *J Biol Chem,* 280**:** 31230-31239, 2005. https://doi.org/10.1074/jbc.M503305200

271. Vaka, R, Parent, S, Risha, Y, Khan, S, Courtman, D, Stewart, DJ, Davis, DR: Extracellular vesicle microRNA and protein cargo profiling in three clinical-grade stem cell products reveals key functional pathways. *Mol Ther Nucleic Acids,* 32**:** 80-93, 2023. https://doi.org/10.1016/j.omtn.2023.03.001
272. Shi, L, Xu, Z, Wu, G, Chen, X, Huang, Y, Wang, Y, Jiang, W, Ke, B: Up-regulation of miR-146a increases the sensitivity of non-small cell lung cancer to DDP by downregulating cyclin J. *BMC Cancer,* 17**:** 138, 2017. https://doi.org/10.1186/s12885-017-3132-9
273. Huang, Y, Wang, H, Wang, Y, Peng, X, Li, J, Gu, W, He, T, Chen, M: Regulation and mechanism of miR-146 on renal ischemia reperfusion injury. *Pharmazie,* 73**:** 29-34, 2018. https://doi.org/10.1691/ph.2018.7776
274. Xue, F, Yang, C, Yun, K, Jiang, C, Cai, R, Liang, M, Wang, Q, Bian, W, Zhou, H, Liu, Z, Zhu, L: RETRACTED ARTICLE: Reduced LINC00467 elevates microRNA-125a-3p to suppress cisplatin resistance in non-small cell lung cancer through inhibiting sirtuin 6 and inactivating the ERK1/2 signaling pathway. *Cell Biol Toxicol,* 39**:** 365, 2023. https://doi.org/10.1007/s10565-021-09637-6
275. Pichiorri, F, Suh, SS, Ladetto, M, Kuehl, M, Palumbo, T, Drandi, D, Taccioli, C, Zanesi, N, Alder, H, Hagan, JP, Munker, R, Volinia, S, Boccadoro, M, Garzon, R, Palumbo, A, Aqeilan, RI, Croce, CM: MicroRNAs regulate critical genes associated with multiple myeloma pathogenesis. *Proc Natl Acad Sci U S A,* 105**:** 12885-12890, 2008. https://doi.org/10.1073/pnas.0806202105
276. Wang, Y, Yu, Y, Tsuyada, A, Ren, X, Wu, X, Stubblefield, K, Rankin-Gee, EK, Wang, SE: Transforming growth factor-beta regulates the sphere-initiating stem cell-like feature in breast cancer through miRNA-181 and ATM. *Oncogene,* 30**:** 1470-1480, 2011. https://doi.org/10.1038/onc.2010.531
277. Marcucci, G, Maharry, K, Radmacher, MD, Mrozek, K, Vukosavljevic, T, Paschka, P, Whitman, SP, Langer, C, Baldus, CD, Liu, CG, Ruppert, AS, Powell, BL, Carroll, AJ, Caligiuri, MA, Kolitz, JE, Larson, RA, Bloomfield, CD: Prognostic significance of, and gene and microRNA expression signatures associated with, CEBPA mutations in cytogenetically normal acute myeloid leukemia with high-risk molecular features: a Cancer and Leukemia Group B Study. *J Clin Oncol,* 26**:** 5078-5087, 2008. https://doi.org/10.1200/JCO.2008.17.5554
278. Ji, J, Yamashita, T, Budhu, A, Forgues, M, Jia, HL, Li, C, Deng, C, Wauthier, E, Reid, LM, Ye, QH, Qin, LX, Yang, W, Wang, HY, Tang, ZY, Croce, CM, Wang, XW: Identification of microRNA-181 by genome-wide screening as a critical player in EpCAM-positive hepatic cancer stem cells. *Hepatology,* 50**:** 472-480, 2009. https://doi.org/10.1002/hep.22989
279. Li, J, Shen, J, Zhao, Y, Du, F, Li, M, Wu, X, Chen, Y, Wang, S, Xiao, Z, Wu, Z: Role of miR-181a-5p in cancer (Review). *Int J Oncol,* 63, 2023. https://doi.org/10.3892/ijo.2023.5556
280. Korhan, P, Erdal, E, Atabey, N: MiR-181a-5p is downregulated in hepatocellular carcinoma and suppresses motility, invasion and branching-morphogenesis by directly targeting c-Met. *Biochem Biophys Res Commun,* 450**:** 1304-1312, 2014. https://doi.org/10.1016/j.bbrc.2014.06.142
281. Liu, Z, Sun, F, Hong, Y, Liu, Y, Fen, M, Yin, K, Ge, X, Wang, F, Chen, X, Guan, W: MEG2 is regulated by miR-181a-5p and functions as a tumour suppressor gene to suppress the proliferation and migration of gastric cancer cells. *Mol Cancer,* 16**:** 133, 2017. https://doi.org/10.1186/s12943-017-0695-7

282. Hummel, R, Wang, T, Watson, DI, Michael, MZ, Van der Hoek, M, Haier, J, Hussey, DJ: Chemotherapy-induced modification of microRNA expression in esophageal cancer. *Oncol Rep,* 26**:** 1011-1017, 2011. https://doi.org/10.3892/or.2011.1381
283. Matuszcak, C, Lindner, K, Eichelmann, AK, Hussey, DJ, Haier, J, Hummel, R: microRNAs: Key regulators of chemotherapy response and metastatic potential via complex control of target pathways in esophageal adenocarcinoma. *Surg Oncol,* 27**:** 392-401, 2018. https://doi.org/10.1016/j.suronc.2018.04.001
284. Liu, XY, Zhang, FR, Shang, JY, Liu, YY, Lv, XF, Yuan, JN, Zhang, TT, Li, K, Lin, XC, Liu, X, Lei, Q, Fu, XD, Zhou, JG, Liang, SJ: Renal inhibition of miR-181a ameliorates 5-fluorouracil-induced mesangial cell apoptosis and nephrotoxicity. *Cell Death Dis,* 9**:** 610, 2018. https://doi.org/10.1038/s41419-018-0677-8
285. Boominathan, L: The tumor suppressors p53, p63, and p73 are regulators of microRNA processing complex. *PLoS One,* 5**:** e10615, 2010. https://doi.org/10.1371/journal.pone.0010615
286. Tsang, J, Zhu, J, van Oudenaarden, A: MicroRNA-mediated feedback and feedforward loops are recurrent network motifs in mammals. *Mol Cell,* 26**:** 753-767, 2007. https://doi.org/10.1016/j.molcel.2007.05.018
287. Seoudi, AM, Lashine, YA, Abdelaziz, AI: MicroRNA-181a - a tale of discrepancies. *Expert Rev Mol Med,* 14**:** e5, 2012. https://doi.org/10.1017/S1462399411002122
288. Xu, M, Feng, M, Peng, H, Qian, Z, Zhao, L, Wu, S: Epigenetic regulation of chondrocyte hypertrophy and apoptosis through Sirt1/P53/P21 pathway in surgery-induced osteoarthritis. *Biochem Biophys Res Commun,* 528**:** 179-185, 2020. https://doi.org/10.1016/j.bbrc.2020.04.097
289. Qi, H, Zhao, Z, Xu, L, Zhang, Y, Li, Y, Xiao, L, Li, Y, Zhao, Z, Fang, J: Antisense Oligonucleotide-Based Therapy on miR-181a-5p Alleviates Cartilage Degradation of Temporomandibular Joint Osteoarthritis via Promoting SIRT1. *Front Pharmacol,* 13**:** 898334, 2022. https://doi.org/10.3389/fphar.2022.898334
290. Wang, R, Li, R, Li, T, Zhu, L, Qi, Z, Yang, X, Wang, H, Cao, B, Zhu, H: Bone Mesenchymal Stem Cell-Derived Exosome-Enclosed miR-181a Induces CD4(+)CD25(+)FOXP3(+) Regulatory T Cells via SIRT1/Acetylation-Mediated FOXP3 Stabilization. *J Oncol,* 2022**:** 8890434, 2022. https://doi.org/10.1155/2022/8890434
291. Su, Y, Silva, JD, Doherty, D, Simpson, DA, Weiss, DJ, Rolandsson-Enes, S, McAuley, DF, O'Kane, CM, Brazil, DP, Krasnodembskaya, AD: Mesenchymal stromal cells-derived extracellular vesicles reprogramme macrophages in ARDS models through the miR-181a-5p-PTEN-pSTAT5-SOCS1 axis. *Thorax,* 78**:** 617-630, 2023. https://doi.org/10.1136/thoraxjnl-2021-218194
292. Sui, X, Liu, W, Liu, Z: Exosomal lncRNA-p21 derived from mesenchymal stem cells protects epithelial cells during LPS-induced acute lung injury by sponging miR-181. *Acta Biochim Biophys Sin (Shanghai),* 53**:** 748-757, 2021. https://doi.org/10.1093/abbs/gmab043
293. Liang, X, Xu, W: miR-181a-5p regulates the proliferation and apoptosis of glomerular mesangial cells by targeting KLF6. *Exp Ther Med,* 20**:** 1121-1128, 2020. https://doi.org/10.3892/etm.2020.8780
294. Yang, S, Wang, P, Wang, S, Cong, A, Zhang, Q, Shen, W, Li, X, Zhang, W, Han, G: miRNA-181a-5p Enhances the Sensitivity of Cells to Cisplatin in

Esophageal Adenocarcinoma by Targeting CBLB. *Cancer Manag Res,* 12**:** 4981-4990, 2020. https://doi.org/10.2147/CMAR.S251264

295. Wu, J, Ma, C, Tang, X, Shi, Y, Liu, Z, Chai, X, Tang, Q, Li, L, Hann, SS: The regulation and interaction of PVT1 and miR181a-5p contributes to the repression of SP1 expression by the combination of XJD decoction and cisplatin in human lung cancer cells. *Biomed Pharmacother,* 121**:** 109632, 2020. https://doi.org/10.1016/j.biopha.2019.109632
296. Barkholt, L, Flory, E, Jekerle, V, Lucas-Samuel, S, Ahnert, P, Bisset, L, Buscher, D, Fibbe, W, Foussat, A, Kwa, M, Lantz, O, Maciulaitis, R, Palomaki, T, Schneider, CK, Sensebe, L, Tachdjian, G, Tarte, K, Tosca, L, Salmikangas, P: Risk of tumorigenicity in mesenchymal stromal cell-based therapies--bridging scientific observations and regulatory viewpoints. *Cytotherapy,* 15**:** 753-759, 2013. https://doi.org/10.1016/j.jcyt.2013.03.005
297. Mishra, PJ, Mishra, PJ, Humeniuk, R, Medina, DJ, Alexe, G, Mesirov, JP, Ganesan, S, Glod, JW, Banerjee, D: Carcinoma-associated fibroblast-like differentiation of human mesenchymal stem cells. *Cancer Res,* 68**:** 4331-4339, 2008. https://doi.org/10.1158/0008-5472.CAN-08-0943
298. Hmadcha, A, Martin-Montalvo, A, Gauthier, BR, Soria, B, Capilla-Gonzalez, V: Therapeutic Potential of Mesenchymal Stem Cells for Cancer Therapy. *Front Bioeng Biotechnol,* 8**:** 43, 2020. https://doi.org/10.3389/fbioe.2020.00043
299. Schwenter, F, Zarei, S, Luy, P, Padrun, V, Bouche, N, Lee, JS, Mulligan, RC, Morel, P, Mach, N: Cell encapsulation technology as a novel strategy for human anti-tumor immunotherapy. *Cancer Gene Ther,* 18**:** 553-562, 2011. https://doi.org/10.1038/cgt.2011.22
300. Johansson, M, Oudin, A, Tiemann, K, Bernard, A, Golebiewska, A, Keunen, O, Fack, F, Stieber, D, Wang, B, Hedman, H, Niclou, SP: The soluble form of the tumor suppressor Lrig1 potently inhibits in vivo glioma growth irrespective of EGF receptor status. *Neuro Oncol,* 15**:** 1200-1211, 2013. https://doi.org/10.1093/neuonc/not054
301. Bregy, A, Shah, AH, Diaz, MV, Pierce, HE, Ames, PL, Diaz, D, Komotar, RJ: The role of Gliadel wafers in the treatment of high-grade gliomas. *Expert Rev Anticancer Ther,* 13**:** 1453-1461, 2013. https://doi.org/10.1586/14737140.2013.840090

# 8 CURRICULUM VITAE

PERSONALIEN

| | |
|---|---|
| Name und Vorname: | Eleonora Scaccia |
| Geburtsdatum: | 13th May 1991 |
| Geburtsort: | Terracina, Italy |

**SCHULISCHER WERDEGANG**

| | |
|---|---|
| (2005) – (2010) | I.T.I.S. Institute "Guglielmo Marconi" **Scientific High School** |

**UNIVERSITÄRER WERDEGANG**

| | |
|---|---|
| (09/2010) – (10/ 2014) | **B.Sc Degree in Biological Sciences**<br>University of Siena, Italy |
| (02/2015) – (10/ 2017) | **Master degree in Genetics and Molecular Biology in basic and biomedical research**<br>"La Sapienza" University of Rome, Italy |
| (04/2019) – (Current) | **Promotion, Dr. sc. Hum (scientiarum humanarum)**<br>Institute of Transfusion Medicine and Immunology, Medical Faculty Mannheim, Heidelberg University.<br>RenalToolBox International Research Training Group<br>Thesis Title: Mechanism of action of adipose mesenchymal stromal cells reducing cisplatin-induced proximal tubular epithelial cell injury |

# 9 SCIENRIFIC OUTPUTS

## 9.1 Publication

1. Renata Skovronova, **Eleonora Scaccia**, Sandra Calcat-I-Cervera, Benedetta Bussolati, Timothy O'Brien, Karen Bieback. “Adipose stromal cells bioproducts as cell-free therapies: manufacturing and therapeutic dose determine in vitro functionality”. J Transl Med. 2023 Oct 16;21(1):723.doi: 10.1186/s12967-023-04602-9.

2. Sandra Calcat-I-Cervera, Erika Rendra, **Eleonora Scaccia**, Francesco Amadeo, Vivien Hanson, Bettina Wilm, Patricia Murray, Timothy O'Brien, Arthur Taylor, Karen Bieback. “Harmonised culture procedures minimise but do not eliminate mesenchymal stromal cell donor and tissue variability in a decentralised multicentre manufacturing approach.” Stem Cell Res Ther. 2023 May 4;14(1):120. doi: 10.1186/s13287-023-03352-1

3. Erika Rendra, **Eleonora Scaccia**, Karen Bieback. „Recent advances in understanding mesenchymal stromal cells.” Review F1000Res . 2020 Feb 27:9:F1000 Faculty Rev-156. doi: 10.12688/f1000research.21862.1. eCollection 2020.

4. Antonella Bordin, Maila Chirivì, Francesca Pagano, Marika Milan, Marco Iuliano, **Eleonora Scaccia**, Orazio Fortunato, Giorgio Mangino, Xhulio Dhori, Elisabetta De Marinis, Alessandra D'Amico, Selenia Miglietta, Vittorio Picchio, Roberto Rizzi, Giovanna Romeo, Fabio Pulcinelli, Isotta Chimenti, Giacomo Frati, Elena De Falco. “Human platelet lysate-derived extracellular vesicles enhance angiogenesis through miR-126.” Cell Prolif 2022 Nov;55(11):e13312. doi: 10.1111/cpr.13312. Epub 2022 Aug 9.

5. **Eleonora Scaccia,** Rita Businaro, Antonella Bordin, Francesca Pagano, Mariangela Corsi, Camilla Siciliano , Raffaele Capoano, Eugenio Procaccini, Bruno Salvati, Vincenzo Petrozza, Pierangela Totta, Maria Teresa Vietri, Giacomo Frati, Elena De Falco . “Platelet lysate-derived neuropeptide Y influences migration and angiogenesis of human adipose tissue-derived stromal cells”. Sci.Rep. 2018 Sep 25;8(1):14365. Doi: 10.1038/s41598-018-32623-8. PMID:30254326.

6. Antonella Bordin , Francesca Pagano , **Eleonora Scaccia**, Matteo Saccucci, Iole Vozza , Noemi Incerti, Antonella Polimeni, Elena Cavarretta , Isotta Chimenti , Elena De Falco. “Oral Plaque from Type 2 Diabetic Patients Reduces the Clonogenic Capacity of Dental Pulp-Derived Mesenchymal Stem Cells.” Stem Cells Int 2019 Jan 14:2019:1516746. doi: 10.1155/2019/1516746

7. Elena De Falco , Antonella Bordin , **Eleonora Scaccia** , Francesca Pagano , Mohsen Ibrahim , Leonardo Schirone , Francesco Angelini , Silvia Palmerio , Michele Madonna , Fianchini L, Isotta Chimenti , Sebastiano Sciarretta , Giacomo

Frati . “Histone acetylation favours the cardiovascular commitment of adipose tissue-derived stromal cells”. Int J Cardiol. 2017 Sep 15;243:421-423. doi: 10.1016/j.ijcard.2017.05.112.PMID: 28610961.

## 9.2 Poster or Oral Presentations

| | |
|---|---|
| September 2019 | Deutsche Gesellschaft für Transfusionsmedizin und Immunhämatologie e.V. (DGTI), Mannheim. Oral presentation<br><br>Antonella Bordin, **Eleonora Scaccia**, Giorgio Mangino, Francesca Pagano, Fabio Pulcinelli, Elena De Falco.<br><br>**Human platelet lysate-derived extravesicles enhance angiogenesis trough Nox4 and production of hydrogen peroxide.** |
| April 2022 | RenalToolBox Annual Meeting, Liverpool. Oral presentation and Poster.<br><br>**Potency assay to predict the renoprotective effect of MSC** |
| September 2022 | Deutsche Gesellschaft für Transfusionsmedizin und Immunhämatologie e.V. (DGTI), Mannheim. Poster<br><br>**Eleonora Scaccia**, Stefanie Uhlig, Harald Klüter, Karen Bieback.<br><br>**miRNA profiling to assess protective effects of MSC-conditioned medium on cisplatin-induced injury in proximal tubule epithelial cells.** |
| May 2023 | Annual Meeting for the International Society for Cellular Therapy, Paris. Poster<br><br>Renata Skovronova, **Eleonora Scaccia**, Sandra Calcat i Cervera, Benedetta Bussolati, Timothy O’Brien, Karen Bieback.<br><br>**Adipose stromal cells-derived secretome has superior immunomodulatory and angiogenic capacity over purified extracellular vesicles: an in vitro multicenter comparison**. |
| September 2023 | Deutsche Gesellschaft für Transfusionsmedizin und Immunhämatologie e.V. (DGTI), Düsseldorf. Oral presentation.<br><br>**Eleonora Scaccia**, Stefanie Uhlig, Francesca Pagano, Harald Klüter, Karen Bieback.<br><br>**miRNA profiling to assess protective effects of MSC-conditioned medium on cisplatin-induced injury in proximal tubule epithelial cells.** |

# 10 ACKNOWLEDGEMENTS

I want to use this part of the thesis to thank all the people who have accompanied and supported me in these years.

I would like to thank Prof. **Karen Bieback** for giving me the opportunity to get a PhD and work in her research lab. Thank you for guiding, supporting me and giving me the opportunity to reach my goal. Also, thank you because this opportunity in addition to allowing me to realize myself professionally, gave me so much on a personal level.

Thanks to all the members of the laboratory for helping, supporting and always encouraging me to give my best. Having created a nice work environment, shared lunches, laughter, birthday parties, and much more.
**Steffi**, the queen of the FACS, thanks for teaching me so much and often helping with bureaucratic issues outside the office.
**Isabell,** you have come close to the end of my PhD but with your skills you were crucial in completing my work. Thank you for your help, your commitment and the laughter we made in the lab... At the end we had fun doing the Western blot**.**
**Corinna** and **Susanne** thank you for the help which often went beyond the professional level.
**Christina** thanks for always helping me with a smile, not only in the work environment but also outside.
**Erika** thanks for your professional help, for all the beautiful moments spent in the lab, during trips and evenings spent together.

Thank you to all the guys of the RTB, especially **Renata** and **Sandra**, we helped and even supported each other from a distance. **Tiziana** a special thanks for having been by my side during these years and sharing important moments of my life.

A mio **marito**, senza di te non so come avrei fatto a completare il mio percorso. Mi sei sempre stato accanto, hai festeggiato con me ogni mio piccolo traguardo professionale, mi hai sostenuto nei miei momenti difficili, ma sopratutto hai creduto in me quando io non lo facevo. Grazie per aver capito quanto questo percorso fosse importante per me.

Ai miei colleghi italiani, **Francesca, Antonella, Elena,**….grazie per avermi spronato a non accontentarmi, aver creduto in me. Anche a distanza in questi anni siete state sempre presenti e pronte ad aiutarmi.
Mi avete sostenuto in un momento in cui ho dovuto scegliere come proseguire la mia carriera e anche se la mia scelta mi ha portato a percorrere una strada diversa so che potrò sempre contare sul vostro aiuto. A mio cugino **Vittorio,** un ringraziamento per essere sempre stato dalla mia parte…resteremo sempre i "cugini picchio" del lab. Frati che fanno tutto insieme e le stesse scelte di vita.

In ultimo, un ringraziamento speciale va alla mia famiglia. Grazie a i mie **genitori** per avermi dato la possibilità di raggiungere questo traguardo con i loro sacrifici. In tutti i miei anni di studio mi avete sempre sostenuto nelle mie scelte, anche quelle che hanno comportato il mio trasferirmi in un altro paese. Grazie di tutto…oggi non sarei una donna realizzata professionalmente e personalmente senza di voi.
A mia **sorella** grazie di esserci sempre per me, di avermi aiutato in tutto…in questi anni sei stata la mia wedding planner, assistente e babysitter.

A mia **figlia**, a te amore mio invece devo chiedere scusa….a volte la mamma era nervosa, stanca o ti ha un po' trascurato per lavorare al computer. Nonostante il tragitto sia stato un po' più lungo e faticoso, non c'è modo più bello di arrivare al traguardo con te nelle mie braccia.